UNIVERSITY OF ALBERTA

# FOURIER TRANSFORM MICROWAVE ROTATIONAL SPECTRA OF VAN DER WAALS COMPLEXES OF $N_2O$

BY

MWANÎKI SILAS NGARÎ

A THESIS SUBMITTED TO THE FACULTY OF GRADUATE STUDIES AND RESEARCH IN PARTIAL FULFILLMENT OF THE REQUIREMENTS FOR THE DEGREE OF DOCTOR OF PHILOSOPHY

DEPARTMENT OF CHEMISTRY

EDMONTON, ALBERTA

FALL 1999

National Library of Canada
Acquisitions and Bibliographic Services
395 Wellington Street
Ottawa ON K1A 0N4
Canada

Bibliothèque nationale du Canada
Acquisitions et services bibliographiques
395, rue Wellington
Ottawa ON K1A 0N4
Canada

Your file Votre référence

Our file Notre référence

The author has granted a non-exclusive licence allowing the National Library of Canada to reproduce, loan, distribute or sell copies of this thesis in microform, paper or electronic formats.

L'auteur a accordé une licence non exclusive permettant à la Bibliothèque nationale du Canada de reproduire, prêter, distribuer ou vendre des copies de cette thèse sous la forme de microfiche/film, de reproduction sur papier ou sur format électronique.

The author retains ownership of the copyright in this thesis. Neither the thesis nor substantial extracts from it may be printed or otherwise reproduced without the author's permission.

L'auteur conserve la propriété du droit d'auteur qui protège cette thèse. Ni la thèse ni des extraits substantiels de celle-ci ne doivent être imprimés ou autrement reproduits sans son autorisation.

0-612-46894-1

Canada

UNIVERSITY OF ALBERTA

LIBRARY RELEASE FORM

NAME OF AUTHOR: Mwanīki Silas Ngarī

TITLE OF THESIS: Fourier Transform Microwave Rotational Spectra of van der Waals Complexes of $N_2O$

DEGREE: Doctor of Philosophy

YEAR THIS DEGREE GRANTED: 1999

Permission is hereby granted to the University of Aberta Library to reproduce single copies of this thesis and to lend or sell such copies for private, scholarly, or scientific research purposes only.

The author reserves all other publication and other rights in association with the copyright in the thesis, and except as hereinbefore provided, neither the thesis nor any substantial portion thereof may be printed or otherwise reproduced in any material form whatever without the author's prior written permission.

Mwanīki Silas Ngarī

Idara ya Kemia

Chuo Kikuu cha Egerton

S. L. P. 536

Njoro

Kenya

Date 30-6-99

THE UNIVERSITY OF ALBERTA

FACULTY OF GRADUATE STUDIES AND RESEARCH

The undersigned certify that they have read, and recommend to the Faculty of Graduate Studies and Research for acceptance, a thesis entitled

FOURIER TRANSFORM MICROWAVE ROTATIONAL SPECTRA OF VAN DER WAALS COMPLEXES OF $N_2O$

submitted by MWANÎKI SILAS NGARÎ in partial fulfillment of the requirements for the degree of DOCTOR OF PHILOSOPHY.

Supervisor Dr. W. Jäger

Dr. R. E. D. McClung

Dr. G. Kotovych

Dr. M. Cowie

Dr. M. R. Freeman

External Examiner Dr. A. G. Adam

University of New Brunswick

Date 29. June 1999

Kwī mwendwa mūtumia wakwa Tabitha Wawīra Mwanīki na ciana ciakwa, Winnie Wangeci Mwanīki na Nelson Ngarī Mwanīki

Kwa mpendwa bibi yangu Tabitha Wawīra Mwanīki na watoto wangu, Winnie Wangeci Mwanīki na Nelson Ngarī Mwanīki

To my wife Tabitha Wawīra Mwanīki and my children, Winnie Wangeci Mwanīki and Nelson Ngarī Mwanīki

# ABSTRACT

Rotational spectra of six van der Waals complexes, namely Ne-$N_2O$, Ar-$N_2O$, $Ar_2$-$N_2O$, $Ne_2$-$N_2O$, ArNe-$N_2O$, and CO-$N_2O$, were measured using a pulsed molecular beam cavity Fourier transform microwave spectrometer. The resulting spectroscopic constants were utilised to derive the geometries, structures, harmonic force fields, and dynamical information about these complexes.

The Ne-$N_2O$ and Ar-$N_2O$ dimers have T-shaped equilibrium geometries. The structural parameters indicate that the rare gas atom is on average closer to the O atom than to the terminal N atom of $N_2O$ in both complexes. The $^{14}N$ nuclear quadrupole hyperfine structures in the rotational spectra were resolved and analysed, to yield quadrupole coupling constants for both terminal and central $^{14}N$ nuclei. Harmonic force field analyses were performed to estimate the frequencies of the van der Waals vibrations in the dimers.

The spectra of $Ar_2$-$N_2O$ and $Ne_2$-$N_2O$ are those of complexes with $C_s$ symmetry; those of ArNe-$N_2O$ are in accord with a complex with $C_1$ symmetry. Both *a*- and *c*-type transitions were measured for all $Ne_2$-$N_2O$ isotopomers. In the case of the mixed, $^{20}Ne^{22}Ne$ containing, isotopomers a small *b*-dipole moment occurs and two *b*-type transitions were measured. For $Ar_2$-$N_2O$ only *b*- and *c*-type transitions occur, while all three types of transitions were measured for ArNe-$N_2O$. Structural parameters were derived and show that all three trimers have distorted tetrahedral structures with the rare gases tilted towards the O atom of the $N_2O$ subunit. Nuclear quadrupole hyperfine structures were analysed and harmonic force field analyses were performed for each complex. The results are discussed in the light of possible three-

body non-additive interactions.

The CO-$N_2O$ dimer has a T-shaped structure, consistent with the CO subunit forming the leg of the T, and the C atom of CO bonded to the central N atom of $N_2O$. Comparison of the nuclear quadrupole coupling constants with those of the $N_2O$ monomer and of other $N_2O$ containing complexes indicate significant electronic charge redistribution at the central nitrogen atom upon complex formation.

# ACKNOWLEDGMENTS

It is a pleasure to acknowledge the inestimable assistance of Dr. W. Jäger, my supervisor, whose inspiring counsel and advice enabled me to overcome many difficult situations during my stay in his research group in the course of the work that culminated in the presentation of this thesis. The support, guidance and assistance of Dr. Jäger were invaluable and necessary in making this thesis possible.

Many colleagues kindly supported me in this endeavour. Not having the possibility to identify and to thank all of them by name, however, I wish to convey my deepest gratitude to the members of our (Dr. Jäger's) research group for the stimulating discussions we have had in our group seminars which greatly aided my understanding of rotational spectroscopy. I would like to thank Dr. Y. Xu in particular, for the many useful suggestions and fruitful discussions regarding my research projects that are presented in this thesis.

Fr. E. Crough of the St. Antony's Catholic Parish, Edmonton, gave me a lot of personal, moral, spiritual, and material support during my residential stay at the Parish quarters. My sincere thanks go to him.

I thank the Department of Chemistry for a teaching assistantship, the Natural Sciences and Engineering Research Council (NSERC) of Canada for financial support, and Egerton University, Kenya, for study leave.

Finally, I take this opportunity to acknowledge my parents, S. N. Ngware and A. W. Ngarī, for taking me to school and instilling into me the value of education, my wife T. W. Mwanīki and my children for their patience during my long absence from home. Thanks be to Almighty God. Amen.

# CONTENTS


| Chapter | | Page |
|---|---|---|
| 1 | Introduction | 1 |
| | References. | 17 |
| 2 | Experimental | 23 |
| | References. | 41 |
| 3 | Study of the Rotational Spectrum of the Ne-$N_2O$ van der Waals Dimer | 43 |
| | 3.1 Introduction. | 43 |
| | 3.2 Experimental. | 44 |
| | 3.3 Results and Discussion. | 45 |
| | 3.3.1 Observed Spectra, Assignments, and Analyses. | 45 |
| | 3.3.2 Harmonic Force Field. | 53 |
| | 3.3.3 Geometry and Structure. | 56 |
| | 3.3.4 $^{14}N$ Nuclear Quadrupole Hyperfine Structure | 60 |
| | 3.4 Conclusion. | 63 |
| | References. | 64 |
| 4 | Ground State Average and Partial Substitution Structures of the Ar-$N_2O$ van der Waals Dimer | 66 |
| | References. | 74 |
| 5 | FTMW Rotational Spectra of the $Ne_2$-$N_2O$ and $Ar_2$-$N_2O$ van der Waals Trimers | 75 |
| | 5.1 Introduction. | 75 |
| | 5.2 Experimental. | 78 |

5.3 Observed Spectra and Analyses. ..... 79

5.3.1 $Ar_2$-$N_2O$. ..... 79

5.3.2 $Ne_2$-$N_2O$. ..... 83

5.4 Results and Discussion. ..... 87

5.4.1 Structural Analyses. ..... 87

5.4.2 Harmonic Force Field Analyses. ..... 94

5.4.3 $^{14}N$ Nuclear Quadrupole Coupling Constants. ..... 99

5.5 Conclusions. ..... 103

References. ..... 105

6 The ArNe-$N_2O$ van der Waals Trimer: A High Resolution Spectroscopic Study of Its Rotational Spectrum, Structure and Dynamics 108

6.1 Introduction. ..... 108

6.2 Experimental Details. ..... 110

6.3 Results and Discussion. ..... 111

6.3.1 Spectral Assignments and Analyses. ..... 111

6.3.2 Structural Analyses. ..... 115

6.3.3 $^{14}N$ Nuclear Quadrupole Hyperfine Structure. ..... 119

6.3.4 Harmonic Force Field Approximation. ..... 122

6.4 Concluding Remarks. ..... 125

References. ..... 127

7 Rotational Spectroscopic Investigation of the Weak Interactions Between CO and $N_2O$ 130

7.1 Introduction. ..... 130

7.2 Experimental Details. ..... 131

7.3 Results and Discussion. ..... 132

7.3.1 Spectral Assignments and Analyses. ..... 132

7.3.2 Nuclear Quadrupole Coupling Constants. ..... 136

7.3.3 Structural Analyses. ..... 144

References. ..... 148

8 General Discussion and Conclusions 150

References. ..... 153

Appendix 154

A1 Tables of the measured transition frequencies for chapter three. ..... 154

A2 Tables of the measured transition frequencies for chapter four. ..... 161

A3 Table of the measured transition frequencies for chapter five. ..... 164

A4 Tables of the measured transition frequencies for chapter six. ..... 180

A5 Tables of the measured transition frequencies for chapter seven. ..... 187

# LIST OF TABLES


Table Page

3.1 Derived spectroscopic constants for Ne-$N_2O$. ..... 48

3.2 Harmonic force field of Ne-$N_2O$. ..... 55

3.3 Observed and calculated centrifugal distortion constants. ..... 55

3.4 Structural parameters of Ne-$N_2O$. ..... 59

4.1 Spectroscopic constants of Ar-$N_2O$. ..... 70

4.2 Structural parameters of the Ar-$N_2O$ van der Waals complex. ..... 73

5.1 Derived spectroscopic constants for $Ar_2$-$N_2O$. ..... 84

5.2 Derived spectroscopic constants for $^{20}Ne^{20}Ne$-$N_2O$ and $^{22}Ne^{22}Ne$-$N_2O$. ... 88

5.3 Derived spectroscopic constants for $^{20}Ne^{22}Ne$-$N_2O$. ..... 89

5.4 The structural parameters of $Ar_2$-$N_2O$, Ar-$N_2O$, $Ar_2$-$CO_2$, Ar-$CO_2$, and $Ar_2$. ..... 90

5.5 The structural parameters of $Ne_2$-$N_2O$, Ne-$N_2O$, Ne-$CO_2$, and $Ne_2$. ..... 90

5.6 The harmonic force field of $Ar_2$-$N_2O$. ..... 96

5.7 The harmonic force field of $Ne_2$-$N_2O$. ..... 97

5.8 Comparison of experimental and calculated quartic centrifugal distortion constants. ..... 98

6.1 Derived spectroscopic constants for ArNe-$N_2O$. ..... 116

6.2 The structural parameters of ArNe-$N_2O$, $Ar_2$-$N_2O$, $Ne_2$-$N_2O$, and the relevant dimers. ..... 118

6.3 Comparison of the $^{14}N$ nuclear quadrupole coupling constants of ArNe-$N_2O$

with those of the dimers Ar-$N_2O$ and Ne-$N_2O$. ..... 122

6.4 The harmonic force field of ArNe-$N_2O$. ..... 123

6.5 Comparison of observed and calculated centrifugal distortion constants. ..... 126

7.1 Spectroscopic constants for the CO-$N_2O$ complex. ..... 137

7.2 Comparison of the nuclear quadrupole coupling constants of $N_2O$ containing complexes and the $N_2O$ monomer. ..... 139

7.3 Structural parameters of the CO-$N_2O$ complex. ..... 147

A1.1 Observed transition frequencies of the $^{14}N$-hyperfine structure of $^{20}Ne$-$^{14}N^{14}NO$ and $^{22}Ne$-$^{14}N^{14}NO$. ..... 155

A1.2 Observed transition frequencies of the $^{14}N$-hyperfine structure of Ne-$^{15}N^{14}NO$ and Ne-$^{14}N^{15}NO$. ..... 158

A2.1 Observed transition frequencies of Ar-$^{15}N^{14}NO$ and Ar-$^{14}N^{15}NO$. ..... 162

A3.1 The measured transition frequencies of the $^{14}N$-hyperfine patterns of $^{40}Ar_2$-$^{14}N_2O$. ..... 165

A3.2 Measured frequencies of the $^{14}N$-hyperfine structure of $^{40}Ar_2$-$^{15}N^{14}NO$ and $^{40}Ar_2$-$^{14}N^{15}NO$. ..... 168

A3.3 Observed transition frequencies of the $^{14}N$-hyperfine structure of $^{20}Ne_2$-$^{14}N_2O$ and $^{22}Ne_2$-$^{14}N_2O$. ..... 170

A3.4 Observed transition frequencies of the $^{14}N$-hyperfine structure of $^{20}Ne^{22}Ne$-$^{14}N_2O$. ..... 173

A3.5 The observed frequencies of the $^{14}N$-hyperfine structure of $^{20}Ne_2$-($^{15}N^{14}NO$, $^{14}N^{15}NO$) and $^{22}Ne_2$-($^{15}N^{14}NO$, $^{14}N^{15}NO$). ..... 175

A3.6 Observed frequencies of the $^{14}N$-hyperfine structure of $^{20}Ne^{22}Ne$-($^{15}N^{14}NO$, $^{14}N^{15}NO$). ..... 178

A4.1 The observed transition frequencies of the $^{14}N$-hyperfine structure of $Ar^{20}Ne$-$N_2O$ and $Ar^{22}Ne$-$N_2O$. ..... 181

A4.2 The observed frequencies of the $^{14}N$-hyperfine structure of $Ar^{20}Ne$-($^{15}N^{14}NO$, $^{14}N^{15}NO$) and $Ar^{22}Ne$-($^{15}N^{14}NO$, $^{14}N^{15}NO$). ..... 184

A5.1 Observed transition frequencies (in MHz) for CO-$^{14}N^{14}NO$ isotopomers. ..... 188

A5.2 Observed transition frequencies (in MHz) for $^{13}C^{16}O$-$^{15}N^{14}NO$ and $^{13}C^{16}O$-$^{14}N^{15}NO$. ..... 196

# LIST OF FIGURES


Figure page

2.1 Schematic showing the relationship between the polarization and the population difference for the case of resonant polarization. ..... 27

2.2 The general set-up of the molecular beam FTMW spectrometer. ..... 29

2.3 The mechanical parts of the molecular beam FTMW spectrometer. ..... 31

2.4 The MW circuit. ..... 33

2.5 Schematic representation of the sequence of pulses in a single experiment. ..... 35

2.6 The results from an automatic scan. ..... 40

3.1 Power spectrum of the $J_{K_aK_c}=1_{11}-0_{00}$ rotational transition of $^{20}Ne-^{14}N^{14}NO$ showing hyperfine components due to the $^{14}N$ nuclei. ..... 50

3.2 Comparison of the $^{14}N$ nuclear quadrupole hyperfine structures of the rotational transition $J_{K_aK_c}=4_{04}-3_{13}$ of $^{20}Ne-^{15}N^{14}NO$, $^{20}Ne-^{14}N^{15}NO$, and $^{20}Ne-^{14}N^{14}NO$. ..... 52

3.3 The rotational constants and the quadrupole coupling constants are consistent with these two orientations of the $N_2O$ monomer with respect to the rare gas atom. ..... 58

4.1 The power spectrum of the rotational transition $J_{K_aK_c}=2_{12}-1_{01}$ of $Ar-^{14}N^{15}NO$ showing hyperfine components due to the terminal $^{14}N$ nucleus. ..... 68

4.2 The $Ar-N_2O$ dimer in its principal inertial axis system. ..... 72

5.1 The equilibrium geometry of the $Ar_2-N_2O$ trimer, derived assuming

pairwise additivity. ..... 80

5.2 The $Ne_2$-$N_2O$ van der Waals trimer in its principal inertial axis system. ..... 81

5.3 Spectrum of the rotational transition $J_{K_aK_c}=3_{22}$-$2_{12}$ of $^{20}Ne_2$-$^{14}N_2O$. ..... 85

6.1 The ArNe-$N_2O$ trimer in its principal inertial axis system. ..... 112

6.2 The spectra of the $J_{K_aK_c}=3_{22}$-$2_{12}$ transition with the assigned hyperfine pattern for the isotopomers $^{40}Ar^{20}Ne$-($^{14}N^{14}NO$, $^{15}N^{14}NO$, and $^{14}N^{15}NO$). ..... 114

7.1 The effective structure of CO-$N_2O$ as determined from the structural analysis. ..... 133

7.2 Observed spectrum of the rotational transition $J_{K_aK_c}=1_{11}$-$0_{00}$ of $^{12}C^{16}O$-$^{14}N^{14}NO$. ..... 135

# CHAPTER ONE

# INTRODUCTION

Atoms and molecules attract one another when they are far apart, as is evident from the existence of molecular and atomic liquids and solids, and repel one another when they are very close to each other - since, for example, densities are finite. The interaction potential energy of a pair of atoms or molecules is positive at small intermolecular distances and negative for large intermolecular distances. At some intermediate distance the potential energy is a minimum and at this point the attractive and repulsive forces balance and the atoms or molecules are bound to each other to form a new species with a separate, unique identity with its own properties which can be studied by some physical-chemical means.

As early as the mid-19$^{th}$ century van der Waals demonstrated that the very existence of condensed phases of matter stems from the attractive forces between molecules, and at the same time that the small compressibility of these condensed phases arises from the repulsive forces which act at short range (*1*). Since the end of the 19$^{th}$ century a considerable amount of work has been devoted to the exact formulation of the connection between the properties of matter in bulk and intermolecular forces. It is such a formulation that represents the ultimate aim of the molecular theory of matter, since, when a theory of this kind is well established, a knowledge of the intermolecular forces is sufficient for the evaluation of all the properties of the bulk materials. However the exact functional forms of these intermolecular forces are not sufficiently well understood even though the physical

origins of these forces are well established.

The extremely important role of intermolecular forces in determining equilibrium and non-equilibrium properties and phenomena of matter is by now a well established point and there have been numerous reviews on the subject (*2*, *3*, *4*, *5*, *6*, *7*). At present, the field of intermolecular interactions represents one of the most important branches of molecular science. The topic is of particular importance especially at the interfaces of chemistry, physics, and biology.

Many important processes, including life itself, depend on two apparently contradictory requirements: stability and change. The type of chemistry that allows both of these requirements is the subject of intermolecular forces. When intermolecular forces are negligible, for example, in the gas phase, no persistent structures appear, even though molecules continuously undergo collisions, and in some cases, chemical reactions. If on the other hand the forces are very strong, for example, in diamond, structure persists forever. This means that dynamics is sacrificed for stability. It is thus the relatively weak *inter*molecular forces and not the strong forces that allow for both stability and change. A protein molecule, for example, may be confined into one of many conformations by weak forces that act between the various interacting functional groups in the molecule. However only a slight change in temperature, pH, or solvent properties is needed to change the conformation, which may in turn change the activity of say an enzyme molecule (*8*). The fundamental questions concerned with the mechanisms of chemical and biochemical catalysis and the paths of chemical reactions can thus be answered by an

understanding of the molecular interactions involved. They account for the stability of such molecules as DNA, and also play an essential role in the mechanisms of enzyme reactions and protein folding (*9*, *10*, *11*).

The study of intermolecular forces is the first step in understanding imperfect gases, liquids, and many other systems. We always come across the existence of intermolecular, interatomic, forces in the studies of collisions of rare gas atoms, surface phenomena, equilibrium geometries of crystals, and in many other problems (9). Intermolecular interactions are also of prime importance in phase transitions (10). The coagulation of colloidal solutions is based upon a balance of the repulsive electrostatic forces and the attractive dispersion forces between particles (*12*).

The basic concepts in the study of intermolecular forces are covered in many physical chemistry textbooks and monographs about the subject (*13*, *14*, *15*, *16*, *17*, *18*, *19*, *20*, *21*). Intermolecular forces have an electrostatic origin. The source of the interaction is thus due to the charged particles that make up matter - the electrons and nuclei. The interactions are repulsive at short range and attractive at long range. The short range forces originate from the approach of the electron clouds of two atoms or molecules, sufficiently close so that the electron density between them is reduced (Pauli exclusion principle). This reduction of electron density causes the positively charged nuclei of the atoms or molecules to be incompletely shielded from each other and therefore to exert a repulsive force on each other. Depending on the nature of the interacting molecules, there are three possible contributions to the attractive force, only one of which is present in all molecular interactions - the London dispersion

force. For simple molecules it is nearly always the greatest contribution to the intermolecular attractive force. The other contributions are electrostatic and induction interactions.

Some molecules, such as nitrous oxide, $N_2O$, have permanent dipole moments due to the electric charge distribution in the molecule. One component of the interaction energy for two such molecules at long range therefore arises from the electrostatic interaction between their dipole moments. This interaction occurs without a distortion of the electron distribution on either molecule and is thus a first-order energy. This energy is strictly pairwise additive and may be attractive or repulsive. The electrostatic energy between two dipoles is a function of their relative orientation. Molecules without a resultant dipole moment, such as $CO_2$, can possess an electric quadrupole moment or higher order moments which contribute to the electrostatic energy in a similar fashion.

Another kind of interaction can involve a molecule with a permanent dipole moment and another molecule which is non-dipolar. The electric field of the dipolar molecule distorts the electron charge distribution of the other molecule, thereby producing an induced dipole moment within it. This induced dipole moment interacts with the inducing dipole to produce an attractive force. This type of interaction relies for its existence upon distortion of electron clouds and is therefore a second-order effect. This induction contribution is simultaneously present with the electrostatic contribution in the case of the interaction of two polar molecules. The induction effects arise from the distortion of a particular molecule in the electric field of all its

neighbours, and are always attractive. Because the fields of several neighbouring molecules may reinforce each other or cancel out, induction is strongly non-additive.

The third type of contribution to the attractive intermolecular force can, for example, involve atoms without permanent electronic multiple moments. This contribution has a purely quantum mechanical origin. Even though the atom has no permanent dipole moment, its electrons are in continuous motion so that its electron density oscillates continuously in time and space. Thus at any instant the atom possesses an instantaneous electric dipole which fluctuates as the electron density fluctuates. This instantaneous dipole in one atom can induce an instantaneous dipole in a second atom. The induced dipole in the second atom and the inducing dipole in the first interact to produce an attractive energy called the dispersion energy. In other words the dispersion energy is due to the correlations between the electron density fluctuations in the two atoms. This energy is second-order since a distortion of the electron density of the molecule is involved, and is present in all interacting molecules.

At the heart of the matter in the study of intermolecular forces is the interaction potential energy surface. This is a functional form of the dependence of the interaction energy on the distance between the interacting atoms or molecules and the orientations of the monomers. For a diatomic molecule or complex, the situation is simplest because the interaction energy is dependent upon only the separation distance between the atoms. The resulting potential energy curve is a mathematical representation of the dependence of the interaction potential energy on the separation

distance. The next type of interaction involves an atom and a linear diatomic or polyatomic molecule. The interaction pair potential will have an additional degree of freedom, which can be the angle between the axis of the linear molecule and the line that connects the center-of-mass of the two subunits. For a complete description, it would also be necessary to consider the internal degrees of freedom of the linear molecule. The multi-dimensional potential energy surfaces can be rather complex if pairs of non-linear molecules are involved, even if only the intermolecular degrees of freedom are considered.

Potential energy surfaces can be constructed solely based on experimental data or from *ab initio* calculations or from a combination of both (semi-empirical potentials). One of the major problems in the construction of empirical and semi-empirical potentials is to produce a realistic model with parameters that have conceptual meaning. These parameters must also be explicable in terms of the basic concepts in the study of intermolecular forces. The ultimate test of *ab initio* potentials is in their ability to reproduce experimental data, and to predict other properties (*22*, *23*, *24*, *25*, *26*, *27*). Thus, a multitude of experimental data is needed for use in construction of semi-empirical and empirical potentials as well as in testing existing potentials and the *ab initio* ones. This calls for the study of prototype systems.

The basic starting point in learning about intermolecular forces is a knowledge of the properties of the individual molecules. Such molecular parameters as the multipole moments and polarizabilities are important parameters in determining how a

given molecule interacts with neighboring atoms or molecules in an ensemble. There are various methods that have been used in the determination of dipole moments (and higher moments), and polarizabilities (see for example ref. *14*, chapter 12). An important method for the determination of dipole moments is the Stark effect in rotational spectroscopy (*28*, *29*, *30*, *31*, *32*, *33*). These molecular properties however are only useful as tools for determining some coefficients that enter into the long range part of the intermolecular potential (*14*). Experimental information about the interactions themselves can be obtained from bulk phase experiments. Such studies include the determination of second virial coefficients of gases. The second virial coefficient of gases has been shown to be dependent on pairs of interacting molecules (*34*). Other bulk properties of gases that have been used for this purpose are viscosity, thermal conductivity, and diffusion coefficients (*14, 15, 19*). The study of liquids and solids has also been a source of data which can be used to provide some insight into the nature of intermolecular forces. Studies in these phases, especially the study of crystal structures are valuable in determining intermolecular and interatomic distances (*19*). The main difficulty in these kinds of data is that they represent averages over a range of relative velocities and orientations. Furthermore they are complicated by the effects of many-body interactions.

The most important source of information on the intermolecular potential function is high resolution spectroscopy, especially spectroscopy of van der Waals complexes. Various spectroscopic methods have been used to study van der Waals complexes. These methods include electronic, infrared, far-infrared, and microwave

(MW) spectroscopies (*35*, *36*, *37*, *38*, *39* ). A collection of one or more types of atoms or molecules (or both) held together by intermolecular attractions are called van der Waals molecules. For example, gaseous Ar is known to contain, at below its boiling point, in addition to Ar atoms a few percent of $Ar_2$ (*40*, *41*, *42*, *43*, *44*). Such dimers have very shallow potential wells with very small dissociation energies compared to those of normal chemical bonds. The dimers, however, have well defined sets of bound quantum states, i.e., electronic, vibrational, and rotational, which are amenable to both experimental as well as theoretical study and characterization. It is well known and documented that there will be traces of such dimers present in any gas especially at low temperatures where the kinetic energy is low, which minimizes the dissociation of the dimers.

In the investigation of van der Waals clusters by the pulsed nozzle Fourier transform (FT) technique, the gas mixture is expanded into an evacuated cavity. The gas pulse that emerges from the nozzle has very low effective translational, rotational and vibrational temperatures. The large number of collisions in the initial stages of the molecular expansion leads to the formation of van der Waals complexes. In the sample cell these molecules move in essentially collisionless paths which increases the lifetimes of the van der Waals molecules and allows their spectra to be studied. The presence of van der Waals molecules in the molecular expansion is not limited to dimers. Many studies have documented the presence of trimers, tetramers, pentamers, and larger clusters in these systems. To date many van der Waals complexes have been characterized and their bibliography is enormous. The extensive

literature on van der Waals complexes can be seen from references *35, 36, 37, 38* and *39* . These complexes can be viewed as intermediate stages between the gaseous and liquid phases of matter. Their study is thus crucial to a better understanding of the forces that hold the condensed phases of matter together.

The method used in this laboratory to study the rotational spectra of van der Waals complexes is based on molecular beams (*45*). Experiments on molecular beams have been performed in many regions of the electromagnetic spectrum as described in ref. *45*. This has been made possible by a great deal of advancement in molecular beams, vacuum chambers, and lasers. These have led to reports of a great variety of studies of van der Waals complexes. One of these spectrometers that is used in this laboratory is the pulsed molecular beam FTMW spectrometer. This instrument was first successfully applied to the study of weakly bound dimers by Flygare *et al.* (*46, 47, 48, 49, 50, 51*) and modified by other groups (*52, 53, 54, 55*). The MW spectroscopic study of the isolated complex allows a wide range of its properties to be determined (*56, 57*). Rotational spectroscopy is an unambigious source of some very important quantities, such as the geometry and structure, force constants, and in suitable cases the electronic environments of the monomers. The details of the spectrometer are summarised in the next chapter.

Several prototype systems, especially those involving rare gas atoms and simple molecules, have been at the forefront in the study of intermolecular forces. These range from rare gas dimers, rare gas-simple molecule dimers, and linear molecule-linear molecule dimers. Some of the corresponding potentials have been

modelled theoretically and in combination with results from high resolution spectroscopy. The most studied rare gas dimer is $Ar_2$ and its potential energy curve is very well characterised (*40, 41, 42, 43, 44*). The use of high resolution spectroscopic data in conjunction with theoretical modelling has also produced highly accurate pair potentials for a number of rare gas-simple molecule van der Waals molecules. Hutson (*58*) has used a least squares method to simultaneously fit molecular beam MW and far-infrared spectroscopic data to two intermolecular potentials for Ar-HCl. These potentials were used to calculate additional bound states for Ar-HCl. This author (*59*) has also derived an intermolecular potential function for Ar-HF. This was done by fitting to the results of high resolution MW, far-infrared, and infrared spectroscopy. LeRoy and Hutson have (*60*), by analysing a combination of data from infrared, MW, elastic and inelastic differential cross section measurements, and virial coefficient data, determined accurate potentials for the Ar-$H_2$, Kr-$H_2$ and Xe-$H_2$ dimers. An improvement of the potential energy surface for Ar-$H_2O$ has been reported by Cohen and Saykally (*61*). This was accomplished by using a direct nonlinear least squares fit to far-infrared, infrared, and MW spectroscopic measurements. This potential was also refined using measurements from vibrational-rotational-tunnelling spectroscopy. This potential is at the same level of accuracy as those of Hutson cited above (*58, 59, 60*). Schmuttenmaer and co-workers (*62*) have reported a spectroscopically determined potential energy surface for Ar-$NH_3$. This was done by use of a combination of far-infrared and MW vibrational-rotational-tunnelling measurements as well as temperature-dependent

second virial coefficients.

The knowledge of such interaction pair potentials is the starting point in the study of the contributions of many-body non-additive forces in clusters and in the condensed phase. The total intermolecular interaction energy of a group of atoms or molecules bound together is not simply the sum of the pair potentials for each interacting pair. There are further contributions from three-body, four-body, and, in general, many-body nonadditive terms. The pair potentials have the largest contribution and have thus to be known very accurately before one embarks on the determination of the contributions from the many-body effects. The beauty of the study of van der Waals molecules is that it is possible to start with a simple dimer study, and then build upon it a trimer, tetramer, pentamer, and even larger clusters, each of which can be studied independently. From a knowledge of the pair potentials one can then study the effects of three-body, four-body, five-body, etc., interactions on the intermolecular potential energy surface. The study of many-body effects hinges on the availability of accurate pair potentials. The results from experimental studies of, for example, a ternary system can be compared with those from rigorous pairwise additive calculations. The discrepancies can then be attributed to three-body non-additive interactions. The first three-body non-additive term developed is that due to Axilrod and Teller, the so-called AT tripole-dipole dispersion or DDD term (*63*). This term was derived to account for three-body interactions in atomic ternary systems. It is the leading term in the corrections to the long-range dispersion energy. The apparent success of the AT tripole-dipole dispersion term was later, however,

attributed to a fortuitous cancellation of higher order terms (*64*, *65*).

One of the most studied van der Waals trimers is $Ar_2$-HCl, the main aim being to measure all spectroscopically accessible states of this trimer and to ultimately characterise the full potential energy surface which, in turn, will provide useful insights into the physical origins of three-body effects. The other reason for the popularity of this trimer is that the pair potentials involved are very well characterised; these are Ar-Ar (*40*, *41*, *42*, *43*, *44*), and Ar-HCl (*58*). Cooper and Hutson (*66*) have done rigorous pairwise additive calculations on the $Ar_2$-HCl trimer and found substantial disparities between the calculated vibrational frequencies, rotational constants, and angular expectation values and those from MW and far-infrared spectroscopy. This indicated that the three-body non-additive effects were important in the total interaction potential. In the same study, they set out to investigate various different physical interactions that could lead to three-body non-additive contributions. They found that the nonadditive dispersion, induced dipole-induced dipole, and exchange overlap interactions were important, though not large enough to resolve the discrepancy between pairwise additive calculations and experiment. The interactions involving the multipole moments of the subunits in the trimer were found to be very important in characterising three-body forces. The interactions of the permanent multipole moments of HCl and the overlap-induced multipoles on the Ar atoms (which produces an exchange quadrupole moment when two Ar atoms are close to each other) were found to substantially improve the agreement between theory and and experiment. In an extension of the above study

Ernesti and Hutson (*67*) have used a more elaborate model of non-additve forces (*68*) to re-calculate the vibrational frequencies, rotational constants, and angular expectation values for $Ar_2$-HCl and $Ar_2$-HF which included hydrogen/deuterium isotope effects. The potential used in this study includes a sophisticated model of the exchange multipole interaction. This report indicates that it is important to include not only dispersion and induction but also short range effects in the modelling of non-additive forces in molecular systems.

The current work is a report of studies done in this laboratory on the characterization of van der Waals complexes. The theme of the report centers around the dimers and trimers of Ar and Ne with $N_2O$, (nitrous oxide). The CO-$N_2O$ dimer has also been studied. The aim of this work was to provide rotational spectroscopic information about the binary rare gas-$N_2O$ complexes and then to utilize these data to predict and to measure the rotational spectra of the ternary (rare gas)$_2$-$N_2O$ complexes. Comparison of the results of the spectral analyses of dimer and trimer complexes would then give information about three-body non-additive contributions.

A particular point of interest in this context is that $N_2O$ contains two $^{14}N$ nuclei with spin $I=1$ and an associated electric quadrupole moment. The nuclear spins can couple with the overall rotation of the complex, resulting in complicated hyperfine splittings of the rotational transitions (*69*, *70*, *71*, *72*, *73*). The coupling of the spin and rotational angular momenta occurs through the interaction of the nuclear quadrupole moment with the non-vanishing electric field gradient at the site of the nucleus (*28* (Chapter 6, pp. 149-173), *29* (Chapter 6, pp. 92-145), *30* (Chapter 5, pp.

114-144), *31* (Chapter IX, pp. 391-449)). Assignments and analyses of such hyperfine structures yield nuclear quadrupole coupling constants, which can, in turn, provide information about the electronic perturbation of, for example, $N_2O$ upon complex formation. Furthermore, the nuclear quadrupole coupling constants contain information about the large amplitude van der Waals bending vibrations within the complex.

Knowledge about weak interactions of $N_2O$ in general is important because of its participatory nature in atmospheric pollution, the fact that it is one of the greenhouse gases, and that it is a popular anaesthetic in medicine and dentistry. The properties of $N_2O$ as an anaesthetic are covered in several textbooks in anaesthesia (*74*, *75*, *76*, *77*, *78*). It is known that it does not undergo any metabolism in the body and that it is excreted unchanged after inhilation (*78* (Chapter 8, pp. 121-138)). This means that its anaesthetic actions involve weak reversible intermolecular interactions, probably involving hydrogen-bond-like interactions with biomolecules in the body. It is also known that, when inhaled in small quantities, it produces some hysteria leading to its trivial name "laughing gas".

$N_2O$ is the most abundant nitrogen oxide in the atmosphere (*79*). Its presence in the atmosphere comes from several sources. $N_2O$ is produced in the soils and oceans as a by-product in the nitrogen cycle. This is done by the action of anaerobic bacteria (*80*). It is stable in the atmosphere from where it is slowly transported into the stratosphere where it is destroyed by UV radiation and reacts with O radicals to produce NO (*81*). In this way it is responsible for the natural destruction of the

stratospheric ozone (*81*, *82*), since NO is one of the notorious nitrogen oxides normally termed $NO_x$. $N_2O$ is also produced through anthropogenic (human) activities especially in forest burning, use of nitrogenous fertilizers, and in the burning of fossil fuels (*83*).

Nitrous oxide is one of the trace gases in the atmosphere that cause the earth to retain heat and, like other greenhouse gases, its atmospheric abundance has been shown to be increasing (*82*, *83*, *84*, *85*, *86*). It is a participant in the formation of smoke aerosols, which have serious climatic and ecological effects, for example, by reflecting sunlight back into space, and preventing heat escape from the earth's atmosphere causing a heating effect on the earth's climate (*82*). The industrial manufacture of $N_2O$ is done by heating ammonium nitrate ($NH_4NO_3$) (*87*).

This thesis is divided into 8 self-contained sections, including the present chapter. Chapter 2 presents a brief discussion of the experimental set-up. In this chapter the basic theory of the method is also briefly presented. The other chapters (3-7) present results of the van der Waals complexes studied in this work. Chapter 3 presents the results of a study of the rotational spectrum of the Ne-$N_2O$ van der Waals dimer. Its structure, harmonic force field, and nuclear electric quadrupole hyperfine structure are discussed. In Chapter 4 the results of isotopomeric studies of the previously studied Ar-$N_2O$ complex (*69*, *88*, *89*, *90*, *91*) are presented. A partial substitution structure and a ground state average structure are derived. Chapter 5 presents the results of studies of two geometrically similar van der Waals trimers, $Ar_2$-$N_2O$ and $Ne_2$-$N_2O$. The results of the spectral analyses indicate the presence of

three-body non-additive interactions. Chapter 6 is an extension of the study of the above trimers. The mixed rare gas-$N_2O$ trimer ArNe-$N_2O$ is reported. The introduction of an exchange dipole moment on the Ar-Ne subunit proceeds to provide additional information about three-body effects. The complex CO-$N_2O$ is reported in Chapter 7. The structure and hyperfine analysis are discussed. The last chapter, Chapter 8, is a general discussion and conclusions section, where the commonness and peculiarities of the various studies are pointed out. The major contributions of these studies to the study of intermolecular interactions are summarised, and future prospects are highlighted in the context of the experiments done in this laboratory, and presented here.

## REFERENCES


1. J. D. van der Waals, On the Continuity of the Gaseous and Liquid States (J. S. Rowlinson, Ed), in "Studies in Statistical Mechanics" (J. L. Lebowitz, Ed), Vol. XIV, pp. 121-282, Elsvier, New York, 1987.

2. C. Schlier, *Annu. Rev. Phys. Chem.* **20,** 191 (1969).

3. A. D. Buckingham and B. D. Utting, *Annu. Rev. Phys. Chem.* **21,** 287 (1970).

4. H. Ratajczak and W. J. Orville-Thomas (Eds), Molecular Interactions, Vols. 1 and 2, John Wiley & Sons, New York, 1980.

5. B. Pullman (Ed), Intermolecular Forces, Proceedings of the Fourteenth Jerusalem Symposium on Quantum Chemistry and Biochemistry held in Jerusalem, Israel, April 13-16, 1981.

6. J. M. Haile and G. A. Mansoori (Eds), Molecular-Based Study of Fluids, in "Advances in Chemistry Series", 204 (M. J. Comstock, Ed). (Based on a symposium jointly sponsored by the ACS Division of Industrial and Engineering Chemistry at the 182nd ACS National Meeting, New York, New York, August 23-28, 1981), American Chemical Society, Washington, D. C. 1983.

7. G. E. Ewing, Angew. *Chem. Int. Ed. Engl.* **11,** 486 (1972).

8. J. Ricard and A. Cornish-Bowden (Eds), Dynamics of Biochemical Systems, NATO ASI Series A: Life Sciencies, Vol. 81, pp. 3-29, Plenum Press, New York and London, Published in Cooperation with NATO Scientific Affairs Division, 1983.

9. A. Rich and N. Davidson (Eds), Structural Chemistry and Molecular Biology, W. H. Freeman and Company, San Francisco, 1968.

10. W. Ferdinand, The Enzyme Molecule, pp. 74-75, 82-84, John Wiley and Sons, London, 1976.

11. A. Kormychev and S. Leikin, *Proc. Natl. Acad. Sci. USA,* **95,** 13579 (1998).

12. C. La Messa, L. Perci, and A. D' Aprano, *Ber. Bunsenges. Phys. Chem.* **10,** 1459 (1998).

13. P. Atkins, Physical Chemistry, 6th Edition, pp. 649-677, W. H. Freeman and Company, New York, 1997.

14. A. J. Stone, The Theory of Intermolecular Forces; International Series of Monographs on Chemistry, 32, pp. 1-11, Clarendon Press, Oxford, 1996.

15. M. Rigby, E. B. Smith, W. A. Wakeman, and G. C. Maitland, The Forces Between Molecules, pp. 1-16, Clarendon Press, 1986.

16. I. G. Kaplan, Theory of Molecular Interactions, in "Studies in Physical Chemistry", 42, pp. 1-12, Elsvier, New York, 1986.

17. J. N. Israelachvilli, Intermolecular and Surface Forces, with Applications to Colloidal and Biological Systems, pp. 1-60, Academic Press, New York, 1985.

18. P. Arrighini, Intermolecular Forces and Their Evaluation by Perturbation Theory, in "Lecture Notes in Chemistry", 25, pp. 1-3, Springer-Verlag, Berlin, 1981.

19. G. C. Maitland, M. Rigby, E. B. Smith, and W. A. Wakeman, Intermolecular Forces - Their Origin and Determination, pp. 1-23, Clarendon Press, Oxford, 1981.

20. H. Ratajczak and W. J. Orville-Thomas, in "Molecular Interactions" (H. Ratajczak and W. J. Orville-Thomas, Eds), Vol. 1, pp. 1-16, John Wiley and Sons, 1980.

21. T. Kihara, Intermolecular Forces, pp. 1-6, John Wiley and Sons, Toronto, 1976.

22. G. Yan, M. Yang, and D. Xie, *Chem. Phys. Lett.* **275,** 494 (1997).

23. J. M. Sorenson and J. K. Gregory, *J. Chem. Phys.* **106,** 849 (1997).

24. F.-M. Tao, Z. Li, and Y.-K. Pan, *Chem. Phys. Lett.* **255,** 179 (1996).

25. R. G. A. Bone, *J. Phys. Chem.* **98,** 3126 (1994).

26. R. J. Bemish, P. A. Block, L. G. Pederson, W. Yang, and R. E. Miller, *J. Chem. Phys.* **99,** 8585 (1993).

27. F.-M. Tao and W. Klemperer, *J. Chem. Phys.* **97,** 440 (1992).

28. C. H. Townes and A. L. Schawlow, Microwave Spectroscopy, Chapter 10, pp. 248-283, Dover Publications, Inc., New York, 1975.

29. T. M. Sugden and C. N. Kenney, Microwave Spectroscopy of Gases, Chapter 7, pp. 146-161, D. van Norstrand Company Ltd., London, 1965.

30. J. E. Wollrab, Rotational Spectra and Molecular Structure, Chapter 8, pp. 244-281, Academic Press, 1967.

31. W. Gordy and R. L. Cook, Microwave Molecular Spectra, Techniques of Chemistry, Vol. XVIII, Chapter X, pp. 451-504, John Wiley and Sons, New York, 1984.

32. J. S. Muenter and R. Bhattacharjee, *J. Mol. Spectrosc.* **190,** 290 (1998).

33. M. Iida, Y. Ohshino, and Y. Endo, *J. Chem. Phys.* **97,** 357 (1993).

34. D. A. McQuarrie, Statistical Mechanics, Harper and Row, New York, 1976.

35. *Faraday Discuss. Chem. Soc.* **97,** 1 (1994).

36. *Chem. Rev.* **94,** 1721 (1994).

37. *Faraday Discuss. Chem. Soc.* **73,** 7 (1982).

38. *Chem. Rev.* **88,** 814 (1988).

39. *Chem. Rev.* **86,** 491 (1986).

40. Y. Tanaka and K. Yoshino, *J. Chem. Phys.* **53,** 2012 (1970).

41. J. M. Parson, P. E. Siaska, and Y. T. Lee, *J. Chem. Phys.* **56,** 1511 (1972).

42. J. A. Barker, R. A. Fisher, and R. O. Watts, *Mol. Phys.* **21,** 657 (1971).

43. E. A. Colbourn and A. E. Douglas, *J. Chem. Phys.* **65,** 1741 (1976).

44. R. A. Aziz, *J. Chem. Phys.* **99,** 4518 (1993).

45. G. Scoles, D. Laine, and U. Valbusa (Eds), Atomic and Molecular Beam Methods, Vol. 2, Oxford University Press, 1992.

46. T. J. Balle and W H. Flygare, *Rev. Sci. Instrum.* **52,** 33 (1981).

47. J. Ekkers and W. H. Flygare, *Rev. Sci. Instrum.* **47,** 448 (1976).

48. J. C. McGurk, H. Mäder, R. T. Hofmann, T. G. Schmalz, and W. H. Flygare, *J. Chem. Phys.* **61,** 3759 (1974).

49. J. C. McGurk, R. T. Hofmann, and W. H. Flygare, *J. Chem. Phys.* **60,** 2922 (1974).

50. W. H. Flygare, Molecular Structure and Dynamics, pp. 423-495, Prentice-Hall, Inc., New Jersey, 1978.

51. J. I. Steinfeld, Molecules and Radiation: An Introduction to Modern Molecular Spectroscopy, pp. 326-403, MIT Press, Cambridge, Massachusetts, 1974.

52. J.-U. Grabow, W. Stahl, and H. Dreizler, *Rev. Sci. Instrum.* **67,** 4072 (1996).

53. H. Dreizler, *Ber. Bunsenges. Phys. Chem.* **99,** 1451 (1995).

54. H. Dreizler, *Mol. Phys.* **59,** 1 (1986).

55. A. C. Legon, *Annu. Rev. Phys. Chem.* **34,** 275 (1983).

56. See for example A. C. Legon, D. J. Millen, and S. C. Rogers, *Proc. Roy. Soc.* **A370,** 213 (1980).

57. A. C. Legon and D. J. Millen, *Faraday Discuss. Chem. Soc.* **73,** 71 (1982).

58. J. M. Hutson, *J. Chem. Phys.* **89,** 4550 (1988).

59. J. M. Hutson, *J. Chem. Phys.* **96,** 6752 (1992).

60. R. J. LeRoy and J. M. Hutson, *J. Chem. Phys.* **86,** 837 (1987).

61. R. C. Cohen and R. J. Saykally, *J. Chem. Phys.* **98,** 6007 (1993).

62. C. A. Schumuttenmaer, R. C. Cohen, and R. J. Saykally, *J. Chem. Phys.* **101,** 146 (1994).

63. B. M. Axilrod and E. Teller, *J. Chem. Phys.* **11,** 299 (1943).

64. G. Chałasiński and M. M. Szczęśniak, *Chem. Rev.* **94,** 1723 (1994).

65. W. J. Meath and M. Koulis, *J. Molec. Struct.* **226,** 1 (1991).

66. A. R. Cooper and J. M. Hutson, *J. Chem. Phys.* **98,** 5337 (1993).

67. A. Ernesti and J. M. Hutson, *J. Chem. Phys.* **106,** 6288 (1997).

68. A. Ernesti and J. M. Hutson, *Phys. Rev.* **A51,** 239 (1995).

69. H. O. Leung, *Chem. Commun.* **1996,** 2525 (1996).

70. H. O. Leung, D. Gangwani, and J.-U. Grabow, *J. Mol. Spectrosc.* **184,** 106 (1997)

71. G. Columberg and A. Bauder, *J. Chem. Phys.* **106,** 504 (1997).

72. M. S. Ngarī and W. Jäger, *J. Mol. Spectrosc.* **192,** 452 (1998).

73. M. S. Ngarī and W. Jäger, *J. Mol. Spectrosc.* **192,** 320 (1998).

74. D. W. Eastwood (Ed), Nitrous Oxide, F. A. Davis Company, Philadelphia, 1964.

75. R. M. Julien, Understanding Anesthesia, Addison-Wesley Publishing Company, 1984.

76. E. I. Eger II (Ed), Nitrous Oxide/$N_2O$, Elsevier, Oxford, 1985.

77. L. E. S. Carrie, P. J. Simpson, and M. T. Popat, Understanding Anaesthesia, Butterworth-Heinman, Oxford, 1996.

78. A. R. Aitkenhead and G. Smith (Eds), Textbook of Anaesthesia, Churchill Livingstone, New York, 1996.

79. Commitee on Medical and Biological Effects of Environmental Pollutants, Nitrogen Oxides, Division of Medical Sciences, Assembly of Life Sciences, National Research Council, National Academy of Sciences, Washington, D. C., pp. 20-30, 99-149, 1977.

80. J. E. Rogers and W. B. Whitman (Eds), Microbial Production and Consumption of Greenhouse Gases: Methane, Nitrogen Oxides, and Halomethanes, pp. 219-235, American Society for Microbiology, Washington, D. C., 1991.

81. A. R. Randy (Ed), The Chemistry of the Atmosphere-Oxidants and Oxidation in the Earths Atmosphere, 7th BOC Priestley Conference, The Royal Society of Chemistry, pp. 83-87, Cambridge, 1995.

82. P. J. Crutzen, *Angew. Chem., Int. Ed. Engl.* **35,** 1759 (1996).

83. P. J. Crutzen and M. O. Andrease, *Science* **250,** 1669 (1990).

84. J. G. Calvert (Ed), The Chemistry of the Atmosphere: Its Impact on Global Change, pp. 363-376, Blackwell Scientific Publications, Oxford, 1994.

85. R. F. Weiss, C. D. Keeling, and H. Craig, *J. Geophys. Res.* **86,** 7197 (1981).

86. R. F. Weiss, *J. Geophys. Res.* **86,** 7185 (1981).

87. Most general chemistry textbooks for example, R. Chang, Chemistry, p. 848, McGraw-Hill, Princeton, New Jersey, 1994.

88. C. H. Joyner, T. A. Dixon, F. A. Baiocchi, and W. Klemperer, *J. Chem. Phys.* **75,** 5285 (1981).

89. J. Hodge, G. D. Hayman, T. R. Dyke, and B. J. Howard, *J. Chem. Soc., Faraday Trans.* 2 **82,** 1137 (1986).

90. T. A. Hu, E. L. Chappel, and S. W. Sharpe, *J. Chem. Phys.* **98,** 6162 (1993).

91. H. O. Leung, D. Gangwani, and J.-U. Grabow, *J. Mol. Spectrosc.* **184,** 106 (1997).

# CHAPTER TWO

# EXPERIMENTAL

The instrument used in this laboratory is a pulsed molecular beam cavity FTMW spectrometer which has been described previously (*1*, *2*). The basic design of the instrument is based on the principles of the famous Balle-Flygare instrument (*3*, *4*, *5*, *6*, *7*, *8*, *9*, *10*, *11*) and later modifications (*1*, *2*, *12*, *13*, *14*, *15*, *16*, *17*, *18*, *19*, *20*). The chapter begins by very briefly discussing the theoretical basis of the experiment, as found in the original literature (*4*, *5*, *8*, *10*). Here the important mathematical equations are explained and their implications for the experimental design are pointed out. In the second part of the chapter the spectrometer configuration, including mechanical and electronic components, is described. Finally, the general strategy used for the search for rotational transitions of new molecular systems is explained.

In the experiment the transient emission signal from the molecular ensemble is observed, immediately after a sudden radiation-induced change in the equilibrium condition of the system. This transient emission occurs as the system relaxes back to equilibrium. This emission must be observed in very short periods of time compared to the relaxation times of the systems. The first step is to prepare a sample in an equilibrium condition, secondly, to change this condition in a very short time and thirdly to observe the system as it relaxes.

Using the density matrix method, Flygare *et al.* (*4*, *5*, *8*, *10*) have rederived the Bloch equations, well known in nuclear magnetic resonance (*21*, *22*, *23*), for the

electric dipole-electric field interaction for a two-level system relevant for this type of time domain spectroscopy. These rederived equations are called the "Electric Field Analogs of the Bloch Equations". A summarized derivation of these equations is given in refs. 13 and 16. This derivation is based on an ensemble of non-degenerate two-level quantum systems interacting with an electromagnetic field through the electric dipole moment. The angular transition frequency is $\omega_0$. It is assumed that each molecular dipole interacts with the electric field independently, and that all molecules of the ensemble obey the same Hamiltonian. This means that molecular interactions are ignored.

The density matrix elements contain ensemble averages of products of complex time-dependent coefficients that describe the wavefunction of the two level system in terms of its stationary wavefunctions. The time-dependence of the density matrix is then evaluated using the time-dependent Schrödinger equation. After introduction of the Hamiltonian that describes the interaction of the two-level system with electromagnetic radiation, explicit expressions for the time derivatives of the density matrix elements are obtained. This set of coupled differential equations is then simplified by transformation into a frame that rotates with the frequency of the external radiation, $\omega$, and by neglecting high frequency terms (rotating wave approximation) (*13, 16*). Finally, new, real variables are introduced that can be related to experimental observables and that are linear combinations of the density matrix elements (*13, 16*):

$s=0$ 2.1

$$\dot{u} = -(\Delta\omega)v \qquad 2.2$$

$$\dot{v} = (\Delta\omega)u - \chi w \qquad 2.3$$

$$\dot{w} = \chi v \qquad 2.4$$

with $\Delta\omega = \omega_0 - \omega$, and the Rabi frequency $\chi = (2\mu_{ab}/\hbar)\varepsilon$, where $\mu_{ab}$ is the transition dipole moment and $\varepsilon$ is the amplitude of the electromagnetic wave. s corresponds to the sum of the populations of the two energy levels involved and is constant; w is the population difference. u and v are terms that describe the coherent behaviour of the system and can be related to the macroscopic polarization of the molecular ensemble (*13, 16*). This macroscopic polarization is proportional to the signal observed in a time-domain experiment. Relaxation effects can be introduced phenomenologically in equations 2.1-2.4 (*13, 16*).

The polarization is created by a MW pulse of duration $t_s = t_1 - t_0$ which is short compared to the relaxation times. After introduction of the initial conditions, $u(t_0) = v(t_0) = 0$; $w(t_0) = w_0$ and assuming $\Delta\omega = 0$ and $\chi \neq 0$, analytical solutions can be found for the equations 2.1-2.4:

$$u(t) = 0$$

$$v(t) = -w_0 \sin(\chi t_s)$$

$$w(t) = w_0 \cos(\chi t_s)$$

A maximum polarization can thus be achieved for $\chi t_s = (2n+1) = \pi/2$, with n=0, 1, 2, .... For example, a $\pi/2$-pulse with n=0 and $t_s = t_{\pi/2}$ converts the initial population difference $w_0$ into macroscopic polarization:

$$u(t_{\pi/2}) = 0$$

$v(t_{\pi/2}) = -w_0$

$w(t_{\pi/2}) = 0$

These relationships are summarised in figure 2.1 (*13*).

The theoretical considerations above dictate that the spectrometer meet certain requirements. The four main parts of the spectrometer are shown schematically in figure 2.2. The first element is a phase-coherent, tunable MW radiation source. The second part of the spectrometer is the sample unit including a pulsed nozzle which is the source of van der Waals clusters. The MW cavity, situated in a vacuum chamber, forms the third feature of the instrument. It is inside this Fabry-Perot cavity with two spherical aluminium mirrors within which the MW pulses and the gas pulses interact. The detection and processing of the transient emission signal from the system is conducted through a superheterodyne detection system which forms the fourth feature of the spectrometer. The mechanical parts of the instrument are shown schematically in figure 2.3, and a schematic of the superheterodyne detection system is shown in figure 2.4. The operation of the spectrometer is automated and can be controlled via a PC.

The instrument operations are governed by the ability to achieve the "$\pi/2$-excitation condition". A number of instrumental settings are important and crucial to the success of the experiment. The sequence of events is: first a pulse of molecules is injected parallel to the cavity axis (*24*); second, after an appropriate delay, a pulse of MWs is coupled into the cavity. The MW power and the excitation pulse length are adjusted to achieve a maximum emission signal, i.e. to come as close as possible

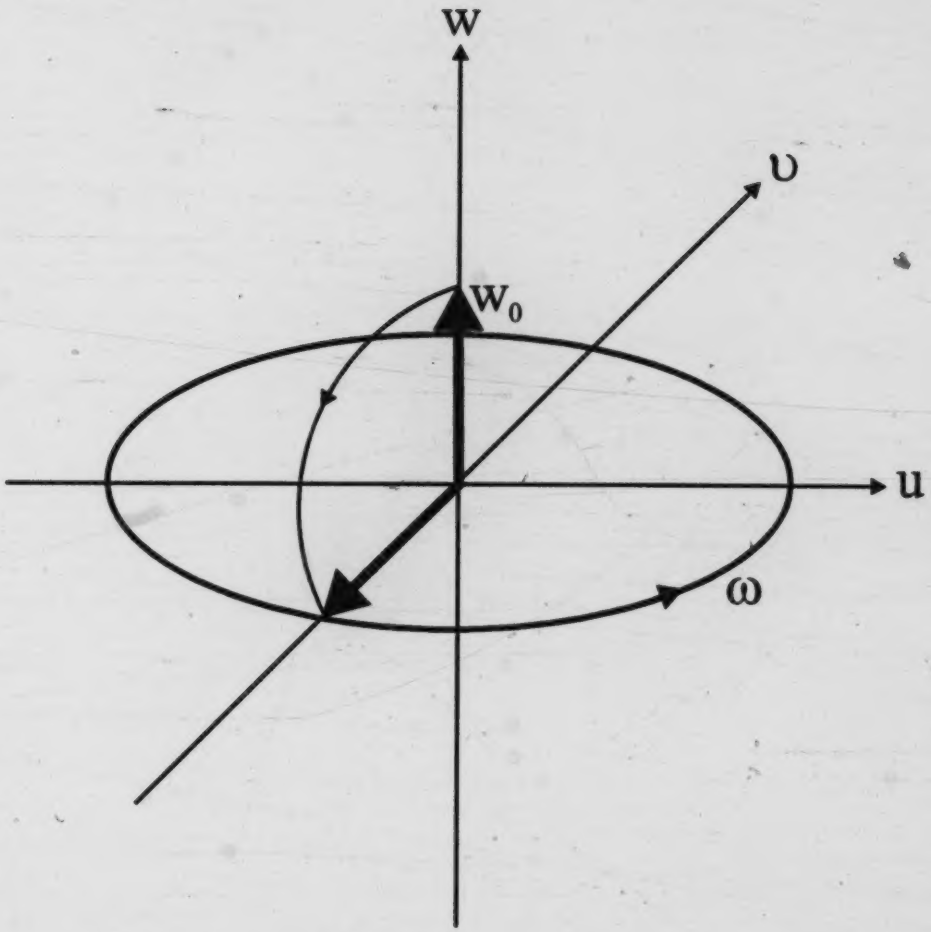


Fig. 2.1. This is a schematic showing the relationship between the polarization and the population difference for the case of resonant polarization, i.e. $\Delta\omega=0$, in the rotating frame. The optimum polarization is obtained for $\chi t_s=\pi/2$, by production of a vector which lies along the $v$ axis. The initial population difference is converted into coherence.

Fig. 2.2. The general set-up of the molecular beam FTMW spectrometer. The diagram indicates the main parts of the instrument. (1) The Hewlett-Packard MW synthesizer, (2) the sample system arrangement, (3) the evacuated chamber that houses the MW cavity where the MWs interact with the pulsed molecular sample, (4) the electronic circuit for the excitation pulse generation and superheterodyne detection of the emission signal. The details of each part are provided in the succeeding figures 2.3 and 2.4.

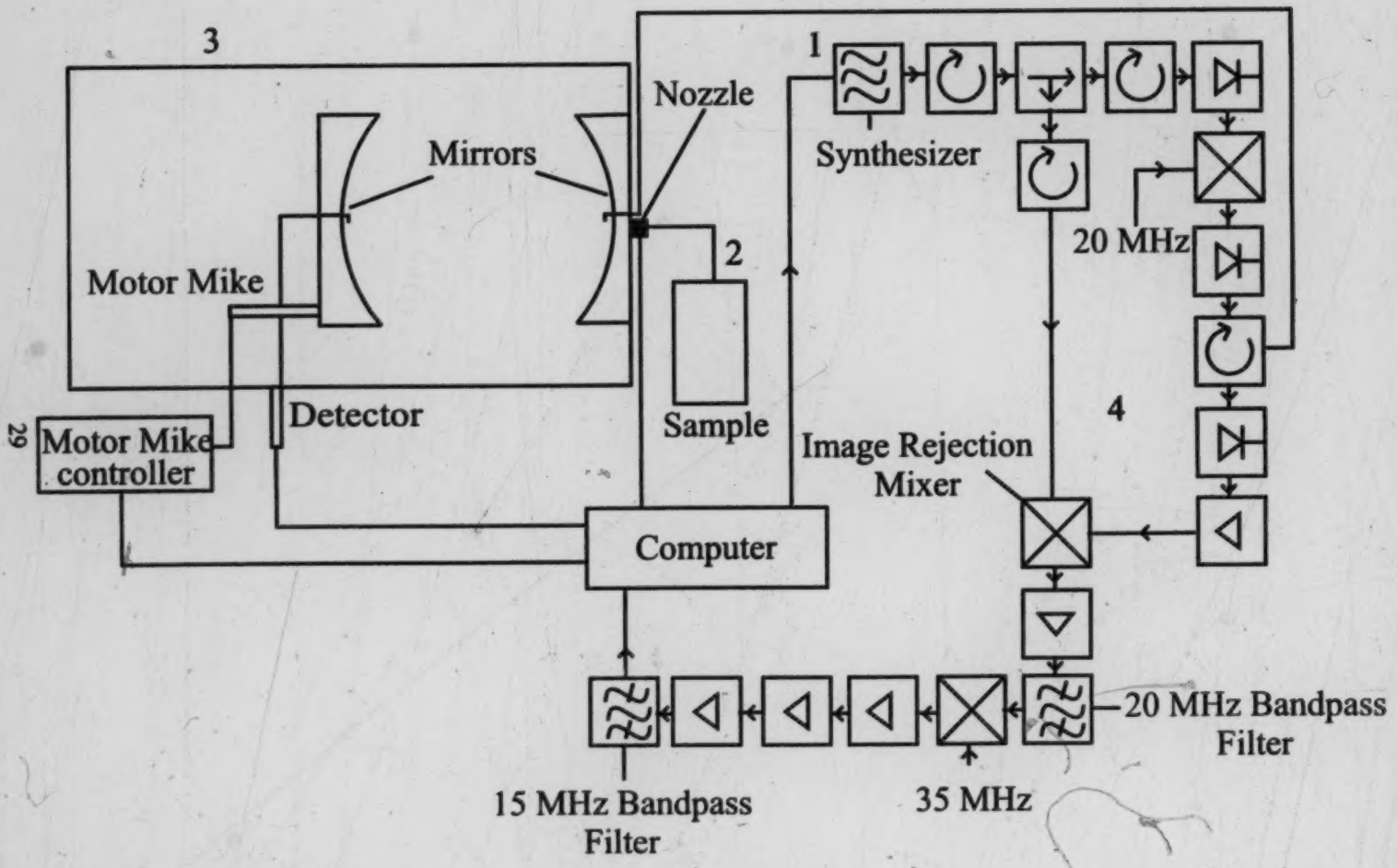
3
1
Nozzle
Mirrors
Synthesizer
20 MHz
2
Motor Mike
Detector
Sample
29
Motor Mike
controller
4
Image Rejection
Mixer
Computer
20 MHz Bandpass
Filter
15 MHz Bandpass
Filter
35 MHz

Fig. 2.3. The mechanical parts of the molecular beam FTMW spectrometer. ⊗ indicates a valve which can be opened or closed. (1) The stainless steel vacuum chamber, (2) and (3) spherical aluminium mirrors, (2) is fixed on the side of the vacuum chamber, while (3) is movable, (4) high precision slide rails on which the movable mirror can slide during movement, (5) the pulsed nozzle source of van der Waals clusters, (6) antenna from where MWs can be coupled in and out of the cavity, (7) antenna through which MWs can be coupled out of the cavity when tuning the cavity into resonance with the MWs, (8) a MW diode detector for detection of the MWs during tuning of the cavity, (9) the Motor Mike which drives the mirror back and forth when tuning the cavity, (10) a 12" diffusion pump for evacuation of the cavity and the sample system, (11) a mechanical pump as fore pump for the diffusion pump, (12) MW detector amplifier, (13) Motor Mike controller, (14) oscilloscope for observation of the analog signal from the MW detector after amplification, (15) personal computer which controls all the operations of the spectrometer, (16) TTL pulse generator for phase coherent control of the spectrometer, (16a) nozzle driver which controls the extent of the nozzle movement in order to determine how much sample is injected into the cavity, (17) a butterfly valve that can be closed or opened and connects the diffusion pump to the chamber, (18) a valve which can be used to vent the chamber, (19) connects the sample to the diffusion pump for evacuation, (20) connects the sample line to the fore pump for evacuation, (21) final exhaust fumes go into the fumehood, (22) flexible vacuum tubing that helps to isolate the instrumentation from the mechanical vibrations of the mechanical pump.

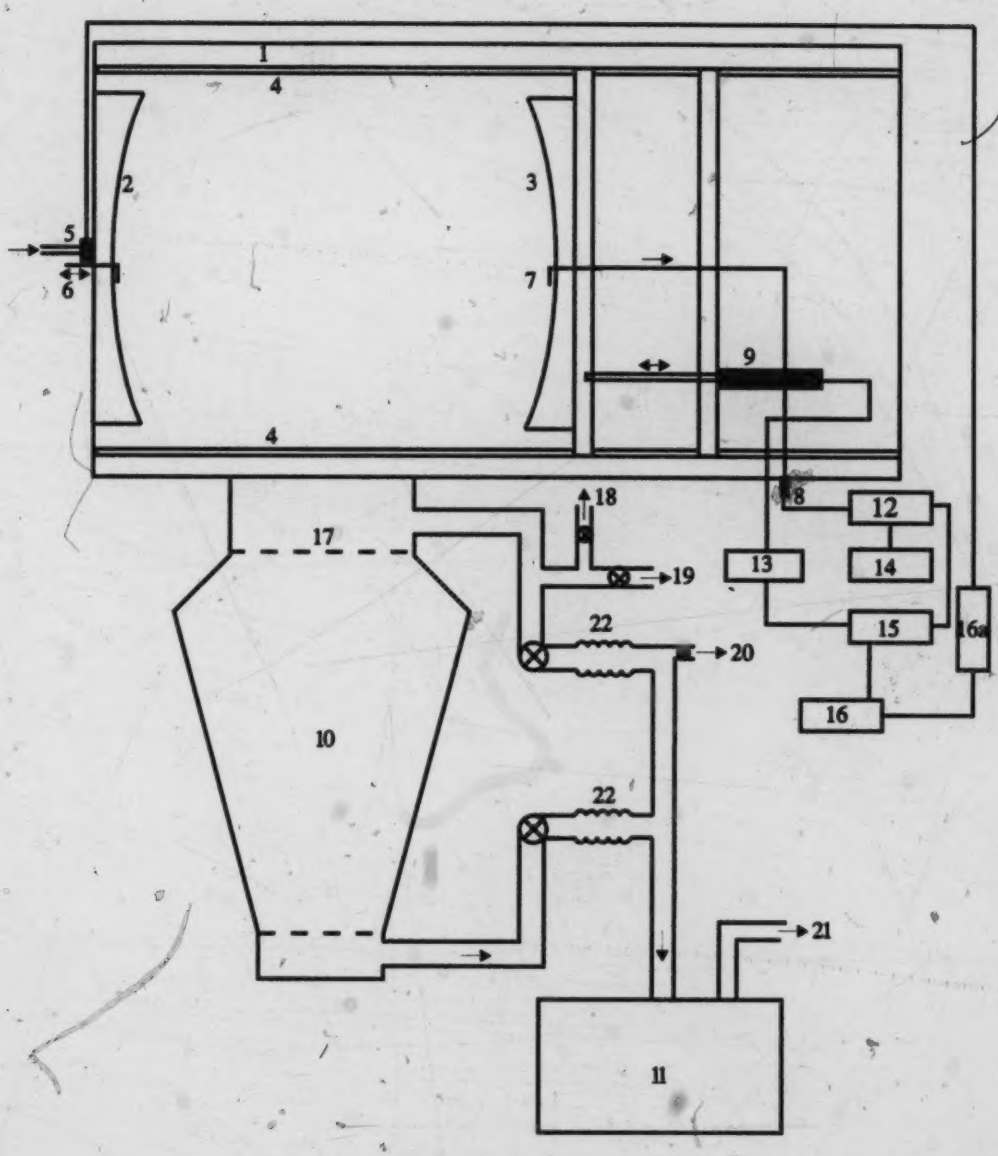
1
4
2
3
5
6
7
9
4
18
8
12
17
13
14
19
22
15
16a
20
16
10
22
21
11

Fig. 2.4. The MW circuit. (1) is the synthesizer (Hewlett-Packard), (2) is a power divider, it divides the MW power from the Synthesizer into two components, one for entry into the chamber as the polarizing radiation and the other for use in the down-conversion of the emission signal for detection, (3) an isolator that makes sure the MW radiation does not reflect back towards the synthesizer, (4) MW *p-i-n* diode switch, (5) a double balanced mixer, (6) MW power amplifier, (7) MW *p-i-n* diode switch; to generate a MW pulse both MW *p-i-n* diode switches 4 and 7 are opened, (8) circulator, allows MWs to move only in the directions chosen, into and out of the cavity in the directions indicated only, (9) MW *p-i-n* diode switch; closed during MW excitation pulse for protection of the detection circuit, (10) a low noise MW amplifier, (11) an image rejection mixer, (12) a radiofrequency (RF) amplifier; after down-conversion of the MW signal, the resultant signal is in the RF region (20 MHz+$\Delta\nu$), (13) 20 MHz bandpass filter, (14) another mixer for the second mixing to frequencies around 15 MHz, (15) 15 MHz bandpass filter, (16) an RF amplifier, (17) a transient recorder with analog-to-digital converter, (18) a PC where the data is analysed, averaged and Fourier transformed to obtain the power spectrum.

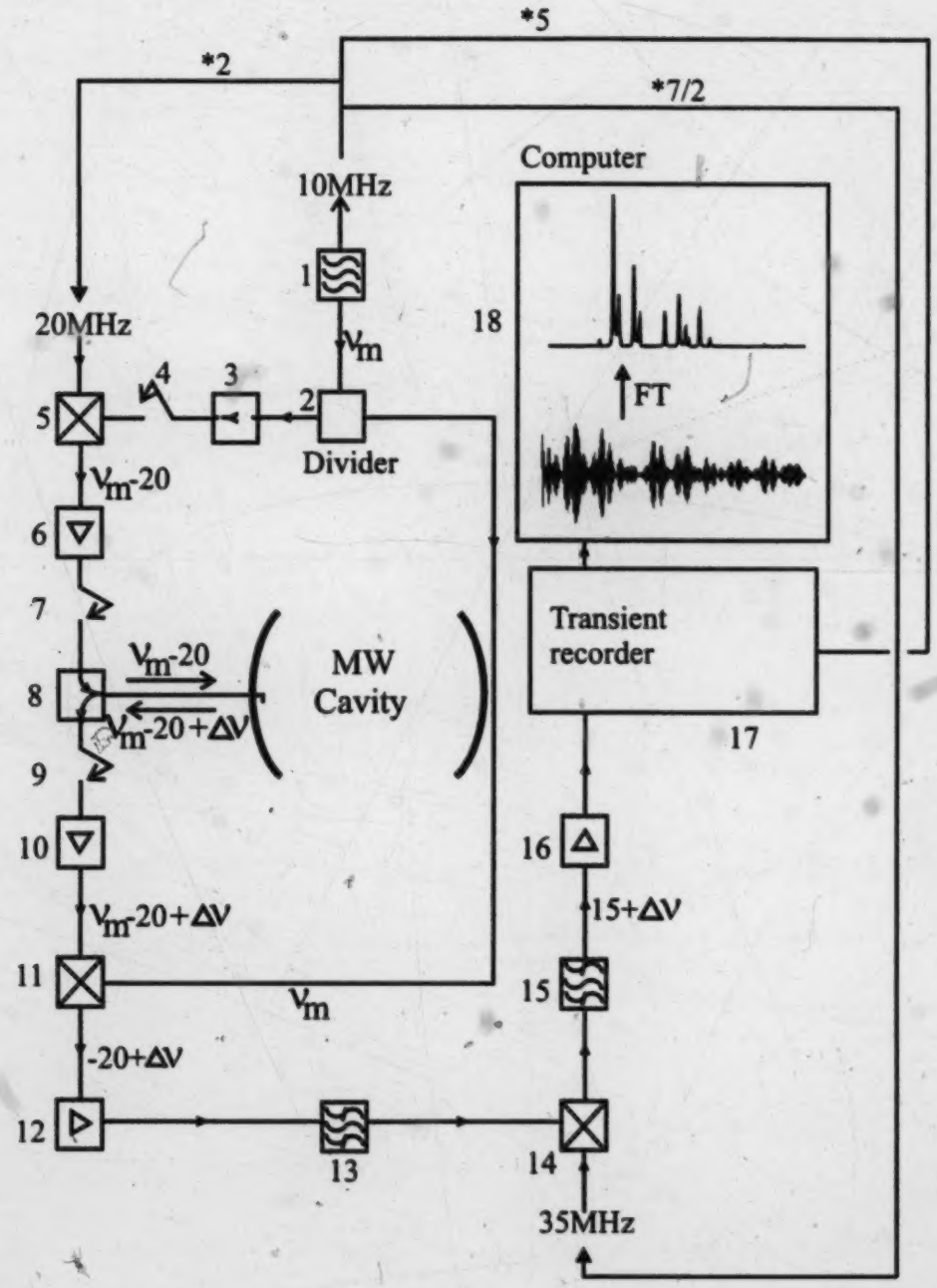
*5
*2
*7/2
Computer
10MHz
1
18
20MHz
$\nu_m$
4
3
2
FT
5
Divider
$\nu_m$-20
6
7
Transient
recorder
$\nu_m$-20
MW
Cavity
8
$\nu_m$-20+ΔV
17
9
10
16
$\nu_m$-20+ΔV
15+ΔV
11
15
$\nu_m$
-20+ΔV
12
13
14
35MHz

to a $\pi/2$-excitation pulse. The molecules will then emit coherently and this transient emission signal (similar to the free induction decay in nuclear magnetic resonance) is coupled out of the cavity and detected via a superheterodyne detection system, analog-to-digital converted, and subsequently Fourier transformed to give the power spectrum from which the transition frequencies are determined. The delay between the end of the MW pulse and the start of the detection phase is required in order to allow the power stored in the cavity to dissipate sufficiently enough so as not to damage the delicate detection circuit. The timing of these events is schematically shown in fig. 2.5. The experiment is fully automated and controlled by an interactive program via a personal computer.

The source of the MW radiation is a Hewlett-Packard synthesized CW generator model HP 83711A which is controlled via an IEEE-bus with a personal computer. It is capable of generating microwaves in the range from 1-20 GHz. The synthesizer contains a 10 MHz crystal that serves as a frequency reference. All events are synchronized with the 10 MHz reference to allow phase coherent averaging of the molecular emission signal.

van der Waals complexes were generated by the pulsed expansion of a sample of a pressurized gas through a nozzle into the evacuated MW cavity. The sample was prepared by mixing a few percent, typically 0.25-1% (for the experiments reported here 0.5% ($N_2O$, CO) and 1% Ar, in Ne were found to be optimum) of the relevant monomer gases in an evacuated sample container system. The sample was then pressurized by addition of a rare gas to boost the pressure to 2-6 atm. In this

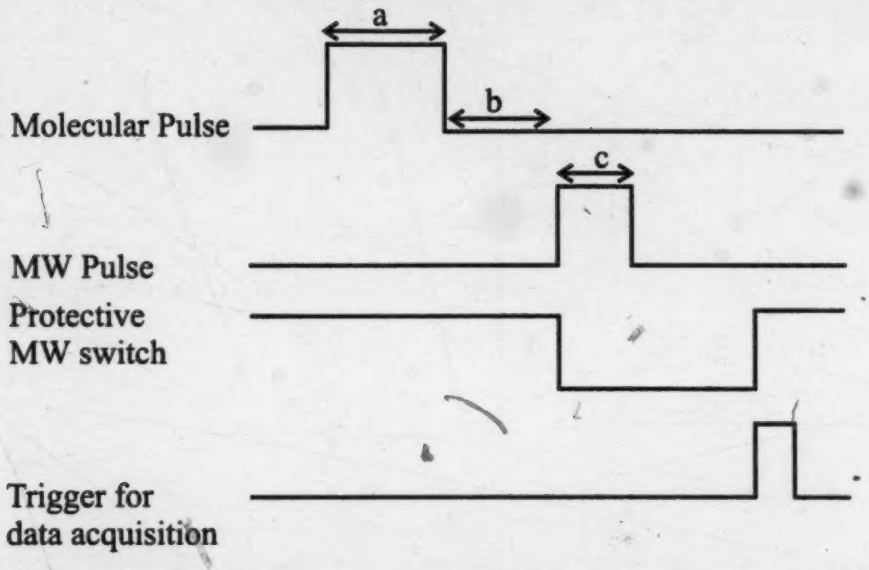


Fig. 2.5. This is a brief schematic representation of the sequence of pulses in a single experiment. At the beginning of one experiment a short pulse (pulse width (a): ~1 msec) of the sample gas mixture is expanded into the evacuated cavity. After a suitable delay (molecular pulse - MW pulse delay (b): ~0.1 msec), a MW pulse (duration (c): order of $\mu$sec), is admitted into the cavity. After some critical delay the detection circuit is opened, and the transient recorder board is triggered to start data collection. This pulse sequence is preceeded by the same sequence without molecular pulse to record the background signal. The molecular signal is obtained by subtracting the signals of the two sequences in the computer. The whole pulse sequence can be repeated for signal averaging. The timing of these events is such that the detection circuit is opened when most of the polarizing radiation has dissipated away, and at the same time most of the emission signal is still strong enough for detection.

laboratory Ne was used as the carrier gas. The pressure used depended on the system under study. Trimers required higher background pressures than dimers. The sample container is then connected through appropriate tubing to the nozzle. The pulsed nozzle employed here was a General Valve Series 9 with an orifice diameter of 0.8 mm. The nozzle was controlled by a pulse generator via a personal computer, thus allowing the amount of sample injected into the cavity to be controlled. The properties of the gas pulse have been discussed in details by Flygare and co-workers (*4*, *5*). The three most important aspects of the molecular expansion are the very low effective translational, rotational and, to some extent, vibrational temperatures of the molecular ensemble (*25*), the high number density of the molecular clusters, and the spatial distribution of the clusters in the pulse. The spatial distribution is important in relation to the lineshapes and resolution of the spectrometer (*4*, *5*, *15*, *26*, *27*).

The MW Fabry-Perot cavity in this instrument consists of two spherical aluminium mirrors with a radius of curvature of 384 mm and a diameter of 280 mm. One of the mirrors is fixed to one end of the vacuum chamber and forms a cover of the vacuum chamber. This mirror contains at its center the pulsed nozzle and a connector for a wire antenna. MWs are coupled in and out of the cavity through this antenna. The other mirror is movable, and can be moved in order to tune the cavity into resonance with the polarizing MW radiation. The cavity has two high precision linear slide rails at the top and at the bottom on which the mirror slides. Below the cavity is a 12" diffusion pump with a pumping speed of 2000 l $s^{-1}$ which is backed by a mechanical vacuum pump (Edwards).

The signals that are emitted by the relaxing molecules are usually very weak. This necessitates the application of a very sensitive detection system. A double superheterodyne detection system is employed. The synthesizer produces radiation of frequency $\nu_m$, which passes through a power divider and is divided into two components of equal power. The component used for polarization passes through an isolator and is mixed with a 20 MHz component, which is obtained by doubling the 10 MHz reference frequency, to produce both the sum and difference of the two frequencies, i.e. $\nu_m$+20 MHz and $\nu_m$-20 MHz. The cavity is tuned into resonance with the sideband at $\nu_m$-20 MHz. The excitation pulse is generated with two *p-i-n* diode switches, amplified, and coupled into the cavity. If the molecules in the molecular pulse have a rotational transition with a frequency near that of the polarizing pulse a macroscopic polarization is induced in the molecular ensemble; as the molecules relax they emit MW radiation with their transition frequencies. This radiation has frequency $\nu_m$-20 MHz+$\Delta\nu$, where $\Delta\nu$ indicates the difference between the polarizing radiation and the molecular transition frequency. The molecular emission signal is amplified and mixed with $\nu_m$ from the synthesizer. The difference, i.e. 20 MHz+$\Delta\nu$, is amplified and passed through a 20 MHz band pass filter. The second step in the detection scheme is mixing down of this signal with a 35 MHz frequency component. This is obtained by multiplication of the 10 MHz frequency reference by 7/2. The difference, 15 MHz+$\Delta\nu$, is passed through a 15 MHz bandpass filter, amplified, sent into a transient recorder board with analog-to-digital

converter and transferred to the computer after which the signal is Fourier transformed to produce the power spectrum from which the transition frequencies are determined.

Generally, the following steps are used in studying a new van der Waals complex. A guess structure is determined from known properties of the monomer units and from properties of similar complexes, such as bond angles and bond distances. This guess structure is input into a program (DHS1CAD) which diagonalises the moment of inertia tensor and provides the three rotational constants, A, B, and C. From the guess structure of the complex and the directions of the inertial axes the types of transitions expected and their relative strengths can be deduced. The type of transitions referred to here are those that result from the components of the dipole moment along the various inertial axes, viz. *a*-type, *b*-type and *c*-type transitions. Armed with this information, the rotational constants and the expected types of transitions are fed into another program (MWDOP4, MWDOP6) to calculate the various transitions and their rigid rotor rotational frequencies. In the case of complexes with a quadrupolar nucleus which is expected to produce resolvable hyperfine structure, another program (Q-FOR) can be used to make a hyperfine pattern prediction for each transition.

The next step in the experiment is the search for the spectrum. The basic consideration is to search first for the strongest transitions. The instrumental settings to use for the search are obtained by consideration of the basic structure of the complex, known dipole moments and projections thereof onto the inertial axes of the

complex, and known settings for other similar complexes. The settings mentioned here are the MW power, MW pulse length and the molecular pulse length. When this has been ascertained and one wants to search for a transition that is predicted at a frequency of say 7000 MHz, the spectrometer will be set at a frequency that is for example 50 MHz below the prediction, i.e. 6950 MHz, and instructed to scan with a step size of, for example, 200 kHz, and to stop at 50 MHz above the prediction, i.e. at 7050 MHz. This would constitute a 100 MHz scan around the prediction. The first step is to tune the cavity into resonance with the initial MW radiation, which is, for the example given above, 6950 MHz. After the program has been started, tuning of MW cavity into resonance with the next higher frequency is done automatically. After a predetermined number of molecular and MW pulses, the accumulated signal amplitude is displayed on a logarithmic scale versus the frequency. The result of such a scan is shown schematically in figure 2.6. To measure the spectrum this frequency region has to be scrutinized more closely with the right instrumental settings, for the detailed measurement of the spectrum. For most of the scan frequency range the signal will be just background noise, so when a resonance emission signal is detected one sees a large signal amplitude against the background noise.

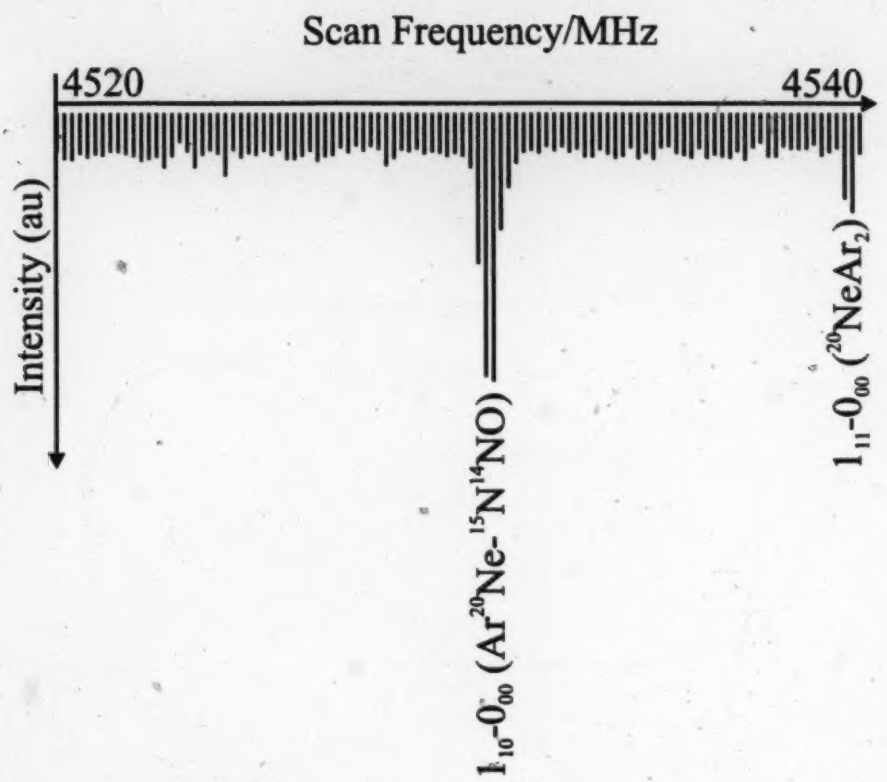


Fig. 2.6. The results from an automatic scan. This scan was performed in the frequency range 4520-4540 MHz, step size: 0.2 MHz, and 20 cycles per step. The regions with large signal amplitudes indicate an emission signal from the gas pulse. These regions have to be scrutinized more closely with the right instrumental settings for the detailed measurement of the spectrum.

## REFERENCES


1. Y. Xu and W. Jäger, *J. Chem. Phys.* **106,** 7968 (1997).

2. V. N. Markov, Y. Xu, and W. Jäger, *Rev. Sci. Instrum.* **69,** 4061 (1998).

3. T. J. Balle and W. H. Flygare, *Rev. Sci. Instrum.* **52,** 33 (1981).

4. E. J. Campbell, L. W. Buxton, T. J. Balle, and W. H. Flygare, *J. Chem. Phys.* **74,** 813 (1981).

5. E. J. Campbell, L. W. Buxton, T. J. Balle, M. R. Keenan, and W. H. Flygare, *J. Chem. Phys.* **74,** 829 (1981).

6. J. Ekkers and W. H. Flygare, *Rev. Sci. Instrum.* **47,** 448 (1976).

7. J. C. McGurk, H. Mäder, R. T. Hofmann, T. G. Schmalz, and W. H. Flygare, *J. Chem. Phys.* **61,** 3759 (1974).

8. J. C. McGurk, T. G. Schmalz, and W. H. Flygare, in "Advances in Chemical Physics" (I. Prigogine and S. A. Rice, Eds), Vol. XXV, pp. 1-68, John Wiley and Sons, New York, 1974.

9. J. I. Steinfeld, Molecules and Radiation, An Introduction to Modern Molecular Spectroscopy, 2nd Edition, pp. 340-355, MIT Press, Cambridge, Massachusetts, 1974.

10. T. G. Schmalz and W. H. Flygare, in "Laser and Coherence Spectroscopy" (J. I. Steinfeld, Ed), pp. 125-196, Plenum Press, New York, 1978.

11. W. H. Flygare, Molecular Structure and Dynamics, pp. 444-495, Prentice-Hall, Inc., Englewood, New Jersey, 1978.

12. A. C. Legon, *Ann. Rev. Phys. Chem.* **34,** 275 (1983).

13. H. Dreizler, *Mol. Phys.* **59,** 1 (1986).

14. F. J. Lovas and R. D. Suenram, *J. Chem. Phys.* **87,** 2010 (1987).

15. A. C. Legon, in "Atomic and Molecular Beam Methods" Vol. 2, (G. Scoles, D. Laine, and U. Valbusa, Eds), pp. 289-308, Oxford University Press, Oxford, 1992.

16. H. Dreizler, *Ber. Bunsenges. Phys. Chem.* **99,** 1451 (1995).

17. J.-U. Grabow, W. Stahl, H. Dreizler, *Rev. Sci. Instrum.* **67,** 4072 (1996).

18. H. O. Leung, D. Gangwani, and J.-U. Grabow, *J. Mol. Spectrosc.* **184,** 106 (1997).

19. H. O. Leung, *J. Chem. Phys.* **107,** 2232 (1997).

20. H. Dreizler, U. Andresen, J.-U. Grabow, and D. H. Sutter, *Z. Naturforsch.* **53a,** 887 (1998).

21. F. Bloch, *Phys. Rev.* **70,** 460 (1946).

22. F. Bloch, *Phys. Rev.* **102,** 104 (1956).

23. R. K. Harris, Nuclear Magnetic Resonance Spectorscopy, A Physicochemical View, pp. 66-94, Pitman, London, 1983.

24. J.-U. Grabow and W. Stahl, *Z. Naturforsch.* **45a,** 1043 (1990).

25. R. E. Smalley, L. Wharton, and D. H. Levy, *Acc. Chem. Res.* **10,** 139 (1977).

26. E. J. Campbell and F. J. Lovas, *Rev. Sci. Instrum.* **64,** 2173 (1993).

27. E. J. Campbell, *Rev. Sci. Instrum.* **64,** 2166-2172 (1993).

# CHAPTER THREE

# STUDY OF THE ROTATIONAL SPECTRUM OF THE Ne-$N_2O$ VAN DER WAALS DIMER[1]

## 3.1 INTRODUCTION

Spectroscopy of van der Waals complexes is well established as an important tool for the study of intermolecular interactions. Binary complexes between rare gas atoms and linear triatomic molecules have attracted considerable interest in the past, One reason is the prototypical nature of these systems. Their structures are defined by only two parameters (assuming that the structure of the linear molecule is unchanged upon complex formation), and their potential energy surfaces show, in addition, usually a fairly large angular anisotropy. The resulting spectra can, for the latter reason, often be interpreted in terms of standard semi-rigid rotor models without using drastic approximations. Examples of such studies are rotational and ro-vibrational spectra of Ar-ClCN (*1*), Ne-,(*2, 3, 4, 5*) Ar-,(*2, 3, 4, 6, 7, 8*) Kr-OCS (*2, 3, 4*), and Ne-, Ar-, Kr-$CO_2$ (*9, 10, 11, 12, 13, 14, 15*) dimers. However, so far only the Ar-variety of the rare gas-$N_2O$ complexes has been studied spectroscopically both in the MW (*16, 17, 18*) and in the infrared ranges (*19, 20*).

We present here the first report on the MW rotational spectrum of the van der Waals complex Ne-$N_2O$. Rotational transitions of six isotopomers of Ne-$N_2O$ were studied. Furthermore, the nuclear quadrupole hyperfine patterns of rotational

---

[1] A version of this chapter has been published. M. S. Ngarí and W. Jäger, *J. Mol. Spectrosc.* **192**, 320 (1998). Copyright © by Academic Press, Inc.

transitions due to the two $^{14}N$ nuclei have been resolved and assigned. Harmonic force field and structural analyses were performed using the experimental rotational and centrifugal distortion constants. The data presented show that the geometry of the complex is T-shaped, similar to that of Ar-$N_2O$ (*16, 17, 18*).

## 3.2 EXPERIMENTAL

Rotational spectra of Ne-$N_2O$ were recorded in the frequency range between 5 and 18 GHz using a pulsed molecular beam cavity FTMW spectrometer of the Balle-Flygare type (*21*). The details of the spectrometer were described before (*22*) and are also discussed in chapter two. In case of weakly dipolar transitions such as the *a*-type transitions of Ne-$N_2O$, a solid state MW power amplifier was used to achieve the $\pi/2$ excitation condition with pulse lengths shorter than 10 $\mu$s. The line frequencies were obtained using a three point interpolation procedure in the frequency domain. In the case of some narrow $^{14}N$ nuclear quadrupole hyperfine splittings, a time domain signal analysis was used to extract the transition frequencies (*23*).

The Ne-$N_2O$ complex was generated by the pulsed expansion of a gas mixture consisting of 0.5% $N_2O$ in Ne at a backing pressure of 3 to 4 atm. The molecular beam ran parallel to the MW propagation direction, resulting in line doubling due to the Doppler effect. The estimated measurement accuracy was about $\pm 1$ kHz, and typical linewidths were $\sim 7$ kHz (full width at half maximum). For the investigation of isotopomers with $^{15}N$, enriched $^{15}N^{14}NO$ (98%) and $^{14}N^{15}NO$ (98%) (Cambridge Isotope Laboratories) were used. The natural abundance of $^{22}Ne$ ($\sim 9\%$) was

sufficient to measure transitions of the species containing this isotope.

## 3.3 RESULTS AND DISCUSSION

### 3.3.1 OBSERVED SPECTRA, ASSIGNMENTS, AND ANALYSES

Initial values for the rotational constants of Ne-$N_2O$ were predicted assuming a T-shaped structure of the complex. The distance between the Ne atom and the central N atom was extrapolated from the corresponding value in Ar-$N_2O$ (*9*) to be 3.2 Å, by comparison with the corresponding distances in the Ne-, Ar-OCS (*4*) and Ne-, Ar-$CO_2$ (*11*) complexes. The Ne-NO angle was taken to be 82°, the same as in Ar-$N_2O$ where Ne is closer to the O atom than to the terminal N atom. In this configuration the $N_2O$ subunit lies approximately parallel to the *b*-principal inertial axis. By projecting the known dipole moment of $N_2O$ (*24*) onto the principal inertial axes of the complex, dipole moment components $\mu_a$=0.02 D and $\mu_b$=0.16 D were obtained. Induction and dispersion contributions to the dipole moment are neglected in this procedure. The rotational constants were used to predict the frequencies of the expected *a*- and *b*-type rotational transitions for the $^{20}$Ne-$^{14}$N$^{14}$NO and $^{22}$Ne-$^{14}$N$^{14}$NO isotopomers. The search for the lines was performed alternately for both isotopomers, with the $^{22}$Ne complex being studied in its natural abundance. The transitions were identified using the observed $^{14}$N nuclear quadrupole hyperfine pattern. The coupling constants used for the prediction of the hyperfine patterns were obtained by projecting the known quadrupole coupling tensor of the $N_2O$ monomer (*24*) onto the principal inertial axes of the complex. A two nuclei program with first

order perturbation treatment of the nuclear quadrupole interaction was used to predict the hyperfine structure of the rotational transitions.

A number of observed lines could be assigned and were used to refine rotational and centrifugal distortion constants. The measurements of further transitions confirmed the assignments. The *a*-type transitions were found to be considerably weaker than the *b*-type transitions. In addition, amplification of the excitation pulses was required in order to optimize the signal-to-noise ratio for *a*-type transitions but was not necessary for *b*-type transitions. These observations are in accord with the dipole moment consideration above.

In total 12 rotational transitions with nuclear quadrupole hyperfine structure were measured for both $^{20}$Ne-$^{14}$N$^{14}$NO and $^{22}$Ne-$^{14}$N$^{14}$NO. A two nuclei program with first order perturbation treatment was used for the evaluation, applying the coupling scheme $\mathbf{I}_1+\mathbf{I}_2=\mathbf{I}$, and $\mathbf{I}+\mathbf{J}=\mathbf{F}$, where $\mathbf{I}_1$ and $\mathbf{I}_2$ are the spin angular momenta of the two $^{14}$N nuclei, $\mathbf{J}$ is the rotational angular momentum of the complex, and $\mathbf{F}$ is the total angular momentum. The frequencies of the nuclear quadrupole hyperfine components were input for the fitting procedure to obtain nuclear quadrupole coupling constants $\chi_{aa}$ and $\chi_{bb}$ for both $^{14}$N nuclei and the hypothetical unsplit center frequencies $\nu_{rot}$ of the rotational transitions. The frequencies of the hyperfine components of the rotational transitions for these two isotopomers are given in Table A1.1 in the appendix, together with their corresponding quantum numbers and the hypothetical unsplit center frequencies. Rotational and centrifugal distortion constants were fitted to the center frequencies $\nu_{rot}$, using Watson's S-reduction, I$^r$-

representation Hamiltonian (25).

The resulting spectroscopic constants, including three rotational constants, four quartic centrifugal distortion constants, i.e. $D_J$, $D_{JK}$, $d_1$, and $d_2$, and two sextic distortion constants, i.e. $H_J$ and $H_{JK}$, as well as the nuclear quadrupole coupling constants $\chi_{aa}(1)$, $\chi_{bb}(1)$, $\chi_{aa}(2)$, and $\chi_{bb}(2)$ are given in Table 3.1 for both $^{20}$Ne-$^{14}$N$^{14}$NO and $^{22}$Ne-$^{14}$N$^{14}$NO. The numbers 1 and 2 in the brackets indicate the terminal and central $^{14}$N nuclei, respectively. The centrifugal distortion constant $D_K$ could not be determined independently from A because only transitions involving energy levels with $K_a=1$ and 0 were measured and because the complex is relatively close to the prolate symmetric top limit with $\kappa$ = -0.848. The value for $D_K$ was obtained from the harmonic force field analysis (see section 3.3.2, Harmonic Force Field) and was held fixed in the rotational fits. An example power spectrum of the $J_{K_aK_c}=1_{11}$-$0_{00}$ transition of the $^{20}$Ne-$^{14}$N$^{14}$NO isotopomer with the hyperfine components is shown in Figure 3.1. This serves to demonstrate the typical signal-to-noise ratio achieved and the usual order of magnitude of hyperfine splittings encountered for this complex.

The rotational constants obtained for these two isotopomers were used to determine an effective structure of the complex, by varying the Ne-N-O angle and the distance between Ne and the central N atom until a best fit was obtained. The refined structure was used to predict rotational constants and then rotational transition frequencies for the next pair of isotopomers, i.e. $^{20}$Ne-$^{15}$N$^{14}$NO and $^{22}$Ne-$^{15}$N$^{14}$NO. A total of 13 rotational transitions were measured and assigned for each of the two

Table 3.1. Derived Spectroscopic Constants for Ne-$N_2O$.

| | $^{20}$Ne-$^{14}$N$^{14}$NO | $^{22}$Ne-$^{14}$N$^{14}$NO | $^{20}$Ne-$^{15}$N$^{14}$NO | $^{22}$Ne-$^{15}$N$^{14}$NO | $^{20}$Ne-$^{14}$N$^{15}$NO | $^{22}$Ne-$^{14}$N$^{15}$NO |
|---|---|---|---|---|---|---|
| **Ground state effective rotational constants /MHz** | | | | | | |
| A | 12913.6654(9) | 12907.9110(1) | 12482.3619(9) | 12476.5969(4) | 12912.4344(1) | 12906.6519(6) |
| B | 3546.6768(1) | 3330.2628(8) | 3521.8251(3) | 3305.4707(2) | 3523.0031(1) | 3306.5130(3) |
| C | 2736.0601(1) | 2605.2740(5) | 2701.0541(8) | 2571.7557(6) | 2721.9255(6) | 2590.6952(9) |
| **Ground state average rotational constants[a] /MHz** | | | | | | |
| $A_z$ | 12729.215 | 12730.571 | 12301.191 | 12302.787 | 12728.734 | 12730.472 |
| $B_z$ | 3471.127 | 3261.912 | 3447.665 | 3238.391 | 3448.303 | 3238.993 |
| $C_z$ | 2726.080 | 2595.614 | 2691.484 | 2562.496 | 2711.986 | 2581.095 |
| **Centrifugal distortion constants /kHz** | | | | | | |
| $D_J$ | 100.47(4) | 91.39(3) | 96.85(2) | 88.18(2) | 99.50(4) | 90.40(1) |
| $D_{JK}$ | 1694.9(7) | 1496.7(8) | 1646.6(1) | 1452.7(9) | 1670.3(5) | 1473.5(2) |
| $D_K$ | -955.2 | -817.1 | -811.7 | -692.5 | -932.1 | -800.1 |
| $d_1$ | -28.049(1) | -23.612(7) | - 28.053(5) | -23.558(7) | -27.580(5) | -23.160(5) |
| $d_2$ | -12.2(5) | -9.1(1) | -12.3(9) | -9.5(8) | -12.0(5) | -8.9(1) |
| $H_J$ | -0.00667(4) | -0.0100(8) | -0.00526(3) | -0.00773(4) | -0.00636(4) | -0.00882(6) |
| $H_{JK}$ | -1.28(1) | -1.04(5) | -1.14(2) | -1.01(3) | -1.23(6) | -1.00(3) |
| **$^{14}$N nuclear quadrupole coupling constants /MHz** | | | | | | |
| $\chi_{aa}(1)$ | 0.3677(2) | 0.3688(7) | | | 0.3635(6) | 0.3649(4) |
| $\chi_{bb}(1)$ | -0.7560(8) | -0.7572(3) | | | -0.7534(3) | -0.7524(3) |
| $\chi_{aa}(2)$ | 0.1186(7) | 0.1132(9) | 0.1248(4) | 0.1251(7) | | |
| $\chi_{bb}(2)$ | -0.2583(1) | -0.2557(8) | -0.2599(4) | -0.2590(9) | | |

Table 3.1. (continued).

| | $^{20}Ne$-$^{14}N^{14}NO$ | $^{22}Ne$-$^{14}N^{14}NO$ | $^{20}Ne$-$^{15}N^{14}NO$ | $^{22}Ne$-$^{15}N^{14}NO$ | $^{20}Ne$-$^{14}N^{15}NO$ | $^{22}Ne$-$^{14}N^{15}NO$ |
|---|---|---|---|---|---|---|
| Inertial defect /amu Å$^2$ | | | | | | |
| $\Delta_o$ | 3.0816 | 3.0769 | 3.1177 | 3.1134 | 3.0795 | 3.0747 |
| $\Delta_i$ [c] | 0.0893 | 0.0736 | 0.1000 | 0.0843 | 0.0876 | 0.0722 |
| Standard deviation /kHz | | | | | | |
| $\sigma$ | 0.5 | 1.0 | 0.9 | 0.3 | 0.6 | 0.6 |

[a] Derived from the force field analysis by subtracting off the harmonic parts of the $\alpha$-constants from the ground state effective values.

[b] Obtained from the force field analysis and held constant in the rotational and centrifugal distortion fit.

[c] Derived from the ground state average rotational constants.

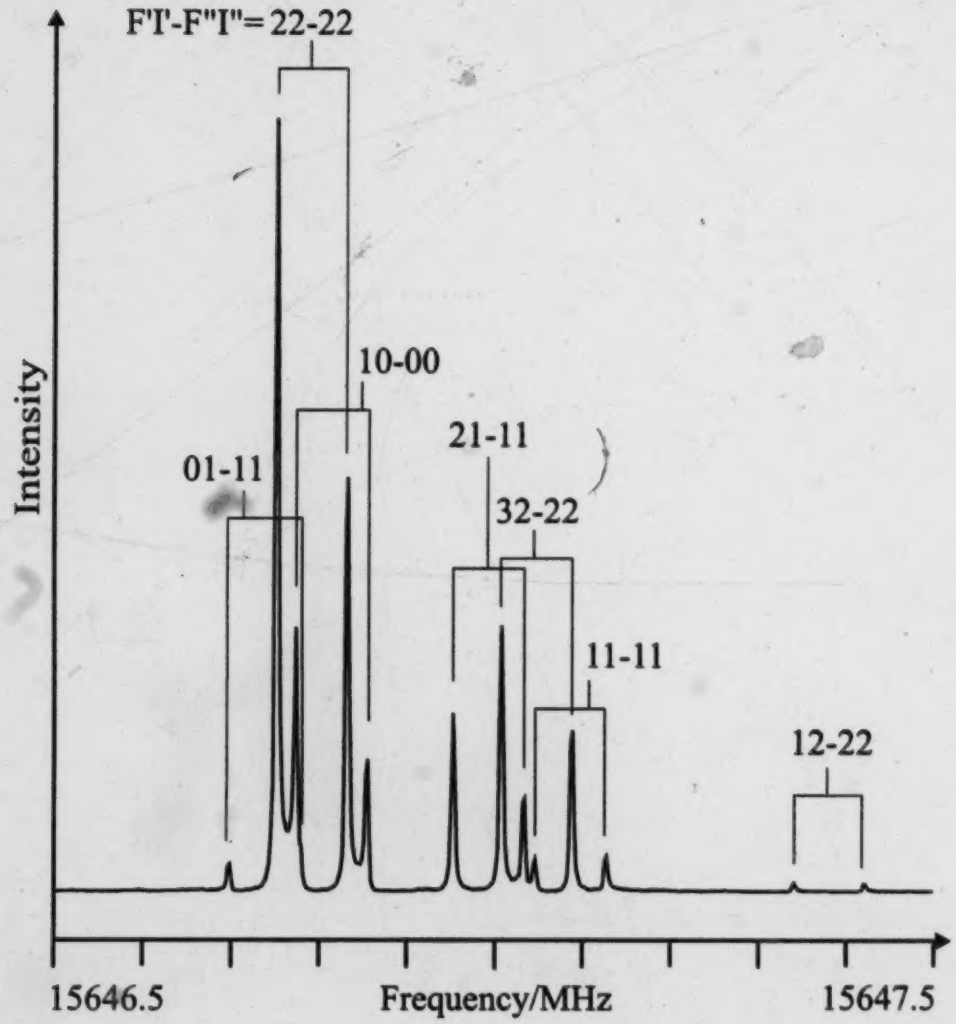


Fig. 3.1. Power spectrum of the $J_{K_aK_c}=1_{11}-0_{00}$ rotational transition of $^{20}Ne$-$^{14}N^{14}NO$ showing the hyperfine components due to the two $^{14}N$ nuclei. Excitation frequency: 15646.6 MHz; sample interval: 60ns; number of points: 4K; 8K FT; number of averaging cycles: 80.

isotopomers. Table A1.2 in the appendix shows the frequencies of the hyperfine components and the resulting hypothetical unsplit rotational transition frequencies of these two isotopomers as well as their quantum number assignments. Assignment and spectroscopic fits followed the procedure outlined above for the first two isotopomers. The nuclear quadrupole coupling constants, rotational constants, and centrifugal distortion constants are given in Table 3.1.

After further refinement of the effective structure of the complex, rotational transitions of complexes with $^{14}N^{15}NO$ were located. In total 13 rotational transitions with hyperfine structure were measured for both $^{20}Ne$-$^{14}N^{15}NO$ and $^{22}Ne$-$^{14}N^{15}NO$. The measured frequencies of the hyperfine components and the hypothetical unsplit center frequencies as well as their quantum number assignments are listed in Table A1.2 (see the appendix section). The derived spectroscopic constants are given in Table 3.1. After locating the spectra of the species containing $^{14}N^{15}NO$ and $^{15}N^{14}NO$ using enriched samples, some low J transitions could be detected in $^{15}N$ natural abundance ($\sim$0.4%) using normal $N_2O$.

A comparison of the nuclear quadrupole hyperfine patterns observed for the $^{20}Ne$-$^{15}N^{14}NO$, $^{20}Ne$-$^{14}N^{15}NO$, and $^{20}Ne$-$^{14}N^{14}NO$ isotopomers is shown in Figure 3.2. The figure shows the power spectra of the rotational transition $J_{K_aK_c}=4_{04}$-$3_{13}$. The narrower splitting in the case of $^{20}Ne$-$^{15}N^{14}NO$ as compared to that of $^{20}Ne$-$^{14}N^{15}NO$ reflects the lower magnitude of the nuclear quadrupole coupling constants of the central $^{14}N$ nucleus as compared to the terminal $^{14}N$ nucleus. A similar effect was previously also observed in the uncomplexed $N_2O$ (*24*). This can be attributed to a

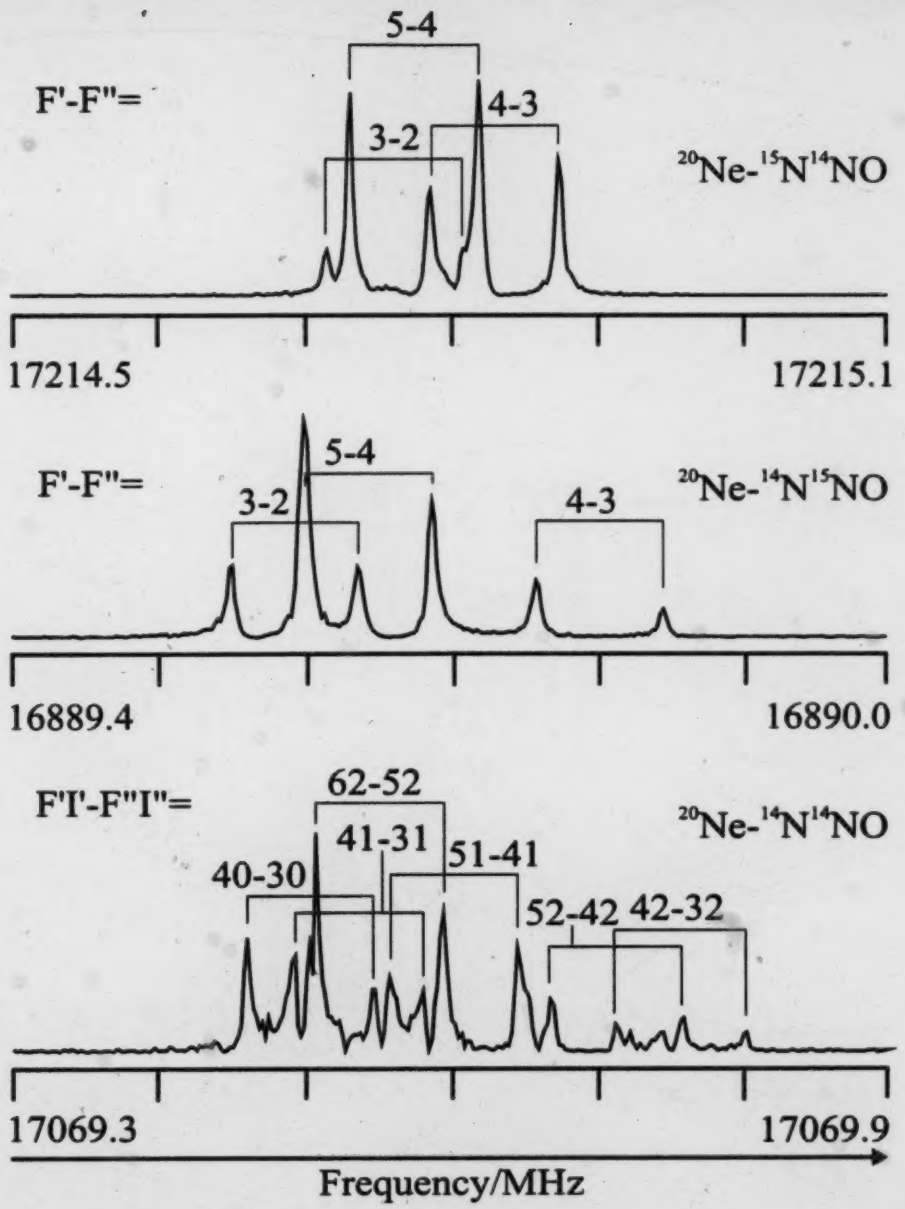


Fig. 3.2. Comparison of the $^{14}$N nuclear quadrupole hyperfine structures of the rotational transition $J_{K_aK_c}=4_{04}$-$3_{13}$ of $^{20}$Ne-$^{15}$N$^{14}$NO, $^{20}$Ne-$^{14}$N$^{15}$NO, and $^{20}$Ne-$^{14}$N$^{14}$NO.

smaller molecular electric field gradient at the site of the central N atom with respect to the end N atom. The bottom spectrum serves to indicate the kind of congested spectra that were observed for species containing normal $N_2O$ with two quadrupolar $^{14}N$ nuclei.

### 3.3.2 HARMONIC FORCE FIELD

The harmonic force field of the complex can be related to the centrifugal distortion constants (*26*). It was possible to carry out a harmonic force field analysis for the Ne-$N_2O$ complex. The force constants of interest are $f_{rr}$, the force constant associated with the van der Waals stretching vibration (defined as the Ne-$N_{central}$ stretch here) and $f_{\theta\theta}$, the force constant associated with the van der Waals bending vibration (defined here as the Ne-$N_{central}$-O angle bend). In this analysis, the force constants for the $N_2O$ monomer (*27*) were assumed to be unchanged by the weak bonding to Ne. The three force constants $f_{NO\ stretch}$, $f_{NN\ stretch}$ and $f_{NNO\ bend}$, and the interaction force constant between two stretching constants $f_{NO\text{-}NN\ interaction}$ were fixed at their corresponding monomer values of 12.0308 mdyn $Å^{-1}$, 18.1904 mdyn $Å^{-1}$, 0.666 mdyn Å $rad^{-2}$, and 1.024 mdyn $rad^{-1}$, respectively. The effective, $r_0$, structure (bottom orientation of Fig. 3.3, see section 3.3.3, Geometry and Structure) was used in the analysis.

The van der Waals force constants were fit to the derived quartic centrifugal distortion constants of all the isotopomers. There were not enough data available to determine the van der Waals interaction force constant and it was constrained to zero

in the fit. An iterative procedure was applied in the force field analysis. This process involved the fitting of rotational and centrifugal distortion constants to the hypothetical center frequencies obtained from the quadrupole fit (see Tables A1.1 and A1.2 in the appendix). Initial quartic centrifugal distortion constants $D_J$, $D_{JK}$, $d_1$ and $d_2$ were obtained from the spectral fits and were used in the initial force field calculation. The distortion constants $D_K$ for the various isotopomers were then predicted from the force field and were constrained to these values in the next spectral fits, which produced new values of the other distortion constants. This procedure was repeated until it converged. It is noted that the four initial quartic centrifugal distortion constants varied only slightly and that the iterative procedure converged quickly in three cycles.

The values obtained for the van der Waals force constants $f_{rr}$ and $f_{\theta\theta}$ are given in Table 3.2, together with the corresponding vibrational frequencies of the normal isotopomer. Also in Table 3.2 are the corresponding values for Ar-$N_2O$ (*16*) for comparison purposes. Ne-$N_2O$ is, as expected, considerably more flexible than the Ar-$N_2O$ complex. Such observation is anticipated since Ne is much smaller in size and is less polarizable than Ar. Similar trends were also observed in the Ne-, (*5*) Ar-OCS (*8*) and Ne-, (*10*) Ar-$CO_2$ (9) pairs.

The quartic centrifugal distortion constants obtained from the rotational fits for the six isotopomers studied are compared with those calculated from the harmonic force field analysis in Table 3.3. One can see that the harmonic force field analysis can predict the quartic centrifugal distortion constants of the complexes reasonably well, despite the severe approximation made in assuming harmonicity of the van der

Table 3.2. Harmonic Force Field of Ne-$N_2O$.

| Parameter | Ne-$N_2O$ | Ar-$N_2O$ [a] |
|---|---|---|
| $f_{rr}$ [b] /mdyn$^{-1}$ | 0.0089(7) | 0.0194(10) |
| $f_{r\theta}$ [c] /mdyn rad$^{-1}$ | 0.0 | 0.0 |
| $f_{\theta\theta}$ /mdyn rad$^{-1}$ | 0.0107(4) | 0.0213(5) |
| $\nu_r$ /cm$^{-1}$ | 33.0 | 39.4(10) |
| $\nu_\theta$ /cm$^{-1}$ | 24.0 | 45.8(8) [d] |

[a] Ref. *16*.

[b] $f_{rr}$ is defined approximately as Ne-N stretch, not as Ne-c.m. of $N_2O$ stretch.

[c] Fixed at 0.0 in the force field analysis.

[d] Hu *et al.* (*20*) have obtained a value of 31.47 cm$^{-1}$ which contrasts with this value.

Table 3.3. Observed and calculated centrifugal distortion constants (kHz).

| Constant | Obs. [a] | Calc. [b] | Obs. [a] | Calc. [b] |
|---|---|---|---|---|
| | $^{20}$Ne-$^{14}$N$^{14}$NO | | $^{22}$Ne-$^{14}$N$^{14}$NO | |
| $D_J$ | 100.47(4) | 100.4716 | 91.39(3) | 91.7692 |
| $D_{JK}$ | 1694.9(7) | 1694.8530 | 1496.7(8) | 1533.1154 |
| $D_K$ | -. | -955.2436 | -. | -817.0988 |
| $d_1$ | -28.049(1) | -26.9829 | -23.612(7) | -22.9194 |
| $d_2$ | -12.2(5) | -10.0925 | -9.1(1) | -8.0481 |
| | $^{20}$Ne-$^{15}$N$^{14}$NO | | $^{22}$Ne-$^{15}$N$^{14}$NO | |
| $D_J$ | 96.85(2) | 97.3595 | 88.18(2) | 88.7506 |
| $D_{JK}$ | 1646.6(1) | 1607.7024 | 1452.7(9) | 1455.4235 |
| $D_K$ | -. | -811.6646 | -. | -692.5351 |
| $d_1$ | -28.053(5) | -26.9130 | -23.558(7) | -22.8293 |
| $d_2$ | -12.3(9) | -10.0928 | -9.5(8) | -8.0650 |
| | $^{20}$Ne-$^{14}$N$^{15}$NO | | $^{22}$Ne-$^{14}$N$^{15}$NO | |
| $D_J$ | 99.50(4) | 99.4631 | 90.40(1) | 90.6533 |
| $D_{JK}$ | 1670.3(5) | 1674.1638 | 1473.5(2) | 1512.9556 |
| $D_K$ | -. | -932.0691 | -. | -800.1110 |
| $d_1$ | -27.580(5) | -26.5070 | -23.160(5) | -22.4871 |
| $d_2$ | -12.0(5) | -9.8392 | -8.9(1) | -7.8476 |

[a] The values are those in Table 3.1.

[b] Calculated from the force constants derived from the centrifugal distortion constants of all measured isotopomers.

Waals vibrational modes. In particular, the procedure predicts the variation in centrifugal distortion constants with isotopomer quite well. This validates the force field analysis and serves as an additional confirmation of the spectral assignment.

The harmonic force field analysis also produced the harmonic contributions to the rotational constants. These were subtracted from the effective rotational constants to obtain the ground state average rotational constants $A_Z$, $B_Z$, and $C_Z$, which are given in Table 3.1. The corresponding inertial defects $\Delta_Z$ calculated from the average rotational constants are given for all isotopomers in Table 3.1. The value of inertial defect for a planar molecule in its ground state is expected to be zero if the molecule was not vibrating. For chemically bound molecules the inertial defect is usually a small positive number, for example 0.0486 amu Å$^2$ for $H_2O$ (*28*). For a planar van der Waals complex, however, this value is larger since the complex undergoes large amplitude motions. The values of the inertial defects $\Delta_0$ of the various isotopomers listed in Table 3.1 are in the order of 3.1 amu Å$^2$. Similar magnitudes have also been observed for other related van der Waals complexes with planar equilibrium geometries, for example 4.4 amu Å$^2$ for Ne-OCS (5), 3.9 amu Å$^2$ for Ne-$CO_2$ (*10*). The values for $\Delta_Z$ are in the order of 0.085 amu Å$^2$. This indicates that the harmonic force field analysis can account for about 97% of the vibrational effects.

## 3.3.3 GEOMETRY AND STRUCTURE

The rotational spectrum of the Ne-$N_2O$ dimer is in accord with a T-shaped complex undergoing large amplitude motions. The variation of the inertial defects

between the six isotopomers is 1.4% at most, indicating that all of the substituted atoms lie in the same plane. Several procedures were used to determine the structural parameters of the Ne-$N_2O$ complex. In the first attempt, the effective rotational constants were used to obtain effective structural parameters. The structure of the $N_2O$ monomer (*29*) was assumed to be unchanged upon weakly binding to Ne in this procedure. Consequently, only two parameters, for example, the distance between the Ne atom and the center of mass of $N_2O$ ($R_{c.m.}$) and the angle $\theta_{c.m.}$ between the $N_2O$ axis and $R_{c.m.}$, need to be determined. $R_{c.m.}$ and $\theta_{c.m.}$ were fitted to the effective moments of inertia $I_a$, $I_b$ and $I_c$ of all the isotopomers given in Table 3.1. The moments of inertia are consistent with two values for $\theta_{c.m.}$. One of them places the Ne atom closer to the O atom ($\theta_{c.m.}$=81.7°) and the other one places Ne closer to the terminal N atom ($\theta_{c.m.}$=98.2°). The values obtained for $R_{c.m.}$ were the same within the error limits for both configurations. Figure 3.3 shows the two possible orientations. The structural parameters of the configuration where the Ne atom is closer to the O atom are given in Table 3.4, assuming that the overall geometry is similar to that found in Ar-$N_2O$.

A similar procedure was carried out using the average rotational constants $A_Z$, $B_Z$, and $C_Z$ of all isotopomers. The structural fit produced again two possible values for $\theta_{c.m.}$ (83.5°, 96.4°). The parameters that correspond to $\theta_{c.m.}$ = 83.5° (Ne closer to O) are given in Table 3.4. There are small variations between the effective and average structural parameters, i.e. $\Delta R_{c.m.} \sim 0.023$ Å, $\Delta\theta_{c.m.} \sim 1.8°$. Such variations are expected since effective structural parameters are affected by the harmonic

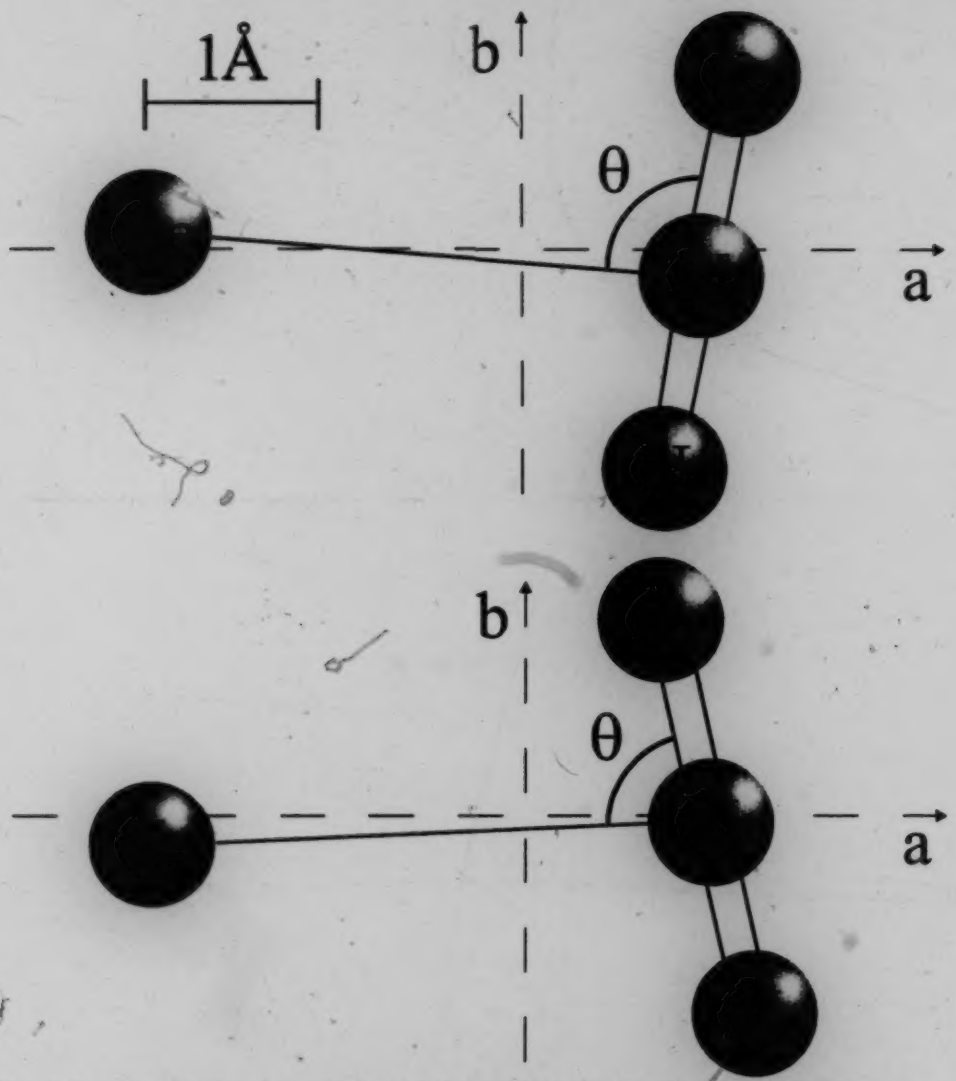


Fig. 3.3. The rotational constants and the quadrupole coupling constants are consistent with these two orientations of the $N_2O$ monomer with respect to the rare gas atom. The $r_s$ structure can however discriminate between these orientations, suggesting that the bottom orientation is, on average, the most likely one, as discussed in the text.

Table 3.4. Structural parameters of Ne-$N_2O$

| | Ne-$N_2O$ | | | Ar-$N_2O$ | | |
|---|---|---|---|---|---|---|
| Parameter | $r_0$ [c] | $r_z$ [d] | $r_s$ [e] | $r_0$ | $r_0$ | $r_0$ |
| $R_{c.m.}$ [a] /Å | 3.225 | 3.249 | -. | 3.470(5) | 3.4666 | 3.47(2) |
| $\theta_{c.m.}$ [a] /(deg) | 81.70 | 84.06 | -. | 81.4(3) | 82.92 | 82.92(1) |
| R(O-RG) [b] /Å | 3.258 | 3.325 | 3.289 | -. | -. | -. |
| $R(N_{terminal}$-RG) [b] /Å | 3.601 | 3.579 | 3.438 | -. | -. | -. |
| $R(N_{central}$-RG) [b] /Å | 3.237 | 3.258 | 3.177 | -. | 3.4766 | 3.48(2) |
| ∠(O-N-RG) [b] /(deg) | 80.39 | 82.76 | 86.18 | 81.70 | -. | -. |
| ∠(N-N-RG) [b] /(deg) | 99.60 | 97.24 | 93.82 | -. | -. | -. |
| Reference | *f* | *f* | *f* | *16* | *19* | *20* |

[a] $R_{c.m.}$ and $\theta_{c.m.}$ are the fitting structural parameters as described in the text. $N_2O$ bondlengths were fixed at r(NN)=1.1278Å and r(NO)=1.1923Å as in Ref. 29.

[b] Calculated from $R_{c.m.}$, $\theta_{c.m.}$, and the $N_2O$ bond lengths as listed above.

[c] Effective structural parameters obtained by fitting to all rotational constants (see text).

[d] Average structural parameters obtained by fitting to the ground state average rotational constants as described in the text.

[e] Substitution structure obtained via Kraitchman's equations (*30*).

[f] This work.

contribution of the vibrations which had been accounted for in the average structural parameters.

Both ground state effective and ground state average rotational constants are consistent with two orientations, as shown in Fig. 3.3. The $^{14}N$ nuclear quadrupole coupling constants (see section 3.3.4, $^{14}N$ Nuclear Quadrupole Hyperfine Structure) cannot discriminate between these two orientations either. The extensive isotopic data available, however, allowed us to determine a partial substitution ($r_s$) structure using Kraitchman's equations (*30*). The oxygen atom coordinates were calculated using the first moment equation since no isotopic substitution was performed for oxygen. The

resulting $r_s$ structural parameters are listed in Table 3.4. Two $r_s$ structure calculations were performed using $^{20}Ne$-$^{14}N^{14}NO$ and $^{22}Ne$-$^{14}N^{14}NO$ as the respective parent molecules. The results of these two calculations were consistent. In particular, the terminal N-atom was found to have a larger *a*-coordinate than the central N-atom. This places the oxygen atom on average closer to Ne than the terminal nitrogen atom. The bottom structure in Fig. 3.3 is thus the preferred one, similar to what was found previously for Ar-$N_2O$ (*16*). From the $r_s$ coordinates the N-N-O angle is calculated to be 176.5°. This slight deviation from linearity is most likely an artefact of the calculation that is caused by the presence of large amplitude motions. The conclusions concerning the overall geometry of the complex are not affected, however, by this deviation from linearity of the $N_2O$ subunit.

### 3.3.4 $^{14}N$ NUCLEAR QUADRUPOLE HYPERFINE STRUCTURE

The observed hyperfine splittings of the rotational transitions are caused by coupling of the spin angular momentum of the $^{14}N$ nuclei with the overall rotational angular momentum of the complex. The underlying mechanism is the interaction of the non-vanishing molecular electric field gradient at the site of the nucleus with the nuclear electric quadrupole moment of $^{14}N$, which arises from the nonspherical distribution of the nuclear charge.

In the past, it has been assumed in many analyses of rotational spectra of van der Waals complexes between a molecular subunit and a rare gas atom that the molecular electric field gradient at the location of a quadrupolar nucleus is unaltered

by the rare gas binding partner. If a linear molecule is involved, the nuclear quadrupole coupling constants $\chi_{gg}$ of the complex are then related to the monomer coupling constant $\chi_{mon}$ by the expression $\chi_{gg} = (½)\chi_{mon} \langle 3 \cos^2 \theta_g - 1 \rangle$. Here, $g$ denotes the $a$, $b$, or $c$ principal inertial axis of the complex, and $\theta_g$ is the angle between the axis of the linear monomer and the $g$ axis. The brackets indicate averaging over the large amplitude bending motion. This expression can be used to derive effective angles $\theta_{g\,(eff)} = \cos^{-1} \sqrt{\langle \cos^2 \theta_g \rangle}$ from the quadrupole coupling constants. The values of $\theta_{b\,(eff)}$ obtained using this relationship for $^{20}$Ne-$^{14}$N$^{14}$NO are 7.3(2)° and 8.5(2)° using the terminal and the central $^{14}$N nucleus, respectively. The numbers in the brackets indicate the uncertainties that result from the uncertainties in the nuclear quadrupole constants.

The difference between the two values of $\theta_{b\,(eff)}$ for terminal and central $^{14}$N nuclei is significantly larger than the uncertainties associated with these values. Such an effect was observed previously by Leung *et al.* (*18*) in the case of the Ar-$N_2O$ complex and was attributed to a perturbation of the electric field gradient at the central $^{14}$N atom by the Ar atom. The planarity of the Ne-$N_2O$ complex makes it possible to directly compare the out-of-plane nuclear quadrupole coupling constants $\chi_{cc}$ with $\chi_{yy}$ of uncomplexed $^{14}N_2O$ since $\chi_{cc}$ (complex) is unaffected by the large amplitude motions. The values for $\chi_{yy}$ are $\chi_{yy}(1) = 386.88(19)$ kHz; $\chi_{yy}(2) = 133.79(27)$ kHz for $^{14}N_2O$ (*24*). For the terminal $^{14}$N nucleus the following values are obtained from the data in Table 3.1 for the various isotopomers of the complex: $^{20}$Ne-$^{14}$N$^{14}$NO, $\chi_{cc}(1) = 388.3(8)$ kHz; $^{22}$Ne-$^{14}$N$^{14}$NO, $\chi_{cc}(1) = 388.4(8)$ kHz;

$^{20}Ne$-$^{14}N^{15}NO$, $\chi_{cc}(1)=389.9(7)$ kHz; $^{22}Ne$-$^{14}N^{15}NO$, $\chi_{cc}(1)=387.5(5)$ kHz. The corresponding values for the central $^{14}N$ nucleus are: $^{20}Ne$-$^{14}N^{14}NO$, $\chi_{cc}(2)=139.7(7)$ kHz; $^{22}Ne$-$^{14}N^{14}NO$, $\chi_{cc}(2)=142.5(12)$ kHz; $^{20}Ne$-$^{15}N^{14}NO$, $\chi_{cc}(2)=135.1(6)$ kHz; $^{22}Ne$-$^{15}N^{14}NO$, $\chi_{cc}(2)=133.9(11)$ kHz. The $\chi_{cc}$ values of the terminal $^{14}N$ nucleus for the various isotopomers all agree within twice their standard deviations; the average (388.5 kHz) agrees also with the corresponding value of free $N_2O$ within twice the standard deviation. In case of the central $^{14}N$ nucleus there is a larger spread, of about 8.5 kHz, between the values of the different isotopomers. The average (137.8 kHz) is larger than the value of uncomplexed $N_2O$ by about 4 kHz (~3%). This deviation is significant and can be attributed to a change of electric field gradient at the central $^{14}N$ nucleus upon complex formation with Ne, whereas the field gradient at the terminal nitrogen atom is virtually unchanged. In the case of Ar-$N_2O$ (*18*) a deviation of 5% was found for the corresponding nuclear quadrupole coupling constant of the central nitrogen atom.

Hutson and co-workers have recently emphasized the importance of using the Eckart axis system as the reference system for interpretation of nuclear quadrupole coupling constants in complexes that undergo large amplitude internal bending motions (*31*, *32*, *33*). The Ne-$N_2O$ complex can be used as a test case for the procedure described in Refs. *31*, *32*, and *33*. Eq. (12) in Ref. *32* was used to calculate the A rotational constant of $^{20}Ne$-$^{14}N^{14}NO$ from the respective nuclear quadrupole coupling constants in Table 3.1 and the $N_2O$ monomer rotational constant. The resulting value is 12951.1 MHz, 0.29% larger than the experimental value (see

Table 3.1). A value of 12833.4 MHz for the A constant is obtained if a different axis system is used, where the nuclear quadrupole coupling constants correspond to projections of the $N_2O$ monomer constants onto the intermolecular vector **R**, the line connecting the Ne atom and the center-of-mass of the $N_2O$ subunit. The deviation here is significantly larger, about 0.99%, supporting the claim that the choice of the Eckart axis system as the reference system is a considerable improvement for the interpretation of nuclear quadrupole coupling constants in van der Waals complexes.

## 3.4 CONCLUSION

We present here the first MW rotational spectrum of the van der Waals dimer Ne-$N_2O$. The FTMW spectrometer was sensitive enough to be able to record the spectra of low J transitions of the species containing $^{14}N^{15}NO$ and $^{15}N^{14}NO$ in natural abundance. Six isotopomers were investigated; their spectra are those of near symmetric prolate rotors. The structural evidence is consistent with a T-shaped geometry of the complex where the Ne atom is on average closer to the oxygen atom than to the terminal nitrogen atom of $N_2O$. The sometimes complex $^{14}N$ nuclear quadrupole hyperfine structures of rotational transitions were observed and assigned. The resulting nuclear quadrupole coupling constants indicate that the molecular electric field gradient at the site of the terminal N nucleus is essentially unchanged from that of free $N_2O$, whereas that at the central N atom deviates slightly.

## REFERENCES


1. M. K. Keenan, D. B. Wozniak, and W. H. Flygare, *J. Chem. Phys.* **75,** 631 (1981).

2. G. D. Hayman, J. Hodge, B. J. Howard, J. S. Muenter, and T. R. Dyke, *Chem. Phys. Lett.* **118,** 12 (1985).

3. G. D. Hayman, J. Hodge, B. J. Howard, J. S. Muenter, and T. R. Dyke, *J. Chem. Phys.* **86,** 1670 (1987).

4. F. J. Lovas and R. D. Suenram, *J. Chem. Phys.* **87,** 2010 (1987).

5. Y. Xu, and M. C. L. Gerry, *J. Mol. Spectrosc.* **169,** 542 (1995).

6. S. J. Harris, K. C. Janda, S. E. Novick, and W. Klemperer, *J. Chem. Phys.* **63,** 881 (1975).

7. J. A. Shea, W. G. Read, and E. J. Campbell, *J. Chem. Phys.* **79,** 2559 (1983).

8. Y. Xu, W. Jäger, and M. C. L. Gerry, *J. Mol. Spectrosc.* **151,** 206 (1992).

9. J. M. Steed, T. A. Dixon, and W. Klemperer, *J. Chem. Phys.* **70,** 4095 (1979).

10. R. W. Randall, M. A. Walsh, and B. J. Howard, *Faraday Discuss.* **85,** 13 (1988).

11. G. T. Fraser, A. S. Pine, and R. D. Suenram, *J. Chem. Phys.* **88,** 6157 (1988).

12. S. W. Sharpe, R. Sheeks, C. Wittig, and R. A. Beaudet, *Chem. Phys. Lett.* **151,** 267 (1991).

13. S. W. Sharpe, D. Reifschneider, C. Wittig, and R. A. Beaudet, *J. Chem. Phys.* **94,** 233 (1991).

14. M. Iida, Y. Ohshima, and Y. Endo, *J. Phys. Chem.* **97,** 357 (1993).

15. H. Mäder, N. Heineking, W. Stahl, W. Jäger, and Y. Xu, *J. Chem. Soc., Faraday Trans.* **92,** 901 (1996).

16. C. H. Joyner, T. A. Dixon, F. A. Baiocchi, and W. Klemperer, *J. Chem. Phys.* 75, 5285 (1981).

17. H. O. Leung, *Chem. Commun.* ***1996,*** 2525 (1996).

18. H. O. Leung, D. Gangwani, and J.-U. Grabow, *J. Mol. Spectrosc.* **184**, 106 (1997).

19. J. Hodge, G. D. Hayman, T. R. Dyke, and B. J. Howard, *J. Chem. Soc.,Faraday Trans. 2,* **82,** 1137 (1986).

20. T. A. Hu, E. L. Chappell, and S. W. Sharpe, *J. Chem. Phys.* **98,** 6162 (1993).

21. T. J. Balle and W. H. Flygare, *Rev. Sci. Instrum.* **52,** 33 (1981).

22. Y. Xu and W. Jäger, *J. Chem. Phys.* **106**, 7968 (1997).

23. J. Haekel and H. Mäder, Z. Naturforsch. **43a**, 203 (1988).

24. J. M. L. J. Reinartz, W. L. Meerts and A. Dymanus, *Chem. Phys.* **31,** 19 (1978).

25. J. K. G. Watson, in "Vibrational Spectra and Structure: A Series of Advances", (J. R. Durig, Ed.), Vol.6, pp. 1-89, Elsevier, New York, 1977.

26. D. Kivelson and E. B. Wilson, Jr., *J. Chem. Phys.* **21,** 1229 (1953).

27. I. Suzuki, *J. Mol. Spectrosc.* **32**, 54 (1969).

28. W. S. Benedict, N. Gailar, and E. K. Plyler, *J. Chem. Phys.* **24**, 1139 (1963).

29. C. C. Costain, *J. Chem. Phys.* **29**, 864 (1958).

30. J. Kraitchman, *Am. J. Phys.* **21**, 17 (1953).

31. A. Ernesti and J. M. Hutson, *Chem. Phys. Lett.* **222**, 257 (1994).

32. A. Ernesti and J. M. Hutson, *J. Chem. Phys.* **101**, 5438 (1994).

33. J. M. Hutson, *Mol. Phys.* **84**, 185 (1995).

# CHAPTER FOUR

## GROUND-STATE AVERAGE AND PARTIAL SUBSTITUTION STRUCTURES OF THE Ar-$N_2O$ VAN DER WAALS DIMER[1]

The rotational spectrum of the Ar-$N_2O$ van der Waals complex was first measured by Joyner *et al.* (*1*) using the molecular beam electric resonance technique. In that work, the Ar-$^{14}N^{14}N^{16}O$ and Ar-$^{15}N^{15}N^{16}O$ isotopomers were studied. The spectra were in accord with a T-shaped geometry of the complex, and the results suggested that the Ar atom is, on average, closer to the O atom than to the terminal N atom of $N_2O$. Hodge *et al.* (*2*), using a pulsed molecular beam diode laser infrared absorption spectrometer, studied the rotationally resolved vibration-rotation spectrum of Ar-$N_2O$ in the region of the asymmetric stretching vibration of $N_2O$. Subsequently, Hu *et al.* (*3*) used an infrared diode laser absorption spectrometer with a pulsed slit expansion to investigate the intermolecular bending vibration in combination with the asymmetric $N_2O$ monomer stretch. The infrared studies confirmed the T-shaped geometry of Ar-$N_2O$ as determined by Joyner *et al.* (*1*). In the molecular beam electric resonance study (*1*) the $^{14}N$ nuclear quadrupole hyperfine structures of transitions of the Ar-$^{14}N^{14}N^{16}O$ isotopomer were not resolved. A MW rotational spectrum of Ar-$^{14}N^{14}N^{16}O$ with resolved hyperfine structure was recorded by Leung and co-workers (*4*, *5*), using an FTMW spectrometer. They were able to determine the $^{14}N$ nuclear quadrupole coupling constants of both central and terminal

---

[1] A version of this chapter has been published. M. S. Ngarí and W. Jäger, *J. Mol. Spectrosc.* **192**, 452 (1998). Copyright © by Academic Press, Inc.

N nuclei in $N_2O$.

This chapter presents the MW spectra of two new isotopomers, namely Ar-$^{15}N^{14}N^{16}O$ and Ar-$^{14}N^{15}N^{16}O$. A harmonic force field analysis was performed using the centrifugal distortion constants from all isotopomers. Ground state effective ($r_0$) and ground state average ($r_z$) structures of Ar-$N_2O$ were determined. Substitution at both N atoms in $N_2O$ made it also possible to determine a partial substitution ($r_s$) structure.

The instrument used was a pulsed molecular beam cavity FTMW spectrometer of the Balle-Flygare type (*6*) the details of which have been described elsewhere (*7*) and in the experimental section, (chapter two of this thesis). The sample was prepared by the pulsed expansion of a mixture of 1% Ar and 0.25% $N_2O$ in Ne at a backing pressure of 3 atm into the MW cavity. Enriched $^{15}N^{14}NO$ and $^{14}N^{15}NO$ (98%, Cambridge Isotope Laboratories) were used for the studies. Typical linewidths were 7 kHz (full width at half maximum), and the measurement accuracy was estimated to be $\pm 1$ kHz.

The structural parameters from the earlier studies (*1, 2, 3, 4, 5*) were used to guide the search for the MW spectra of the two new isotopomers. Transitions were easily found and the spectral assignments were confirmed by the $^{14}N$ nuclear quadrupole hyperfine patterns. Figure 4.1 shows the hyperfine components of the transition $J_{K_aK_c} = 2_{12} - 1_{01}$ of Ar-$^{14}N^{15}NO$, and serves to demonstrate the signal-to-noise ratio and the resolution achieved. A total of 15 rotational transitions with hyperfine components were measured for each isotopomer. Table A2.1 in the appendix

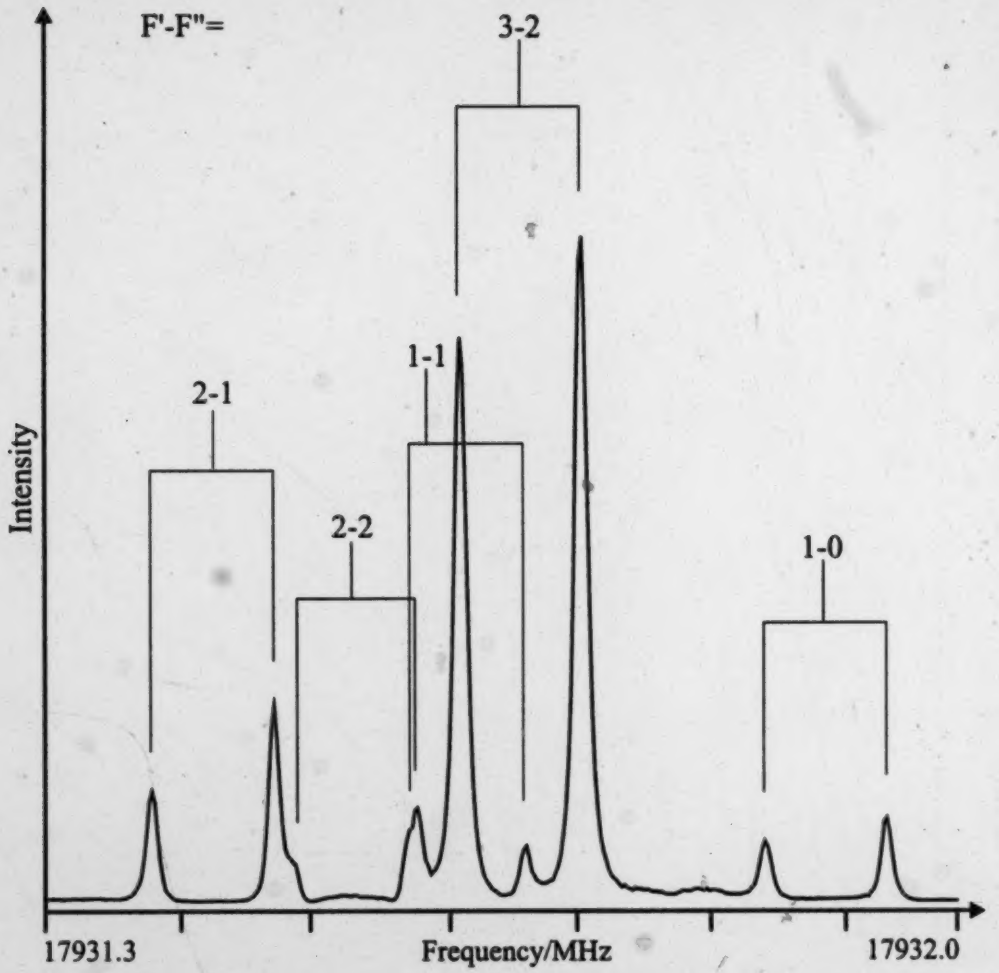


Fig. 4.1. The power spectrum of the rotational transition $J_{K_aK_c}=2_{12}-1_{01}$ of Ar-$^{14}N^{15}NO$ showing hyperfine components due to the terminal $^{14}N$ nucleus. Excitation frequency: 17931.9 MHz; sample interval: 60 ns; number of points: 4K; 8K FT; averaging cycles: 400. The *F* quantum numbers correspond to the total angular momentum **F=J+I**, where **J** is the overall rotational and **I** the $^{14}N$ spin angular momentum.

contains the frequencies and quantum number assignments of all observed transitions. The frequencies of the hyperfine components were input into a global fitting program (*8*) to obtain rotational and centrifugal distortion constants as well as the $^{14}N$ nuclear quadrupole coupling constants simultaneously. The rotational Hamiltonian employed was Watson's S-reduction Hamiltonian in its $I^r$-representation (*9*). The spectroscopic constants obtained are given in Table 4.1. The centrifugal distortion constants $D_K$ and $d_2$ could not be determined and were fixed at the values estimated from the harmonic force field analysis in the fit.

In the harmonic force field analysis, the force constants of the van der Waals bending and stretching vibrational modes were fit to the quartic centrifugal distortion constants of four isotopomers, namely Ar-$^{15}N^{14}N^{16}O$, Ar-$^{14}N^{15}N^{16}O$, Ar-$^{15}N^{15}N^{16}O$ (*1*), and Ar-$^{14}N^{14}N^{16}O$ (*5*). The constants from Joyner *et al.* (*1*) were recomputed by using Watson's S-reduction Hamiltonian in the $I^r$-representation (*9*), for consistency. Values for the centrifugal distortion constants $D_K$ and $d_2$ were determined in the initial force field analysis. These values were then used in the next spectroscopic fit to produce a new set of centrifugal distortion constants. This iterative procedure was repeated until it converged. The interaction force constant $f_{r\theta}$ could not be determined and was fixed at 0.0 in the force field analysis and the force constants of the $N_2O$ monomer (*10*) were assumed to be unchanged. Values for the van der Waals stretching ($f_{rr}$ = 0.020(3) mdyn Å$^{-1}$) and bending force constants ($f_{\theta\theta}$ = 0.023(2) mdyn rad$^{-1}$) as well as for the corresponding vibrational frequencies ($\nu_r$ = 40.1 cm$^{-1}$, $\nu_\theta$ = 33.0 cm$^{-1}$) were obtained. The vibrational frequencies compare favourably with those given by

Table 4.1. Spectroscopic Constants of Ar-$N_2O$

| | Ar-$^{15}N^{14}NO$ | Ar-$^{14}N^{15}NO$ |
|---|---|---|
| **Ground state effective rotational constants /MHz** | | |
| A | 12366.3520(6) | 12791.3829(8) |
| B | 1995.1845(6) | 1996.1192(3) |
| C | 1705.3946(0) | 1714.1140(8) |
| **Ground state average rotational constants /MHz** | | |
| $A_z$ | 12281.582 | 12705.723 |
| $B_z$ | 1975.424 | 1976.339 |
| $C_z$ | 1701.535 | 1710.154 |
| **Centrifugal distortion constants /kHz** | | |
| $D_J$ | 15.52(8) | 15.73(2) |
| $D_{JK}$ | 294.6(8) | 297.9(6) |
| $D_K$[a] | -76.6 | -99.5 |
| $d_1$ | -2.444(7) | -2.364(3) |
| $d_2$[a] | -0.619 | -0.595 |
| **$^{14}N$ nuclear quadrupole coupling constants /MHz** | | |
| $\chi_{aa}$ | | 0.3706(3) |
| $\chi_{bb}(1)-\chi_{cc}(1)$ | | -1.1430(9) |
| $\chi_{aa}(2)$ | 0.1176(9) | |
| $\chi_{bb}(2)-\chi_{cc}(2)$ | -0.3987(3) | |
| **Standard deviation /kHz** | | |
| | 1.5 | 1.3 |

[a] Obtained from the force field analysis and held constant in the global fit.

Hu *et al.* ($\nu_t$ = 38.07 cm$^{-1}$, $\nu_\theta$ = 32.16 cm$^{-1}$) (*3*). The predicted centrifugal distortion constants are in good agreement with the experimental ones for all of the four isotopomers. This serves as an additional confirmation of the spectral assignment. Ground state average rotational constants (Table 4.1) were obtained by subtracting the harmonic contributions calculated in the force field analysis from the effective rotational constants. Comparison of the resulting inertial defects ($\Delta_z$=0.0311 amu Å$^2$ and 0.0262 amu Å$^2$ for Ar-$^{15}N^{14}NO$ and Ar-$^{14}N^{15}NO$, respectively) with those derived

from the effective rotational constants ($\Delta_0$= 2.1747 amu Å$^2$ and 2.1478 amu Å$^2$) indicates that the force field analysis can account for about 98% of the vibrational effects.

Asuming the structure of $N_2O$ (*11*) to be unchanged upon complex formation with Ar, there remain only two structural parameters to be determined for this complex. The parameters chosen are the distance from the center of mass (c.m.) of the $N_2O$ monomer to the Ar atom, $R_{c.m.}$, and the angle Ar - c.m. of $N_2O$ - O, $\theta_{c.m.}$, as shown in figure 4.2. The ground state effective structure ($r_0$), was determined by fitting $R_{c.m.}$ and $\theta_{c.m.}$ to the effective rotational constants of all four isotopomers. The results are given in Table 4.2 together with the parameters from earlier studies for comparison. The average rotational constants obtained from the force field analysis were used to derive the ground state average structural parameters given in Table 4.2.

The substitution coordinates of the two nitrogen atoms were calculated via Kraitchman's equations (*12*). The coordinates of O and Ar were then obtained from the first moment condition and the moment of inertia equations. The resulting structural parameters are given in Table 4.2 under the heading "$r_s$". The $r_s$ coordinates of the two nitrogen atoms determine unambiguously that the oxygen end of the $N_2O$ axis is tilted towards the Ar atom, rather than the nitrogen end.

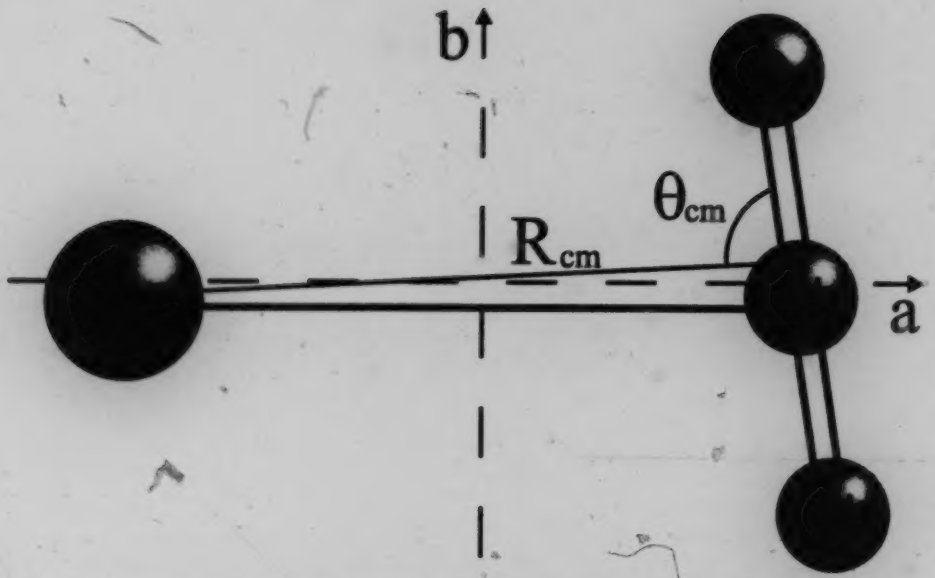


Fig. 4.2. The Ar-$N_2O$ dimer in its principal inertial axis system. The structural fitting parameters $R_{cm}$ and $\theta_{cm}$ are represented as shown in this figure. This figure shows the most likely orientation of the Ar atom with respect to the $N_2O$ axis, as determined by the substitution structure.

Table 4.2. Structural Parameters of the Ar-$N_2O$ van der Waals Complex

| Parameter | $r_0$[c] | $r_z$[d] | $r_s$[e] | $r_0$ | $r_0$ | $r_0$ |
|---|---|---|---|---|---|---|
| $R_{c.m.}$[a]/Å | 3.465 | 3.473 | -. | 3.470 | 3.47 | 3.467 |
| $\theta_{c.m.}$[a]/(deg) | 82.6 | 84.0 | -. | 81.4 | 82.9 | 82.9 |
| R(O-RG)[b]/Å | 3.501 | 3.519 | 3.501 | -. | -. | -. |
| $R(N_{outer}$-RG)[b]/Å | 3.811 | 3.809 | 3.819 | -. | -. | -. |
| $R(N_{inner}$-RG)[b]/Å | 3.475 | 3.483 | 3.499 | -. | 3.48 | 3.477 |
| ∠(O-N-RG)[b]/(deg) | 81.4 | 81.9 | 84.6 | 81.7 | -. | -. |
| Reference | *f* | *f* | *f* | *1* | *2* | *3* |

[a] $R_{c.m.}$ and $\theta_{c.m.}$ are the fitting structural parameters as described in the text. $N_2O$ bond lengths were fixed at R(NN)=1.1278Å, R(NO)=1.1923Å (*11*).

[b] Calculated from $R_{c.m.}$, $\theta_{c.m.}$ and the $N_2O$ bond lengths as listed above.

[c] Effective structural parameters obtained by fitting to all rotational constants as described in the text.

[d] Average structural parameters obtained by fitting to the ground state average rotational constants as described in the text.

[e] Partial substitution structure obtained via Kraitchman's (*12*) equations (see text).

[f] This work.

## REFERENCES


1. C. H. Joyner, T. A. Dixion, F. A. Baiocchi, and W. Klemperer, *J. Chem. Phys.* **75,** 5285 (1981).

2. J. Hodge, G. D. Hayman, T. R. Dyke, and B. J. Howard, *J. Chem. Soc., Faraday trans.* 2, **82,** 1137 (1986).

3. T. A. Hu, E. L. Chappel, and S. W. Sharpe, *J. Chem. Phys.* **98,** 6162 (1993).

4. H. O. Leung, *Chem. Commun.* **1996,** 2525 (1996).

5. H. O. Leung, D. Gangwani, and J.-U. Grabow, *J. Mol. Spectrosc.* **184,** 106 (1997).

6. T. J. Balle and W. H. Flygare, *Rev. Sci. Instrum.* **52,** 33 (1981).

7. Y. Xu and W. Jäger, *J. Chem. Phys.* **106,** 7968 (1997).

8. H. M. Pickett, *J. Mol. Spectrosc.* **148,** 371 (1991).

9. J. K. G. Watson, in "Vibrational Spectra and Structure" ( J. R. Durig, Ed.), Vol. 6, pp. 1-89, Elsevier Scientific, Amsterdam, 1977.

10. I. Suzuki, *J. Mol. Spectrosc.* **32,** 54 (1969).

11. C. C. Costain, *J. Chem. Phys.* **29,** 864 (1958).

12. J. Kraitchman, *Am. J. Phys.* **21,** 17 (1953)

# CHAPTER FIVE

# FTMW ROTATIONAL SPECTRA OF $Ne_2$-$N_2O$ AND $Ar_2$-$N_2O$ VAN DER WAALS TRIMERS[1]

## 5.1 INTRODUCTION

A detailed understanding of the effects of many-body non-additive contributions in intermolecular interactions is of considerable importance for the understanding of macroscopic systems in terms of the microscopic properties of the constituent atoms and molecules. Much work has been done on the exploration of non-additive effects in atomic systems (*1*). For example, the famous Axilrod-Teller triple-dipole dispersion term (*2*) was the first introduced to account for non-additive contributions in atomic systems. However, its apparent success was later attributed to a fortuitous cancellation of higher order corrections (*1*, *3*, *4*). Today, a complete elucidation of many-body interactions remains a subject of much interest and debate, especially in the context of systems that involve molecular subunits where relatively little experimental information is available.

With the rapid developments in high resolution spectroscopic techniques for the investigation of van der Waals complexes, considerable advances have been made in the understanding of intermolecular interactions. Concerted efforts of experimentalists and theoreticians have resulted in the characterization of the potential energy surfaces of several binary systems with almost spectroscopic accuracy (for

---

[1] A version of this chapter has been accepted for publication. M. S. Ngarí and W. Jäger, 1999. *Journal of Chemical Physics*. Copyright © 1999 by American Institute of Physics.

example: $Ar_2$ (*5*, *6*, *7*), Ar-HCl (*8*), Ar-HF (*9*), Ar-$H_2$ (*10*), Ar-$H_2O$ (*11*), and Ar-$NH_3$ (*12*)). This, however, is only a first, though crucial, step towards a complete description of macroscopic systems. It is also of utmost importance to investigate the deviations from pairwise additive descriptions in larger systems, i.e. the various three- and more-body non-additive terms.

In the past few years, significant progress has been made in the understanding of three-body non-additive interactions in molecular systems through experimental and theoretical studies of a few ternary prototype systems. Among these prototype systems are $Ar_2$-HCl (*13*, *14*, *15*, *16*), $Ar_2$-HF (*17*, *18* ,*19*) and $Ar_2$-$CO_2$ (*20*, *21*, *22*). In particular, it was found that the electric multipole moments on the molecular subunits give rise to additional non-additive interactions, that are not present in atomic systems. Specifically, Hutson and co-workers found in the cases of $Ar_2$-HCl *(15*, *23)* and $Ar_2$-HF *(15)* that the interaction of an $Ar_2$ exchange quadrupole moment with the electric dipole moment of the molecular monomer is a significant contributor to the non-additive interaction energy. It is of present interest to provide experimental spectroscopic data for further systems in order to test the broader applicability of the new terms. A substitution of the $Ar_2$ subunit with $Ne_2$, for example, would result in a smaller exchange quadrupole moment and the corresponding non-additive contribution should be reduced. However, there are so far no reports about high resolution infrared or MW spectroscopic studies of any $Ne_2$-molecule complexes.

Ternary van der Waals complexes that contain the $N_2O$ and (rare gas)$_2$ subunits are relatively simple ball-ball-stick prototype systems and their investigations promise

to be rewarding for the further elucidation of non-additive interactions. Of importance in this context is the fact that the corresponding dimer interactions, i.e. $Ar_2$ (5,6,7), $Ne_2$ (*24*, *25*), Ne-$N_2O$ (*26*, *27*), and Ar-$N_2O$ (*28*, *29*, *30*, *31*, *32*, *33*) have been relatively well characterized spectroscopically or by other methods. In addition, the $Ar_2$-$CO_2$ trimer, isoelectronic to $Ar_2$-$N_2O$, has been studied extensively in MW (*20*) and infrared (*21*) ranges and theoretically (22). A comparison with the current systems may lead to the discovery of trends and differences that could be attributed to, for example, the magnitudes of the electric dipole and quadrupole moments of the respective molecular subunits. Of further importance is the presence of two quadrupolar $^{14}N$ nuclei in the molecular $N_2O$ subunit. The resulting nuclear quadrupole coupling constants depend in the most sensitive way upon an average orientation of the $N_2O$ subunit within the principal inertial axes system of the complex, and can provide a delicate measure of the angular anisotropy of the interaction potential energy surface. The extent of perturbation of the electronic structure of $N_2O$ at the site of the central $^{14}N$ nucleus upon complex formation has been the focus of high resolution FTMW studies of several other $N_2O$ containing complexes, such as $H_2O$-$N_2O$ (*34*), HCCH-$N_2O$ (*35*), and $N_2$-$N_2O$ (*36*). In the present study we hoped that the variation in the $^{14}N$ nuclear quadrupole coupling constants with the number of rare gas atoms would provide information about three-body non-additive effects.

This chapter presents the first spectroscopic studies of the van der Waals trimers $Ne_2$-$N_2O$ and $Ar_2$-$N_2O$. Rotational spectra, including $^{14}N$ nuclear quadrupole

hyperfine structure, of several isotopomers were recorded and analysed. The resulting spectroscopic constants were used to derive structural parameters, to determine the extents of the large amplitude bending motions, and to find indications for deviations from pairwise additivity. Harmonic force field analyses were used to estimate the frequencies of the van der Waals vibrational modes.

## 5.2 EXPERIMENTAL

The rotational spectra of the $Ne_2$-$N_2O$ and $Ar_2$-$N_2O$ clusters were measured with a pulsed molecular beam cavity FTMW spectrometer of the Balle-Flygare type (*37*). The details of the instrument have been described elsewhere (*38*, *39*), and in Chapter two. A personal computer based transient recorder with 8 bit resolution was used to digitize the emission signal at sampling intervals of 20, 60, or 120 ns, depending on the required resolution. All transitions were split into doublets due to the Doppler effect because the molecular expansion ran parallel to the axis of the MW cavity. The estimated accuracy of the measurements is $\pm 1$ kHz with linewidths of about 7 kHz (full width at half height). The measurements were done in the frequency range from 3 to 18 GHz.

The sample gas mixtures consisted of 0.5% $N_2O$ in Ne and 0.5% $N_2O$, 1% Ar in Ne, respectively, at backing pressures of 6 atm. Higher backing pressures were found not to improve the signal-to-noise ratio in these systems. Enriched $^{15}N^{14}NO$ (98%) and $^{14}N^{15}NO$ (98%) (Cambridge Isotope Laboratories) were used for the measurements of the spectra involving these isotopomers. For these species, 0.25%

$N_2O$ was used in the gas samples. This was found to be adequate though not optimum.

## 5.3 OBSERVED SPECTRA AND ANALYSES

The initial geometries of the $Ne_2$-$N_2O$ and $Ar_2$-$N_2O$ complexes were derived assuming pairwise additivity, analogous to the procedures used in the studies of $Ar_2$-$CO_2$ (*20*) and $Ar_2$-OCS (*40*). The $Ne_2$-$N_2O$ and $Ar_2$-$N_2O$ complexes thus predicted have distorted tetrahedral geometries (see Figures 5.1 and 5.2). When accurately known, the bond lengths and bond angles were taken from those of the respective dimers, i.e. Ar-$N_2O$ (*32, 33*) and Ne-$N_2O$ (*26, 27*). The Ne-Ne and Ar-Ar bond lengths were estimated from the MW spectra of trimers containing these subunits, for example, $Ne_2$-Ar, $Ar_2$-Ne (*41*), $Ar_2$-OCS (*40*), and $Ar_2$-$CO_2$ (*20*). The structural parameters of the $N_2O$ subunit (*42*) were assumed to be unaffected by the weak interactions with the rare gas atoms. From the resulting structures, rotational constants were estimated for each complex and rotational spectra calculated. With the above assumptions, the structures of the parent isotopomers of both complexes have $C_s$ symmetry.

### 5.3.1 $Ar_2$-$N_2O$

In the case of $Ar_2$-$N_2O$, the $N_2O$ subunit lies in the *bc*-plane, i.e. the plane of symmetry of the complex. Consequently, only *b*- and *c*-type transitions are possible because there is no dipole moment component along the *a* axis. The *c*-type

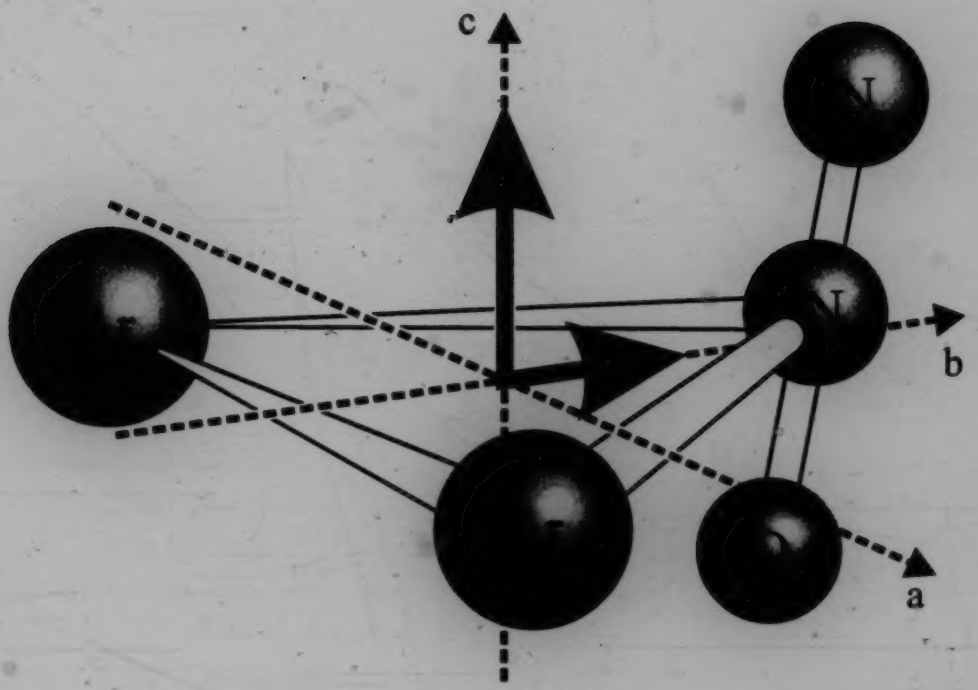


Fig. 5.1. Shown is the equilibrium geometry of the $Ar_2$-$N_2O$ trimer, derived assuming pairwise additivity. Indicated are also the principal inertial axes and the non-vanishing dipole moment components along *b*- and *c*-axes. Note that the $N_2O$ subunit lies in the *bc*-inertial plane.

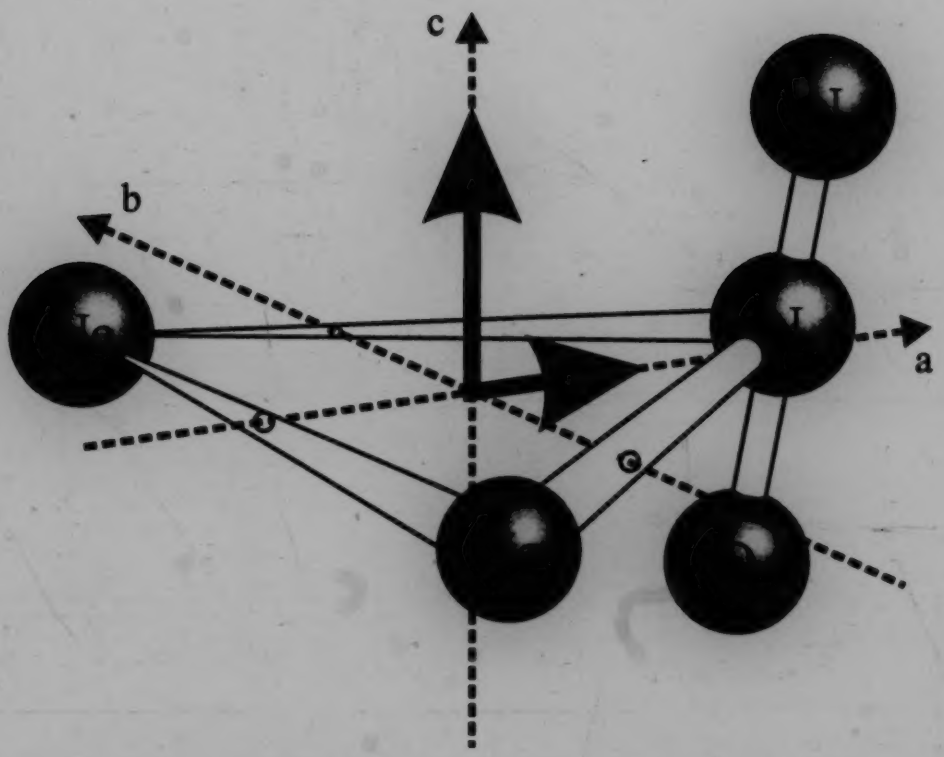


Fig. 5.2. The $Ne_2$-$N_2O$ van der Waals trimer in its principal inertial axis system. The $N_2O$ subunit lies in the *ac*-inertial plane for the isotopomers with $C_s$ symmetry. Note that a non-vanishing *b*-dipole moment component arises for isotopomers that contain the $^{20}Ne^{22}Ne$ subunit.

transitions are expected to be stronger than *b*-types because the *c*-inertial axis runs approximately parallel to the $N_2O$ axis. Since the $N_2O$ subunit contains two quadrupolar nitrogen nuclei (nuclear spin I=1), nuclear quadrupole coupling constants due to both central and terminal $^{14}N$ nuclei were also predicted. This was done by projecting the known coupling tensor of the $N_2O$ monomer (*43*) onto the principal inertial axes of the complex, assuming that the principal nuclear quadrupole coupling constants do not change upon complex formation. The resulting constants were used to predict hyperfine structures of the rotational transitions.

Initial searches were done in the frequency range from 6.3 to 6.5 GHz for the rotational transition $J_{K_aK_c} = 3_{13}$-$2_{02}$ of the normal isotopomer. After some searching a number of transitions with multiplet structures were found and identified by comparing the measured with the predicted hyperfine patterns. More lines were predicted and measured in an iterative procedure. In total, 22 rotational transitions with 261 hyperfine components were measured for the parent isotopomer. All measured transition frequencies of $Ar_2$-$N_2O$ are given in Table A3.1 (see the appendix) together with the quantum number assignments. The analysis was done using Watson's A-reduction Hamiltonian in the $I^r$-representation (*44*). Pickett's global fitting program (*45*) was used in the analysis. The hyperfine structure analysis was performed using the coupling scheme $\mathbf{I}_1+\mathbf{J} = \mathbf{F}_1$, $\mathbf{F}_1+\mathbf{I}_2 = \mathbf{F}_2$, where $\mathbf{I}_1$ and $\mathbf{I}_2$ are nuclear spin angular momentum vectors of terminal and central $^{14}N$ nuclei, respectively, and $\mathbf{J}$ is the overall rotational angular momentum vector of the complex. For the isotopomers with only one $^{14}N$ nucleus the coupling scheme $\mathbf{I}+\mathbf{J} = \mathbf{F}$ was

used. The resulting rotational and centrifugal distortion constants, and the $^{14}N$ nuclear quadrupole coupling constants $\chi_{aa}(1)$, $\chi_{bb}(1)$, $\chi_{cc}(1)$ and $\chi_{aa}(2)$, $\chi_{bb}(2)$, $\chi_{cc}(2)$ for terminal and central nitrogen nuclei, respectively, are given in Table 5.1.

The rotational constants obtained from the above analysis were used to calculate an effective ground state ($r_o$) structure. From this structure, the spectra of the two further isotopomers involving $^{15}N^{14}NO$ and $^{14}N^{15}NO$ were predicted, located, and measured. For the $Ar_2$-$^{15}N^{14}NO$ isotopomer 19 rotational transitions with 95 hyperfine components were measured and for $Ar_2$-$^{14}N^{15}NO$, 17 transitions with 85 hyperfine components were detected (See Table A3.2 for a list of transition frequencies together with the quantum number assignments). The resulting spectroscopic constants are in Table 5.1.

### 5.3.2 $Ne_2$-$N_2O$

The search for the spectrum of $Ne_2$-$N_2O$ followed a similar procedure as described for $Ar_2$-$N_2O$. However, in this complex the *a*- and *b*-inertial axes are interchanged with respect to the $Ar_2$-$N_2O$ inertial axes. As a result, weaker *a*- and stronger *c*-type transitions are predicted to occur for the species with $C_s$ symmetry. The corresponding frequencies of the normal isotopomer were predicted, measured, and assigned to the respective J, K, and F quantum numbers (see Table A3.3 for a list of the observed transition frequencies and their quantum number assignments for this isotopomer). Figure 5.3 shows the rotational transition $J_{K_aK_c} = 3_{22}$-$2_{12}$ of $^{20}Ne_2$-$^{14}N_2O$ with the assigned hyperfine pattern as an example of the sensitivity and the resolution

Table 5.1. Derived Spectroscopic Constants for $Ar_2$-$N_2O$.

| | $Ar_2$-$^{14}N^{14}NO$ | $Ar_2$-$^{15}N^{14}NO$ | $Ar_2$-$^{14}N^{15}NO$ |
|---|---|---|---|
| Ground state effective rotational constants /MHz | | | |
| A | 1832.13862(11) | 1800.19318(17) | 1810.04167(17) |
| B | 1516.16060(13) | 1509.9598(2) | 1516.1484(2) |
| C | 948.74984(9) | 942.47234(13) | 942.75833(19) |
| Ground state Average rotational constants /MHz | | | |
| $A_z$ | 1820.789 | 1789.213 | 1798.872 |
| $B_z$ | 1508.191 | 1502.090 | 1508.178 |
| $C_z$ | 946.420 | 940.172 | 940.458 |
| Centrifugal distortion constants /kHz | | | |
| $\Delta_J$ | 10.693(6) | 10.4780(10) | 10.702(13) |
| $\Delta_{JK}$ | -18.48(3) | -18.02(4) | -18.69(5) |
| $\Delta_K$ | 27.96(2) | 26.88(4) | 27.75(5) |
| $\delta_j$ | 4.193(3) | 4.124(5) | 4.212(5) |
| $\delta_k$ | 1.271(15) | 1.010(19) | 1.17(2) |
| $^{14}N$ nuclear quadrupole coupling constants /MHz | | | |
| $\chi_{aa}(1)$ | 0.3759(6) | | 0.3704(5) |
| $\chi_{bb}(1)$ | 0.3687(9) | | 0.3715(10) |
| $\chi_{cc}(1)$ | -0.7446(9) | | -0.7419(10) |
| $\chi_{aa}(2)$ | 0.1262(9) | 0.1311(5) | |
| $\chi_{bb}(2)$ | 0.1226(16) | 0.1193(10) | |
| $\chi_{cc}(2)$ | -0.2488(16) | -0.2504(10) | |
| Planar moments /amu Å$^2$ | | | |
| $P_a$ | 295.0830 | 295.0940 | 295.0933 |
| Standard deviation /kHz | | | |
| | 1.4 | 1.2 | 1.0 |

achieved with our spectrometer.

It should be noted that the searches and assignments of the rotational transitions were rather complex, mainly because of the uncertainty in the Ne-Ne distance, the large number of transitions accessible, and the presence of several isotopomers, i.e. $^{20}Ne_2$, $^{22}Ne_2$, and $^{20}Ne^{22}Ne$ containing species, simultaneously in the

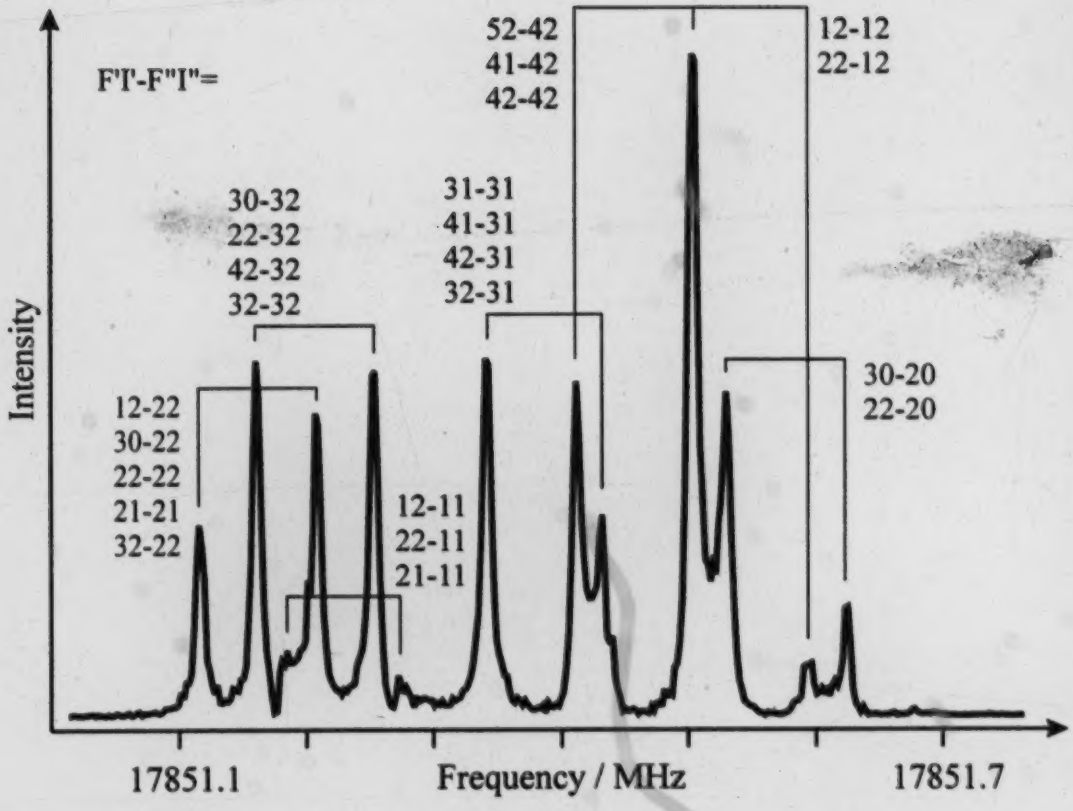


Fig. 5.3. Spectrum of the rotational transition $J_{K_aK_c}=3_{22}-2_{12}$ of $^{20}Ne_2$-$^{14}N_2O$, showing $^{14}N$ nuclear quadrupole hyperfine structure due to both central and terminal $^{14}N$ atoms of the $N_2O$ subunit. The signal was recorded using 1000 averaging cycles at a sampling interval of 60 ns. Excitation frequency: 17851.1 MHz. The spectrum was obtained after an 8K Fourier transformation.

molecular expansion. Isotopomers with $^{20}Ne_2$, $^{22}Ne_2$, and $^{20}Ne^{22}Ne$ subunits have natural abundances of 83%, 0.8%, and 16%, respectively. However, the intensities of the spectra of all these species are of similar order of magnitude which can be attributed to an isotopic enrichment effect. The abundances of the heavier isotopomers with lower zero point energies are significantly increased in the initial phase of the molecular expansion, as a result of repeated dissociation and recombination of the complexes.

In the cases of complexes that contain the $^{20}Ne^{22}Ne$ subunit it was possible to measure *b*-type transitions. The substitution of one Ne atom breaks the $C_s$ symmetry of the complex and leads to a small dipole moment component along the *b*-axis. Two *b*-type transitions could be measured and assigned for each isotopomer involving $^{20}Ne^{22}Ne$. The *b*-type transitions were, as expected, very weak compared to the *a*- and *c*- type transitions. In the isotopomers with $C_s$ symmetry it was not possible to detect *b*-type transitions, despite accurate frequency predictions from the sets of spectroscopic constants. The observation of *b*-type transitions only in the mixed isotopomers serves thus to confirm the assumed $C_s$ equilibrium geometry of $Ne_2$-$N_2O$.

In total, the spectra of nine isotopomers of $Ne_2$-$N_2O$ were studied. We measured and assigned 15 rotational transitions comprising 188 hyperfine components for $^{20}Ne^{20}Ne$-$^{14}N_2O$ (Table A3.3), 19 transitions with 216 hyperfine components for $^{20}Ne^{22}Ne$-$^{14}N_2O$ (Table A3.4), and 14 transitions involving 147 hyperfine components in the spectrum of $^{22}Ne^{22}Ne$-$^{14}N_2O$ (Table A3.3). 14 rotational transitions were assigned for each of the symmetric isotopomers $^{20}Ne^{20}Ne$-, $^{22}Ne^{22}Ne$-$^{15}N^{14}NO$ and

$^{20}Ne^{20}Ne$-, $^{22}Ne^{22}Ne$-$^{14}N^{15}NO$ with 60 hyperfine components for the first three and 56 for the last species (Table A3.5). For the mixed isotopomers that contain $^{20}Ne^{22}Ne$, two extra *b*-type transitions were recorded; thus in total 16 rotational transitions were measured for each (Table A3.6).

The analyses of the spectra were performed as described above for $Ar_2$-$N_2O$. All $Ne_2$-$N_2O$ spectra required the inclusion of the sextic centrifugal distortion constant $\Phi_K$ in order to obtain standard deviations of the fits that are comparable to the measurement uncertainty. The isotopomer $^{20}Ne^{22}Ne$-$^{14}N_2O$ also required the sextic distortion constant $\Phi_3$ to fit all of the 19 rotational transitions, mainly because it was possible to measure two additional transitions that involve energy levels with $K_a=3$ (see Table A3.4). The spectroscopic constants of the isotopomers with $C_s$ symmetry are given in Table 5.2, those of the species that contain the $^{20}Ne^{22}Ne$ subunit are in Table 5.3.

## 5.4 RESULTS AND DISCUSSION

### 5.4.1 STRUCTURAL ANALYSES

The observed spectra of both $Ar_2$-$N_2O$ and $Ne_2$-$N_2O$ are in accord with the initially assumed distorted tetrahedral geometries of these complexes. Three additional parameters are required for their structural descriptions if it is assumed that the structure of the $N_2O$ subunit (*42*) does not change upon complex formation. These could be, for example, the distance from the center-of-mass of the $Ar_2$ ($Ne_2$) moiety to the center-of-mass of $N_2O$ ($R_{c.m.}$), the angle this distance makes with the

Table 5.2. Derived Spectroscopic Constants for $^{20}Ne^{20}Ne$-$N_2O$ and $^{22}Ne^{22}Ne$-$N_2O$.

| | $^{20}Ne^{20}Ne$-$^{14}N^{14}NO$ | $^{22}Ne^{22}Ne$-$^{14}N^{14}NO$ | $^{20}Ne^{20}Ne$-$^{15}N^{14}NO$ | $^{22}Ne^{22}Ne$-$^{15}N^{14}NO$ | $^{20}Ne^{20}Ne$-$^{14}N^{15}NO$ | $^{22}Ne^{22}Ne$-$^{14}N^{15}NO$ |
|---|---|---|---|---|---|---|
| Ground state effective rotational constants /MHz | | | | | | |
| A | 3432.3057(6) | 3214.3408(7) | 3400.4692(9) | 3186.3572(8) | 3432.2309(9) | 3214.2671(9) |
| B | 2521.4621(2) | 2424.2975(2) | 2483.0922(2) | 2386.8489(3) | 2500.8041(3) | 2403.2222(3) |
| C | 1859.0647(2) | 1742.4597(2) | 1847.3827(2) | 1731.1407(2) | 1847.7203(2) | 1731.4559(3) |
| Ground state average rotational constants /MHz | | | | | | |
| $A_z$ | 3386.996 | 3171.941 | 3356.139 | 3144.837 | 3386.971 | 3171.907 |
| $B_z$ | 2491.952 | 2396.148 | 2454.582 | 2359.659 | 2471.634 | 2375.412 |
| $C_z$ | 1846.805 | 1731.530 | 1835.313 | 1720.381 | 1835.620 | 1720.676 |
| Centrifugal distortion constants /kHz | | | | | | |
| $\Delta_J$ | 63.442(9) | 56.915(11) | 61.041(13) | 54.645(13) | 62.566(13) | 56.120(15) |
| $\Delta_{JK}$ | -85.68(4) | -75.93(5) | -79.93(7) | -70.63(7) | -85.96(7) | -76.21(7) |
| $\Delta_K$ | 402.4(4) | 354.3(5) | 387.0(7) | 338.6(6) | 404.4(7) | 356.4(6) |
| $\delta_J$ | 18.987(6) | 17.223(7) | 18.081(8) | 16.448(8) | 18.804(8) | 17.049(9) |
| $\delta_K$ | -39.64(5) | -30.10(5) | -41.98(6) | -31.82(6) | -38.12(6) | -28.70(7) |
| $\Phi_K$ | -2.86(8) | -2.13(8) | -2.50(12) | -2.39(10) | -2.68(12) | -1.95(11) |
| $^{14}N$ nuclear quadrupole coupling constants /MHz | | | | | | |
| $\chi_{aa}(1)$ | 0.3670(6) | 0.3652(8) | | | 0.3671(7) | 0.3690(7) |
| $\chi_{bb}(1)$ | 0.3720(13) | 0.3723(15) | | | 0.3672(13) | 0.3649(15) |
| $\chi_{cc}(1)$ | -0.7390(12) | -0.7375(15) | | | -0.7343(13) | -0.7339(15) |
| $\chi_{aa}(2)$ | 0.1209(11) | 0.1299(16) | 0.1205(7) | 0.1221(7) | | |
| $\chi_{bb}(2)$ | 0.1266(21) | 0.1191(27) | 0.1314(14) | 0.1276(13) | | |
| $\chi_{cc}(2)$ | -0.2475(21) | -0.2491(27) | -0.2519(14) | -0.2497(13) | | |
| Planar moments /amu Å$^2$ | | | | | | |
| $P_b$ | 109.3284 | 119.4000 | 109.3286 | 119.4032 | 109.3367 | 119.4093 |
| Standard deviation /kHz | | | | | | |
| $\sigma$ | 1.7 | 1.7 | 1.6 | 1.0 | 1.5 | 1.2 |

Table 5.3. Derived Spectroscopic Constants for $^{20}Ne^{22}Ne$-$N_2O$.

| | $^{20}Ne^{22}Ne$-$^{14}N^{14}NO$ | $^{20}Ne^{22}Ne$-$^{15}N^{14}NO$ | $^{20}Ne^{22}Ne$-$^{14}N^{15}NO$ |
|---|---|---|---|
| Ground state effective rotational constants /MHz | | | |
| A | 3330.5903(3) | 3300.4477(6) | 3330.3873(6) |
| B | 2466.2058(3) | 2428.5094(2) | 2445.4524(2) |
| C | 1799.0096(3) | 1787.4987(2) | 1787.8247(2) |
| Ground state average rotational constants /MHz | | | |
| $A_z$ | 3286.680 | 3257.468 | 3286.527 |
| $B_z$ | 2437.456 | 2400.739 | 2417.042 |
| $C_z$ | 1787.440 | 1776.109 | 1776.405 |
| Centrifugal distortion constants /kHz | | | |
| $\Delta_J$ | 59.060(8) | 56.799(12) | 58.252(12) |
| $\Delta_{JK}$ | -67.51(3) | -62.99(6) | -68.34(6) |
| $\Delta_K$ | 371.35(10) | 346.5(6) | 365.6(6) |
| $\delta_J$ | 17.62(5) | 16.767(7) | 17.426(8) |
| $\delta_K$ | -27.81(15) | -32.73(6) | -29.39(6) |
| $\Phi_K$ | -0.292(7) | -2.40(11) | -1.85(12) |
| $\Phi_J$ | 0.424(18) | -.- | -.- |
| $^{14}N$ nuclear quadrupole coupling constants /MHz | | | |
| $\chi_{aa}(1)$ | 0.3641(7) | | 0.3664(7) |
| $\chi_{bb}(1)$ | 0.3726(13) | | 0.3677(13) |
| $\chi_{cc}(1)$ | -0.7367(13) | | -0.7341(13) |
| $\chi_{aa}(2)$ | 0.1353(12) | 0.1222(6) | |
| $\chi_{bb}(2)$ | 0.1133(22) | 0.1288(13) | |
| $\chi_{cc}(2)$ | -0.2486(22) | -0.2510(13) | |
| Standard deviation /kHz | | | |
| $\sigma$ | 1.4 | 1.2 | 1.5 |

$N_2O$ axis [$\theta_{c.m.} = \angle$(rare gas)$_{2\ c.m.}$-$N_2O_{c.m.}$-O)], and the Ar-Ar (Ne-Ne) distance ($R_{Ar\text{-}Ar}$, $R_{Ne\text{-}Ne}$).

Ground state effective, $r_o$, structural parameters were obtained by fitting to the rotational constants of all isotopomers. The resulting values for $R_{c.m.}$, $\theta_{c.m.}$, and $R_{Rg\text{-}Rg}$ (Rg=Ne or Ar) are given in Tables 5.4 and 5.5 for $Ar_2$-$N_2O$ and $Ne_2$-$N_2O$, respectively. In these fits the structure of $N_2O$ was assumed to be unchanged upon

Table 5.4. The structural parameters of $Ar_2$-$N_2O$, Ar-$N_2O$, $Ar_2$-$CO_2$, Ar-$CO_2$, and $Ar_2$.

| Parameter | $Ar_2$-$N_2O$ | | Ar-$N_2O$ | | $Ar_2$-$CO_2$ | Ar-$CO_2$ | $Ar_2$ |
|---|---|---|---|---|---|---|---|
| | $r_o$ | $r_z$ | $r_o$ | $r_z$ | | | |
| $R_{c.m.}$[a]/Å | 2.8795 | 2.8905 | 3.465 | 3.473 | 2.9355 | -. | -. |
| $\theta_{c.m.}$[a]/(deg) | 78.87 | 82.66 | 82.6 | 84.0 | -. | -. | -. |
| R(Ar-Ar)[a]/Å | 3.8419 | 3.8466 | -. | -. | 3.8431 | -. | 3.822 |
| R(Ar-$N_{inner}$)[b]/Å | 3.4742 | 3.4806 | 3.475 | 3.483 | 3.5085 | 3.5048 | -. |
| ∠ Ar$N_{inner}$O)[b]/(deg) | 79.55 | 82.68 | 81.4 | 81.9 | -. | -. | -. |
| ∠ Ar$N_{inner}$Ar)[b]/(deg) | 67.13 | 67.09 | -. | -. | -. | -. | -. |
| Reference | this work | this work | 33 | 33 | 20 | 47 | 6 |

[a] $R_{c.m.}$, $\theta_{c.m.}$, and R(Ar-Ar) are the $r_o$ structural parameters obtained from a fitting procedure as described in the text. $N_2O$ bond lengths were fixed at R(N-N)=1.1278Å, R(N-O)=1.1923Å, and R($N_{inner}$-c.m. of $N_2O$)=0.0745Å (from Ref.42).

[b] Calculated from $R_{c.m.}$, $\theta_{c.m.}$, R(Ar-Ar), and the $N_2O$ bond lengths listed above. $N_{inner}$ is to be substituted with C for the $CO_2$ containing complexes.

Table 5.5. The structural parameters of $Ne_2$-$N_2O$, Ne-$N_2O$, Ne-$CO_2$, and $Ne_2$.

| Parameter | $Ne_2$-$N_2O$ | | Ne-$N_2O$ | | $Ne_2$ |
|---|---|---|---|---|---|
| | $r_o$ | $r_z$ | $r_o$ | $r_z$ | |
| $R_{c.m.}$[a]/Å | 2.7611 | 2.7789 | 3.225 | 3.249 | -. |
| $\theta_{c.m.}$[a]/(deg) | 77.02 | 77.24 | 81.70 | 84.06 | -. |
| R(Ne-Ne)[a]/Å | 3.3074 | 3.3229 | -. | -. | 3.290 |
| R(Ne-$N_{inner}$)[b]/Å | 3.2336 | 3.2526 | 3.237 | 3.258 | -. |
| ∠ Ne$N_{inner}$O)[b]/(deg) | 77.60 | 77.78 | 80.39 | 82.76 | -. |
| ∠ Ne$N_{inner}$Ne)[b]/(deg) | 61.52 | 61.44 | -. | -. | -. |
| Reference | this work | this work | 27 | 27 | 7 |

[a] $R_{c.m.}$, $\theta_{c.m.}$, and R(Ne-Ne) are the $r_o$ structural parameters obtained from the fitting procedure described in the text. $N_2O$ bond lengths were fixed at R(N-N)=1.1278Å, R(N-O)=1.1923Å, and R($N_{inner}$-c.m. of $N_2O$) =0.0745Å (from Ref.42).

[b] Calculated from $R_{c.m.}$, $\theta_{c.m.}$, R(Ne-Ne), and the $N_2O$ bond lengths listed above.

complex formation with Ar or Ne. In the case of the $Ne_2$-$N_2O$ trimer isotopic shifts in $R_{Ne\text{-}Ne}$ and $R_{c.m.}$ were taken into account in the structural fits. The Ne-Ne bond shortening upon substitution with $^{22}Ne$ was estimated from the planar moments $P_b$ of the $^{20}Ne_2$ and $^{22}Ne_2$ containing species (see below). The shortening of $R_{c.m.}$ upon substitution with $^{22}Ne$, $^{15}N$ (central), and $^{15}N$ (terminal) was estimated using the respective C-rotational constants of the Ne-$N_2O$ dimer (*27*) and the expression $\mu R_{c.m.}^2 = 505379\ (1/C - 1/b_o)$, where $\mu$ is the reduced mass of the dimer in a pseudo-diatomic approximation and $b_o$ is the rotational constant of free $N_2O$ (*46*). Other structural parameters calculated from the fitting results are also given in Tables 5.4 and 5.5 to allow comparison with the corresponding values of the related $Ar_2$-$CO_2$ trimer (*20*), the Ar-$CO_2$ dimer (*47*), and the (rare gas)$_2$ dimers (*6, 25*). The $r_o$ structure determinations put the oxygen end of the $N_2O$ subunit closer to the (rare gas)$_2$ unit in both instances. This is consistent with the structures of the corresponding dimers where the oxygen end of $N_2O$ was also found to be closer to the respective rare gas atom.

Ground state average, $r_z$, structures were determined using the results from the force field analyses described below (Section 5.4.2). The ground state average rotational constants $A_z$, $B_z$, and $C_z$ (see Table 5.1 for $Ar_2$-$N_2O$ and Tables 5.2 and 5.3 for $Ne_2$-$N_2O$), obtained by subtracting the harmonic contributions to the $\alpha$-constants from the ground state rotational constants, were input for fitting procedures to give the $r_z$ structural parameters in Tables 5.4 ($Ar_2$-$N_2O$) and 5.5 ($Ne_2$-$N_2O$). Isotopic shifts were taken into account in the case of $Ne_2$-$N_2O$ as described for the $r_o$ structure

determination. There are, in general, only relatively small variations between $r_o$ and $r_z$ structural parameters. These variations can be attributed mainly to the large amplitude van der Waals vibrational motions which were partly accounted for in the force field analyses.

The availability of sets of rotational constants for several isotopomers allowed us to determine partial substitution structures for the trimers using Kraitchman's equations (*48*). For $Ar_2$-$N_2O$, substitutions were made at both nitrogen atoms. The resulting *a*-coordinates for the nitrogen atoms are small or imaginary, confirming that the $N_2O$ unit lies in the *bc*-plane. The *b*-coordinates are 1.847 and 1.885 Å for central and terminal nitrogen, respectively, consistent with the finding from the $r_o$ and $r_z$ structure fits that the oxygen end of $N_2O$ is tilted towards, and the terminal nitrogen atom away from, the $Ar_2$ subunit. For $Ne_2$-$N_2O$, the two nitrogen atoms have small *b*-coordinates, consistent with the fact that $N_2O$ lies in the *ac*-plane. The *a*-coordinates are 1.298 Å and 1.313 Å for central and terminal N, respectively. The difference, though small, is in accord with the findings from the $r_o$ and $r_z$ structure determinations, that the oxygen end of $N_2O$ is slightly tilted towards the $Ne_2$ subunit. Substitutions at the Ne atoms made it possible to calculate an $r_s$ Ne-Ne distance which came to 3.179 Å.

The planar moments of inertia are also good indicators of molecular geometry and structure. They are defined as: $P_\alpha = (I_\beta+I_\gamma-I_\alpha)/2$; $\alpha, \beta, \gamma = a, b, c$ and cyclic permutations thereof (*49*). In the case of $Ar_2$-$N_2O$, $P_a$ depends only on the *a*-coordinates of the atoms. As seen in Table 5.1, $P_a$ is basically invariant (less than

0.004% variation) to isotopic substitution of the $^{14}N$ atoms in $Ar_2$- $N_2O$ with $^{15}N$. This is further confirmation that the $N_2O$ unit lies in the *bc*-plane, the symmetry plane of the complex. The main contributions to $P_a$ in $Ar_2$-$N_2O$ are therefore from the two Ar atoms. The planar moment $P_a$ was thus used to calculate the Ar-Ar distance in the complex; values of 3.8430 Å and 3.8473 Å were obtained for $r_o$ and $r_z$, respectively. The corresponding values from the fitting procedures described above are 3.8419 Å and 3.8466 Å, respectively (see Table 5.4). In the case of the $Ne_2$-$N_2O$ trimer there is also little variation (less than 0.008%) in the values of $P_b$ upon $^{14}N \rightarrow {}^{15}N$ substitution (see Table 5.5) for the isotopomers with $C_s$ symmetry, thus confirming that the $N_2O$ unit lies in the *ac*-plane of the complex. The Ne-Ne separation derived via the $P_b$ planar moments gives ground state effective values for the Ne-Ne distance of 3.3071Å for $^{20}Ne^{20}Ne$-$^{14}N^{14}NO$ and 3.2953Å for $^{22}Ne^{22}Ne$-$^{14}N^{14}NO$. The respective $r_z$ values are 3.3177 Å and 3.3055 Å. These calculated values may be compared with the values 3.3074 Å and 3.3229 Å from the $r_o$ and $r_z$ fitting procedures, respectively (see Table 5.5).

These geometries and the derived structural parameters in Tables 5.4 and 5.5 are consistent with dominance of pairwise additive contributions to the total interaction energy. The relevant parameters, for example the distance between rare gas atom and the central nitrogen of $N_2O$ and the angle between this distance and the $N_2O$ axis, are very similar in the trimers and the corresponding dimers. An indication of three-body non-additive effects can be found, however, in the significant bond lengthening of the Ar-Ar (3.842 Å) and Ne-Ne bonds (3.307 Å), as compared to

the bond lengths of the free dimers. The $r_o$ dimer bond lengths are 3.822 Å for the Ar-Ar dimer (calculated from the $B_o$ rotational constant of Ref. 6) and 3.290 Å for the Ne-Ne dimer (derived from the Ne dimer potential in Ref. 25). Similar lengthening of the Ar-Ar bond was previously also observed in the $Ar_2$-HCl (*105*), $Ar_2$-OCS (*40*), and $Ar_2$-$CO_2$ (*20*) trimers. There is no previous high resolution spectroscopic report of another $Ne_2$-molecule complex and the Ne-Ne bond lengthening noted in this work is the first such observation.

## 5.4.2 HARMONIC FORCE FIELD ANALYSES

The experimental centrifugal distortion constants contain information about the force constants of the trimers. For an asymmetric top molecule the $\tau$'s are related to the force constants by the expression (*50*),

$$\tau_{\alpha\beta\gamma\delta} = -\frac{\hbar^3}{4\pi}\,\frac{1}{I_{\alpha\alpha} I_{\beta\beta} I_{\gamma\gamma} I_{\delta\delta}} \sum_i \sum_j J_{\alpha\beta}^{(i)} \left(f^{-1}\right)_{ij} J_{\gamma\delta}^{(j)} \qquad (5.1)$$

where $I_{\alpha\alpha}$ represent the moments of inertia at the equilibrium configuration, $J_{\alpha\beta}^{(i)} = (\partial I_{\alpha\beta}/\partial R_i)_e$ are the inertial tensor component derivatives with respect to the $i^{th}$ internal coordinate evaluated at the equilibrium geometry, $R_i$ is an internal coordinate of the molecule, $(f^{-1})_{ij}$ is an element of the inverse force constant matrix and $\alpha$, $\beta$, $\gamma$, and $\delta$ are the *a*, *b*, *c*. The distortion constants given in Tables 5.1, 5.2, and 5.3 are related to the $\tau$'s of Equation 5.1 by the expressions in Ref. *51*.

For simplification and for consistency in the treatments of $Ar_2$-$N_2O$ and $Ne_2$-$N_2O$ only the symmetric isotopomers of $Ne_2$-$N_2O$ will be considered in the

following. All these (rare gas)$_2$-$N_2O$ trimers have $C_s$ symmetry. The nine vibrational modes transform as 6A′+3A″ under the operations of the $C_s$ point group. The A′ symmetry modes are; the N-N stretch ($\nu_1$), the N-O stretch ($\nu_2$), the in-plane N-N-O linear bend ($\nu_3$), the symmetric Ar-N-Ar stretch ($\nu_4$), the Ar-Ar stretch ($\nu_5$), and the $Ar_2$-$N_2O$ "wag" ($\nu_6$), where both Ar atoms move towards $N_2O$ in the same direction. For A″ symmetry there are the out-of-plane N-N-O linear bend ($\nu_7$), the Ar-N-Ar asymmetric stretch ($\nu_8$), and the $Ar_2$-$N_2O$ "twist" ($\nu_9$), where the Ar atoms move towards $N_2O$ in opposite directions. These modes can be approximated by the symmetry coordinates shown in Tables 5.6 ($Ar_2$-$N_2O$) and 5.7 ($Ne_2$-$N_2O$).

The internal vibrational modes of $N_2O$ were assumed to be unchanged as a result of complexation with the two rare gas atoms (*52*). The values of the force constants of $N_2O$ were fixed at those of Ref. *53*. Symmetry considerations preclude the interaction between modes of different symmetry, and all corresponding interaction force constants were set to zero. All other interaction force constants were fixed at zero in the fitting procedures since there was not sufficient data available for their determinations. Furthermore, the force constants $f_{66}$ corresponding to the (rare gas)$_2$-$N_2O$ wagging vibrations were fixed at values of $f_\theta/2$ of the corresponding rare gas-$N_2O$ dimers. The force constants obtained from fitting to the experimental centrifugal distortion constants of the three isotopomers of $Ar_2$-$N_2O$ are shown in Table 5.6, those of $Ne_2$-$N_2O$ are in Table 5.7. The estimated van der Waals vibrational frequencies of the normal isotopomers are also listed. A comparison of the experimental centrifugal distortion constants and those calculated from the

Table 5.6. The harmonic force field of $Ar_2$-$N_2O$.

| Structure parameters | |
|---|---|
| $r(Ar1\text{-}Ar2)=r=3.8419$Å | |
| $r(Ar1\text{-}N_{inner})=r_1=r(Ar2\text{-}N_{inner})=r_2=3.4742$Å | |
| $r(NN)=r_3=1.1278$Å | |
| $r(NO)=r_4=1.1923$Å | |
| $\sphericalangle(Ar1NN)=\alpha_1=\sphericalangle(Ar2NN)=\beta_1=100.43°$ | |
| $\sphericalangle(Ar1NO)=\alpha_2=\sphericalangle(Ar2NO)=\beta_2=79.57°$ | |
| **Symmetry coordinates** | |
| A′: | $S_1=\Delta r_3$ |
| | $S_2=\Delta r_4$ |
| | $S_3$=in-plane NNO linear bend |
| | $S_4=(1/2)^{1/2}(\Delta r_1+\Delta r_2)$ |
| | $S_5=\Delta r$ |
| | $S_6=(1/2)(\Delta\alpha_1-\Delta\alpha_2+\Delta\beta_1-\Delta\beta_2)$ |
| A″: | $S_7$=out-of-plane NNO linear bend |
| | $S_8=(1/2)^{1/2}(\Delta r_1-\Delta r_2)$ |
| | $S_9=(1/2)(\Delta\alpha_1-\Delta\alpha_2-\Delta\beta_1+\Delta\beta_2)$ |
| **Harmonic force constants** | |
| $f_{11}$/mdyn Å$^{-1}$ | 18.1904[a] |
| $f_{12}$/mdyn Å$^{-1}$ | 1.024[a] |
| $f_{22}$/mdyn Å$^{-1}$ | 12.0308[a] |
| $f_{33}$/mdyn Å rad$^{-2}$ | 0.666[a] |
| $f_{44}$/mdyn Å$^{-1}$ | 0.0189(7) |
| $f_{55}$/mdyn Å$^{-1}$ | 0.00839(6) |
| $f_{46}$/mdyn rad$^{-1}$ | 0.0[b] |
| $f_{66}$/mdyn Å rad$^{-2}$ | 0.0115[b] |
| $f_{77}$/mdyn Å rad$^{-2}$ | 0.666[a] |
| $f_{88}$/mdyn Å$^{-1}$ | 0.0193(4) |
| $f_{89}$/mdyn Å rad$^{-2}$ | 0.0[b] |
| $f_{99}$/mdyn Å rad$^{-2}$ | 0.013(1) |

Predicted van der Waals vibrational frequencies (cm$^{-1}$)

| $\nu_4$ | $\nu_5$ | $\nu_8$ | $\nu_9$ |
|---|---|---|---|
| 44.4 | 23.8 | 35.7 | 28.0 |

[a] Constrained at the values of Ref. 53.
[b] Constrained. See discussion in the text.

resulting force constants is given in Table 5.8. The force constants derived from the harmonic force field analysis reproduce the centrifugal distortion constants quite well,

Table 5.7. The harmonic force field of $Ne_2$-$N_2O$.

| Structure parameters | |
|---|---|
| r(Ne1-Ne2)=r=3.3074Å | |
| r(Ne1-$N_{inner}$)=$r_1$=r(Ne2-$N_{inner}$)=$r_2$=3.2277Å | |
| r(NN)=$r_3$=1.1278Å | |
| r(NO)=$r_4$=1.1923Å | |
| ∢(Ne1NN)=$\alpha_1$=∢(Ne2NN)=$\beta_1$=97.83° | |
| ∢(Ne1NO)=$\alpha_2$=∢(Ne2NO)=$\beta_2$=82.17° | |
| **Symmetry coordinates** | |
| A′: | $S_1=\Delta r_3$ |
| | $S_2=\Delta r_4$ |
| | $S_3$=in-plane NNO linear bend |
| | $S_4=(1/2)^{1/2}(\Delta r_1+\Delta r_2)$ |
| | $S_5=\Delta r$ |
| | $S_6=(1/2)(\Delta\alpha_1-\Delta\alpha_2+\Delta\beta_1-\Delta\beta_2)$ |
| A″: | $S_7$=out-of-plane NNO linear bend |
| | $S_8=(1/2)^{1/2}(\Delta r_1-\Delta r_2)$ |
| | $S_9=(1/2)(\Delta\alpha_1-\Delta\alpha_2-\Delta\beta_1+\Delta\beta_2)$ |
| **Harmonic force constants** | |
| $f_{11}$/mdyn Å$^{-1}$ | 18.1904[a] |
| $f_{12}$/mdyn Å$^{-1}$ | 1.024[a] |
| $f_{22}$/mdyn Å$^{-1}$ | 12.0308[a] |
| $f_{33}$/mdyn Å rad$^{-2}$ | 0.666[a] |
| $f_{44}$/mdyn Å$^{-1}$ | 0.0071(2) |
| $f_{55}$/mdyn Å$^{-1}$ | 0.0021(1) |
| $f_{46}$/mdyn rad$^{-1}$ | 0.0[b] |
| $f_{66}$/mdyn Å rad$^{-2}$ | 0.00535[b] |
| $f_{77}$/mdyn Å rad$^{-2}$ | 0.666[a] |
| $f_{88}$/mdyn Å$^{-1}$ | 0.0099(5) |
| $f_{89}$/mdyn Å rad$^{-2}$ | 0.0[b] |
| $f_{99}$/mdyn Å rad$^{-2}$ | 0.0063(3) |

**Predicted van der Waals vibrational frequencies (cm$^{-1}$)**

| $\nu_4$ | $\nu_5$ | $\nu_8$ | $\nu_9$ |
|---|---|---|---|
| 33.1 | 16.8 | 32.2 | 19.8 |

[a] Constrained at the values of Ref. 53.
[b] Constrained. See discussion in the text.

especially their variations with isotopomers. This shows that the variations are mostly mass and geometry dependent, and serves to confirm the spectral assignments and the distorted tetrahedral geometries of the complexes.

Table 5.8. Comparison of experimental and calculated quartic centrifugal distortion constants.[a]

| Constant | Obs.[b] | Calc.[c] | Obs.[b] | Calc.[c] | Obs.[b] | Calc.[c] |
|---|---|---|---|---|---|---|
| | $Ar_2$-$^{14}N^{14}NO$ | | $Ar_2$-$^{15}N^{14}NO$ | | $Ar_2$-$^{14}N^{15}NO$ | |
| $\Delta_J$ | 10.693(6) | 10.70 | 10.4780(10) | 10.54 | 10.701(13) | 10.68 |
| $\Delta_{JK}$ | -18.48(3) | -18.50 | -18.02(4) | -18.19 | -18.69(5) | -18.61 |
| $\Delta_K$ | 27.96(2) | 28.03 | 26.88(4) | 26.84 | 27.75(5) | 27.73 |
| $\delta_j$ | 4.193(3) | 4.19 | 4.124(5) | 4.14 | 4.212(5) | 4.20 |
| $\delta_k$ | 1.271(15) | 1.31 | 1.010(19) | 1.01 | 1.17(2) | 1.16 |
| | $^{20}Ne^{20}Ne$-$^{14}N^{14}NO$ | | $^{20}Ne^{20}Ne$-$^{15}N^{14}NO$ | | $^{20}Ne^{20}Ne$-$^{14}N^{15}NO$ | |
| $\Delta_J$ | 63.442(9) | 62.55 | 61.041(13) | 59.67 | 62.566(13) | 61.66 |
| $\Delta_{JK}$ | -85.68(4) | -78.43 | 79.93(7) | -71.81 | -85.96(7) | -78.02 |
| $\Delta_K$ | 402.4(4) | 384.41 | 387.0(7) | 370.00 | 404.4(7) | 384.89 |
| $\delta_j$ | 18.987(6) | 17.60 | 18.081(8) | 16.49 | 18.804(8) | 17.38 |
| $\delta_k$ | -39.64(5) | -39.63 | -41.98(6) | -39.23 | -38.12(6) | -38.38 |
| | $^{22}Ne^{22}Ne$-$^{14}N^{14}NO$ | | $^{22}Ne^{22}Ne$-$^{15}N^{14}NO$ | | $^{22}Ne^{22}Ne$-$^{14}N^{15}NO$ | |
| $\Delta_J$ | 56.915(11) | 58.23 | 54.645(13) | 55.52 | 56.120(15) | 57.35 |
| $\Delta_{JK}$ | -75.93(5) | -79.51 | -70.63(7) | -73.10 | -76.21(7) | -78.87 |
| $\Delta_K$ | 354.3(5) | 355.42 | 338.6(6) | 342.60 | 356.4(6) | 355.66 |
| $\delta_j$ | 17.223(7) | 16.96 | 16.448(8) | 15.91 | 17.049(9) | 16.73 |
| $\delta_k$ | -30.10(5) | -32.30 | -31.82(6) | -31.58 | -28.70(7) | -31.08 |

[a] Values are given in kHz.
[b] These are the values from Tables 5.1 and 5.2.
[c] Calculated using the force constants from the harmonic force field analyses.

The harmonic force field analyses also provide information about the $\alpha$-constants, i.e. about the contributions of the harmonic parts of the vibrations to the rotational constants. When these are subtracted from the ground state effective rotational constants the ground state average rotational constants, $A_z$, $B_z$, and $C_z$, are obtained. These are given in Tables 5.1, 5.2, and 5.3, and were used to determine ground state average, $r_z$, structures (see Section 5.4.1, and Tables 5.4 and 5.5).

The derived force constants can be compared with the respective dimer constants. It is found that the averages of the symmetric ($\nu_4$) and asymmetric ($\nu_8$) rare gas-N-rare gas stretching force constants $f_{44}$ and $f_{88}$, respectively, are the same as

the rare gas-$N_2O$ stretching force constants $f_s$ of the respective rare gas-$N_2O$ dimers ($f_{s\ Ar\text{-}N_2O}$=0.020(3) mdyn Å$^{-1}$, $f_{s\ Ne\text{-}N_2O}$=0.0089(7) mdyn Å$^{-1}$) (*33*, *27*) within the error limits. Furthermore, the values of $f_{44}$ and $f_{88}$ are close, indicating that there is negligible interaction between the two rare gas-$N_2O$ stretches. Similar arguments hold for the symmetric ("wag", $\nu_6$) and asymmetric ("twist", $\nu_9$) (rare gas)$_2$-$N_2O$ bending vibrations. The sums of $f_{66}$ and $f_{99}$ are, within the error limits, equal to the bending force constants $f_b$ in the corresponding rare gas-$N_2O$ dimers ($f_{b\ Ar\text{-}N_2O}$=0.023(3) mdyn Å rad$^{-2}$, $f_{b\ Ne\text{-}N_2O}$=0.0107(4) mdyn Å rad$^{-2}$) (*33*, *27*). It appears thus that the relatively low levels of precision of the force constants do not allow for the detection of any non-additive three-body interactions. On the other hand, the consistency of the force constants from the rare gas-$N_2O$ dimers and the (rare gas)$_2$-$N_2O$ trimers is a nice confirmation of the validity of the harmonic force field procedure. The value of the Ar-Ar stretching force constant, $f_{55}$, is slightly larger than that estimated for the $Ar_2$ dimer (0.0078 mdyn Å$^{-1}$) (*17*) and very close to the corresponding values of $Ar_2$-OCS (0.00842 mdyn Å$^{-1}$) (*40*) and $Ar_2$-$CO_2$ (0.00816 mdyn Å$^{-1}$) (*20*).

### 5.4.3 $^{14}$N NUCLEAR QUADRUPOLE COUPLING CONSTANTS

The $^{14}$N nuclear quadrupole coupling constants obtained from the spectral analyses contain information about the structures and the large amplitude motions of the complexes, and about the change of the electronic charge distribution at the sites of the $^{14}$N nuclei upon complex formation. Assuming that the electronic perturbation is negligible, the coupling constants of the complex are related to the $N_2O$ monomer

constants by the expression

$$\chi_{gg}=(1/2)\chi_{mon}<3\cos^2\theta_g -1> \qquad (5.2)$$

where $g=a$, $b$ or $c$ and $\theta_g$ represents the angle between the $g$ inertial axis of the complex and the $N_2O$ monomer axis. The proper choice of axis system for the interpretation of nuclear quadrupole coupling constants of van der Waals molecules which undergo large amplitude bending motions has been pointed out by Hutson and co-workers (*54*, *55*, *56*). It was emphasized, in particular, that it is important to use an Eckart axis system to achieve an optimal separation of rotational and vibrational motions. This treatment, however, has thus far not been extended to ternary systems, and we assume instead that the angles in the above expression correspond to an instantaneous inertial axis system.

The nuclear quadrupole coupling constants from the spectral analyses can be used to derive effective angles, $\theta_g$, between the $N_2O$ axis and the $g$-inertial axis. The resulting angles no longer place the $N_2O$ subunits into the respective planes of symmetry in the cases of the isotopomers with $C_s$ symmetry, as a result of the averaging over the large amplitude out-of-symmetry-plane motions with a $cos^2\theta$ term. This makes it rather difficult to make useful comparisons with the effective, $r_o$, structural parameters. For example, the value of $\theta_b$ ($\theta_a$) of $Ar_2$-$N_2O$ ($Ne_2$-$N_2O$) from the quadrupole coupling constants can be compared with the corresponding value derived from the $r_o$ structural parameters. The values given below were derived from the quadrupole coupling constants of the terminal $^{14}N$ nucleus, since it has been shown in previous studies that these constants are least affected by electronic perturbations

caused by complex formation. The values for $\theta_b$ are 84.4° (from $^{14}N$) and 76.7° (from $r_o$) for $Ar_2$-$^{14}N_2O$ and are 82.5° (from $^{14}N$) and 73.0° (from $r_o$) for $\theta_a$ in the case of $^{20}Ne_2$-$^{14}N_2O$. The $^{14}N$ values are larger than the $r_o$ values by about eight to ten degrees. Such discrepancies, albeit of smaller magnitude, were also found in the Ne-$N_2O$ (*27*) and Ar-$N_2O$ dimers (*32*, *33*) and may be attributed to the choice of axis system (see remarks above) and to the different averaging over the large amplitude motions for moments of inertia and the nuclear quadrupole coupling constants.

Further insight can be gained from a consideration of the coupling constants $\chi_{aa}$ and $\chi_{bb}$ of $Ar_2$-$N_2O$ and $Ne_2$-$N_2O$, respectively. These constants contain information about an average excursion of the $N_2O$ subunit from the *bc*- ($Ar_2$-$N_2O$) or *ac*- ($Ne_2$-$N_2O$) plane of symmetry. The resulting values from the terminal $^{14}N$ quadrupole coupling constants are 84.2° for $\theta_a$ in $Ar_2$-$N_2O$ and 83.5° for $\theta_b$ in $Ne_2$-$N_2O$. Such amplitudes of less than 15° of the out-of-plane motions indicate that the complexes are comparatively rigid, and support the use of the semi-rigid rotor model in the spectral analyses discussed above.

The electronic perturbation of the $N_2O$ subunit upon complex formation has been analysed in previous studies of $N_2O$ containing van der Waals dimers. For example, in Ne-$N_2O$ (*27*) and Ar-$N_2O$ (*32*) noticeable perturbation was found at the site of the central N nucleus, whereas negligible effect was detected at the terminal N nucleus. The presence of electronic perturbations of the $N_2O$ subunit becomes apparent when comparing the values $\chi_{gg}/\chi_{G\,(mon)}$ of terminal and central $^{14}N$ nuclei. Here, $\chi_{G\,(mon)}$ is the respective monomer coupling constant of the $N_2O$ monomer, and

G=X, Y, Z, are the principal axes of the nuclear quadrupole coupling tensor in the $N_2O$ monomer. These values of $\chi_{gg}/\chi_{G\,(mon)}$ would be the same for both nuclei in the absence of electronic perturbations since both central and terminal $^{14}N$ nuclei are equally affected by geometry and large amplitude motions. The values for $Ar_2$-$^{14}N_2O$ are: $\chi_{aa}/\chi_{X\,(mon)}$=0.971 (terminal), 0.943 (central); $\chi_{bb}/\chi_{Y\,(mon)}$=0.953 (terminal), 0.916 (central); $\chi_{cc}/\chi_{Z\,(mon)}$=0.962 (terminal), 0.930 (central). Those for $^{20}Ne_2$-$^{14}N_2O$ are: $\chi_{aa}/\chi_{X\,(mon)}$=0.949 (terminal), 0.904 (central); $\chi_{bb}/\chi_{Y\,(mon)}$=0.962 (terminal), 0.946 (central); $\chi_{cc}/\chi_{Z\,(mon)}$=0.955 (terminal), 0.925 (central). In all cases, the values for the central $^{14}N$ nucleus are smaller.

It was hoped that the nuclear quadrupole coupling constants, in particular the comparisons of these constants for central and terminal nitrogen nuclei, would reveal information about non-additivity in the trimer systems studied. For this purpose, we will compare the values of $\chi_{bb}/\chi_{Z\,(mon)}$ of the Ar-$^{14}N_2O$ dimer with the values of $\chi_{cc}/\chi_{Z\,(mon)}$ of the $Ar_2$-$N_2O$ trimer, because the *b*-axis in the dimer corresponds to the *c*-axis in the trimer. For the Ar-$^{14}N_2O$ dimer the values of $\chi_{bb}/\chi_{Z\,(mon)}$ of terminal and central $^{14}N$ nuclei are 0.981(1) and 0.964(3), respectively. The ratio of these values is 1.018(3), and its deviation from the value of one can be attributed to the electronic perturbation of the $^{14}N_2O$ subunit at the site of the central $^{14}N$ nucleus. For the $Ar_2$-$N_2O$ trimer, the values of $\chi_{cc}/\chi_{Z\,(mon)}$ of terminal and central $^{14}N$ nuclei are 0.962(1) and 0.930(6), respectively. The ratio of these two values is 1.035(7). Here, the deviation from one is about twice as large as in the Ar-$^{14}N_2O$ dimer. This is expected in the limit of pairwise additivity. It appears that the electronic perturbation

at the site of the central $^{14}N$ nucleus in $N_2O$ upon complex formation, as measured by the nuclear quadrupole coupling constants, does not indicate the presence of three-body non-additive interactions in $Ar_2$-$N_2O$. For $Ne_2$-$N_2O$, a similar analysis can be made. The ratios $\chi_{bb}/\chi_{Z\,(mon)}$ of the $^{20}Ne$-$^{14}N_2O$ dimer are compared with $\chi_{cc}/\chi_{Z\,(mon)}$ of the $^{20}Ne_2$-$^{14}N_2O$ trimer. For the $^{20}Ne$-$^{14}N_2O$ dimer, a ratio of 1.012(2) is obtained. For the $^{20}Ne_2$-$^{14}N_2O$ trimer the corresponding ratio is 1.033(9), which deviates from one, within the error limits, by about twice the dimer amount. For the $^{22}Ne$ containing isotopomers, the obtained ratios are 1.024(4) and 1.024(11) for the $^{22}Ne$-$^{14}N_2O$ dimer and the $^{22}Ne_2$-$^{14}N_2O$ trimer, respectively. The deviation from one of the ratio of the trimer is thus not quite twice the dimer amount within the error limits. It appears that the precision of the nuclear quadrupole coupling constant is not high enough to be able to unambiguously detect three-body non-aditive effects.

## 5.5 CONCLUSIONS

In summary, rotational spectra of several isotopomers of the van der Waals trimers $Ar_2$-$N_2O$ and $Ne_2$-$N_2O$ were measured with a pulsed beam FTMW spectrometer. It was possible to resolve and to assign the sometimes rather complex $^{14}N$ nuclear quadrupole hyperfine structures of the rotational transitions. The spectroscopic analyses yielded rotational, centrifugal distortion, and $^{14}N$ nuclear quadrupole coupling constants. Several observations confirm unambiguously the equilibrium geometries of the $Ar_2$-$N_2O$ and $Ne_2$-$N_2O$ trimers shown in Figures 5.1 and 5.2. Among these observations are the independence of $P_a$ ($P_b$) upon isotopic

substitution in the $N_2O$ subunit, the observation of additional *b*-type transitions in the mixed $Ne_2$-$N_2O$ complexes, and the failure to observe *a*-type (*b*-type) transitions in $Ar_2$-$N_2O$ ($^{20}Ne_2$-$N_2O$, $^{22}Ne_2$-$N_2O$) despite accurate frequency predictions. The possible presence of three-body non-additive interactions could not be unambiguously confirmed by the harmonic force field analyses and the analyses of the nuclear quadrupole coupling constants. However, the structural analyses revealed noticeable lengthening of the Ar-Ar and Ne-Ne bonds, as compared to those of the respective rare gas dimers and such bond lengthening could be attributed to three-body non-additive effects.

## REFERENCES


1. W. J. Meath and M. Koulis, *J. Mol. Struct.* **226**, 1 (1991).

2. B. M. Axilrod and E. Teller, *J. Chem. Phys.* **11**, 299 (1943).

3. P. J. Kortbeek and J. A. Schouten, *Mol. Phys.* **69**, 981 (1990).

4. G. Chałasiński, M. M. Szczęśniak, and S. Scheiner, *J. Chem. Phys.* **94**, 2807 (1991).

5. E. A. Colbourn and A. E. Douglas, *J. Chem. Phys.* **65**, 1741 (1976).

6. P. R. Herman, P. E. LaRocque, and B. P. Stoicheff, *J. Chem. Phys.* **89**, 4535 (1988).

7. R. A. Aziz, *J. Chem. Phys.* **99**, 4518 (1993).

8. J. M. Hutson, *J. Chem. Phys.* **96**, 4237 (1992).

9. J. M. Hutson, *J. Chem. Phys.* **96**, 6752 (1992).

10. R. J. Le Roy and J. M. Hutson, *J. Chem. Phys.* **86**, 837 (1987).

11. R. C. Cohen and R. J. Saykally, *J. Chem. Phys.* **98**, 6007 (1993).

12. C. A. Schmuttenmaer, R. C. Cohen, and R. J. Saykally, *J. Chem. Phys.* **101**, 146 (1994).

13. T. D. Klots, C. Chuang, R. S. Ruoff, T. Emilsson, and H. S. Gutowsky, *J. Chem. Phys.* **86**, 569 (1987).

14. M. J. Elrod, R. J. Saykally, A. R. Cooper, and J. M. Hutson, *Mol. Phys.* **81**, 579 (1994).

15. A. Ernesti and J. M. Hutson, *J. Chem. Phys.* **106**, 6288 (1997).

16. D. T. Anderson, S. Davis, and D. J. Nesbitt, *J. Chem. Phys.* **107**, 1115 (1997).

17. H. S. Gutowsky, T. D. Klots, C. Chuang, C. A. Schmuttenmaer, and T. Emilsson, *J. Chem. Phys.* **86**, 569 (1987).

18. J. T. Farrel Jr. and D. J. Nesbitt, *J. Chem. Phys.* **105**, 9421 (1996).

19. R. Moszynzki, P. E. S. Wormer, T. G. A. Heijmen, and A. van der Avoird, *J. Chem. Phys.* **108**, 579 (1998).

20. Y. Xu, W. Jäger, and M. C. L. Gerry, *J. Mol. Spectrosc.* **157,** 132 (1993).

21. J. M. Sperhac, M. J. Weida, and D. J. Nesbitt, *J. Chem. Phys.* **104,** 2202 (1996).

22. J. Rak, M. M. Szczęśniak, G. Chałasiński, and S. M. Cybulski, *J. Chem. Phys.* **106**, 10215 (1997).

23. A. Ernesti and J. M. Hutson, *Phys. Rev.* A **51**, 239 (1995).

24. Y. Tanaka and K. Yoshino, *J. Chem. Phys.* **57,** 2964 (1972).

25. R. A. Aziz and M. J. Slaman, *Chem. Phys.* **130**, 187 (1989).

26. W. A. Herrebout, H.-B. Qian, H. Yamaguchi, and B. J. Howard, *J. Mol. Spectrosc.* **189,** 235 (1998).

27. M. S. Ngarī and W. Jäger, *J. Mol. Spectrosc.* **192**, 320 (1998).

28. C. H. Joyner, T. A. Dixon, F. A. Baiocchi, and W. Klemperer, *J. Chem. Phys.* **75,** 5285 (1981).

29. J. Hodge, G. D. Hayman, T. R. Dyke, and B. J. Howard, *J. Chem. Soc., Faraday trans. II* **82,** 1137 (1986).

30. T. A. Hu, E. L. Chappel, and S. W. Sharpe, *J. Chem. Phys.* **98,** 6162 (1993).

31. H. O. Leung, *Chem. Commun.* **1996,** 2525 (1996).

32. H. O. Leung, D. Gangwani, and J.-U. Grabow, *J. Mol. Spectrosc.* **184,** 106 (1997).

33. M. S. Ngarī and W. Jäger, *J. Mol. Spectrosc.* **192**, 452 (1998).

34. D. Zolandz, D. Yaron, K. I. Peterson, and W. Klemperer, *J. Chem. Phys.* **97**, 2861 (1992).

35. H. O. Leung, *J. Chem. Phys.* **107**, 2232 (1997).

36. H. O. Leung, *J. Chem. Phys.* **110**, 4394 (1999).

37. T. J. Balle and W. H. Flygare, *Rev. Sci. Instrum.* **52,** 33 (1981).

38. Y. Xu and W. Jäger, *J. Chem. Phys.* **106,** 7968 (1997).

39. V. N. Markov, Y. Xu, and W. Jäger, *Rev. Sci. Instrum.* **69**, 4061 (1998).

40. Y. Xu, M. C. L. Gerry, J. P. Connelly, and B. J. Howard, *J. Chem. Phys.* **98,** 2735 (1993).

41. Y. Xu and W. Jäger, *J. Chem. Phys.* **107,** 4788 (1997).

42. C. C. Costain, *J. Chem. Phys.* **29,** 864 (1958).

43. J. M. L. J. Reinartz, W. L. Meerts, and A. Dymanus, *Chem. Phys.* **31,** 19 (1978).

44. J. K. G. Watson, in *Vibrational Spectra and Structure: A Series of Advances,* edited by J. R. Durig (Elsevier, New York, 1977) Vol. 6, pp.1-89.

45. H. M. Pickett, *J. Mol. Spectrosc.* **148,** 371 (1991).

46. B. A. Andreev, A. V. Burenin, E. N. Karyakin, A. F. Krupnov, and S. M. Shapin, *J. Mol. Spectrosc.* **62,** 125 (1976).

47. G. T. Fraser, A. S. Pine, and R. D. Suenram, *J. Chem. Phys.* **88,** 6157 (1988).

48. J. Kraitchman, *Am. J. Phys.* **21,** 17 (1953).

49. W. Gordy and R. L. Cook, *Microwave Molecular Spectra* (Wiley, New York, 1984).

50. D. Kivelson and E. B. Wilson, Jr., *J. Chem. Phys.* **21,** 1229 (1953).

51. J. K. G. Watson, *J. Chem. Phys.* **46,** 1935 (1967).

52. J. A. Shea, W. G. Read, and E. J. Campbell, *J. Chem. Phys.* **79,** 2559 (1983).

53. I. Suzuki, *J. Mol. Spectrosc.* **32,** 54 (1969).

54. A. Ernesti and J. M. Hutson, *Chem. Phys. Lett.* **222,** 257 (1994).

55. A. Ernesti and J. M. Hutson, *J. Chem. Phys.* **101,** 5438 (1994).

56. J. M. Hutson, *Mol. Phys.* **84,** 185 (1995).

# CHAPTER SIX

# THE ArNe-$N_2O$ VAN DER WAALS TRIMER: A HIGH RESOLUTION SPECTROSCOPIC STUDY OF ITS ROTATIONAL SPECTRUM, STRUCTURE AND DYNAMICS

## 6.1 INTRODUCTION

The high resolution spectroscopic studies of van der Waals clusters provide us with an opportunity to study the effects of weak intermolecular interactions at the molecular level. Most high resolution spectroscopic studies of van der Waals complexes involving the rare gases were concentrated around dimer systems. The geometric and structural information obtained from these studies (of dimers) have allowed the derivation of very accurate pairwise interaction potential energy curves for a variety of systems. These include potential energy functions for Ar-Ar (*1*, *2*), Ar-HCl (*3*), Ar-HF (*4*), Ar-$H_2$ (*5*), Ar-$H_2O$ (*6*), and Ar-$NH_3$ (*7*).

Studies of trimeric and higher order van der Waals complexes comprise a relatively small proportion of the work on weakly bound clusters compared to dimer systems although the number of trimers and larger clusters investigated is steadily rising. After the pioneering work of Gutowsky and co-workers in their studies of $Ar_2$-HX complexes (X=F (*8*), Cl (*9*, *10*), CN (*11*)) several other reports on trimer systems of the type (rare gas)$_2$-linear molecule have appeared in the literature.

With well known pair potentials such as those cited above (*1*, *2*, *3*, *4*, *5*, *6*, *7*), the construction of potential energy surfaces by both *ab initio* computational (*12*, *13*, *14*) and semiempirical methods (*15*, *16*, *17*) for trimeric species has been an active area of investigation. In many cases the Axilrod-Teller (A-T) triple-dipole dispersion

term (*18*) has been used to account for the effects of three-body forces in van der Waals trimers. The apparent success of this term has, however, been shown to be due to a cancellation of errors in higher order terms (*19*) and (*20*).

In the construction of the potential energy surface for $Ar_2$-HCl and $Ar_2$-HF, Ernesti and Hutson (*17*) found that the A-T term was insufficient to account for three-body effects in the interaction potentials. In attempts to fit the potential energy surface to the experimental data they found that in addition to the pairwise additive contributions the introduction of a new three-body term was needed to reduce the discrepancy between experimental data and the calculations. This term was called the "exchange quadrupole" term and accounts for the interaction between the dipole moment of HCl and the exchange quadrupole moment of $Ar_2$. The resulting potential was found to account only partly for the three-body nonadditive effects, and inclusion of other physical effects will be required in future potential energy surfaces to narrow the gap between the results from calculations and experimental data.

It is now of importance to investigate further ternary systems in order to explore the significance of the new proposed "exchange quadrupole" term. For example, substitution of the $Ar_2$ subunit with ArNe would introduce an additional "exchange dipole" term. Thus far only two spectroscopic studies of rare gas-rare gas'-linear molecule complexes can be found in the literature. The MW rotational spectrum the ArNe-HCl van der Waals trimer has been measured by Xu *et al.* (*21*). This trimer was found to have a planar equilibrium structure with the H-atom pointing towards the ArNe bond. An observed lengthening of the ArCl and ArNe distances,

as compared to the respective dimer distances, was interpreted as a result of three-body non-additive interactions. The trimer ArNe-$CO_2$ has been studied in the MW range by Xu and Jäger (*22*). Its structure is that of a distorted tetrahedron. Only small variations in the bond lengths, as compared to the respective dimer values were observed.

We report here the identification and analysis of the MW rotational spectrum of six isotopomers of the ArNe-$N_2O$ trimer. This study is an extension of our previous studies of Ar-$N_2O$ (*23*), Ne-$N_2O$ (*24*), $Ar_2$-$N_2O$ and $Ne_2$-$N_2O$ (see chapter 5). It was possible to resolve hyperfine structures of the rotational transitions that are due to the quadrupolar $^{14}N$ nuclei. The resulting spectroscopic constants were used to determine the structure of the trimer system. A harmonic force field analysis provided estimates for the frequencies of the van der Waals vibrational motions.

## 6.2 EXPERIMENTAL DETAILS

The spectra of ArNe-$N_2O$ were recorded between 4 and 14 GHz with a pulsed nozzle molecular beam Fabry-Pérot cavity FTMW spectrometer. The details of the spectrometer, which is based on the design of the Balle and Flygare instrument (*25*) were reported previously (*26*, *27*). The design and principles of operation of the spectrometer have been described in Chapter 2. The measurement accuracy is estimated to be about $\pm 1$ kHz, with typical linewidths of 7 kHz (full width at half height).

The samples were prepared by the pulsed expansion of a gas mixture made of

1% Ar and 0.5% $N_2O$ in Ne as the backing gas at pressures of about 6 atm. The measurements of the spectra of isotopomers containing $^{22}Ne$ were done in their natural abundances (~9%), while enriched $N_2O$ was used for isotopomers containing $^{15}N^{14}NO$ (98%) and $^{14}N^{15}NO$ (98%) (Cambridge Isotope Laboratories). For these isotopomers 0.25% $N_2O$ was used in the gas mixture. This was found to be adequate though not optimal.

## 6.3 RESULTS AND DISCUSSION

### 6.3.1 SPECTRAL ASSIGNMENTS AND ANALYSES

The structure of the trimer (see Figure 6.1) was assumed to be similar to those of $Ne_2$-$N_2O$ and $Ar_2$-$N_2O$ (see Chapter 5), $Ar_2$-$CO_2$ (*28*), $Ar_2$-OCS (*29*), and ArNe-$CO_2$ (*22*), all of which have been shown to have distorted tetrahedral geometries. The initial guess structure was determined from a consideration of the bond lengths and bond angles found in the constituent dimers, i.e. Ar-Ne (*30*), Ar-$N_2O$ (*23*, *31*, *32*, *33*, *34*, *35*), and Ne-$N_2O$ (*24*, *36*). Rotational constants were estimated and the resultant rotational spectrum predicted, followed by the search for the spectrum. This trimer was predicted to have $C_1$ symmetry, and all three types of rotational transitions were therefore expected. The *c*-type transitions were expected to be stronger than *a*- and *b*-type transitions. The reason is that the *c* principle inertial axis runs approximately parallel to the $N_2O$ molecular axis.

The search for the spectrum started with the isotopomer $^{40}Ar^{20}Ne$-$^{14}N_2O$. The spectra were expected to show nuclear electric quadrupole hyperfine structure due to

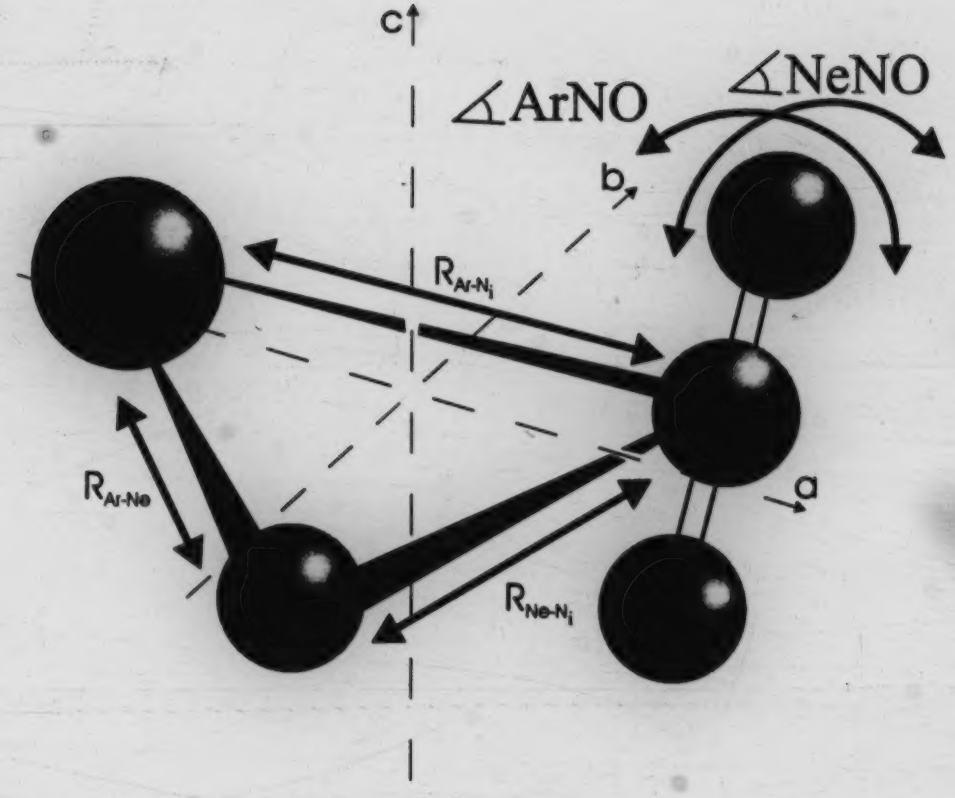


Fig. 6.1. The ArNe-$N_2O$ trimer in its principal inertial axis system.

the two $^{14}N$ nuclei in $N_2O$ (nuclear spin $I=1$). The hyperfine patterns due to both nuclei were expected to be similar to those observed in $Ne_2$-$N_2O$ and $Ar_2$-$N_2O$ (see Chapter 5). The hyperfine prediction was based upon the projection of the known quadrupole coupling tensor of the $N_2O$ monomer (*37*) onto the principal inertial axes of the complex. Using the predicted hyperfine pattern the observed transitions could be identified. The search for the spectrum was conducted alternately for $^{40}Ar^{20}Ne$-$^{14}N_2O$ and $^{40}Ar^{22}Ne$-$^{14}N_2O$, with the $^{40}Ar^{22}Ne$-$^{14}N_2O$ isotopomer being studied in its natural abundance (~9%). The first few lines that were observed were used to refine the rotational and centrifugal distortion constants. These constants were used to predict the location of other transitions which were found, measured and assigned. In total 14 rotational transitions were measured; the measured transition frequencies are given in Table A4.1 with their quantum number assignments. Using the rotational constants from these two isotopomers a refined effective ground state structure was determined and used to predict the spectra of the next four isotopomers, namely: $^{40}Ar^{20}Ne$-$^{15}N^{14}NO$, $^{40}Ar^{22}Ne$-$^{15}N^{14}NO$, $^{40}Ar^{20}Ne$-$^{14}N^{15}NO$, and $^{40}Ar^{22}Ne$-$^{14}N^{15}NO$. 14 rotational transitions were located, measured and assigned for each of these four isotopomers (see Table A4.2). The hyperfine stucture analyses were less cumbersome since only one nucleus is quadrupolar in these cases. Figure 6.2 shows the spectra of the $J_{K_aK_c}=3_{22}$-$2_{12}$ transition with the assigned hyperfine pattern for the isotopomers involving the $^{40}Ar^{20}Ne$ unit. The figure shows narrower hyperfine structure for the isotopomers involving $^{15}N^{14}NO$ as a result of the lower electric field gradient at the location of the inner N atom in $N_2O$ (*37*). Watson's A-reduction Hamiltonian in its

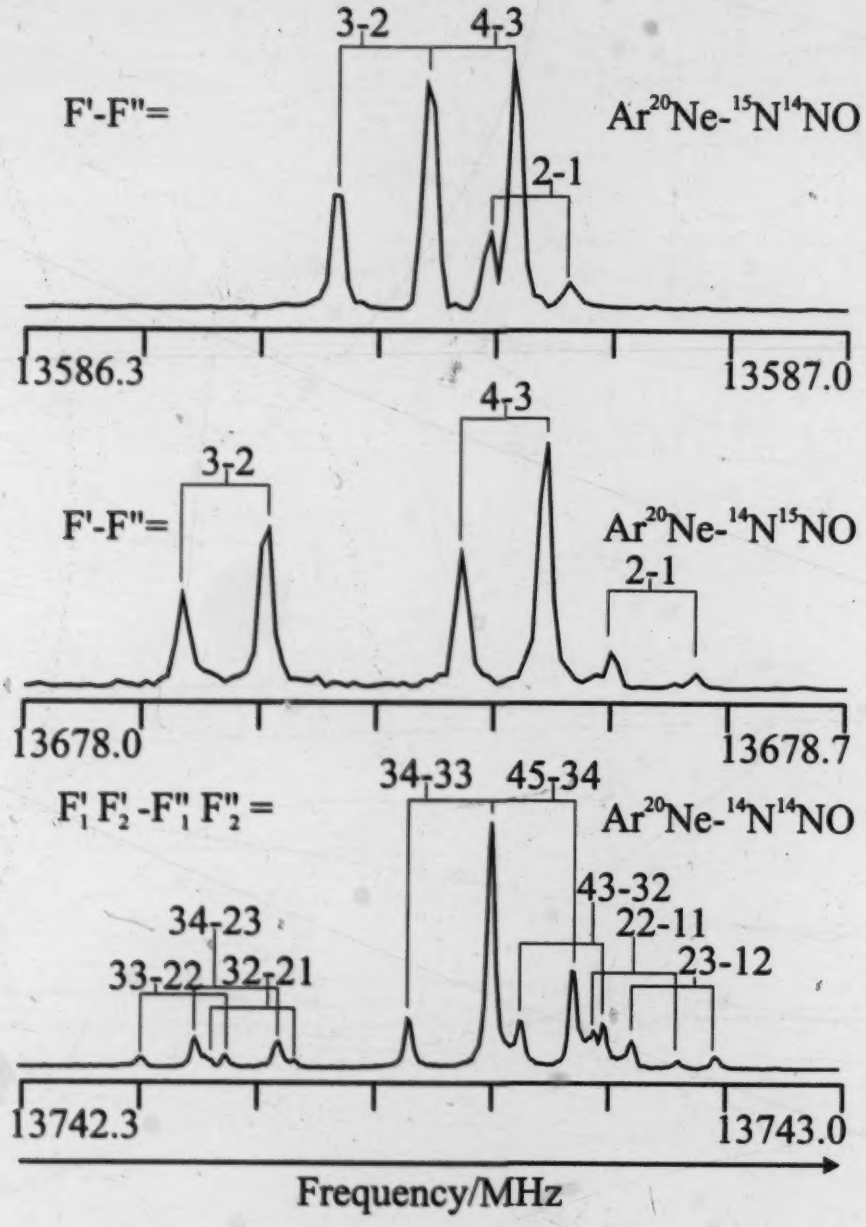


Fig. 6.2. The spectra of the $J_{K_aK_c}=3_{22}-2_{12}$ transition with the assigned hyperfine pattern for the isotopomers $^{40}Ar^{20}Ne$-($^{14}N^{14}NO$, $^{15}N^{14}NO$, and $^{14}N^{15}NO$).

I$^r$-representation (*38*) was used for the spectral analysis. Pickett's least-squares global fitting program (*39*) was used. The coupling scheme used in the hyperfine pattern analysis is based on the scheme, $I_1+J=F_1$, $F_1+I_2=F_2$, for isotopomers involving two $^{14}$N quadrupolar nuclei, and $I+J=F$, for those involving only one quadrupolar nucleus. In this scheme $I$ is the nuclear spin angular momentum, $J$ is the overall rotational angular momentum of the complex, and $F$ is the total angular momentum. The quadrupole coupling constants $\chi_{aa}$ and $\chi_{bb}$-$\chi_{cc}$ were fit to the observed hyperfine structure. The spectroscopic constansts obtained from this fit are listed in Table 6.1 including the standard deviations of the fits. The standard deviations are within the estimated errors in the frequency measurements.

## 6.3.2 STRUCTURAL ANALYSES

The spectra of the ArNe-$N_2O$ isotopomers are in accord with a distorted tetrahedral structure of the complex. The following parameters were chosen to describe its structure: the Ar-$N_{inner}$ distance ($R_{Ar\text{-}N_i}$), the Ne-$N_{inner}$ distance ($R_{Ne\text{-}N_i}$), angle $\angle ArN_iO$, angle $\angle NeN_iO$, and the dihedral angle $\angle ArN_iNe$. The structural parameters were fit to the rotational constants A, B, and C of all six isotopomers to determine a ground state effective, $r_0$, structure. This procedure was done assuming that the structure of the $N_2O$ subunit was unchanged as a result of complexation with the two rare gas atoms (*40*). The structural parameters obtained from this fit, and those that have been calculated from the ensuing geometry, are shown in Table 6.2 together with those of $Ar_2$-$N_2O$ and $Ne_2$-$N_2O$ (Chapter 5). High resolution spectra of

Table 6.1. Derived Spectroscopic Constants for ArNe-$N_2O$.

| | $Ar^{20}Ne$-$^{14}N^{14}NO$ | $Ar^{22}Ne$-$^{14}N^{14}NO$ | $Ar^{20}Ne$-$^{15}N^{14}NO$ | $Ar^{22}Ne$-$^{15}N^{14}NO$ | $Ar^{20}Ne$-$^{14}N^{15}NO$ | $Ar^{22}Ne$-$^{14}N^{15}NO$ |
|---|---|---|---|---|---|---|
| **Ground state effective rotational constants /MHz** | | | | | | |
| A | 2857.6182(3) | 2702.6752(3) | 2827.1825(4) | 2673.8569(4) | 2849.2225(4) | 2693.5988(4) |
| B | 1725.0363(2) | 1722.0556(2) | 1703.4135(2) | 1700.9418(2) | 1711.9750(2) | 1709.4644(2) |
| C | 1283.2972(2) | 1249.1642(2) | 1273.9631(2) | 1240.2035(2) | 1274.3373(2) | 1240.5586(2) |
| **Ground state average rotational constants[a] /MHz** | | | | | | |
| $A_z$ | 2835.148 | 2681.495 | 2805.153 | 2653.067 | 2826.793 | 2672.449 |
| $B_z$ | 1712.876 | 1709.746 | 1691.634 | 1689.012 | 1699.985 | 1697.324 |
| $C_z$ | 1278.457 | 1244.564 | 1269.193 | 1235.674 | 1269.577 | 1236.039 |
| **Centrifugal distortion constants /kHz** | | | | | | |
| $\Delta_J$ | 10.41(1) | 10.38(1) | 10.01(1) | 9.99(1) | 10.10(1) | 10.15(1) |
| $\Delta_{JK}$ | 105.40(4) | 99.30(4) | 102.40(5) | 96.90(5) | 104.48(5) | 98.51(5) |
| $\Delta_K$ | -34.02(7) | -36.01(8) | -32.95(9) | -35.12(9) | -32.57(9) | -34.89(9) |
| $\delta_j$ | 1.676(7) | 1.871(7) | 1.556(8) | 1.753(8) | 1.637(8) | 1.831(8) |
| $\delta_k$ | 32.72(8) | 32.75(7) | 30.61(9) | 31.31(7) | 32.20(9) | 33.11(7) |
| **$^{14}N$ nuclear quadrupole coupling constants /MHz** | | | | | | |
| $\chi_{aa}(1)$ | 0.3718(8) | 0.3738(8) | | | 0.3718(6) | 0.3716(6) |
| $\chi_{bb}(1)$ | 0.370(1) | 0.369(1) | | | 0.368(1) | 0.366(1) |
| $\chi_{aa}(2)$ | 0.122(1) | 0.128(1) | 0.1184(6) | 0.1239(6) | | |
| $\chi_{bb}(2)$ | 0.126(2) | 0.119(2) | 0.132(1) | 0.124(1) | | |
| **Planar moments /amu Å$^2$** | | | | | | |
| $P_a$ | 254.9635 | 255.5280 | 257.3136 | 257.8033 | 257.2049 | 257.6970 |
| $P_b$ | 138.8495 | 149.0458 | 139.3847 | 149.6936 | 139.3770 | 149.6833 |
| $P_c$ | 38.0038 | 37.9464 | 39.3724 | 39.3140 | 37.9975 | 37.9390 |

Table 6.1. (continued)

| | $Ar^{20}Ne$-$^{14}N^{14}NO$ | $Ar^{22}Ne$-$^{14}N^{14}NO$ | $Ar^{20}Ne$-$^{15}N^{14}NO$ | $Ar^{22}Ne$-$^{15}N^{14}NO$ | $Ar^{20}Ne$-$^{14}N^{15}NO$ | $Ar^{22}Ne$-$^{14}N^{15}NO$ |
|---|---|---|---|---|---|---|
| Standard deviation /kHz | | | | | | |
| $\sigma$ | 1.7 | 1.4 | 1.3 | 1.5 | 1.1 | 1,1 |

[a] Derived from the force field analysis by subtracting off the harmonic parts of the $\alpha$-constants from the ground state effective values.

[c] Derived from the ground state average rotational constants.

Table 6.2. Structural Parameters of ArNe-$N_2O$, $Ar_2$-$N_2O$, $Ne_2$-$N_2O$, and the relevant Dimers.

| | $r_0$ | | | | $r_z$ |
|---|---|---|---|---|---|
| Parameter | ArNe-$N_2O$ | $Ar_2$-$N_2O$[c] | $Ne_2$-$N_2O$[c] | Dimers | |
| $R(Ar\text{-}N_{inner})$[a]/Å | 3.4602 | 3.4742 | -. | 3.4686 (Ar-$N_2O$)[d] | 3.4660 |
| $R(Ne\text{-}N_{inner})$[a]/Å | 3.2196 | -. | 3.2336 | 3.237 (Ne-$N_2O$)[e] | 3.2254 |
| R(Ar-Ne)[b]/Å | 3.6637 | -. | -. | 3.607 (Ar-Ne)[f] | 3.6802 |
| $\angle(ArN_{inner}O)$[a]/(deg) | 79.97 | 79.55 | -. | 82.92 (Ar-$N_2O$)[d] | 82.61 |
| $\angle(NeN_{inner}O)$[a]/(deg) | 77.82 | -. | 77.60 | 80.39 (Ne-$N_2O$)[e] | 80.46 |
| $\angle(ArN_{inner}Ne)$[a]/(deg) | 66.41 | -. | -. | -. | 59.82 |

[a] Obtained from the structural fit as described in the text. $N_2O$ bondlengths were fixed at R(NN)=1.1278Å, R(NO)=1.1923Å, and $R(N_{inner}$-c.m. of $N_2O)$=0.0745Å as in ref.40.

[b] Calculated from the resulting geometry after the structural fit described in the text and the $N_2O$ bond lengths as listed above.

[c] See chapter 5, [d] See ref. 36, [e] See ref. 24, [f] See ref. 30.

all three dimer subunits of the ArNe-$N_2O$ trimer have been reported previously. These are the Ar-Ne (*30*), Ar-$N_2O$ (*23, 31, 32, 33, 34, 35*), and Ne-$N_2O$ (*24, 36*) dimers. The resulting structural parameters are also given in Table 6.2 for comparison purposes. There is indication for a slight shrinkage of the Ar-$N_i$ and Ne-$N_i$ bonds as compared to the corresponding dimer values. The differences in dimer and trimer bond lengths are rather small, especially in light of the relatively large uncertainities associated with these values. However, a similar trend with similar variations in bond lengths was observed in ArNe-$CO_2$ (*22*). There is thus growing confidence that there is a real shrinkage in the Ne-$N_i$ and Ar-$N_i$ bonds, that can be attributed to three-body non-additive effects. A clearer manifestation of these effects

can be found in the lengthening of the Ar-Ne bond in the trimer as compared to the Ar-Ne dimer. The same effect was observed previously in ArNe-$CO_2$ (*22*).

We also performed a harmonic force field approximation as described in section 6.3.4. This analysis provides the harmonic contributions of the vibrations to the rotational constants. When these contributions are subtracted from the ground state effective rotational constants, we obtain the ground state average rotational constants, i.e. constants that are partly corrected for the effects of zero-point vibrations. The resulting rotational constants are given in Table 6.1. A structural fit was carried out to these rotational constants in the same way as was described for the effective structure. The resulting structural parameters are listed under $r_z$ in Table 6.2.

### 6.3.3 $^{14}$N NUCLEAR QUADRUPOLE HYPERFINE STRUCTURE

The coupling of the spins of the $^{14}$N nuclei with the overall rotation of the complex results in a splitting of the rotational energy levels into several components (*41*). An analysis of the resulting $^{14}$N nuclear quadrupole hyperfine structures of the rotational transitions yields nuclear quadrupole coupling constants $\chi_{aa}$, $\chi_{bb}$, $\chi_{cc}$, which, in turn, provide information about structure, large amplitude motions, and electronic perturbation at the site of the $^{14}$N nucleus upon complex formation. In comparatively rigid complexes, the coupling constants $\chi_{gg}$ can be regarded as projections of the monomer coupling constants $\chi_{mon}$ onto the principal inertial axes of the complex:

$$\chi_{gg}=(1/2)\chi_{mon}<3\cos^2\theta_g-1>, \qquad (6.1)$$

where g=*a*,*b* or *c* and $\theta_g$ is the angle between the g-inertial axis of the complex and the monomer axis. This expression assumes that $\chi_{mon}$ is unchanged by complex formation, i.e. that the field gradient at the site of the $^{14}N$ nucleus does not change upon complex formation.

An important consideration in the analysis and interpretation of the coupling constants in van der Waals complexes is the choice of the proper axis system. In particular, Hutson and Ernesti (*42*, *43*) have pointed out that the use of an Eckart axis system for the interpretation of coupling constants in van der Waals complexes is most appropriate. The appropriate formalism for the application of such an axis system has thus far, however, not been extended beyond dimer systems. Hence, in this work we present a simplified interpretation using projections of the monomer constants onto the instantaneous inertial axes of the complex. The coupling constants of the $N_2O$ monomer are known for both the terminal and middle N atoms (37). These are -0.77376(27) MHz and -0.26758(38) MHz for the outer and inner N nuclei, respectively.

The following structural analysis is based on the coupling constants of the outer $^{14}N$ nucleus, since it has been shown that those of the inner $^{14}N$ nucleus can be significantly affected by electronic perturbation of the complex binding partner (*24*, *35*, *44*, *45*, *46*). The values of $\theta_g$ obtained from Equation 6.1 are $\theta_a$=83.5(0.3)°, $\theta_b$=96.9(0.4)°, and $\theta_c$=9.5(0.6)° for the outer N atom. The errors shown in the brackets reflect the uncertainties in the coupling constants of the complex. The values calculated from the structural parameters shown in Table 6.2 ($r_0$ structure) are

$\theta_a$=80.8°, $\theta_b$=102.9°, and $\theta_c$=9.2°. The relatively small discrepancies between $^{14}N$ values and $r_0$ values are attributable to the choice of axis system and to the different averaging over the large amplitude motions for moments of inertia and nuclear quadrupole coupling constants.

Clear indication about an electronic perturbation at the site of the central $^{14}N$ nucleus can be found by comparing the ratios of the complex coupling constants $\chi_{gg}$, g=*a*,*b*,*c*, over the respective monomer coupling constants $\chi_G$, G=X, Y, Z, of outer and inner $^{14}N$ nuclei. Values for these ratios are compiled in Table 6.3, together with those of Ne-$N_2O$ (*24*) and Ar-$N_2O$ (*35*). In the limit of no electronic perturbation, the values $\chi_{gg}$ /$\chi_{G(mon)}$ would be the same for the outer and inner $^{14}N$ nuclei. In all instances, however, the central $^{14}N$ values are significantly smaller. This is consistent with previous observations of significant electronic perturbation at the site of the inner $^{14}N$ in other $N_2O$ containing complexes (*24*, *35*, *44*, *45*, *46*).

It is instructive to compare the coupling constants of the trimer with those of the respective dimer subunits, i.e. Ar-$N_2O$ (*35*) and Ne-$N_2O$ (24). Specifically, the values $\chi_{cc}$ /$\chi_{Z(mon)}$ of the trimer can be compared with $\chi_{bb}$ /$\chi_{Z(mon)}$ of the dimer since these correspond to components that are approximately parallel to the $N_2O$ subunit and approximately perpendicular to the rare gas-$N_2O$ bonds (see Figures 3.3 and 4.2) The ratios of the values $\chi_{gg}$ /$\chi_{G(mon)}$ of outer and inner $^{14}N$ nuclei are also given in Table 6.3 for the ArNe-$N_2O$ trimer and the dimer subunits. The deviation of these values from one is a measure of the electronic perturbation at the inner $^{14}N$ nucleus. Within the error limits, the deviation of this ratio from one in ArNe-$N_2O$ equals the

Table 6.3.[a] Comparison of the $^{14}N$ nuclear quadrupole coupling constants of ArNe-$N_2O$ with those of the dimers Ar-$N_2O$ and Ne-$N_2O$

| | ArNe-$N_2O$ | | Ar-$N_2O$[b] | | Ne-$N_2O$[c] | | |
|---|---|---|---|---|---|---|---|
| | $N_o$ | $N_i$ | $N_o$ | $N_i$ | $N_o$ | $N_i$ | $N_o/N_i$ |
| $\chi_{aa}/\chi_{X(mon)}$ | 0.961(2) | 0.912(8) | | | | | |
| $\chi_{bb}/\chi_{Y(mon)}$ | 0.956(3) | 0.942(15) | | | | | |
| $\chi_{cc}/\chi_{Z(mon)}$ | 0.959(1) | 0.927(8) | | | | | 1.036(9) |
| $\chi_{bb}/\chi_{Z(mon)}$ | | | 0.981(1) | 0.964(1) | | | 1.018(1) |
| $\chi_{bb}/\chi_{Z(mon)}$ | | | | | 0.977(1) | 0.965(1) | 1.012(1) |

[a] $N_o$=outer N, $N_i$=inner N.
[b] Ref. 24.
[c] Ref. 36.

sum of these deviations in Ar-$N_2O$ and Ne-$N_2O$. This is expected in the limit of pairwise additivity. The errors associated with the nuclear quadrupole coupling constants appear thus to be too large for an unambiguous detection of three-body effects.

## 6.3.4 HARMONIC FORCE FIELD APPROXIMATION

An approximation of the van der Waals force field in ArNe-$N_2O$ was obtained by an analysis based on the quartic centrifugal distortion constants, similar to that described in Chapters 3-5. ArNe-$N_2O$ has no axes or planes of symmetry, and belongs to the $C_1$ point group. The nine vibrational modes in this complex can be approximated by the symmetry coordinates given in Table 6.4. The vibrational modes are: the N-N stretch ($\nu_1$) with force constant $f_{11}$, the N-O stretch ($\nu_2$) associated with force constant $f_{22}$, the in-plane N-N-O linear bend ($\nu_3$) with force constant $f_{33}$, the Ar-$N_i$-Ne

Table 6.4. The Harmonic Force Field of ArNe-$N_2O$

| Structure Parameters | |
|---|---|
| r(Ar-Ne)=r=3.6238Å | |
| $r(Ar\text{-}N_{inner})=r_1=3.4703$Å, $r(Ne\text{-}N_{inner})=r_2=3.2387$Å | |
| $r(NN)=r_3=1.1278$Å, $r(NO)=r_4=1.1923$Å | |
| $\sphericalangle(ArNN)=\alpha_1=99.84°$, $\sphericalangle NeNN)=\beta_1=102.37°$ | |
| $\sphericalangle(ArNO)=\alpha_2=80.16°$, $\sphericalangle NeNO)=\beta_2=77.63°$ | |
| **Symmetry Coordinates** | |
| $S_1=\Delta r_3$, $S_2=\Delta r_4$, $S_3$=in-plane NNO linear bend | |
| $S_4=(1/2)^{1/2}(\Delta r_1+\Delta r_2)$, $S_5=\Delta r$, $S_6=(1/2)(\Delta\alpha_1-\Delta\alpha_2+\Delta\beta_1-\Delta\beta_2)$ | |
| $S_7$=out-of-plane NNO linear bend, $S_8=(1/2)^{1/2}(\Delta r_1-\Delta r_2)$ | |
| $S_9=(1/2)(\Delta\alpha_1-\Delta\alpha_2-\Delta\beta_1+\Delta\beta_2)$ | |
| **Harmonic Force Constants** | |
| $f_{11}$/mdyn Å$^{-1}$ | 18.1904[a] |
| $f_{12}$/mdyn Å$^{-1}$ | 1.024[a] |
| $f_{22}$/mdyn Å$^{-1}$ | 12.0308[a] |
| $f_{33}$/mdyn Å rad$^{-2}$ | 0.666[a] |
| $f_{44}$/mdyn Å$^{-1}$ | 0.022(5) |
| $f_{55}$/mdyn Å$^{-1}$ | 0.0032(1) |
| $f_{46}$/mdyn rad$^{-1}$ | 0.0 |
| $f_{66}$/mdyn Å rad$^{-2}$ | 0.008425[b] |
| $f_{77}$/mdyn Å rad$^{-2}$ | 0.666[a] |
| $f_{88}$/mdyn Å$^{-1}$ | 0.018(2) |
| $f_{89}$/mdyn Å rad$^{-2}$ | 0.0 |
| $f_{99}$/mdyn Å rad$^{-2}$ | 0.0065(6) |

Predicted van der Waals Vibrational Frequencies (cm$^{-1}$)

| $\nu_4$ | $\nu_5$ | $\nu_8$ | $\nu_9$ |
|---|---|---|---|
| 53.0 | 20.1 | 37.1 | 18.3 |

[a] Constrained at the values of ref.47.
[b] Constrained. See discussion in the text.

"symmetric" stretch in which the Ar-$N_i$ and Ne-$N_i$ bonds are stretching in the same direction ($\nu_4$) whose force constant is designated $f_{44}$, the Ar-Ne stretch ($\nu_5$) with the corresponding force constant $f_{55}$, the ArNe-$N_2O$ "wag" ($\nu_6$) with force constant $f_{66}$, where both Ar and Ne atoms bend towards $N_2O$ in the same direction, the out-of-plane N-N-O bend ($\nu_7$) and its force constant $f_{77}$, the Ar-$N_i$-Ne asymmetric stretch ($\nu_8$)

with a force constant $f_{88}$, and the ArNe-$N_2O$ "twist" ($\nu_9$) in which the Ar and Ne atoms are moving towards $N_2O$ in opposite directions with a force constant labelled $f_{99}$. Some of these van der Waals vibrations are shown schematically in Figure 6.1. In the force field analysis the force constants of $N_2O$ monomer were fixed at their monomer values (*47*). These values are given in Table 6.4.

Four force constants, associated with the van der Waals vibrational modes of the complex were fit to six sets of quartic centrifugal distortion constants. The force constant $f_{66}$ could not be determined in the analysis and its value was estimated from the bending force constants in Ne-$N_2O$ (*24*) and Ar-$N_2O$ (*23*). This was taken as the arithmetic mean of the two force constants of the above dimers and fixed in the analysis. The off-diagonal force constants also could not be determined and were thus constrained to zero in the analysis. The resulting force constants are given in Table 6.4, together with the van der Waals vibrational frequencies. The stretching force constants $f_{44}$ and $f_{88}$ may be compared with the corresponding stretching force constants in Ar-$N_2O$ ($f_s$=0.020(3) mdyn $Å^{-1}$) (*23*) and Ne-$N_2O$ ($f_s$=0.0089(7) mdyn $Å^{-1}$) (*24*). The arithmetic mean of $f_{44}$ and $f_{88}$ agrees with the value of the Ar-$N_2O$ force constant within the error limits. This indicates that these stretching modes are dominated by contributions from the Ar-$N_i$ vibration, and this can possibly be attributed to the presence of three-body interactions. The sum of $f_{66}$ and $f_{99}$, the ArNe-$N_2O$ bending force constants, on the other hand, equals the arithmetic mean of the bending force constants in Ar-$N_2O$ ($f_b$=0.023(3) mdyn Å $rad^{-2}$) (*23*) and Ne-$N_2O$ ($f_b$=0.0107(4) mdyn Å $rad^{-2}$) (*24*). This is expected in the limit of pairwise

additivity. The value of 0.0032 mdyn $Å^{-1}$ for $f_{55}$, the Ar-Ne stretch force constant, results in an Ar-Ne vibrational frequency of 20 $cm^{-1}$. This compares favourably with the value of 19 $cm^{-1}$ for the free Ar-Ne dimer, estimated from a potential energy calculation (*48*).

The observed and calculated quartic centrifugal distortion constants from the harmonic force field analysis are compared in Table 6.5. The harmonic force field approximation is seen to reproduce the distortion constants very well despite the drastic approximation made in the analysis. This is especially true for the reproduction of their variation with isotopomer. This serves as a further confirmation of the spectral assignment since the variations of the centrifugal distortion constants are mainly geometry and mass dependent.

## 6.4 CONCLUDING REMARKS

We have studied the mixed rare gas-rare gas-$N_2O$ van der Waals trimer, ArNe-$N_2O$, for the first time. Rotational spectra of six isotopomers of the trimer were measured and analysed to yield accurate rotational and centrifugal distortion constants as well as $^{14}N$ nuclear quadrupole coupling constants. The nuclear quadrupole coupling constants were analysed in terms of the electronic perturbation at the site of the central $^{14}N$ nucleus. However, no clear indication about the presence of three-body interactions was found. It appears, from the results of the force field analysis, that the ArNe-$N_2O$ stretching modes, $\nu_4$ and $\nu_8$, are dominated by the Ar-$N_i$

Table 6.5. Comparison of observed and calculated centrifugal distortion constants (kHz).

| Constant | Obs.[a] | Calc.[b] | Obs.[a] | Calc.[b] | Obs.[a] | Calc.[b] |
|---|---|---|---|---|---|---|
| | $Ar^{20}Ne$-$^{14}N^{14}NO$ | | $Ar^{22}Ne$-$^{14}N^{14}NO$ | | $Ar^{20}Ne$-$^{15}N^{14}NO$ | |
| $\Delta_J$ | 10.41 | 10.23 | 10.38 | 10.40 | 10.01 | 9.78 |
| $\Delta_{JK}$ | 105.40 | 103.95 | 99.30 | 100.62 | 102.40 | 99.48 |
| $\Delta_K$ | -34.02 | -57.64 | -36.01 | -62.25 | -32.95 | -52.36 |
| $\delta_j$ | 1.676 | 1.965 | 1.871 | 2.141 | 1.556 | 1.843 |
| $\delta_k$ | 32.72 | 32.31 | 32.75 | 34.54 | 30.61 | 29.80 |
| | $Ar^{22}Ne$-$^{15}N^{14}NO$ | | $Ar^{20}Ne$-$^{14}N^{15}NO$ | | $Ar^{22}Ne$-$^{14}N^{15}NO$ | |
| $\Delta_J$ | 9.99 | 9.88 | 10.10 | 9.94 | 10.15 | 10.07 |
| $\Delta_{JK}$ | 96.90 | 96.66 | 104.48 | 102.07 | 98.51 | 99.06 |
| $\Delta_K$ | -35.12 | -57.17 | -32.57 | -54.24 | -34.89 | -59.10 |
| $\delta_j$ | 1.753 | 1.985 | 1.637 | 1.908 | 1.831 | 2.059 |
| $\delta_k$ | 31.31 | 32.10 | 32.20 | 31.72 | 33.11 | 33.92 |

[a] These values are those found in Table 6.1.

[b] Calculated from the force constants derived from the centrifugal distortion constants of all the measured isotopomers.

stretch. This can possibly be attributed to three-body interactions. The small lengthening of the Ne-$N_i$ and Ar-$N_i$ bonds and the significant lengthening of the Ar-Ne bond in the trimer as compared to the respective dimers units are clear manifestations of three-body non-additive contributions to the total interaction energy.

## REFERRENCES


1. E. A. Colbourn and A. E. Douglas, *J. Chem. Phys.* **65,** 1741 (1976).

2. R. A. Aziz, *J. Chem. Phys.* **99,** 4518 (1993).

3. J. M Hutson, *J. Chem. Phys.* **96,** 4237 (1992).

4. J. M. Hutson, *J. Chem. Phys.* **96,** 6752 (1992).

5. R. J. Le Roy and J. M. Hutson, *J. Chem. Phys.* **86,** 837 (1987).

6. R. C. Cohen and R. J. Saykally, *J. Chem. Phys.* **98,** 6007 (1993).

7. C. A. Schmuttenmaer, R. C. Cohen, and R. J. Saykally, *J. Chem. Phys.* **101,** 146 (1994).

8. H. S. Gutowsky, T. D. Klots, C. Chuang, C. A. Schmuttenmaer, and T. Emilsson, *J. Chem. Phys.* **86,** 569 (1987).

9. T. D. Klots, C. Chuang, R. S. Ruoff, T. Emilsson, and H. S. Gutowsky, *J. Chem. Phys.* **86,** 5315 (1987).

10. T. D. Klots and H. S. Gutowsky, *J. Chem. Phys.* **91,** 63 (1989).

11. H. S. Gutowsky, T. D. Klots, and C. E. Dykstra, *J. Chem. Phys.* **93,** 6216 (1990).

12. G. Chałasiński, M. M. Szczęśniak, and B. Kukawska-Tarnawska, *J. Chem. Phys.* **94,** 6677 (1991).

13. M. M. Szczęśniak, G. Chałasiński, and P. Piecuch, *J. Chem. Phys.* **99,** 6732 (1993).

14. S. M. Cybulski, M. M. Szczęśniak, and G. Chałasiński, *J. Chem. Phys.* **101,** 10708 (1994).

15. A. Ernesti and J. M. Hutson, *Phys. Rev.* A **51,** 239 (1995).

16. A. R. Cooper and J. M. Hutson, *J. Chem. Phys.* **98,** 5337 (1993).

17. A. Ernesti and J. M. Hutson, *J. Chem. Phys.* **106,** 6288 (1997).

18. B. M. Axilrod and E. Teller, *J. Chem. Phys.* **11,** 299 (1943).

19. W. J. Meath and M. Koulis, *J. Molec. Struct.* **226,** 1 (1991).

20. G. Chałasiński and M. M. Szczęśniak, *Chem. Rev.* **94,** 1723 (1994).

21. Y. Xu, G. S. Armstrong, and W. Jäger, *J. Chem. Phys.* **110,** 4354 (1999).

22. Y. Xu and W. Jäger, *Molec. Phys.* **93,** 727 (1998).

23. M. S. Ngarī and W. Jäger, *J. Mol. Spectrosc.* **192,** 452 (1998).

24. M. S. Ngarī and W. Jäger, *J. Mol. Spectrosc.* **192,** 320 (1998).

25. T. J. Balle and W. H. Flygare, *Rev. Sci. Instrum.* **52,** 33 (1981).

26. Y. Xu and W. Jäger, *J. Chem. Phys.* **106,** 7968 (1997).

27. V. N. Markov, Y. Xu, and W. Jäger, *Rev. Sci. Instrum.* **69,** 4061 (1998).

28. Y. Xu, W. Jäger, and M. C. L. Gerry, *J. Mol. Spectrosc.* **157,** 132 (1993).

29. Y. Xu, M. C. L. Gerry, J. P. Connelly, and B. J. Howard, *J. Chem. Phys.* **98,** 2735 (1993).

30. J.-U. Grabow, A. S. Pine, G. T. Fraser, F. J. Lovas, T. Emilsson, E. Arunan, and H. S. Gutowsky, *J. Chem. Phys.* **102,** 1181 (1995).

31. C. H. Joyner, T. A. Dixon, F. A. Baiocchi, and W. Klemperer, *J. Chem. Phys.* **75,** 5285 (1981).

32. J. Hodge, G. D. Hayman, T. R. Dyke, and B. J. Howard, *J. Chem. Soc. Faraday Trans. 2,* **82,** 1137 (1986).

33. T. A. Hu, E. L. Chappel, and S. W. Sharpe, *J. Chem. Phys.* **98,** 6162 (1993).

34. H. O. Leung, *Chem. Commun.* **1996,** 2525 (1996).

35. H. O. Leung, D. Gangwani, and J.-U. Grabow, *J. Mol. Spectrosc.* **184,** 106 (1997).

36. W. A. Herrebout, H.-B. Qian, H. Yamaguchi, and B. J. Howard, *J. Mol. Spectrosc.* **189,** 135 (1998).

37. J. M. L. J. Reinartz, W. L. Meerts, and A. Dymanus, *Chem. Phys.* **31,** 19 (1978).

38. J. K. G. Watson, *Vibrational Spectra and Structure: A Series of Advances,* (Durig, J. R., Ed), Vol. 6, Elsevier, New York, p.1. 1977.

39. H. M. Pickett, *J. Mol. Spectrosc.* **148,** 371 (1991).

40. C. C. Costain, *J. Chem. Phys.* **29,** 864 (1958).

41. W. Gordy and R. L. Cook, *Microwave Molecular Spectra*, (New York: Wiley). 1984.

42. A. Ernesti and J. M. Hutson, *J. Chem. Phys.*, **101,** 5438 (1994).

43. J. M. Hutson, *Molec. Phys.* **84,** 185 (1995).

44. H. O. leung, *J. Chem. Phys.* **107,** 2232 (1997).

45. H. O. Leung, *J. Chem. Phys.* **108,** 3955 (1998).

46. H. O. Leung, *J. Chem. Phys.* **110,** 4394 (1999).

47. I. Suzuki, *J. Mol. Spectrosc.* **32,** 54 (1969).

48. D. A. Barrow, and R. A. Aziz, *J. Chem. Phys.*, **89,** 6189 (1988).

# CHAPTER SEVEN

# ROTATIONAL SPECTROSCOPIC INVESTIGATION OF THE WEAK INTERACTION BETWEEN CO AND $N_2O$[1]

## 7.1 INTRODUCTION

High resolution spectroscopic investigations of a variety of complexes containing either CO or $N_2O$, for example, CO-Ar (*1*), CO-$N_2$ (*2*), CO-$CO_2$ (*3*), and $CO_2$-$N_2O$ (*4*, *5*) have been reported in the past. This interest in weak interactions involving nitrous oxide ($N_2O$) and carbon monoxide (CO) is in part a result of the various roles these species play in the atmospheric environment. CO and $N_2O$ are two important greenhouse gases that cause the earth to retain heat and their atmospheric abundances have been shown to be increasing (*6*). The spectroscopic studies can provide important information about weak interactions that involve these two molecules. $N_2O$ containing complexes have been the target systems for a series of recent high resolution rotational spectroscopic investigations, with the aim to understand how the electronic structure of $N_2O$ is affected by another molecule (*5*, *7*, *8*, *9*).

So far, there are two reports on high resolution spectra of the CO-$N_2O$ complex (*10*, *11*). Utilizing infrared diode laser and molecular beam techniques, Xu and McKellar (*10*) studied the *a*-type transitions of CO-$N_2O$ in the carbon monoxide stretching region around 2150 $cm^{-1}$, while Qian and Howard (*11*) reported the

---

[1] A version of this chapter has been accepted for publication. M. S. Ngarí, Y. Xu, and W. Jäger, 1999. *Journal of Molecular Spectroscopy*. Copyright © 1999 by Academic Press, Inc.

observation of *b*-type transitions of the complex in the region of the $\nu_3$ vibrational mode of the $N_2O$ monomer. It was established from these investigations that the CO-$N_2O$ complex has a T-shaped geometry, with CO forming the leg of the T. However, it was not possible to determine the exact structure, in particular the orientation of CO and the tilting direction of $N_2O$ in the complex, mainly because of the lack of isotopic data.

This Chapter describes the first high resolution rotational spectroscopic observation of the complex. Five isotopomers, namely, $^{12}C^{16}O$-$^{14}N^{14}NO$, $^{13}C^{16}O$-$^{14}N^{14}NO$, $^{13}C^{18}O$-$^{14}N^{14}NO$, $^{13}C^{16}O$-$^{15}N^{14}NO$, and $^{13}C^{16}O$-$^{14}N^{15}NO$, were investigated using a pulsed molecular beam cavity FTMW spectrometer. The nuclear quadrupole hyperfine structures due to the two $^{14}N$ nuclei were observed and analyzed. The resulting nuclear quadrupole coupling constants indicate that there is a considerable distortion of the electronic structure of $N_2O$ as a result of complex formation. Possible sources of this distortion are discussed. The isotopic data made it possible to determine the structure of the complex, and, in particular, to establish the orientation of CO and the tilting direction of the $N_2O$ subunit within the complex.

## 7.2 EXPERIMENTAL DETAILS

The spectra were recorded with a pulsed molecular beam FTMW spectrometer, which has been described in detail elsewhere (*12*, *13*), and also in Chapter 2. The sample was injected along the MW cavity axis, parallel to the MW propagation direction (*14*). As a result, each line is split into two Doppler

components. Typical line widths are 7 kHz (full width at half height) and the estimated measurement accuracy is ±1 kHz.

The complex was generated using a sample gas mixture of 0.5% CO and 0.5% $N_2O$ in Ne carrier gas at a backing pressure of ~3atm. Isotopomers with $^{13}CO$ and $^{13}C^{18}O$ were measured using enriched $^{13}CO$ (Cambridge Isotope Laboratories Inc., 99% $^{13}C$ and 10% $^{18}O$); enriched $^{14}N^{15}NO$ and $^{15}N^{14}NO$ (Cambridge Isotope Laboratories Inc., 98% $^{15}N$) were used for the isotopomers containing these two labelled subunits.

## 7.3 RESULTS AND DISCUSSION

### 7.3.1 SPECTRAL ASSIGNMENTS AND ANALYSES

The rotational constants from the previous infrared studies (*10,11*) were used to predict the pure rotational spectrum of the normal isotopomer of CO-$N_2O$. For a T-shaped planar structure with CO forming the leg and $N_2O$ forming the top, one expects to observe both *a*- and *b*-type transitions, with the *a*-type dipole moment mainly provided by the CO subunit and the *b*-type dipole moment largely contributed by the $N_2O$ subunit (see Figure 7.1). Since the CO monomer dipole moment was determined to be 0.1098 Debye (*15*), comparable to that of the $N_2O$ monomer (0.16088 Debye) (*16*), one expects similar intensities for both *a*- and *b*-type transitions in the semirigid rotor limit. If the complex were non-planar, one should also be able to observe *c*-type transitions. Furthermore, each rotational transition is expected to split into a fairly complex hyperfine pattern due to the two quadrupolar

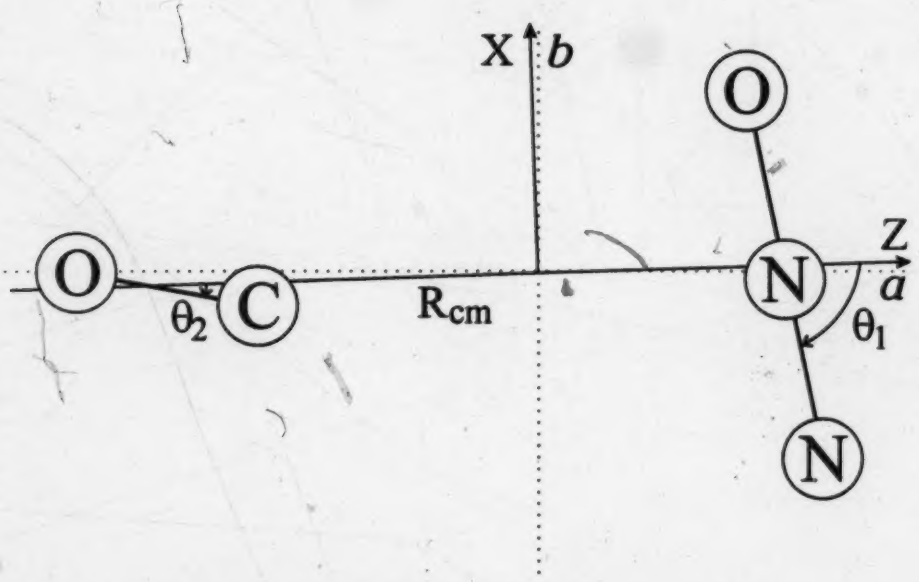


Fig. 7.1. The effective structure of CO-$N_2O$ as determined from the structural analysis. *a* and *b* are the principal inertial axes. Also shown is the coordinate system used in the analysis for CO-$N_2O$. The relative positions of the CO and $N_2O$ subunits in the complex are defined by $\mathbf{R}_{cm}$, the distance between the centers of mass of CO and $N_2O$, and the angles $\theta_1$ and $\theta_2$ as depicted. The Z-axis is along the intermolecular axis of the complex, while the X- and Y-axes are perpendicular to the Z-axis in the in- and out-of-plane directions, respectively.

$^{14}N$ nuclei. Even though the distortion constants, in particular $D_K$ and $d_2$, were not well determined in the infrared studies, the assignments of the observed transitions were relatively straightforward using the nuclear quadrupole hyperfine patterns to aid identification. A first order, two quadrupolar nuclei program was used to provide initial predictions of the hyperfine structure. In some instances, extra transitions were observed and some of these transitions were later identified as transitions arising from Ne-$N_2O$ (7) by removing CO from the sample gas mixture. Figure 7.2 shows an example rotational transition $J_{K_aK_c}=1_{11}$-$0_{00}$ of $^{12}C^{16}O$-$^{14}N^{14}NO$ with $^{14}N$ nuclear quadrupole hyperfine components as a demonstration of the resolution and the sensitivity achieved.

The spectral searches for the other minor isotopomers were guided by the structure proposed in the previous infrared studies (*10,11*). The spectra of the $^{13}C^{16}O$-$^{14}N^{14}NO$ and $^{13}C^{18}O$-$^{14}N^{14}NO$ isotopomers show hyperfine structure patterns similar to those of the normal isotopomer, while the spectra of the other two minor isotopomers containing either $^{14}N^{15}NO$ or $^{15}N^{14}NO$ have much simpler patterns since only one quadrupolar nucleus is involved.

In all, 25 rotational transitions with 385 nuclear hyperfine components were measured and analyzed for the $^{12}C^{16}O$-$^{14}N^{14}NO$ isotopomer. There are 18 rotational transitions with 269 hyperfine components for $^{13}C^{16}O$-$^{14}N^{14}NO$, 18 rotational transition with 238 hyperfine components for $^{13}C^{18}O$-$^{14}N^{14}NO$, and 14 rotational transitions with 73 hyperfine components for the other two isotopomers containing $^{14}N^{15}NO$ or $^{15}N^{14}NO$. All the measured transition frequencies are listed in Tables A5.1 and A5.2,

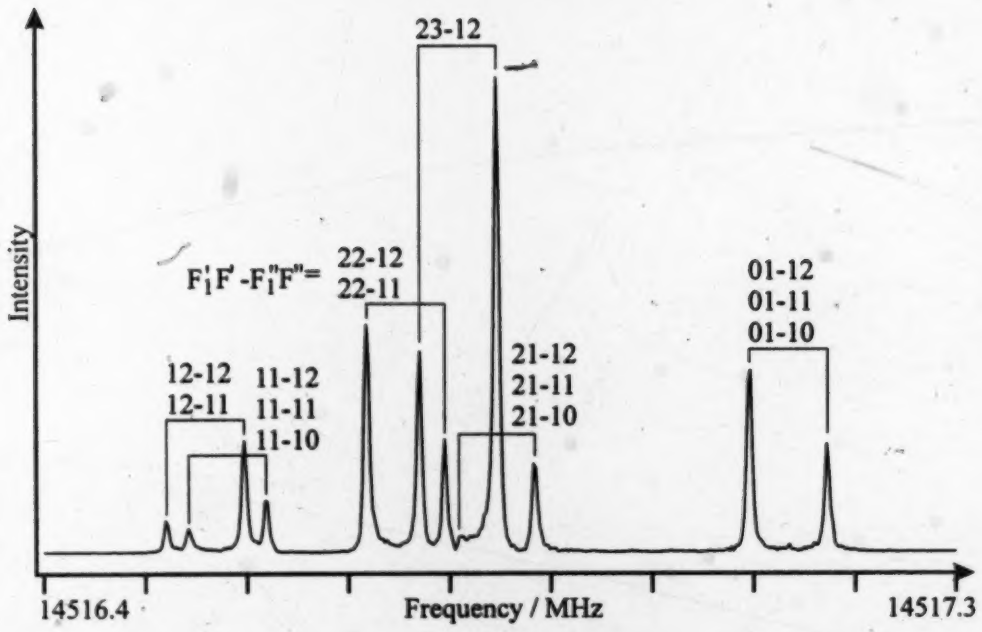


Fig. 7.2. Observed spectrum of the rotational transition $J_{K_aK_c}=1_{11}-0_{00}$ of $^{12}C^{16}O-{}^{14}N^{14}NO$, showing the nuclear quadrupole coupling components due to the two $^{14}N$ nuclei. The spectrum was recorded using 50 averaging cycles with 60 ns sampling interval, 4K data points and an 8K FT.

along with their quantum number assignments. In Table A5.1, the quantum numbers F and $F_1$ are given in the coupling scheme: $\mathbf{F}=\mathbf{F}_1+\mathbf{I}_2$, $\mathbf{F}_1=\mathbf{J}+\mathbf{I}_1$; where $\mathbf{I}_1$ and $\mathbf{I}_2$ are the nuclear spin angular momenta of the terminal and the central $^{14}N$ nuclei, respectively, and **J** is the rotational angular momentum. In cases of the $^{14}N^{15}NO$ or $^{15}N^{14}NO$ containing isotopomers (see Table A5.2), the quantum number F is given in the coupling scheme: $\mathbf{F}=\mathbf{J}+\mathbf{I}$, where **I** represents the spin angular momentum of the $^{14}N$ nucleus involved. No extra splittings due to $^{15}N$ (spin 1/2) were observed. All the data were analyzed using Pickett's complete diagonalization program (*17*) including the interactions with one or two quadrupolar nuclei when appropriate. Watson's S-reduction, $I^r$-representation Hamiltonian was used (*18*). The resulting spectroscopic constants are listed in Table 7.1. The standard deviations of the fits are in the order of 1.2 to 1.9 kHz, comparable to the estimated experimental measurement accuracy.

## 7.3.2 NUCLEAR QUADRUPOLE COUPLING CONSTANTS

The effect of complex formation on the electric field gradient in $N_2O$ has been the focal point of several FTMW studies of $N_2O$ containing complexes (*5, 7, 8, 9*). It was found, in general, that the electric field gradient at the site of the central $^{14}N$ nucleus is considerably perturbed upon complex formation. For example, the values of the out-of-plane coupling constant $\chi_{cc}$ are about 4% larger than the unperturbed value in case of Ne-$N_2O$ (*7*) and 21% in case of HCCH-$N_2O$ (*9*). The electric field gradient at the terminal $^{14}N$ nucleus, on the other hand, was found to be basically

Table 7.1. Spectroscopic Constants for the CO-$N_2O$ Complex.[a]

| Constant | $^{12}C^{16}O$-$^{14}N^{14}NO$ | $^{13}C^{16}O$-$^{14}N^{14}NO$ | $^{13}C^{18}O$-$^{14}N^{14}NO$ | $^{13}C^{16}O$-$^{15}N^{14}NO$ | $^{13}C^{16}O$-$^{14}N^{15}NO$ |
|---|---|---|---|---|---|
| **Rotational Constants / MHz** | | | | | |
| A | 12862.14654(17) | 12848.48853(15) | 12846.83365(19) | 12450.14390(31) | 12848.33001(29) |
| B | 1914.445924(64) | 1892.869817(95) | 1790.64531(12) | 1873.16179(25) | 1876.73032(23) |
| C | 1655.641475(48) | 1639.363603(61) | 1562.026210(81) | 1617.84898(19) | 1627.24519(18) |
| **Centrifugal Distortion Constants / kHz** | | | | | |
| $D_J$ | 8.1965(11) | 8.0548(16) | 7.3296(12) | 7.6241(30) | 7.9388(28) |
| $D_{JK}$ | 359.7913(75) | 343.386(13) | 318.562(26) | 336.033(46) | 338.491(42) |
| $D_K$ | 282.097(53) | | | | |
| $d_1$ | -1.31910(79) | -1.3106(16) | -1.1009(35) | -1.251(10) | -1.2492(99) |
| $d_2$ | -0.6734(12) | -0.9410(25) | -0.751(82) | -1.07(31) | -0.72(32) |
| **Nuclear Quadrupole Coupling Constants / kHz** | | | | | |
| $\chi_{aa}(N_{terminal})$ | 341.71(45) | 338.95(47) | 341.77(51) | N/A | 340.81(52) |
| $\chi_{bb}$-$\chi_{cc}(N_{terminal})$ | -1136.76(84) | -1135.48(92) | -1136.16(96) | N/A | -1130.8(11) |
| $\chi_{aa}(N_{central})$ | 84.93(84) | 91.47(87) | 81.2(10) | 86.05(55) | N/A |
| $\chi_{bb}$-$\chi_{cc}(N_{central})$ | -396.4(13) | -393.3(15) | -401.4(15) | -400.8(11) | N/A |
| **Standard Deviation / kHz** | | | | | |
| $\sigma$ | 1.7 | 1.9 | 1.5 | 1.3 | 1.2 |

[a] Watson's S-reduction $I^r$-representation Hamiltonian (*18*) was used in the frequency fits.

unperturbed in cases of rare gas-$N_2O$ complexes (*7, 8*), and perturbed to only a minor degree in case of HCCH-$N_2O$ (*9*).

Such perturbation is also expected to occur in the CO-$N_2O$ complex. Three diagonal elements of the nuclear quadrupole coupling constants $\chi_{aa}$, $\chi_{bb}$, and $\chi_{cc}$ of all the isotopomers investigated are given in Table 7.2, along with the $\chi^{\circ}_{xx}$, $\chi^{\circ}_{yy}$ and $\chi^{\circ}_{zz}$ values of the $N_2O$ monomer, and the coupling constants of several other $N_2O$ containing planar complexes for comparison purposes. Assuming that there is no perturbation of the electronic structure upon complex formation, the quadrupole coupling constants of the complex can be related to the coupling constants of the free $N_2O$ monomer using the following expression:

$$\chi_{gg}=\chi^{\circ}<(3\cos^2\theta_g-1)(1/2)>, \qquad (7.1)$$

where $g$ = $a$, $b$, or $c$, $\theta_g$ is the angle between the $N_2O$ axis and the Eckart $g$-axis of the complex, and $\chi^{\circ}$ is the coupling constant of the free $N_2O$ monomer.

For a planar complex like CO-$N_2O$, it is most convenient to use $\chi_{cc}$ to examine the effect of complex formation on the quadrupole coupling constants. The reason is that the *y*-principal axis of the nuclear quadrupole coupling tensor coincides with the *c*-principal inertial axis of the complex in the limit of rigidity, and $\chi_{cc}=\chi^{\circ}_{yy}$. This is in contrast to the values of $\chi_{aa}$ and $\chi_{bb}$ which depend on the particular orientation of the *a*- and *b*-principal axes in the complex plane. This statement is true for both terminal and central $^{14}N$ nuclei. However, from Table 7.2, one can see that the values of $\chi_{cc}$ are quite different from those of $\chi^{\circ}_{yy}$ for both terminal and central $^{14}N$ nuclei. If these deviations were a result solely of the out-of-plane vibrational

Table 7.2. Comparison of the Nuclear Quadrupole Coupling Constants of $N_2O$ Containing Complexes and the $N_2O$ monomer

| | $^{12}C^{16}O$-$^{14}N^{14}NO$ | $^{13}C^{16}O$-$^{14}N^{14}NO$ | $^{13}C^{18}O$-$^{14}N^{14}NO$ | $^{13}C^{16}O$-$^{15}N^{14}NO$ | $^{13}C^{16}O$-$^{14}N^{15}NO$ | HCCH-$^{14}N^{14}NO$[a] | $CO_2$-$^{14}N^{14}NO$[b] | Ar-$^{14}N^{14}NO$[c] | Ne-$^{14}N^{14}NO$[d] | $^{14}N^{14}NO$[e] |
|---|---|---|---|---|---|---|---|---|---|---|
| Terminal $^{14}N$ nucleus | | | | | | | | | | |
| $\chi_{aa}$ | 341.71(45) | 338.95(47) | 341.77(51) | N/A | 340.81(52) | 377.49(44) | -96.55(43) | 371.48(43) | 367.7(2) | $\chi^o_{xx}$ 386.88(14) |
| $\chi_{bb}$ | -739.24(48) | -737.22(52) | - 738.96(54) | N/A | -735.80(61) | -773.12(45) | -311.11(38) | -758.89(42) | -756.0(8) | $\chi^o_{zz}$ -773.76(27) |
| $\chi_{cc}$ | 397.52(48) | 398.26(52) | 397.20(54) | N/A | 395.00(61) | 395.63(45) | 407.66(38) | 387.41(42) | 388.3(8) | $\chi^o_{yy}$ 386.88(14) |
| Central $^{14}N$ nucleus | | | | | | | | | | |
| $\chi_{aa}$ | 84.93(84) | 91.47(87) | 81.2(10) | 86.05(55) | N/A | 84.08(87) | -41.13(64) | 117.19(86) | 118.6(7) | $\chi^o_{xx}$ 133.79(19) |
| $\chi_{bb}$ | -240.66(77) | -242.38(87) | -241.30(90) | -243.42(61) | N/A | -246.59(71) | -96.83(56) | -257.84(64) | -258.3(1) | $\chi^o_{zz}$ -267.58(38) |
| $\chi_{cc}$ | 155.74(77) | 150.92(87) | 160.10(90) | 157.38(61) | N/A | 162.51(71) | 137.96(56) | 140.66(64) | 139.7(7) | $\chi^o_{yy}$ 133.79(19) |

[a]Ref. 9., [b]Ref. 5., [c]Ref. 8., [d]Ref. 7., [e]Ref. 16.

motions, one would expect the $\chi_{cc}/\chi^{o}_{yy}$ ratio to be close to and smaller than one, and to be the same for both terminal and central $^{14}N$ nuclei. However, this is not the case here. For the normal isotopomer, the $\chi_{cc}/\chi^{o}_{yy}$ ratio is 1.0275(13) for the terminal $^{14}N$ and 1.1641(60) for the central $^{14}N$. On one hand, the ratio is very close to 1.0 for the terminal $^{14}N$, supporting the argument for a planar structure with only small out-of-plane vibrational amplitude. On the other hand, the ratio for the central $^{14}N$ nucleus is significantly larger than 1.0, indicating an imaginary $\theta_c$ value associated with it. Clearly, there are other contributions, such as changes in the field gradients at the sites of these nuclei, that must be considered.

It is of interest to also compare the corresponding ratios associated with $\chi_{aa}$ and $\chi_{bb}$ to get a more complete picture of the perturbations. The ratios of $\chi_{aa}/\chi^{o}_{xx}$ and $\chi_{bb}/\chi^{o}_{zz}$ are 0.8832(12) and 0.9554(7), respectively, for the terminal $^{14}N$ nucleus; while those for the central $^{14}N$ nucleus are 0.6348(63) and 0.8994(31). If one assumes there are no electronic perturbations upon complex formation, it is possible to calculate the "hypothetical" values of these ratios by utilizing the result from the structural analysis and Equation 7.1. To simplify the calculation, the angle between the $N_2O$ subunit and the *a*-axis is approximated to be the same as $\theta_1$ since the *a*-axis nearly coincides with the intermolecular axis *Z* (see Figure 7.1). Furthermore, the Eckart axis system required in Equation 7.1 is being approximated with the usual principal inertial axis system. The uncertainties in the angles involved, due to vibrational amplitudes or the approximations made, are assumed to be about 5°, which is a reasonable assumption for a more rigidly bound complex like CO-$N_2O$. The "hypothetical" ratios with the

uncertainties thus estimated are 0.92(6) and 0.96(5) for $\chi_{aa}/\chi^{o}_{xx}$ and $\chi_{bb}/\chi^{o}_{zz}$, respectively, and are the same for both central and terminal $^{14}N$. It is apparent that the differences between observed and "hypothetical" values for the central $^{14}N$ nucleus are considerably larger than the uncertainties inherent in the experimental data or the approximations, while the differences for the terminal $^{14}N$ nucleus are still within the proposed uncertainties.

In the following, we focus on the coupling constants of the central $^{14}N$ nucleus since the perturbations detected are significantly larger than those at the terminal $^{14}N$. To facilitate easier comparisons with the previous FTMW investigations of $N_2O$ containing complexes, a new set of coupling constants, i.e., $\chi_{xx}$, $\chi_{yy}$, and $\chi_{zz}$, designed to separate the effects of electronic perturbation at the site of the quadrupolar nucleus and the effects of geometry or vibrational averaging associated with Equation (1), is introduced. Here, $\chi_{xx}$, $\chi_{yy}$, and $\chi_{zz}$ are the "perturbed" coupling constants of the central $^{14}N$ nucleus of the $N_2O$ subunit in the complex environment, with the $x$, $y$, $z$ directions defined as in the $N_2O$ monomer. In other words, these are the constants to be used instead of $\chi^{o}$, the monomer value, in order to obtain the geometry or vibrational averaging information. $\chi_{yy}$ is the out-of-plane component and is given the experimental value of $\chi_{cc}$ of the central $^{14}N$, assuming that the out-of-plane vibrational amplitudes are negligible. $\chi_{xx}$ and $\chi_{zz}$ are calculated using the values of the above "hypothetical" ratios and the experimental values of $\chi_{aa}$ and $\chi_{bb}$ of the central $^{14}N$. The result is that the $\chi_{xx}$, $\chi_{yy}$, and $\chi_{zz}$ coupling constants of the central $^{14}N$ of the $N_2O$ subunit in the CO-$N_2O$ complex change by +15.7%, -8.2% and -6.5% of the value

of $\chi^{o}_{zz}$, if compared with the $\chi^{o}_{xx}$, $\chi^{o}_{yy}$, and $\chi^{o}_{zz}$ of the monomer. The corresponding changes are +17.8%, -10.7% and -7.1% for HCCH-$N_2O$, +4.4%, -2.6%, -1.8% for Ar-$N_2O$, and +3.4%, -2.2%, -1.2% for Ne-$N_2O$. The sum of the variations is zero for each complex since the Laplace equation holds also for the "perturbed" coupling constants $\chi_{xx}$, $\chi_{yy}$, and $\chi_{zz}$ of $N_2O$ in the complex. It should be noted that all of the above $N_2O$ containing complexes are planar with the central nitrogen atom bound directly to the other partner. $CO_2$-$N_2O$ is not included here for comparison since the two subunits are in a slipped parallel arrangement with the terminal N bound to the C atom and the central N to the O atom. Both terminal and central $^{14}N$ nuclei experience considerable perturbations (*5*). It is interesting to note the surprising regularities in the trends discussed above for the various $N_2O$ containing complexes. This is despite the fact that the properties of the binding partners are quite different ranging from nonpolar rare gas atoms such as Ne to dipolar or quadrupolar molecules such as CO and HCCH. Not only the signs of the changes for the corresponding coupling constants are the same in all these complexes, but also the relative magnitudes of the changes in $\chi_{xx}$, $\chi_{yy}$, and $\chi_{zz}$ in each complex are very similar, with the absolute magnitudes getting larger from Ne to HCCH.

At present, we are not able to explain the regularities observed quantitatively. However, some qualitative explanations are offered here. The most plausible contribution comes from the redistribution of electronic charge in $N_2O$ upon bonding to the CO subunit. The larger deviation noticed for the central $^{14}N$ coupling constants can then be explained by the more direct bonding to CO, resulting in a more

significant perturbation of the local electronic structure at the site of the central $^{14}N$ nucleus. As in HCCH-$N_2O$ where the central N atom is bound to the negative $\pi$ cloud of the C≡C bond, the central N atom in CO-$N_2O$ is directly bound to the negative end of CO, i.e. the C end (*19*). This would tend to make the central N more positive, thus making the charge distribution surrounding it more spherical, and thus making the coupling constants smaller (*20*). In more detail, the charge along the intermolecular axis, which is directly related to $\chi_{xx}$, is depleted most effectively, resulting in a significant reduction of the coupling constant in this direction. The constant $\chi_{zz}$, along the $N_2O$ axis which is approximately perpendicular to the intermolecular axis, is considerably less affected and has only a minor reduction. The out-of-plane component $\chi_{yy}$, however, has an opposite change, as if the charge pushed out of the bonding direction is being redirected into the out-of-plane direction. Similar variations in the $\chi$ components are also observed for the terminal $^{14}N$ nucleus, although the effects on the terminal $^{14}N$ are much less pronounced since the bonding is less direct. This supports the proposed mechanism. Other possible mechanisms, such as the additional field gradients generated directly by the polar or quadrupolar binding partner and a possible deviation from linear geometry of $N_2O$ upon complex formation, have been discussed in detail in the previous analyses of HCCH-$N_2O$ (*9*) and were found not to be able to account for the observed phenomena.

Another interesting observation is that the coupling constants of the terminal $^{14}N$ nucleus of isotopomers with substitution only in the CO subunit are very similar. This supports the results from the structural analysis (see section 7.3.3) that the C and

O atoms lie very close to the *a*-axis, and that the principal axis system does not tilt significantly upon substitution in the CO subunit. The variations in the quadrupole coupling constants of the central $^{14}N$ nucleus indicate that the degree of perturbation varies as a function of isotopic substitution in CO. Such variation provides a subtle isotopic probe of the corresponding interaction potential.

### 7.3.3 STRUCTURAL ANALYSIS

The values for the inertial defect calculated from the rotational constants in Table 7.1 are 1.9728, 1.9529, 1.9690, 1.9849 and 1.9522 amu Å$^2$ for $^{12}C^{16}O$-$^{14}N^{14}NO$, $^{13}C^{16}O$-$^{14}N^{14}NO$, $^{13}C^{18}O$-$^{14}N^{14}NO$, $^{13}C^{16}O$-$^{15}N^{14}NO$, and $^{13}C^{16}O$-$^{14}N^{15}NO$, respectively. The variations between isotopomers are relatively small. This observation is consistent with a planar structure of CO-$N_2O$. Further evidence for the planar structure comes from the failure to observe *c*-type transitions of the complex, despite accurate frequency prediction available from the *a*- and *b*-type rotational fit. Overall, the CO-$N_2O$ complex can be well characterised by a semirigid rotor model, in contrast to much floppier systems such as CO-$N_2$ (*21*) where the semirigid rotor model fails to describe the system adequately. The van der Waals vibrational amplitudes of the CO-$N_2O$ complex are expected to be relatively small.

Since all atoms in the complex, except the oxygen atom of $N_2O$, were substituted, it was possible in the structural analysis to determine the absolute coordinates for these atoms using Kraitchman's equations (*22*), and then to use the first moment equation to locate the oxygen atom. $^{13}C^{16}O$-$^{14}N^{14}N^{16}O$ was used as

parent molecule so that one can use the simple single substitution equations. From the coordinates obtained, it is unambiguous that the C-end of the CO monomer is pointing towards $N_2O$, and that the O-end of $N_2O$ is closer to the CO monomer than the N-end. However, in this substitution approach, no use is made of the common assumption that the monomer structural parameters remain the same as in their respective free forms upon complex formation. It is known that the substitution procedure described above has severe limitations in dealing with van der Waals complexes. For example, the result for the $r_s$ bond length of CO in the CO-$N_2O$ complex is 1.086 Å, significantly shorter than the monomer value of 1.131 Å (*23*). To obtain more reliable structural parameters of the complex, another approach was taken.

We chose the same coordinate system as Qian and Howard (*11*) to describe the structure of the complex. Assuming that the monomer geometries remain unchanged upon complex formation, three additional structural parameters are needed to describe the complex, for example: $R_{cm}$, the distance between the centers of mass of the two monomers, and $\theta_1$ and $\theta_2$ describing the orientations of the $N_2O$ and the CO subunits in the complex, respectively. The coordinates are shown in Figure 7.1. The *X*, *Y*, and *Z* axes are chosen such that the *Z*-axis coincides with the intermolecular axis along $R_{cm}$ and that the out-of-plane *Y*-axis coincides with the *c*-principal axis of the complex. Note that this axis system is different from the *x*, *y*, *z* axis system used for the coupling constants. The instantaneous moment of inertia tensor elements are related to these three structural parameters as outlined in Ref.11. This moment of

inertia tensor can then be diagonalized to obtain the principal moments that are related to the effective rotational constants of the complex. Since several isotopomers have been investigated, the three structural parameters were fit to the rotational constants of all the isotopomers. Here, the bond lengths of $N_2O$ and CO were fixed at the respective monomer values (*23*, *24*). The effective structural parameters thus obtained are listed in Table 7.3. It is also possible to obtain a "pseudo-substitution" structure by fitting to the differences of the inertial moments between the normal isotopomer and the substituted isotopomers. The "pseudo-substitution" parameters are also listed in Table 7.3.

In the previous infrared study, Qian and Howard (*11*) used a model developed by Muenter (*25*) to estimate a potential energy surface for CO-$N_2O$ to aid their structural analysis. In this model, the electrostatic interaction is described in terms of a distributed multipole interaction between the two monomers, while the repulsive and dispersion interactions are described by atom-atom Lennard-Jones potentials (*26*). They found that the potential minimum is at $R_{cm}$=3.87 Å, $\theta_1$=86°, and $\theta_2$=15°. These values are very close to the "pseudo-substitution" structural parameters obtained from the present study, suggesting that the "pseudo-substitution" procedure has been reasonably effective in removing the van der Waals vibrational effects.

Table 7.3. Structural Parameters of the CO-$N_2O$ Complex.

| Parameters | Effective | Pseudo-substitution[a] | Equilibrium[b] |
|---|---|---|---|
| $r_{CO}$[c] | 1.1310 Å | 1.1310 Å | 1.1310 Å |
| $r_{NO}$[d] | 1.1923 Å | 1.1923 Å | 1.1923 Å |
| $r_{NN}$[d] | 1.1278 Å | 1.1278 Å | 1.1278 Å |
| $R_{cm}$ | 3.863 Å | 3.879 Å | 3.87 Å |
| $\theta_1$ | 80.8° | 88.7° | 86° |
| $\theta_2$ | 10.8° | 15.7° | 15° |

[a]See text for the definition., [b]Ref. 11., [c]Fixed at the value from Ref. 23. [d]Fixed at the values from Ref. 24.

## REFERENCES


1. A. R. W. McKellar, Y. P. Zeng, S. W. Sharpe, C. Wittig, and R. A.Beaudet, *J. Mol. Spectrosc.* **153**, 475 (1992).

2. Y. Xu and A. R. W. McKellar, *J. Chem. Phys.* **104**, 2488 (1996).

3. A. C. Legon and A. P. Suckley, *J. Chem. Phys.* **91**, 4440 (1989).

4. C. Dutton, A. Sazonov, and R. A. Beaudet, *J. Phys. Chem.* **100** 17772 (1996)

5. H. O. Leung, *J. Chem. Phys.* **108**, 3955 (1998).

6. R. F. Weiss, *J. Geophys. Res.* **86**, 7185 (1981).

7. M. S. Ngarī and W. Jäger, *J. Mol. Spectrosc.* **192**, 320 (1998).

8. H. O. Leung, D. Gangwani, and J.-U. Grabow, *J. Mol. Spectrosc.* **184**, 106 (1997).

9. H. O. Leung, *J. Chem. Phys.* **107**, 2232 (1997).

10. Y. Xu and A. R. W. McKellar, *J. Mol. Spectrosc.* **180**, 164 (1996).

11. H.-B. Qian and B. J. Howard, *J. Mol. Spectrosc.* **184**, 156 (1997).

12. Y. Xu and W. Jäger, *J. Chem. Phys.* **106**, 7968 (1997).

13. V. N. Markov, Y. Xu, and W. Jäger, *Rev. Sci. Instrum.* **69**, 4061 (1998).

14. J.-U. Grabow and W. Stahl, *Z. Naturforsch. Teil A* **45**, 1043 (1990).

15. J. S. Muenter, *J. Mol. Spectrosc.* **55**, 490 (1975).

16. J. M. L. J. Reinartz, W. L. Meerts, and A. Dymanus, *Chem. Phys.* **31**, 22 (1978); K. H. Casleton and S. G. Kukolich, *J. Chem. Phys.* **62**, 2696 (1975).

17. J. M. Pickett, *J. Mol. Spectrosc.* **148**, 371 (1991).

18. J. K. G. Watson, *in "Vibrational Spectra and Structure: A series of Advances"*, (J. R. Durig, Ed.), Vol. 6, pp. 1-89, Elsevier, New York, 1977.

19. B. Rosenblum, A. H. Nethercot, and C. H. Townes, *Phys. Rev.* **109**, 400 (1958).

20. C. H. Townes and A. L. Schawlow, *"Microwave Spectroscopy"*, pp. 238, Dover, New York, 1975.

21. Y. Xu and A. R. W. McKellar, *J. Chem. Phys.* **104**, 2488 (1996).

22. J. Kraitchamn, *Am. J. Phys.* **21**, 17 (1953).

23. F. J. Lovas and P. H. Krupenie, *J. Phys. Chem. Ref. Data* **3**, 245 (1974).

24. C. C. Costain, *J. Chem. Phys.* **29**, 864 (1958).

25. J. S. Muenter, *J. Chem. Phys.* **94**, 2781 (1991).

26. A. J. Stone, *Chem. Phys. Lett.* **83**, 233 (1981); A. D. Buckingham and P. W. Fowler, *Can. J. Chem.* **63**, 2018 (1985).

# CHAPTER EIGHT

## GENERAL DISCUSSION AND CONCLUSIONS

Rotational spectra of six van der Waals complexes that contain a nitrous oxide subunit were studied and presented in this thesis with the aim of improving our understanding of the interactions of rare gas atoms with linear triatomic molecules. Several isotopomers were studied for each complex. Very accurate spectroscopic constants were obtained, and the equilibrium geometries, structural parameters, and information about the large amplitude van der Waals motions, i.e. the intermolecular dynamics, were derived. Harmonic force field analyses provided force constants for the van der Waals vibrational modes and estimates of the corresponding frequencies. All of these are important parameters in determining the intermolecular forces involved in the interactions. When used in combination with data from other sources, such as infrared spectroscopy and *ab initio* calculations, these data are invaluable in the construction of the potential energy surfaces for these clusters.

The spectra of the van der Waals dimers Ne-$N_2O$ and Ar-$N_2O$ showed that they have T-shaped geometries, and, in particular, that the rare gas atom prefers to lie near the oxygen side of the $N_2O$ monomer. This was unambiguously determined from the substitution structures via Kraitchman's relationships. The actual reason for the preference of the oxygen side by the rare gas atom in rare gas-$N_2O$ complexes is difficult to rationalize. Unlike the rare gas-OCS complexes (*1*, *2*, *3*) where the tilt towards the oxygen atom of OCS was argued to be a result of the larger van der Waals radius of the sulfur atom as compared to the oxygen atom, this proposition

would not be plausible for $N_2O$ because the O and N atoms are very similar in size. From the various studies reported for rare gas-$N_2O$ dimers we see that the trend in the rare gas-$N_{inner}$ distances is what one would expect. In the series Ne-, Ar-, Kr-, and Xe-$N_2O$, the $r_0$ bond lengths are 3.237 Å (*4*), 3.475 Å (*5*), 3.5936(3) Å (*6*), 3.7806(2) Å (6). This trend is in accord with the increasing size of the rare gas atom.

With the dimers $Ne_2$, $Ar_2$, ArNe, Ne-$N_2O$, and Ar-$N_2O$ already characterised, by high resolution spectroscopic or other methods, the trimers $Ar_2$-$N_2O$, $Ne_2$-$N_2O$, and ArNe-$N_2O$ were studied in order to probe three-body effects in the intermolecular interactions. Towards this end, structural parameters, the extents of the large amplitude van der Waals motions, and information about the electronic perturbation of the $N_2O$ subunit in the ternary systems were compared with the corresponding dimer properties. It transpired that the harmonic force field analyses and the analyses of the nuclear quadrupole coupling constants gave no indication of the presence of three-body non-additive interactions. However, the significant bond lengthening of the Ar-Ar, Ne-Ne, and Ar-Ne bonds in the ternary systems as compared to the respective dimer values can unambiguously be attributed to non-additive interactions.

The structure of CO-$N_2O$ is a T-shape, with CO forming the leg of the T. The C atom points toward the central nitrogen atom while the O end of CO is tilted towards the O end of $N_2O$. This is similar to the rare gas-$N_2O$ and (rare gas)$_2$-$N_2O$ trimers where the rare gases also prefered the O end of the $N_2O$ monomer. In all these complexes there are indications of significant perturbation of the electronic

environment around the central N nucleus in $N_2O$ caused by direct bonding with the other subunits in the complexes.

The present work can be a foundation for the investigation of larger, quarternary, clusters, such as $Ne_3$-$N_2O$, $Ar_3$-$N_2O$, etc. The signal-to-noise ratios achieved for the ternary systems indicate that there is a possiblity for the detection of such species. The complexes studied here promise also to be rewarding candidates for high level *ab initio* calculations since, apart from Ar, only second row elements are involved. Recently developed perturbation methods, such as the symmetry adapted perturbation theory (*7*), promise to further our understanding of intermolecular interactions in terms of their physical origins, i.e. exchange, electrostatic, induction, and dispersion interactions. The same *ab initio* methods can also be used for the study of non-additive three-body effects in ternary systems (*8*).

## REFERENCES


1. G. D. Hayman, J. Hodge, B. J. Howard, J. S. Muenter, and T. R. Dyke, *Chem. Phys. Lett.* **118,** 12 (1985).

2. F. J. Lovas and R. D. Suenram, *J. Chem. Phys.* **87,** 2010 (1987).

3. Y. Xu and M. C. L. Gerry, *J. Mol. Spectrosc.* **169,** 181 (1995).

4. M. S. Ngarī and W. Jäger, *J. Mol. Spectrosc.* **192,** 320 (1998).

5. M. S. Ngarī and W. Jäger, *J. Mol. Spectrosc.* **192,** 452 (1998).

6. W. A. Herrebout, H.-B. Qian, H. Yamaguchi, and B. J. Howard, *J. Mol. Spectrosc.* **189,** 235 (1998).

7. K. Szalewicz and B. Jeziorski, in "Molecular Interactions: From van der Waals to Strongly Bound Complexes", (S. Scheiner, Ed), pp. 3-43, John Wiley and Sons Ltd, New York, 1997.

8. M. M. Szczęśniak and G. Chałasiński, in "Molecular Interactions: From van der Waals to Strongly Bound Complexes", (S. Scheiner, Ed), pp.45-79, John Wiley and Sons, New York, 1997.

# APPENDIX

## A1

## TABLES OF THE MEASURED TRANSITION FREQUENCIES FOR CHAPTER THREE

Table A1.1. Observed transition frequencies of the $^{14}N$-hyperfine structure of $^{20}Ne$-$^{14}N^{14}NO$ and $^{22}Ne$-$^{14}N^{14}NO$.

| $J'K_a'K_c'$-$J''K_a''K_c''$ F'I'-F''I'' | $\nu_{rot}$ [a] $\nu_{obs}$ | $\Delta\nu_{rot}$ [b] $\Delta\nu$ [c] | $\nu_{rot}$ [a] $\nu_{obs}$ | $\nu_{rot}$ [b] $\Delta\nu$ [c] | $J'K_a'K_c'$-$J''K_a''K_c''$ F'I'-F''I'' | $\nu_{rot}$ [a] $\nu_{obs}$ | $\Delta\nu_{rot}$ [b] $\Delta\nu$ [c] | $\nu_{rot}$ [a] $\nu_{obs}$ | $\Delta\nu_{rot}$ [b] $\Delta\nu$ [c] |
|---|---|---|---|---|---|---|---|---|---|
| | $^{20}Ne$-$^{14}N^{14}NO$ | | $^{22}Ne$-$^{14}N^{14}NO$ | | | $^{20}Ne$-$^{14}N^{14}NO$ | | $^{22}Ne$-$^{14}N^{14}NO$ | |
| 101-000 | 6282.3345 | 0.5 | 5935.1710 | 0.1 | 111-000 | 15646.9959 | -0.3 | 15510.7330 | 0.3 |
| 1 2-2 2 | 6282.1458 | 0.0 | 5934.9831 | 0.9 | 0 1-1 1 | 15646.7412 | -1.1 | 15510.4785 | -1.3 |
| 1 2-1 1 | 6282.1458 | 0.0 | 5934.9831 | 0.9 | 2 2-2 2 | 15646.7943 | -0.3 | 15510.5315 | -0.2 |
| 1 2-0 0 | 6282.1458 | 0.0 | 5934.9831 | 0.9 | 2 2-1 1 | 15646.7943 | -0.3 | 15510.5315 | -0.2 |
| 1 1-2 2 | 6282.2901 | -0.5 | 5935.1265 | -1.8 | 1 0-2 2 | 15646.8171 | 0.0 | 15510.5535 | -0.6 |
| 1 1-1 1 | 6282.2901 | -0.5 | 5935.1265 | -1.8 | 1 0-1 1 | 15646.8171 | 0.0 | 15510.5535 | -0.6 |
| 1 1-0 0 | 6282.2901 | -0.5 | 5935.1265 | -1.8 | 1 0-0 0 | 15646.8171 | 0.0 | 15510.5535 | -0.6 |
| 3 2-2 2 | 6282.3111 | 0.9 | 5935.1473 | 0.4 | 2 1-2 2 | 15646.9959 | 1.6 | 15510.7328 | 1.0 |
| 2 1-2 2 | 6282.3352 | 0.8 | 5935.1707 | 0.6 | 2 1-1 1 | 15646.9959 | 1.6 | 15510.7328 | 1.0 |
| 2 1-1 1 | 6282.3352 | 0.8 | 5935.1707 | 0.6 | 3 2-2 2 | 15647.0506 | 4.0 | 15510.7853 | 1.6 |
| 1 0-2 2 | 6282.4211 | -0.2 | 5935.2580 | 0.1 | 1 1-2 2 | 15647.0891 | -0.5 | 15510.8260 | -0.2 |
| 1 0-1 1 | 6282.4211 | -0.2 | 5935.2580 | 0.1 | 1 1-1 1 | 15647.0891 | -0.5 | 15510.8260 | -0.2 |
| 1 0-0 0 | 6282.4211 | -0.2 | 5935.2580 | 0.1 | 1 1-0 0 | 15647.0891 | -0.5 | 15510.8260 | -0.2 |
| 2 2-2 2 | 6282.4327 | 0.8 | 5935.2680 | -0.3 | 1 2-2 2 | 15647.3838 | -1.3 | 15511.1229 | 0.2 |
| 2 2-1 1 | 6282.4327 | 0.8 | 5935.2680 | -0.3 | 1 2-1 1 | 15647.3838 | -1.3 | 15511.1229 | 0.2 |
| 0 1-1 1 | 6282.4540 | -2.1 | 5935.2927 | 1.2 | 1 2-0 0 | 15647.3838 | -1.3 | 15511.1229 | 0.2 |
| 110-101 | 10175.0529 | 0.1 | 10300.3616 | 0.6 | 202-101 | 12511.9416 | 0.1 | 11828.5683 | -1.3 |
| 1 2-0 1 | 10174.7313 | 0.5 | 10300.0388 | -1.3 | 1 2-0 1 | 12511.7482 | -1.2 | | |
| 1 2-2 2 | 10174.7545 | -0.4 | 10300.0626 | -0.7 | 0 2-1 0 | 12511.7482 | -1.4 | | |
| 1 2-1 0 | 10174.7657 | 0.1 | 10300.0738 | 0.0 | 2 0-2 2 | 12511.7609 | 0.4 | 11828.3843 | -1.4 |
| 1 1-0 1 | 10174.8814 | -0.1 | 10300.1893 | -1.3 | 2 0-1 0 | 12511.7710 | -0.2 | 11828.3978 | 1.6 |
| 3 2-2 2 | 10174.9323 | 3.2 | 10300.2400 | 2.3 | 1 2-2 2 | 12511.7710 | -2.6 | 11828.3978 | -0.7 |
| 1 1-2 1 | 10175.0033 | 0.1 | 10300.3114 | -0.6 | 1 2-1 0 | 12511.7852 | 0.9 | | |
| 1 0-0 1 | 10175.0263 | 2.9 | 10300.3361 | 2.9 | 2 0-3 2 | 12511.8811 | -1.1 | | |
| 3 2-2 1 | 10175.0263 | -0.4 | 10300.3361 | 0.2 | 1 1-0 1 | 12511.8893 | -1.4 | 11828.5224 | 2.1 |
| 1 0-2 2 | 10175.0473 | -0.3 | | | 2 1-2 1 | 12511.8986 | -1.4 | | |
| 2 1-2 1 | | | 10300.3633 | -1.2 | 3 2-2 2 | 12511.9215 | -0.3 | 11828.5510 | 0.7 |
| 1 1-1 1 | 10175.0473 | 0.3 | | | 4 2-3 2 | 12511.9353 | -0.6 | 11828.5595 | -2.6 |
| 3 2-3 2 | 10175.0473 | -3.5 | | | 3 1-2 1 | 12511.9399 | 0.5 | 11828.5688 | 3.0 |
| 2 1-2 1 | 10175.0548 | 0.0 | | | 2 2-2 2 | 12511.9399 | 0.2 | 11828.5688 | 1.3 |
| 2 2-1 0 | 10175.0704 | 0.3 | | | 2 1-1 1 | 12511.9451 | 1.3 | 11828.5688 | -0.6 |
| 2 1-3 2 | 10175.0808 | 1.9 | | | 3 1-3 2 | 12511.9608 | -2.8 | | |
| 0 1-1 0 | 10175.0987 | 0.5 | | | 1 1-2 1 | 12512.0140 | 1.6 | 11828.6441 | 2.4 |
| 2 1-1 1 | 10175.0987 | 0.2 | | | 0 2-1 2 | 12512.0244 | -0.7 | | |
| 1 0-2 1 | 10175.1442 | -0.9 | | | 3 2-3 2 | 12512.0463 | 2.8 | 11828.6711 | -0.6 |
| 2 2-2 1 | 10175.1548 | -2.2 | 10300.4669 | 0.3 | 2 0-1 2 | 12512.0463 | -0.3 | 11828.6711 | -0.7 |
| 2 2-3 2 | 10175.1815 | 0.4 | 10300.4899 | 0.1 | 1 1-1 1 | 12512.0612 | 5.0 | 11828.6819 | -1.6 |
| 1 0-1 1 | 10175.1879 | -1.0 | | | 1 2-1 2 | 12512.0612 | 1.5 | 11828.6819 | -2.7 |
| 0 1-1 1 | 10175.2277 | -1.1 | 10300.5359 | -1.1 | | | | | |
| 1 0-1 2 | 10175.3340 | 0.3 | 10300.6440 | 1.5 | 211-110 | 13365.1558 | -0.3 | 12586.3589 | 1.0 |
| 2 2-1 2 | 10175.3463 | 0.8 | 10300.6535 | -1.0 | 2 1-2 1 | 13365.0508 | -1.1 | 12586.2547 | -0.3 |
| 0 1-1 2 | 10175.3721 | -1.5 | | | 0 2-1 2 | 13365.1035 | 0.6 | 12586.3067 | 0.1 |
| | | | | | 2 1-1 1 | 13365.1035 | 0.1 | 12586.3067 | -0.9 |

Table A1.1. (continued)

| $J'K_a'K_c'$-$J''K_a''K_c''$ F'I'-F''I'' | $\nu_{rot}$ [a] $\nu_{obs}$ | $\Delta\nu_{rot}$ [b] $\Delta\nu$ [c] | $\nu_{rot}$ [a] $\nu_{obs}$ | $\Delta\nu_{rot}$ [b] $\Delta\nu$ [c] | $J'K_a'K_c'$-$J''K_a''K_c''$ F'I'-F''I'' | $\nu_{rot}$ [a] $\nu_{obs}$ | $\Delta\nu_{rot}$ [b] $\Delta\nu$ [c] | $\nu_{rot}$ [a] $\nu_{obs}$ | $\Delta\nu_{rot}$ [b] $\Delta\nu$ [c] |
|---|---|---|---|---|---|---|---|---|---|
| | $^{20}Ne$-$^{14}N^{14}NO$ | | $^{22}Ne$-$^{14}N^{14}NO$ | | | $^{20}Ne$-$^{14}N^{14}NO$ | | $^{22}Ne$-$^{14}N^{14}NO$ | |
| 212-111 | 11745.7180 | -0.3 | 11137.8932 | 0.2 | 4 2-3 2 | 13365.1096 | -0.2 | 12586.3128 | -0.3 |
| 1 2-1 2 | 11745.4149 | 1.1 | 11137.5892 | 0.5 | 3 1-2 1 | 13365.1527 | 1.0 | 12586.3560 | 2.1 |
| 2 0-1 2 | 11745.4307 | -0.6 | 11137.6078 | 1.4 | 3 1-3 2 | 13365.1794 | -0.4 | 12586.3830 | 0.5 |
| 0 2-1 2 | 11745.4589 | -1.8 | | | 2 0-1 2 | 13365.1602 | 2.8 | | |
| 1 1-1 1 | 11745.5377 | -1.4 | 11137.7148 | -0.2 | 1 2-1 2 | 13365.1902 | 0.2 | 12586.3929 | -0.1 |
| 3 2-3 2 | 11745.5707 | -2.3 | 11137.7458 | -2.5 | 1 1-0 1 | 13365.1902 | 0.0 | | |
| 3 2-2 1 | 11745.6271 | 1.8 | 11137.8025 | 2.3 | 3 2-2 2 | 13365.2371 | 1.6 | 12586.4396 | 1.0 |
| 2 1-1 1 | 11745.6774 | -0.7 | 11137.8535 | -1.0 | 2 2-2 2 | 13365.2803 | -0.5 | | |
| 4 2-3 2 | 11745.7042 | -0.8 | 11137.8805 | 0.0 | 2 2-1 0 | 13365.2938 | 1.1 | 12586.4956 | 0.2 |
| 3 1-2 1 | 11745.7188 | -0.7 | 11137.8948 | 0.9 | 3 2-3 2 | 13365.3641 | -1.6 | 12586.5669 | -2.3 |
| 2 2-1 0 | 11745.7788 | 0.9 | 11137.9540 | 1.2 | 1 1-1 1 | 13365.3702 | -1.8 | | |
| 2 2-2 2 | 11745.8004 | 0.0 | 11137.9757 | 0.4 | 2 2-2 1 | 13365.3813 | -1.7 | | |
| 1 1-1 0 | 11745.8155 | 4.0 | 11137.9877 | 0.6 | | | | | |
| 2 0-2 1 | 11745.8250 | 2.8 | 11137.9999 | 2.7 | 303-202 | 18637.5113 | 0.6 | 17639.3103 | -0.1 |
| 3 2-2 2 | 11745.8250 | 0.0 | 11137.9999 | -0.4 | 4 2-3 2 | 18637.4935 | 1.9 | 17639.2927 | 0.1 |
| 1 1-0 1 | 11745.8863 | -0.1 | 11138.0600 | -1.4 | 2 1-1 1 | 18637.4935 | 1.0 | 17639.2927 | -0.7 |
| 1 2-1 0 | 11745.9802 | -1.6 | 11138.1577 | 0.5 | 3 2-2 2 | 18637.4935 | 0.0 | 17639.2927 | -2.3 |
| 2 0-1 0 | 11746.0014 | 2.1 | 11138.1749 | -0.1 | 4 1-3 1 | 18637.5124 | 2.4 | 17639.3096 | 0.9 |
| 1 2-2 2 | 11746.0014 | -3.0 | 11138.1749 | -4.8 | 3 2-3 2 | 18637.5124 | 1.1 | 17639.3096 | -2.6 |
| 2 0-2 2 | 11746.0219 | 0.1 | 11138.1973 | -0.1 | 5 2-4 2 | 18637.5124 | -1.9 | 17639.3096 | -2.7 |
| 1 2-0 1 | 11746.0568 | 0.1 | | | 1 2-1 2 | 18637.5201 | 3.1 | 17639.3181 | 3.3 |
| | | | | | 3 1-2 1 | 18637.5201 | 0.8 | 17639.3181 | 1.3 |
| 211-202 | 11028.2673 | -0.1 | 11058.1554 | -0.3 | 4 1-4 2 | 18637.5394 | 1.6 | 17639.3360 | 0.3 |
| 0 2-1 1 | 11027.9396 | -3.5 | | | 3 0-2 0 | 18637.5394 | -1.2 | 17639.3360 | -2.0 |
| 2 0-2 2 | 11027.9748 | 2.0 | 11057.8610 | 1.4 | 2 2-1 2 | 18637.5437 | -2.7 | 17639.3461 | 1.9 |
| 2 0-3 2 | 11027.9917 | 1.0 | 11057.8764 | -0.4 | 1 2-0 2 | 18637.5484 | -3.3 | 17639.3511 | 2.6 |
| 1 2-2 2 | 11028.0042 | -1.3 | 11057.8907 | -1.3 | 3 2-3 1 | 18637.5883 | -2.9 | | |
| 1 2-1 1 | 11028.0310 | 0.7 | 11057.9159 | -0.2 | | | | | |
| 0 2-1 2 | 11028.0832 | -1.2 | | | 313-212 | 17583.6117 | 0.0 | 16678.6012 | 0.0 |
| 2 1-1 1 | 11028.0958 | 1.4 | | | 2 2-2 0 | 17583.5509 | 0.0 | | |
| 4 2-3 2 | 11028.1190 | 1.7 | 11058.0044 | 0.7 | 1 2-0 2 | 17583.5696 | 4.7 | | |
| 2 0-1 2 | 11028.1404 | 1.5 | 11058.0257 | -2.9 | 2 2-1 2 | 17583.5696 | 1.3 | | |
| 2 0-2 0 | 11028.1531 | 1.2 | 11058.0420 | 0.6 | 4 1-4 2 | 17583.5696 | -5.2 | | |
| 2 1-3 1 | 11028.1707 | 3.3 | 11058.0584 | 1.4 | 3 0-2 0 | 17583.5797 | 0.9 | 16678.5692 | 1.3 |
| 3 1-2 2 | 11028.1707 | 1.2 | 11058.0584 | 2.5 | 3 1-2 1 | 17583.6045 | 1.0 | 16678.5920 | -0.9 |
| 1 2-1 2 | 11028.1707 | -0.8 | 11058.0584 | -2.7 | 3 2-3 2 | 17583.6045 | -0.3 | 16678.5920 | -2.0 |
| 1 2-2 0 | 11028.1838 | -0.8 | | | 5 2-4 2 | 17583.6104 | 0.9 | 16678.6006 | 1.7 |
| 3 1-3 2 | 11028.1838 | -3.5 | | | 1 2-1 2 | 17583.6104 | -1.4 | 16678.6006 | -1.0 |
| 1 2-0 2 | 11028.2079 | 1.7 | 11058.0979 | 3.1 | 4 1-3 1 | 17583.6104 | -2.1 | 16678.6006 | -1.0 |
| 2 1-2 1 | 11028.2079 | 1.1 | 11058.0979 | 2.8 | 3 2-2 2 | 17583.6298 | 0.4 | 16678.6189 | -0.2 |
| 4 2-4 2 | 11028.2263 | 1.4 | 11058.1125 | -0.9 | 2 1-1 1 | 17583.6352 | 1.3 | 16678.6252 | 1.2 |
| 3 1-3 1 | 11028.2677 | 0.5 | 11058.1549 | -1.0 | 4 2-3 2 | 17583.6352 | 0.9 | 16678.6252 | 0.9 |
| 1 1-2 2 | 11028.3342 | 0.6 | 11058.2274 | 1.8 | 3 1-3 1 | 17583.6551 | -2.4 | | |
| 3 2-2 2 | 11028.3538 | -1.6 | 11058.2430 | 0.3 | | | | | |
| 1 1-1 1 | 11028.3630 | 0.0 | | | 312-303 | 12398.2949 | 0.0 | 12265.0202 | 0.0 |

Table A1.1. (continued)

| $J'K_a'K_c'$-$J''K_a''K_c''$ F'I'-F''I'' | $\nu_{rot}$ [a] $\nu_{obs}$ | $\Delta\nu_{rot}$ [b] $\Delta\nu$ [c] | $\nu_{rot}$ [a] $\nu_{obs}$ | $\Delta\nu_{rot}$ [b] $\Delta\nu$ [c] | $J'K_a'K_c'$-$J''K_a''K_c''$ F'I'-F''I'' | $\nu_{rot}$ [a] $\nu_{obs}$ | $\Delta\nu_{rot}$ [b] $\Delta\nu$ [c] | $\nu_{rot}$ [a] $\nu_{obs}$ | $\Delta\nu_{rot}$ [b] $\Delta\nu$ [c] |
|---|---|---|---|---|---|---|---|---|---|
| | $^{20}Ne$-$^{14}N^{14}NO$ | | $^{22}Ne$-$^{14}N^{14}NO$ | | | $^{20}Ne$-$^{14}N^{14}NO$ | | $^{22}Ne$-$^{14}N^{14}NO$ | |
| 3 2-3 2 | 11028.3730 | -0.2 | 11058.2596 | -0.3 | 2 2-3 2 | 12398.1012 | -0.7 | | |
| 2 2-2 2 | 11028.4004 | -0.4 | 11058.2860 | -1.5 | 3 0-3 0 | 12398.1655 | 0.6 | 12265.8924 | -0.3 |
| 2 2-3 2 | 11028.4187 | 0.1 | 11058.3018 | -3.0 | 4 1-3 2 | 12398.2112 | 1.0 | | |
| 1 1-2 1 | 11028.4740 | -1.4 | | | 3 1-3 1 | 12398.2112 | 0.2 | 12265.9387 | 1.0 |
| 3 2-4 2 | 11028.4809 | 0.0 | 11058.3697 | 0.2 | 2 2-2 2 | 12398.2112 | -3.7 | 12265.9429 | 0.9 |
| 1 1-1 2 | 11028.5017 | 2.0 | 11058.3953 | 0.6 | 5 2-5 2 | 12398.2291 | -0.1 | 12265.9547 | -0.9 |
| 3 2-2 0 | 11028.5330 | -1.5 | 11058.4243 | -0.2 | 2 2-1 2 | 12398.2426 | -1.7 | | |
| 2 2-1 2 | 11028.5669 | 0.1 | 11058.4556 | -1.0 | 4 1-4 1 | 12398.2919 | 0.5 | 12266.0161 | -0.9 |
| | | | | | 4 2-3 2 | 12398.4128 | 2.4 | | |
| 303-212 | 10039.0756 | -0.3 | 8754.4213 | 0.3 | 2 1-2 1 | 12398.4128 | -1.6 | 12266.1362 | -0.9 |
| 1 2-0 2 | 10038.8800 | 1.4 | 8754.2213 | 0.8 | 4 2-4 2 | 12398.4308 | 0.7 | 12266.1514 | -1.1 |
| 3 0-2 0 | 10038.9179 | -0.6 | 8754.2608 | -0.1 | 3 2-3 2 | 12398.4822 | -0.5 | 12266.2053 | 1.0 |
| 1 2-1 2 | 10038.9256 | 0.1 | 8754.2676 | -0.6 | 2 1-1 2 | 12398.5314 | 0.2 | | |
| 2 2-2 0 | 10038.9376 | 0.2 | 8754.2770 | -2.8 | 4 2-3 0 | 12398.5449 | 2.5 | 12266.2742 | 2.5 |
| 2 2-1 2 | 10038.9561 | 1.2 | 8754.2978 | 0.2 | 3 2-2 2 | 12398.5960 | 0.2 | 12266.3231 | -1.1 |
| 3 1-2 1 | 10038.9879 | 0.0 | 8754.3310 | -0.8 | | | | | |
| 5 2-4 2 | 10039.0088 | -2.0 | 8754.3529 | -2.1 | 404-313 | 17069.6057 | 0.0 | 15406.3511 | 0.0 |
| 3 1-3 1 | 10039.0402 | -1.6 | 8754.3858 | -1.0 | 4 0-3 0 | 17069.5029 | -1.6 | 15406.2462 | 1.0 |
| 4 1-3 1 | 10039.0719 | -0.1 | 8754.4171 | 0.3 | 4 1-3 1 | 17069.5352 | -3.2 | 15406.2798 | -0.7 |
| 2 1-2 1 | 10039.0719 | -1.7 | | | 6 2-5 2 | 17069.5498 | -2.0 | 15406.2939 | -0.6 |
| 1 2-1 1 | 10039.0940 | -1.8 | 8754.4389 | 0.6 | 3 1-3 1 | 17069.6014 | 2.0 | 15406.3462 | 2.6 |
| 4 2-4 2 | 10039.0940 | -1.7 | | | 5 1-4 1 | 17069.6014 | 0.2 | 15406.3462 | 0.3 |
| 3 0-3 2 | 10039.1138 | -1.6 | 8754.4570 | -1.0 | 2 2-2 1 | 17069.6353 | 2.7 | 15406.3724 | 0.3 |
| 2 2-2 2 | 10039.1597 | 0.8 | 8754.5037 | 1.7 | 4 0-4 2 | 17069.6494 | 3.5 | 15406.3838 | -2.1 |
| 2 1-1 1 | 10039.2127 | 0.1 | 8754.5617 | -0.3 | 3 2-3 2 | 17069.6942 | 1.3 | 15406.4286 | -1.8 |
| 4 2-3 2 | 10039.2277 | 0.0 | 8754.5760 | -1.2 | 3 1-2 1 | 17069.7172 | 0.7 | 15406.4509 | -1.1 |
| 2 1-2 2 | 10039.2500 | 3.7 | 8754.5992 | 3.0 | 5 2-4 2 | 17069.7129 | -0.4 | 15406.4649 | 0.6 |
| 3 2-3 2 | 10039.2500 | 2.6 | 8754.5992 | 2.4 | 4 2-3 2 | 17069.7567 | 0.7 | 15406.5100 | 1.2 |
| 3 2-2 2 | 10039.2730 | 1.1 | 8754.6220 | 0.1 | | | | | |

[a] Hypothetical center frequencies in MHz from the quadrupole fit.

[b] Deviations in kHz from the center frequencies from the rotational fit.

[c] Observed-calculated frequencies in kHz from the quadrupole fit.

Table A1.2. Observed frequencies of the $^{14}N$-hyperfine structure of Ne-$^{15}N^{14}NO$ and Ne-$^{14}N^{15}NO$ isotopomers.

| $J'K_a'K_c'$-$J''K_a''K_c''$ F' - F'' | $\nu_{rot}$ [a] $\nu_{obs}$ | $\Delta\nu_{rot}$ [b] $\Delta\nu$ [c] | $\nu_{rot}$ [a] $\nu_{obs}$ | $\Delta\nu_{rot}$ [b] $\Delta\nu$ [c] | $\nu_{rot}$ [a] $\nu_{obs}$ | $\Delta\nu_{rot}$ [b] $\Delta\nu$ [c] | $\nu_{rot}$ [a] $\nu_{obs}$ | $\Delta\nu_{rot}$ [b] $\Delta\nu$ [c] |
|---|---|---|---|---|---|---|---|---|
| | $^{20}Ne$-$^{15}N^{14}NO$ | | $^{22}Ne$-$^{15}N^{14}NO$ | | $^{20}Ne$-$^{14}N^{15}NO$ | | $^{22}Ne$-$^{14}N^{15}NO$ | |
| 101-000 | 6222.4914 | 0.4 | 5876.8739 | -0.3 | 6244.5296 | 0.9 | 5896.8473 | 0.8 |
| 0 - 1 | 6222.4294 | 0.4 | 5876.8116 | 0.2 | 6244.3466 | -1.3 | 5896.6643 | -0.5 |
| 2 - 1 | 6222.4853 | 0.2 | 5876.8676 | -0.1 | 6244.5119 | 0.4 | 5896.8294 | 0.4 |
| 1 - 1 | 6222.5220 | -0.6 | 5876.9051 | -0.1 | 6244.6214 | 0.9 | 5896.9387 | 0.2 |
| 111-000 | 15180.6544 | 0.2 | 15045.8770 | 0.1 | 15631.6591 | -0.5 | 15494.9271 | 0.0 |
| 1 - 1 | 15180.5879 | -1.5 | 15045.8112 | -1.1 | 15631.4710 | 0.3 | 15494.7387 | -0.2 |
| 2 - 1 | 15180.6698 | 2.4 | 15045.8922 | 2.2 | 15631.6975 | 0.8 | 15494.9656 | 0.9 |
| 0 - 1 | 15180.7834 | -0.9 | 15046.0053 | -1.2 | 15632.0347 | -1.1 | 15495.3026 | -0.7 |
| 110-101 | 9778.7087 | 0.8 | 9902.5299 | 0.3 | 10187.9851 | 0.0 | 10313.7127 | 0.4 |
| 0 - 1 | 9778.6084 | -1.5 | 9902.4303 | -1.4 | 10187.6988 | -0.5 | 10313.4269 | -0.8 |
| 2 - 1 | 9778.6718 | 1.1 | 9902.4923 | 0.3 | 10187.8760 | 1.3 | 10313.6029 | 0.9 |
| 2 - 2 | 9778.7094 | 1.2 | 9902.5317 | 2.2 | 10187.9844 | 0.6 | 10313.7124 | 0.9 |
| 1 - 1 | 9778.7094 | -1.8 | 9902.5317 | -0.5 | | | | |
| 1 - 2 | 9778.7497 | 1.0 | | | 10188.0992 | -1.6 | 10313.8265 | -1.3 |
| 1 - 0 | 9778.8049 | 0.0 | 9902.6253 | -0.7 | 10188.2645 | 0.2 | 10313.9923 | 0.3 |
| 202-101 | 12388.8693 | -1.0 | 11709.3837 | -0.2 | 12437.6202 | 0.1 | 11753.0048 | 0.5 |
| 1 - 1 | 12388.8119 | 0.6 | 11709.3244 | -0.6 | 12437.4489 | -1.5 | 11752.8326 | -0.2 |
| 1 - 2 | 12388.8486 | -0.1 | 11709.3627 | 0.2 | | | | |
| 2 - 1 | 12388.8667 | 1.8 | | | 12437.6068 | -1.5 | 11752.9927 | -1.7 |
| 3 - 2 | 12388.8667 | -1.2 | 11709.3823 | 0.2 | 12437.6168 | 1.0 | 11753.0019 | 1.9 |
| 2 - 2 | 12388.9030 | 0.7 | 11709.4182 | 0.8 | 12437.7170 | -0.3 | | |
| 1 - 0 | 12388.9030 | -1.9 | 11709.4182 | -0.6 | 12437.7253 | 2.3 | 11753.1065 | 0.0 |
| 212-111 | 11616.1612 | 0.5 | 11012.8248 | 0.1 | 11679.7564 | -0.4 | 11070.5185 | 0.4 |
| 1 - 0 | 11616.0657 | 0.7 | | | 11679.4771 | -0.1 | 11070.2393 | 0.2 |
| 2 - 2 | 11616.1126 | -1.8 | | | 11679.6206 | -0.6 | 11070.3826 | -1.4 |
| 3 - 2 | 11616.1577 | -0.1 | 11012.8218 | 0.3 | 11679.7468 | 0.2 | 11070.5085 | 0.0 |
| 1 - 2 | 11616.1810 | -0.9 | 11012.8449 | -0.5 | | | | |
| 2 - 1 | 11616.1932 | 0.8 | 11012.8564 | 0.3 | 11679.8487 | 1.5 | 11070.6105 | 0.8 |
| 1 - 1 | 11616.2612 | 1.3 | 11012.9229 | -0.2 | 11680.0412 | -1.0 | 11070.8040 | 0.5 |
| 211-110 | 13255.9081 | 0.4 | 12478.7471 | 0.3 | 13280.1460 | 0.1 | 12500.6724 | -0.1 |
| 1 - 1 | 13255.8101 | 0.7 | 12478.6498 | 0.9 | 13279.8608 | 0.6 | 12500.3868 | -0.6 |
| 3 - 2 | 13255.8970 | 0.7 | 12478.7351 | -0.2 | 13280.1111 | -0.6 | 12500.6381 | 0.1 |
| 1 - 0 | 13255.9083 | -2.4 | 12478.7505 | 1.2 | 13280.1537 | 1.0 | 12500.6790 | 1.0 |
| 2 - 1 | 13255.9403 | 1.0 | 12478.7787 | 0.3 | 13280.2375 | 0.6 | 12500.7641 | 0.5 |
| 2 - 2 | 13255.9798 | -0.1 | 12478.8164 | -2.2 | 13280.3523 | -1.6 | 12500.8790 | -0.9 |
| 211-202 | 10645.7504 | -0.7 | 10671.8943 | -0.2 | 11030.5110 | 0.0 | 11061.3804 | -0.2 |
| 1 - 2 | 10645.6585 | -0.2 | 10671.8010 | -1.1 | 11030.2423 | -1.4 | 11061.1112 | -0.2 |

Table A1.2. (continued)

| $J'K_a'K_c'$-$J''K_a''K_c''$ F'- F'' | $\nu_{rot}$ [a] $\nu_{obs}$ | $\Delta\nu_{rot}$ [b] $\Delta\nu$ [c] | $\nu_{rot}$ [a] $\nu_{obs}$ | $\Delta\nu_{rot}$ [b] $\Delta\nu$ [c] | $\nu_{rot}$ [a] $\nu_{obs}$ | $\Delta\nu_{rot}$ [b] $\Delta\nu$ [c] | $\nu_{rot}$ [a] $\nu_{obs}$ | $\Delta\nu_{rot}$ [b] $\Delta\nu$ [c] |
|---|---|---|---|---|---|---|---|---|
| | $^{20}Ne$-$^{15}N^{14}NO$ | | $^{22}Ne$-$^{15}N^{14}NO$ | | $^{20}Ne$-$^{14}N^{15}NO$ | | $^{22}Ne$-$^{14}N^{15}NO$ | |
| 3 - 2 | 10645.7084 | 3.3 | 10671.8490 | 0.6 | 11030.3792 | 1.0 | 11061.2470 | 1.2 |
| 1 - 1 | 10645.7112 | -1.1 | 10671.8568 | -0.2 | 11030.4022 | 0.6 | 11061.2731 | 0.0 |
| 3 - 3 | 10645.7400 | 0.5 | 10671.8847 | 1.1 | 11030.4803 | 0.5 | 11061.3496 | -0.1 |
| 2 - 2 | 10645.7878 | -0.8 | 10671.9311 | -0.5 | 11030.6192 | -1.2 | 11061.4869 | -0.7 |
| 2 - 3 | 10645.8224 | -0.7 | 10671.9670 | 0.1 | 11030.7222 | 0.3 | 11061.5918 | 0.2 |
| 2 - 1 | 10645.8412 | -1.0 | 10671.9864 | -0.1 | 11030.7786 | 0.3 | 11061.6489 | -0.4 |
| 303-202 | 18444.6798 | -0.2 | 17454.2115 | -0.2 | 18529.1819 | 0.4 | 17528.6424 | -0.5 |
| 2 - 2 | 18444.6331 | -3.6 | | | 18529.0529 | -0.9 | | |
| 3 - 2 | 18444.6708 | -2.5 | 17454.2040 | -1.8 | 18529.1656 | 1.3 | 17528.6279 | 1.0 |
| 4 - 3 | 18444.6809 | 0.3 | 17454.2126 | 0.5 | 18529.1853 | 1.3 | 17528.6430 | -0.7 |
| 2 - 1 | 18444.6928 | 2.5 | 17454.2228 | 1.3 | 18529.2134 | 1.6 | 17528.6706 | -0.3 |
| 3 - 3 | 18444.7111 | 3.3 | | | 18529.2626 | -3.3 | | |
| 303-212 | 10259.2228 | 0.4 | 8981.7661 | 0.1 | 9899.9189 | -0.4 | 8613.0476 | 0.1 |
| 2 - 1 | 10259.1724 | -0.4 | 8981.7155 | 0.3 | 9899.7717 | -0.6 | 8612.8993 | 0.9 |
| 4 - 3 | 10259.2051 | -1.3 | 8981.7491 | -0.2 | 9899.8685 | -2.1 | 8612.9973 | -0.8 |
| 3 - 3 | 10259.2334 | -0.1 | 8981.7773 | -1.0 | 9899.9527 | 0.2 | 8613.0848 | -0.5 |
| 2 - 2 | 10259.2424 | 2.1 | | | 9899.9704 | 3.1 | 8613.0915 | -0.7 |
| 3 - 2 | 10259.2765 | -0.4 | 8981.8222 | 0.9 | 9900.0773 | -0.5 | 8613.2110 | 1.1 |
| 313-212 | 17387.4460 | -0.2 | 16489.6015 | 0.0 | 17485.4590 | 0.0 | 16578.2147 | 0.0 |
| 3 - 3 | | | | | 17485.3503 | -2.5 | | |
| 2 - 1 | 17387.4364 | 2.3 | 16489.5867 | -2.8 | 17485.4252 | 1.0 | 16578.1791 | -0.5 |
| 4 - 3 | 17387.4453 | -0.2 | 16489.6014 | 0.5 | 17485.4571 | -0.2 | 16578.2137 | 1.0 |
| 3 - 2 | 17387.4504 | -2.1 | 16489.6104 | 2.2 | 17485.4789 | 0.7 | 16578.2339 | -0.5 |
| 2 - 2 | | | | | 17485.6203 | 1.1 | | |
| 312-303 | 12042.6587 | 0.2 | 11901.8842 | 0.0 | 12382.2713 | 0.0 | 12252.1647 | 0.1 |
| 2 - 3 | | | | | 12382.0436 | -0.6 | 12251.9315 | -1.8 |
| 4 - 3 | | | | | 12382.1411 | 0.2 | 12252.0321 | 2.0 |
| 2 - 2 | 12042.6178 | -0.1 | 11901.8442 | -0.4 | 12382.1551 | 0.4 | 12252.0525 | 1.5 |
| 4 - 4 | 12042.6410 | -0.7 | 11901.8670 | -0.7 | 12382.2237 | 1.0 | 12252.1172 | -0.1 |
| 3 - 3 | 12042.7106 | 0.9 | 11901.9349 | 1.1 | 12382.4168 | -0.3 | 12252.3060 | -0.8 |
| 3 - 4 | 12042.7341 | -2.7 | | | 12382.4996 | 0.7 | 12252.3928 | -1.2 |
| 3 - 2 | 12042.7487 | 2.4 | | | 12382.5262 | -1.4 | 12252.4248 | 0.3 |
| 404-313 | 17214.7934 | 0.0 | 15564.9028 | 0.0 | 16889.6862 | 0.0 | 15222.5584 | 0.1 |
| 3 - 2 | 17214.7649 | 2.0 | 15564.8720 | 1.0 | 16889.5953 | -0.4 | 15222.4632 | -1.0 |
| 5 - 4 | 17214.7779 | -2.0 | 15564.8873 | -1.3 | 16889.6457 | -0.2 | 15222.5155 | -0.6 |
| 4 - 3 | 17214.8328 | 0.0 | 15564.9443 | 0.2 | 16889.8040 | 0.5 | 15222.6827 | 1.6 |
| 413-404 | 14073.2918 | 0.0 | 13676.1128 | 0.0 | 14339.2089 | 0.0 | 13963.0410 | 0.0 |
| 3 - 3 | 14073.2484 | -0.5 | 13676.0720 | 0.5 | 14339.0880 | 1.3 | 13962.9236 | 1.0 |
| 5 - 4 | 14073.2572 | 3.8 | | | | | | |

Table A1.2. (continued)

| $J'K_a'K_c'$-$J''K_a''K_c''$ F'- F'' | $\nu_{rot}$ [a] $\nu_{obs}$ | $\Delta\nu_{rot}$ [b] $\Delta\nu$ [c] | $\nu_{rot}$ [a] $\nu_{obs}$ | $\Delta\nu_{rot}$ [b] $\Delta\nu$ [c] | $\nu_{rot}$ [a] $\nu_{obs}$ | $\Delta\nu_{rot}$ [b] $\Delta\nu$ [c] | $\nu_{rot}$ [a] $\nu_{obs}$ | $\Delta\nu_{rot}$ [b] $\Delta\nu$ [c] |
|---|---|---|---|---|---|---|---|---|
| | $^{20}Ne$-$^{15}N^{14}NO$ | | $^{22}Ne$-$^{15}N^{14}NO$ | | $^{20}Ne$-$^{14}N^{15}NO$ | | $^{22}Ne$-$^{14}N^{15}NO$ | |
| 5 - 5 | 14073.2680 | -2.0 | 13676.0911 | -0.7 | 14339.1464 | -0.3 | 13962.9804 | -0.3 |
| 4 - 4 | 14073.3505 | -1.3 | 13676.1709 | 0.1 | 14339.3790 | -1.0 | 13963.2061 | -0.7 |

[a] Hypothetical center frequencies in MHz from the quadrupole fit.

[b] Deviations in kHz from the center frequencies from the rotational fit.

[c] Observed-calculated frequencies in kHz from the quadrupole fit.

# A2

# TABLE OF THE MEASURED TRANSITION FREQUENCIES FOR CHAPTER FOUR

Table A2.1. Observed Transition Frequencies of Ar-$^{15}N^{14}NO$ and Ar-$^{14}N^{15}NO$

| $J'K_aK_c'$-$J''K_aK_c''$ F'-F'' | Ar-$^{15}N^{14}NO$ $\nu_{obs}$ | $\Delta\nu^a$ | Ar-$^{14}N^{15}NO$ $\nu_{obs}$ | $\Delta\nu^a$ |
|---|---|---|---|---|
| 111-000 | | | | |
| 1-1 | 14071.1152 | -1.9 | 14504.7573 | -0.4 |
| 2-1 | 14071.1932 | -1.4 | 14504.9825 | -2.3 |
| 0-1 | 14071.3078 | -3.0 | 14505.3237 | -1.6 |
| 110-101 | | | | |
| 0-1 | 10660.3316 | -3.7 | 11076.4762 | -1.0 |
| 2-1 | 10660.3973 | -1.3 | 11076.6519 | 0.9 |
| 2-2 | 10660.4342 | 0.4 | 11076.7622 | 0.0 |
| 1-1 | 10660.4412 | 0.5 | 11076.7622 | -4.7 |
| 1-2 | 10660.4745 | -1.5 | 11076.8770 | -1.1 |
| 1-0 | 10660.5278 | -1.1 | 11077.0442 | -0.6 |
| 202-101 | | | | |
| 1-1 | 7394.6142 | -2.8 | 7414.3294 | -0.3 |
| 3-2 | 7394.6716 | -0.7 | 7414.5033 | -1.1 |
| 2-1 | 7394.6716 | -1.4 | 7414.5033 | -4.3 |
| 1-0 | 7394.7020 | -3.2 | 7414.6079 | 0.2 |
| 2-2 | 7394.7020 | -6.3 | 7414.6185 | -0.3 |
| 212-101 | | | | |
| 2-1 | 17480.3714 | -0.0 | 17931.4302 | 1.2 |
| 2-2 | 17480.4076 | 0.9 | 17931.5400 | -0.2 |
| 1-1 | 17480.4429 | 1.2 | 17931.6227 | 0.6 |
| 211-110 | | | | |
| 1-0 | 7689.2008 | 0.5 | 7700.7067 | 2.1 |
| 2-1 | 7689.2226 | -1.3 | 7700.7949 | 1.5 |
| 2-2 | 7689.2644 | -1.7 | 7700.9088 | -0.5 |
| 211-202 | | | | |
| 1-2 | 10954.8636 | 1.0 | 11362.6750 | 0.7 |
| 3-2 | 10954.9096 | 0.9 | 11362.8110 | 1.6 |
| 1-1 | 10954.9188 | 0.2 | 11362.8526 | 0.4 |
| 3-3 | 10954.9465 | 1.8 | 11362.9258 | 2.0 |
| 2-2 | 10954.9920 | 0.4 | 11363.0540 | 1.3 |
| 2-3 | 10955.0288 | 1.1 | 11363.1672 | 0.2 |
| 2-1 | 10955.0513 | 3.6 | 11363.2307 | 0.1 |
| 303-202 | | | | |
| 2-2 | 11076.0875 | -0.6 | 11107.0590 | 0.8 |
| 3-2 | 11076.1355 | 0.7 | 11107.2122 | 3.9 |
| 4-3 | 11076.1355 | -0.8 | 11107.2122 | 0.7 |
| 2-1 | 11076.1470 | 2.9 | 11107.2361 | 0.0 |
| 3-3 | 11076.1735 | 2.7 | 11107.3236 | 0.9 |
| 313-212 | | | | |
| 3-3 | 10660.1300 | -0.1 | 10700.9825 | -2.4 |
| 2-1 | 10660.1560 | 0.2 | 10701.0479 | -2.2 |
| 312-303 | | | | |
| 4-3 | 11407.7028 | 0.3 | 11802.1096 | 0.1 |
| 2-2 | 11407.7160 | 0.1 | 11802.1613 | 0.2 |
| 4-4 | 11407.7390 | 1.9 | 11802.2214 | 0.7 |
| 3-3 | 11407.7986 | 0.8 | 11802.3917 | 0.6 |
| 3-4 | 11407.8331 | 0.7 | 11802.5007 | -1.6 |
| 3-2 | 11407.8452 | 0.7 | 11802.5422 | 0.9 |
| 404-303 | | | | |
| 3-3 | 14738.6279 | 1.9 | 14782.4095 | -3.3 |
| 4-3 | 14738.6703 | 4.6 | 14782.5408 | -2.4 |
| 5-4 | 14738.6703 | 1.6 | 14782.5518 | 1.1 |
| 3-2 | 14738.6703 | -2.4 | 14782.5638 | 0.9 |
| 4-4 | 14738.7011 | 0.8 | 14782.6562 | 1.8 |
| 414-313 | | | | |
| 4-4 | 14205.2526 | -1.4 | 14260.3279 | -0.2 |
| 3-2 | 14205.2864 | 1.2 | 14260.4078 | -0.4 |
| 5-4 | 14205.2864 | -2.9 | 14260.4197 | 0.3 |
| 4-3 | 14205.2864 | -5.2 | 14260.4277 | 0.2 |
| 3-3 | 14205.3334 | -2.6 | 14260.5428 | 0.5 |
| 413-312 | | | | |
| 3-3 | 15362.6189 | 0.3 | 15386.4607 | 0.9 |

Table A2.1. (continued)

| $J'K_a'K_c'$-$J''K_a''K_c''$ F'-F'' | $\nu_{obs}$ | $\Delta\nu^a$ | $\nu_{obs}$ | $\Delta\nu^a$ | $J'K_a'K_c'$-$J''K_a''K_c''$ F'-F'' | $\nu_{obs}$ | $\Delta\nu^a$ | $\nu_{obs}$ | $\Delta\nu^a$ | $J'K_a'K_c'$-$J''K_a''K_c''$ F'-F'' | $\nu_{obs}$ | $\Delta\nu^a$ | $\nu_{obs}$ | $\Delta\nu^a$ |
|---|---|---|---|---|---|---|---|---|---|---|---|---|---|---|
| | Ar-$^{15}N^{14}NO$ | | Ar-$^{14}N^{15}NO$ | | | Ar-$^{15}N^{14}NO$ | | Ar-$^{14}N^{15}NO$ | | | Ar-$^{15}N^{14}NO$ | | Ar-$^{14}N^{15}NO$ | |
| 3-2 | 17480.4523 | 0.4 | 17931.6664 | 2.1 | 4-3 | 10660.1672 | -0.5 | 10701.0838 | -0.4 | 5-4 | 15362.7398 | 0.1 | 15386.8177 | -0.4 |
| 1-0 | 17480.5303 | 0.4 | 17931.9001 | 0.0 | 3-2 | 10660.1766 | 1.4 | 10701.1086 | -0.4 | 4-3 | 15362.7458 | 0.8 | 15386.8397 | 5.1 |
| | | | | | 2-2 | 10660.2278 | 1.8 | 10701.2423 | -0.9 | 3-2 | 15362.7458 | -1.4 | 15386.8397 | -0.3 |
| 212-111 | | | | | | | | | | 4-4 | 15362.8397 | -0.5 | 15387.1169 | 0.7 |
| 1-0 | 7109.6798 | 2.5 | 7136.5616 | 1.9 | 312-211 | | | | | | | | | |
| 2-2 | 7109.7249 | 1.7 | 7136.7068 | -0.4 | 2-2 | 11528.8123 | -0.1 | 11546.1649 | -1.8 | 413-404 | | | | |
| 3-2 | 7109.7681 | -0.3 | 7136.8318 | 0.5 | 4-3 | 11528.9291 | 0.4 | 11546.5068 | -1.7 | 3-4 | 12031.7500 | -0.6 | 12406.3069 | -0.9 |
| 2-1 | 7109.8027 | 2.0 | 7136.9359 | 1.7 | 3-2 | 11528.9413 | 0.3 | 11546.5460 | -0.8 | 5-4 | 12031.7769 | 0.4 | 12406.3835 | -1.0 |
| 1-1 | 7109.8710 | 0.1 | 7137.1283 | 1.0 | 2-1 | 11528.9413 | -0.1 | 11546.5460 | 0.9 | 3-3 | 12031.7902 | -0.2 | 12406.4382 | -0.1 |
| | | | | | 3-3 | 11529.0236 | -0.4 | 11546.7881 | -2.0 | 5-5 | 12031.8059 | -2.2 | 12406.4872 | -1.0 |
| 211-110 | | | | | | | | | | 4-4 | 12031.8761 | -0.9 | 12406.6821 | -0.5 |
| 1-1 | 7689.0944 | -0.4 | 7700.4155 | 0.5 | 312-303 | | | | | 4-5 | 12031.9081 | -0.5 | 12406.7865 | 0.2 |
| 3-2 | 7689.1828 | -0.3 | 7700.6663 | 0.3 | 2-3 | 11407.6695 | 0.3 | 11802.0113 | 0.3 | 4-3 | 12031.9168 | 0.0 | 12406.8134 | 0.4 |

[a] observed-calculated frequencies (kHz), $\nu_{obs}$ in MHz

# A3

# TABLES OF THE MEASURED TRANSITION FREQUENCIES FOR CHAPTER FIVE

Table A3.1. The measured transition frequencies of the $^{14}N$-hyperfine patterns of $^{40}Ar_2$-$^{14}N_2O$.

| $J'K_a'K_c'$-$J''K_a''K_c''$ $F_1'F_2'$-$F_1''F_2''$ | $\nu_{obs}$[a] | $\Delta\nu$[b] | $J'K_a'K_c'$-$J''K_a''K_c''$ $F_1'F_2'$-$F_1''F_2''$ | $\nu_{obs}$[a] | $\Delta\nu$[b] | $J'K_a'K_c'$-$J''K_a''K_c''$ $F_1'F_2'$-$F_1''F_2''$ | $\nu_{obs}$[a] | $\Delta\nu$[b] |
|---|---|---|---|---|---|---|---|---|
| 110-000 | | | 221-111 | | | 312-221 | | |
| 10-11 | 3348.0000 | 2.2 | 11-01 | 7012.4727 | -1.9 | 32-21 | 6946.2742 | -1.7 |
| 12-12 | 3348.0495 | 1.2 | 12-01 | 7012.4894 | -1.2 | 34-23 | 6946.2825 | 0.3 |
| 12-11 | 3348.0495 | 1.2 | | | | 33-22 | 6946.2962 | -1.0 |
| 11-12 | 3348.0700 | -0.3 | 331-220 | | | | | |
| 11-11 | 3348.0700 | -0.3 | 22-11 | 10221.1610 | 2.1 | 330-220 | | |
| 11-10 | 3348.0700 | -0.3 | 23-12 | 10221.1752 | 0.8 | 34-34 | 10390.5267 | -1.3 |
| 22-12 | 3348.2462 | 0.9 | 44-34 | 10221.1752 | 0.5 | 22-11 | 10390.6850 | -1.0 |
| 22-11 | 3348.2462 | 0.9 | 21-11 | 10221.2307 | 1.6 | 44-34 | 10390.6850 | -2.6 |
| 23-12 | 3348.2964 | 0.6 | 33-23 | 10221.2307 | 0.3 | 33-23 | 10390.7094 | 1.9 |
| 21-12 | 3348.3365 | -0.6 | 45-34 | 10221.2307 | 0.0 | 23-12 | 10390.7094 | -1.0 |
| 21-11 | 3348.3365 | -0.6 | 44-33 | 10221.2411 | 3.0 | 33-22 | 10390.7497 | 1.2 |
| 21-10 | 3348.3365 | -0.6 | 33-22 | 10221.2709 | -0.5 | 43-32 | 10390.7497 | 2.5 |
| 01-12 | 3348.6284 | -0.6 | 32-21 | 10221.2801 | 3.8 | 44-33 | 10390.7497 | -1.3 |
| 01-11 | 3348.6284 | -0.6 | 34-23 | 10221.2801 | 2.4 | 45-34 | 10390.7497 | -5.0 |
| 01-10 | 3348.6284 | -0.6 | 23-23 | 10221.5267 | -0.7 | 34-23 | 10390.7620 | -2.1 |
| | | | | | | 32-21 | 10390.7620 | -3.5 |
| 212-101 | | | 313-202 | | | | | |
| 10-11 | 4677.9524 | 2.0 | 23-23 | 6461.9606 | 0.4 | 312-202 | | |
| 12-12 | 4677.9918 | -0.0 | 21-11 | 6462.2400 | -1.8 | 33-22 | 9695.8112 | 0.8 |
| 11-12 | 4678.0228 | -0.7 | 43-32 | 6462.2981 | 0.7 | 23-22 | 9695.8602 | 4.2 |
| 34-23 | 4678.2428 | 1.2 | 45-34 | 6462.2981 | 0.5 | 34-23 | 9695.8602 | 1.7 |
| 33-22 | 4678.2837 | 0.1 | 32-22 | 6462.3111 | -1.4 | 21-22 | 9695.8602 | 0.4 |
| 12-01 | 4678.2837 | -1.4 | 23-12 | 6462.3111 | -2.1 | 32-21 | 9695.8751 | -1.2 |
| 23-12 | 4678.3688 | 0.5 | 21-10 | 6462.3202 | -0.7 | 44-33 | 9696.0530 | 1.3 |
| 22-11 | 4678.4239 | 0.8 | 44-33 | 6462.3268 | -0.6 | 45-34 | 9696.1246 | 1.0 |
| 23-23 | 4678.4935 | 0.2 | 22-11 | 6462.3552 | -3.5 | 32-32 | 9696.1246 | 1.0 |
| | | | 32-21 | 6462.3677 | -1.4 | 43-32 | 9696.1542 | 1.3 |
| 221-110 | | | 34-23 | 6462.3776 | 0.5 | 22-11 | 9696.2135 | 0.0 |
| 12-01 | 6444.5452 | -0.9 | 33-22 | 6462.4126 | -2.2 | 23-12 | 9696.2503 | 0.3 |
| 23-23 | 6444.6888 | -0.4 | 34-34 | 6462.6141 | 1.0 | | | |
| 32-21 | 6444.7885 | -1.0 | 32-32 | 6462.6141 | -2.3 | 321-211 | | |
| 34-23 | 6444.8166 | 0.3 | | | | 33-22 | 9645.3254 | -0.7 |
| 33-22 | 6444.8307 | -1.8 | 322-211 | | | 34-23 | 9645.3477 | -2.3 |
| 22-11 | 6444.8910 | -1.5 | 21-10 | 8341.9016 | -1.5 | 32-22 | 9645.3895 | 4.3 |
| 22-12 | 6444.9127 | -1.8 | 23-12 | 8341.9287 | -0.3 | 44-33 | 9645.3895 | 1.7 |
| 23-12 | 6444.9359 | -0.7 | 22-12 | 8341.9287 | -0.3 | 21-10 | 9645.4097 | 6.2 |
| 21-10 | 6444.9954 | -0.2 | 21-11 | 8341.9450 | 0.4 | 23-12 | 9645.4097 | 4.4 |
| 12-12 | 6445.1261 | -0.6 | 22-11 | 8341.9450 | 0.4 | 45-34 | 9645.4097 | 1.3 |
| | | | 43-32 | 8341.9783 | 1.6 | 22-22 | 9645.5692 | -0.6 |
| 220-111 | | | 32-32 | 8341.9783 | 1.6 | 23-23 | 9645.5917 | -0.1 |
| 22-11 | 7363.0114 | -0.5 | 45-34 | 8341.9904 | -0.5 | | | |
| 21-10 | 7363.0305 | -2.2 | 34-34 | 8341.9904 | -0.5 | 322-212 | | |
| 23-12 | 7363.0416 | -0.5 | 44-34 | 8341.9904 | -0.5 | 21-22 | 10043.7170 | 0.4 |
| 23-23 | 7363.1644 | -0.1 | 33-33 | 8342.0271 | 2.9 | 23-22 | 10043.7170 | 0.4 |

Table A3.1. (continued)

| $J'K_a'K_c'$-$J''K_a''K_c''$ $F_1'F_2'$-$F_1''F_2''$ | $\nu_{obs}$[a] | $\Delta\nu$[b] | $J'K_a'K_c'$-$J''K_a''K_c''$ $F_1'F_2'$-$F_1''F_2''$ | $\nu_{obs}$[a] | $\Delta\nu$[b] | $J'K_a'K_c'$-$J''K_a''K_c''$ $F_1'F_2'$-$F_1''F_2''$ | $\nu_{obs}$[a] | $\Delta\nu$[b] |
|---|---|---|---|---|---|---|---|---|
| 33-22 | 7363.3123 | 0.1 | 34-33 | 8342.0271 | 2.9 | 22-22 | 10043.7170 | 0.4 |
| 34-23 | 7363.4015 | 1.0 | 44-33 | 8342.0271 | 2.9 | 32-22 | 10043.7170 | 0.4 |
| 32-22 | 7363.4015 | -1.0 | 43-33 | 8342.0271 | 2.9 | 33-22 | 10043.7170 | 0.4 |
| 32-21 | 7363.4471 | -0.7 | 21-21 | 8342.1091 | 1.9 | 23-23 | 10043.7595 | -0.8 |
| 11-01 | 7363.6528 | -0.0 | 22-21 | 8342.1091 | 1.8 | 22-23 | 10043.7595 | -0.8 |
| 12-01 | 7363.6829 | 0.4 | 32-21 | 8342.1091 | 1.9 | 34-23 | 10043.7595 | -0.8 |
| | | | 33-23 | 8342.1163 | 0.9 | 33-23 | 10043.7595 | -0.8 |
| 202-111 | | | 22-23 | 8342.1163 | 0.8 | 21-21 | 10043.7755 | -1.4 |
| 12-12 | 4262.0830 | -0.7 | 34-23 | 8342.1163 | 0.9 | 22-21 | 10043.7755 | -1.4 |
| 32-22 | 4262.2731 | 1.8 | 23-23 | 8342.1163 | 0.8 | 32-21 | 10043.7755 | -1.4 |
| 10-01 | 4262.3262 | 4.5 | 21-22 | 8342.1362 | -0.8 | 33-33 | 10043.9455 | 1.1 |
| 34-23 | 4262.3262 | 3.1 | 23-22 | 8342.1362 | -0.8 | 34-33 | 10043.9455 | 1.1 |
| 33-22 | 4262.3596 | -2.1 | 22-22 | 8342.1362 | -0.8 | 44-33 | 10043.9455 | 1.1 |
| 11-01 | 4262.4032 | 2.4 | 32-22 | 8342.1362 | -0.8 | 43-33 | 10043.9455 | 1.1 |
| 23-12 | 4262.4383 | 1.6 | 33-22 | 8342.1362 | -0.8 | 45-34 | 10044.0124 | 0.4 |
| 22-11 | 4262.4892 | 0.7 | | | | 34-34 | 10044.0124 | 0.4 |
| 23-23 | 4262.5591 | -0.0 | 321-212 | | | 44-34 | 10044.0124 | 0.4 |
| | | | 33-22 | 11346.9051 | -0.7 | 43-32 | 10044.0402 | -0.4 |
| 211-101 | | | 34-23 | 11346.9943 | -0.6 | 32-32 | 10044.0402 | -0.4 |
| 21-10 | 6379.9950 | -0.7 | 32-21 | 11347.0249 | -0.2 | 21-11 | 10044.1047 | -0.4 |
| 23-12 | 6380.0130 | -0.2 | 44-33 | 11347.3081 | 0.1 | 22-11 | 10044.1047 | -0.5 |
| 22-21 | 6380.1381 | 0.5 | 45-34 | 11347.4310 | 1.5 | 23-12 | 10044.1363 | -0.5 |
| 23-23 | 6380.1381 | -0.1 | 43-32 | 11347.4731 | -0.7 | 22-12 | 10044.1363 | -0.5 |
| 21-21 | 6380.1713 | 4.0 | 22-11 | 11347.5394 | 1.4 | 21-10 | 10044.1889 | -0.5 |
| 33-22 | 6380.2023 | -1.5 | 23-12 | 11347.6129 | -0.2 | | | |
| 33-23 | 6380.2300 | 0.6 | | | | 331-221 | | |
| 34-23 | 6380.2638 | 1.1 | 303-212 | | | 33-22 | 10572.2803 | -1.3 |
| 32-21 | 6380.2985 | 0.7 | 23-23 | 6341.0281 | 0.8 | 34-23 | 10572.3048 | -1.9 |
| 12-01 | 6380.4956 | 2.8 | 22-22 | 6341.0596 | 1.6 | 32-21 | 10572.3127 | 0.3 |
| | | | 45-34 | 6341.3811 | 1.8 | 44-34 | 10572.3127 | 0.1 |
| 220-110 | | | 43-32 | 6341.3811 | -0.0 | 22-11 | 10572.3350 | -2.2 |
| 11-01 | 6795.7083 | 0.0 | 23-12 | 6341.4040 | 0.2 | 44-33 | 10572.3478 | 1.0 |
| 23-23 | 6795.7198 | 1.6 | 44-33 | 6341.4040 | 0.2 | 21-10 | 10572.3687 | 4.0 |
| 12-01 | 6795.7382 | 0.2 | 22-11 | 6341.4486 | 2.1 | 23-12 | 10572.3687 | 2.4 |
| 22-11 | 6795.9024 | -0.3 | 44-34 | 6341.4741 | 2.7 | 45-34 | 10572.3687 | 0.1 |
| 32-21 | 6795.9416 | 1.9 | 33-22 | 6341.4741 | 0.5 | 43-32 | 10572.3687 | -1.6 |
| 33-22 | 6795.9416 | 0.4 | | | | | | |
| 34-23 | 6795.9542 | 0.0 | 330-221 | | | 414-303 | | |
| 23-12 | 6795.9658 | 0.2 | 34-34 | 10741.6663 | 0.4 | 56-45 | 8310.8736 | 0.6 |
| 32-22 | 6796.0316 | 0.0 | 32-32 | 10741.6663 | -2.1 | 54-43 | 8310.8736 | -1.6 |
| 21-10 | 6796.0316 | -0.2 | 33-22 | 10741.7577 | -1.0 | 34-23 | 8310.8905 | 3.5 |
| 11-11 | 6796.2673 | 0.3 | 34-23 | 10741.7943 | 1.3 | 55-44 | 8310.8905 | -0.9 |
| 12-12 | 6796.3185 | -0.2 | 44-33 | 10741.8595 | -0.2 | 32-21 | 8310.8905 | -3.4 |
| | | | 45-34 | 10741.8914 | -1.1 | 43-32 | 8310.9182 | -0.6 |
| 221-111 | | | 23-12 | 10741.9054 | 3.1 | 45-34 | 8310.9182 | -1.0 |
| 22-11 | 7012.0009 | -0.8 | 21-10 | 10741.9054 | -0.2 | 44-33 | 8310.9402 | -2.1 |

Table A3.1. (continued)

| $J'K_a'K_c'$-$J''K_a''K_c''$ $F_1'F_2'$-$F_1''F_2''$ | $\nu_{obs}$[a] | $\Delta\nu$[b] | $J'K_a'K_c'$-$J''K_a''K_c''$ $F_1'F_2'$-$F_1''F_2''$ | $\nu_{obs}$[a] | $\Delta\nu$[b] | $J'K_a'K_c'$-$J''K_a''K_c''$ $F_1'F_2'$-$F_1''F_2''$ | $\nu_{obs}$[a] | $\Delta\nu$[b] |
|---|---|---|---|---|---|---|---|---|
| 23-12 | 7012.0129 | -0.2 | 43-33 | 10741.9481 | 1.9 | | | |
| 22-21 | 7012.1363 | 2.6 | 21-11 | 10741.9481 | -0.2 | 404-313 | | |
| 23-23 | 7012.1363 | 0.8 | | | | 56-45 | 8286.2239 | 0.5 |
| 11-10 | 7012.1607 | -1.5 | 312-221 | | | 54-43 | 8286.2239 | -2.0 |
| 21-21 | 7012.1607 | -3.6 | 22-11 | 6946.1369 | -2.8 | 34-23 | 8286.2414 | 2.7 |
| 12-12 | 7012.2019 | -1.3 | 21-11 | 6946.1486 | -1.7 | 55-44 | 8286.2414 | 0.8 |
| 33-22 | 7012.2019 | -1.5 | 43-32 | 6946.1693 | -2.7 | 32-21 | 8286.2488 | 2.7 |
| 12-11 | 7012.2147 | 0.7 | 33-33 | 6946.1846 | 2.4 | 33-22 | 8286.2656 | 2.2 |
| 33-23 | 7012.2263 | -2.0 | 45-34 | 6946.1846 | 0.5 | 43-32 | 8286.2656 | 0.3 |
| 34-23 | 7012.2631 | 0.5 | 44-33 | 6946.2067 | -3.3 | 45-34 | 8286.2656 | 0.1 |
| 32-21 | 7012.2966 | -0.9 | 33-23 | 6946.2742 | -0.8 | 44-33 | 8286.2879 | 0.4 |

[a] Measured frequencies in MHz.

[b] Observed-calculated frequencies in kHz.

Table A3.2. Measured frequencies of the $^{14}N$-hyperfine structure of $^{40}Ar_2$-$^{15}N^{14}NO$ and $^{40}Ar_2$-$^{14}N^{15}NO$.

| $J'K_a'K_c'$-$J''K_a''K_c''$ F'-F'' | $\nu_{obs}$[a] | $\Delta\nu$[b] | $\nu_{obs}$[a] | $\Delta\nu$[b] | $J'K_a'K_c'$-$J''K_a''K_c''$ F'-F'' | $\nu_{obs}$[a] | $\Delta\nu$[b] | $\nu_{obs}$[a] | $\Delta\nu$[b] | $J'K_a'K_c'$-$J''K_a''K_c''$ F'-F'' | $\nu_{obs}$[a] | $\Delta\nu$[b] | $\nu_{obs}$[a] | $\Delta\nu$[b] |
|---|---|---|---|---|---|---|---|---|---|---|---|---|---|---|
| | $^{40}Ar_2$-$^{15}N^{14}NO$ | | $^{40}Ar_2$-$^{14}N^{15}NO$ | | | $^{40}Ar_2$-$^{15}N^{14}NO$ | | $^{40}Ar_2$-$^{14}N^{15}NO$ | | | $^{40}Ar_2$-$^{15}N^{14}NO$ | | $^{40}Ar_2$-$^{14}N^{15}NO$ | |
| 212-101 | | | | | 221-111 | | | | | 312-202 | | | | |
| 1-1 | 4627.4154 | 0.2 | 4637.9384 | -0.8 | 1-0 | 6910.2732 | 2.1 | 6946.1846 | -0.4 | 2-2 | 9625.1304 | -0.2 | 9668.8841 | 0.1 |
| 3-2 | 4627.5009 | 1.6 | 4638.1835 | 0.7 | | | | | | 3-3 | 9625.1988 | 1.6 | 9669.0729 | 0.3 |
| 1-0 | 4627.5155 | 1.9 | 4638.2167 | -0.3 | 313-202 | | | | | 4-3 | 9625.2040 | -0.6 | 9669.1002 | 0.8 |
| 2-1 | 4627.5391 | -1.4 | 4638.3106 | 0.5 | 2-2 | 6405.3077 | 1.9 | 6415.0707 | 0.6 | 2-1 | 9625.2497 | -0.1 | 9669.2332 | -0.4 |
| 2-2 | 4627.5788 | -1.0 | 4638.4209 | -0.3 | 4-3 | 6405.4167 | -1.9 | 6415.4021 | 0.3 | | | | | |
| | | | | | 2-1 | 6405.4243 | -0.7 | 6415.4189 | -0.8 | 331-221 | | | | |
| 221-110 | | | | | 3-2 | 6405.4453 | 0.0 | 6415.4835 | 1.0 | 3-3 | 10412.0002 | 2.4 | 10466.1381 | -0.5 |
| 1-0 | 6342.6351 | -0.8 | 6372.2768 | 0.1 | 3-3 | 6405.5221 | 0.2 | 6415.7070 | -0.3 | 3-2 | 10412.0405 | 0.6 | 10466.2583 | 0.7 |
| 2-2 | 6342.6831 | 0.1 | 6372.4256 | 0.3 | | | | | | 2-1 | 10412.0605 | 0.3 | 10466.3202 | 2.5 |
| 3-2 | 6342.7239 | -1.2 | 6372.5446 | 0.2 | 321-212 | | | | | 4-3 | 10412.0605 | -0.9 | 10466.3202 | -0.1 |
| 2-1 | 6342.7579 | -0.2 | 6372.6490 | 1.2 | 3-2 | 11260.2443 | 0.3 | 11321.2690 | 0.8 | 2-2 | 10412.1257 | -0.1 | 10466.5037 | 0.7 |
| 1-1 | 6342.8233 | -0.3 | 6372.8329 | -0.2 | 2-2 | 11260.3232 | -0.2 | 11321.5067 | 0.0 | | | | | |
| | | | | | 3-3 | 11260.3232 | -1.3 | 11321.5067 | -3.4 | 330-220 | | | | |
| 220-111 | | | | | 4-3 | 11260.3842 | 0.9 | 11321.6866 | 0.8 | 3-3 | 10232.7458 | 1.5 | 10284.9128 | -0.2 |
| 2-1 | 7273.2799 | -0.3 | 7312.2974 | 0.5 | 2-1 | 11260.4496 | 1.1 | 11321.8807 | -0.3 | 2-1 | 10232.8070 | 2.6 | 10285.0863 | 0.5 |
| 2-2 | 7273.3166 | 0.7 | 7312.4079 | -0.4 | | | | | | 4-3 | 10232.8203 | -0.1 | 10285.1331 | -0.4 |
| 3-2 | 7273.3926 | 0.0 | 7312.6333 | 0.3 | 321-211 | | | | | 3-2 | 10232.8203 | -0.6 | 10285.1331 | -4.7 |
| 1-1 | 7273.4002 | 0.8 | 7312.6435 | -3.0 | 3-3 | 9558.1442 | -0.6 | 9601.5733 | -0.9 | 2-2 | 10232.9252 | 1.6 | 10285.4350 | -0.5 |
| 1-0 | 7273.4874 | -1.4 | 7312.9242 | -0.9 | 3-2 | 9558.1832 | 0.1 | 9601.6919 | -1.7 | | | | | |
| | | | | | 2-1 | 9558.2028 | -0.0 | 9601.7545 | 4.8 | 312-221 | | | | |
| 211-101 | | | | | 4-3 | 9558.2028 | -0.8 | 9601.7545 | 1.2 | 2-1 | 6966.0538 | -1.9 | 6979.9509 | 0.3 |
| 2-1 | 6329.6002 | -1.1 | 6357.8835 | -1.2 | 2-2 | 9558.2637 | 1.3 | 9601.9349 | -0.5 | 3-3 | 6966.0677 | -1.5 | 6979.9811 | 0.5 |
| 2-2 | 6329.6412 | 0.5 | 6357.9962 | 0.3 | | | | | | 4-3 | 6966.0778 | 1.3 | 6980.0070 | -0.4 |
| 1-1 | 6329.6621 | 1.1 | 6358.0702 | -0.3 | 322-212 | | | | | 3-2 | 6966.1119 | 0.6 | 6980.0992 | -0.5 |
| 3-2 | 6329.6798 | 0.8 | 6358.1158 | 0.6 | 3-2 | 9929.4630 | -0.6 | 9977.4393 | 0.2 | 2-2 | 6966.1222 | 0.9 | 6980.1355 | -0.4 |
| 1-0 | 6329.7603 | 1.0 | 6358.3499 | 1.6 | 2-2 | 9929.4630 | -0.6 | 9977.4393 | 0.2 | | | | | |
| | | | | | 3-3 | 9929.5448 | 0.7 | 9977.6770 | -0.6 | 330-221 | | | | |

Table A3.2. (continued)

| $J'K_a'K_c'$-$J''K_a''K_c''$ F′-F″ | $\nu_{obs}$[a] | $\Delta\nu$[b] | $\nu_{obs}$[a] | $\Delta\nu$[b] | $J'K_a'K_c'$-$J''K_a''K_c''$ F′-F″ | $\nu_{obs}$[a] | $\Delta\nu$[b] | $\nu_{obs}$[a] | $\Delta\nu$[b] | $J'K_a'K_c'$-$J''K_a''K_c''$ F′-F″ | $\nu_{obs}$[a] | $\Delta\nu$[b] | $\nu_{obs}$[a] | $\Delta\nu$[b] |
|---|---|---|---|---|---|---|---|---|---|---|---|---|---|---|
| | $^{40}Ar_2$-$^{15}N^{14}NO$ | | $^{40}Ar_2$-$^{14}N^{15}NO$ | | | $^{40}Ar_2$-$^{15}N^{14}NO$ | | $^{40}Ar_2$-$^{14}N^{15}NO$ | | | $^{40}Ar_2$-$^{15}N^{14}NO$ | | $^{40}Ar_2$-$^{14}N^{15}NO$ | |
| 220-110 | | | | | 4-3 | 9929.5448 | 0.7 | 9977.6770 | -0.6 | 3-3 | 10595.9399 | -3.0 | 10651.5942 | -0.1 |
| 2-2 | 6705.8466 | -0.5 | 6739.0007 | -0.2 | 2-1 | 9929.5884 | -0.4 | 9977.8102 | 0.2 | 3-2 | 10595.9835 | -1.5 | 10651.7136 | 0.2 |
| 1-0 | 6705.8548 | 1.2 | 6739.0163 | -0.4 | | | | | | 4-3 | 10596.0196 | 0.7 | 10651.8150 | 0.2 |
| 2-1 | 6705.9233 | 1.1 | 6739.2259 | 2.4 | 303-212 | | | | | 2-1 | 10596.0196 | -2.6 | 10651.8288 | 2.9 |
| 3-2 | 6705.9233 | -0.4 | 6739.2259 | 0.2 | 2-2 | 6302.2356 | 1.1 | 6310.4877 | 0.0 | 2-2 | 10596.0855 | -2.2 | 10652.0106 | -0.5 |
| 1-1 | 6706.0399 | -1.5 | 6739.5728 | -0.3 | 4-3 | 6302.3496 | -1.3 | 6310.8319 | -0.2 | | | | | |
| | | | | | 2-1 | 6302.3600 | 0.3 | 6310.8594 | 0.8 | 331-220 | | | | |
| 221-111 | | | | | 3-2 | 6302.3723 | -0.6 | 6310.8939 | -2.3 | 3-3 | 10048.8000 | 0.8 | 10099.4559 | -1.3 |
| 2-1 | 6910.1154 | -0.7 | 6945.7214 | 0.2 | 3-3 | 6302.4541 | 0.8 | 6311.1356 | 0.9 | 2-1 | 10048.8413 | -1.2 | 10099.5777 | 0.0 |
| 2-2 | 6910.1502 | -1.7 | 6945.8333 | 0.6 | | | | | | 4-3 | 10048.8621 | -0.7 | 10099.6396 | 0.6 |
| 1-1 | 6910.1811 | -0.5 | 6945.9066 | 0.1 | 312-202 | | | | | 3-2 | 10048.8766 | 0.7 | 10099.6810 | -1.0 |
| 3-2 | 6910.1945 | 0.5 | 6945.9519 | 0.2 | 3-2 | 9625.1192 | -1.4 | 9668.8482 | 0.3 | 2-2 | 10048.9622 | 0.5 | 10099.9272 | -0.2 |
| 414-303 | | | | | | | | | | | | | | |
| 3-3 | 8247.5222 | 0.4 | | | | | | | | | | | | |
| 5-4 | 8247.6521 | -2.6 | | | | | | | | | | | | |
| 3-2 | 8247.6611 | 1.0 | | | | | | | | | | | | |
| 4-3 | 8247.6731 | 2.4 | | | | | | | | | | | | |
| 4-4 | 8247.7723 | -0.9 | | | | | | | | | | | | |
| 322-211 | | | | | | | | | | | | | | |
| 2-1 | 8227.3447 | 1.6 | | | | | | | | | | | | |
| 3-3 | 8227.3619 | -2.5 | | | | | | | | | | | | |
| 4-3 | 8227.3619 | -2.5 | | | | | | | | | | | | |
| 3-2 | 8227.4028 | 0.1 | | | | | | | | | | | | |
| 2-2 | 8227.4028 | 0.1 | | | | | | | | | | | | |

[a] Measured frequencies in MHz, [b] Observed-calculated frequencies in kHz.

Table A3.3. Observed transition frequencies of the $^{14}N$-hyperfine structure of $^{20}Ne_2$-$^{14}N_2O$ and $^{22}Ne_2$-$^{14}N_2O$.

| $J'K_a'K_c'$-$J''K_a''K_c''$ $F_1'F_2'$-$F_1''F_2''$ | $\nu_{obs}$[a] | $\Delta\nu$[b] | $\nu_{obs}$[a] | $\Delta\nu$[b] | $J'K_a'K_c'$-$J''K_a''K_c''$ $F_1'F_2'$-$F_1''F_2''$ | $\nu_{obs}$[a] | $\Delta\nu$[b] | $\nu_{obs}$[a] | $\Delta\nu$[b] |
|---|---|---|---|---|---|---|---|---|---|
| | $^{20}Ne^{20}Ne$-$^{14}N^{14}NO$ | | $^{22}Ne^{22}Ne$-$^{14}N^{14}NO$ | | | $^{20}Ne^{20}Ne$-$^{14}N^{14}NO$ | | $^{22}Ne^{22}Ne$-$^{14}N^{14}NO$ | |
| 101-000 | | | | | 312-202 | | | | |
| 01-12 | 4380.0852 | 0.7 | 4166.3412 | 0.2 | 44-33 | 16412.2256 | 1.5 | 15717.6624 | 0.0 |
| 01-11 | 4380.0852 | 0.7 | 4166.3412 | 0.2 | 45-34 | 16412.3000 | 3.2 | 15717.7377 | 3.1 |
| 01-10 | 4380.0852 | 0.7 | 4166.3412 | 0.2 | 43-32 | 16412.3235 | -1.8 | 15717.7623 | -1.1 |
| 21-12 | 4380.2289 | 0.3 | 4166.4819 | -1.2 | 22-11 | 16412.3765 | -0.3 | | |
| 21-11 | 4380.2289 | 0.3 | 4166.4819 | -1.1 | 23-12 | 16412.4185 | 1.5 | 15717.8574 | 1.1 |
| 21-10 | 4380.2289 | 0.3 | 4166.4819 | -1.2 | | | | | |
| 23-12 | 4380.2500 | 1.4 | 4166.5066 | 1.8 | 212-111 | | | | |
| 22-12 | 4380.2738 | 0.6 | 4166.5324 | 1.5 | 12-11 | 8097.1363 | 0.8 | | |
| 22-11 | 4380.2738 | 0.6 | 4166.5324 | 1.5 | 11-11 | 8097.1685 | 1.5 | | |
| 11-12 | 4380.3602 | 0.6 | 4166.6161 | 0.0 | 32-22 | 8097.3211 | 3.0 | | |
| 11-11 | 4380.3602 | 0.6 | 4166.6161 | 0.1 | 32-21 | 8097.3654 | 0.6 | 7650.5351 | 0.2 |
| 11-10 | 4380.3602 | 0.6 | 4166.6161 | 0.1 | 34-23 | 8097.3750 | 2.8 | 7650.5460 | 2.1 |
| 12-12 | 4380.373 | 2.8 | 4166.6259 | -1.3 | 33-22 | 8097.4161 | 2.3 | 7650.5889 | 1.7 |
| 12-11 | 4380.3732 | 2.8 | 4166.6259 | -1.3 | 12-01 | 8097.4161 | 1.2 | 7650.5889 | 2.2 |
| 10-11 | 4380.3973 | 2.3 | 4166.6531 | -0.2 | 21-10 | 8097.4582 | 2.2 | 7650.6324 | 3.0 |
| | | | | | 23-12 | 8097.5010 | 2.8 | 7650.6726 | 2.3 |
| 110-000 | | | | | 22-11 | 8097.5538 | 1.1 | 7650.7273 | 2.5 |
| 10-11 | 5953.0364 | -0.5 | 5637.9497 | -1.0 | 23-23 | 8097.6241 | 2.0 | 7650.7953 | 1.9 |
| 12-12 | 5953.0871 | -0.0 | 5638.0022 | 1.0 | 21-21 | | | 7650.7953 | -1.2 |
| 12-11 | 5953.0871 | -0.0 | 5638.0022 | 1.0 | | | | | |
| 11-12 | 5953.1094 | 0.5 | 5638.0231 | 0.1 | 211-101 | | | | |
| 11-11 | 5953.1094 | 0.5 | 5638.0231 | 0.1 | 21-10 | | | 10484.8612 | -4.3 |
| 11-10 | 5953.1094 | 0.4 | 5638.0231 | 0.1 | 22-12 | | | 10484.8612 | -1.5 |
| 22-12 | 5953.2825 | -0.1 | 5638.1974 | 1.3 | 22-11 | 10994.1273 | 1.4 | | |
| 22-11 | 5953.2825 | -0.1 | 5638.1974 | 1.3 | 23-12 | 10994.1361 | -1.3 | 10484.8833 | -0.3 |
| 23-12 | 5953.3353 | 2.5 | 5638.2479 | 1.3 | 23-23 | 10994.2574 | -1.8 | 10485.0047 | -1.3 |
| 21-12 | 5953.3732 | -0.7 | 5638.2897 | 1.6 | 21-21 | 10994.2854 | -2.2 | 10485.0323 | -3.5 |
| 21-11 | 5953.3732 | -0.7 | 5638.2897 | 1.6 | 11-12 | | | 10485.0549 | -1.5 |
| 21-10 | 5953.3732 | -0.7 | 5638.2897 | 1.6 | 12-12 | | | 10485.0711 | -0.5 |
| 01-12 | 5953.6625 | -1.0 | 5638.5767 | -0.1 | 33-22 | 10994.3240 | -2.1 | 10485.0711 | -1.7 |
| 01-11 | 5953.6625 | -1.0 | 5638.5767 | -0.1 | 34-23 | 10994.3857 | 0.6 | 10485.1328 | 1.3 |
| 01-10 | 5953.6625 | -1.0 | 5638.5767 | -0.1 | 32-21 | 10994.4192 | -0.5 | 10485.1671 | 0.2 |
| | | | | | 12-22 | | | 10485.1671 | -0.7 |
| 202-101 | | | | | 11-01 | 10994.5948 | -0.7 | | |
| 12-12 | 8506.5041 | -2.5 | | | 12-01 | 10994.6105 | -1.0 | 10485.3574 | -0.4 |
| 11-10 | 8506.5041 | -3.4 | | | | | | | |
| 11-12 | 8506.5303 | -1.8 | | | 220-110 | | | | |
| 32-21 | 8506.7267 | 0.4 | 8041.8239 | 0.1 | 11-01 | 12401.6308 | -0.2 | | |
| 34-23 | 8506.7267 | -2.6 | 8041.8239 | -2.8 | 12-01 | 12401.6534 | -3.1 | 11669.5077 | 1.2 |
| 10-01 | 8506.7467 | -3.5 | | | 23-23 | 12401.6821 | -0.6 | 11669.5210 | -1.6 |
| 33-22 | 8506.7570 | -2.2 | 8041.8551 | -3.3 | 10-01 | 12401.6962 | -2.6 | | |
| 21-10 | 8506.7714 | -1.7 | | | 33-23 | 12401.8322 | 0.4 | | |
| 12-01 | 8506.7917 | -0.8 | | | 22-11 | 12401.8702 | -1.2 | 11669.7085 | -0.2 |

Table A3.3. (continued)

| $J'K_a'K_c'$-$J''K_a''K_c''$ $F_1'F_2'$-$F_1''F_2''$ | $\nu_{obs}$[a] | $\Delta\nu$[b] | $\nu_{obs}$[a] | $\Delta\nu$[b] | $J'K_a'K_c'$-$J''K_a''K_c''$ $F_1'F_2'$-$F_1''F_2''$ | $\nu_{obs}$[a] | $\Delta\nu$[b] | $\nu_{obs}$[a] | $\Delta\nu$[b] |
|---|---|---|---|---|---|---|---|---|---|
| | $^{20}Ne^{20}Ne$-$^{14}N^{14}NO$ | | $^{22}Ne^{22}Ne$-$^{14}N^{14}NO$ | | | $^{20}Ne^{20}Ne$-$^{14}N^{14}NO$ | | $^{22}Ne^{22}Ne$-$^{14}N^{14}NO$ | |
| 11-01 | | | 8041.9105 | -3.1 | 33-22 | | | 11669.7228 | -2.6 |
| 21-11 | | | 8041.9105 | -1.0 | 34-23 | 12401.8835 | -2.7 | 11669.7341 | 1.4 |
| 23-12 | 8506.8063 | -4.8 | 8041.9105 | -4.0 | 22-12 | 12401.8913 | -1.9 | 11669.7341 | 3.6 |
| 22-11 | 8506.8525 | -4.5 | 8041.9606 | -2.5 | 23-12 | 12401.9298 | 1.4 | 11669.7686 | 0.6 |
| 23-23 | 8506.9293 | -3.6 | 8042.0321 | -4.8 | 21-10 | 12401.9931 | 1.1 | | |
| | | | | | 11-12 | | | 11670.0539 | -1.2 |
| 211-110 | | | | | 12-11 | | | 11670.0607 | 0.5 |
| 11-01 | 9421.0171 | 0.7 | 9013.1071 | 0.4 | 12-12 | 12402.2330 | 0.1 | 11670.0812 | -0.9 |
| 12-01 | 9421.0328 | 0.3 | 9013.1215 | -0.5 | | | | | |
| 23-23 | 9421.1756 | 0.6 | | | 221-111 | | | | |
| 33-23 | | | 9013.3614 | 4.3 | 22-12 | 12811.8120 | 0.2 | | |
| 32-21 | 9421.2739 | -0.4 | 9013.3614 | -0.5 | 22-11 | 12811.8239 | 1.0 | | |
| 34-23 | 9421.3019 | 1.0 | 9013.3917 | 2.1 | 23-12 | 12811.8348 | 1.7 | 12061.5239 | -0.2 |
| 33-22 | 9421.3159 | -0.9 | 9013.4057 | -2.0 | 23-23 | 12811.9589 | 1.9 | 12061.6488 | 1.6 |
| 22-11 | 9421.3756 | -1.0 | 9013.4670 | 0.2 | 21-21 | 12811.9870 | 0.8 | 12061.6749 | -0.5 |
| 22-12 | 9421.3980 | -0.4 | | | 12-12 | | | 12061.7122 | 3.0 |
| 23-12 | 9421.4224 | 1.8 | 9013.5123 | 2.7 | 33-22 | 12812.0240 | 1.6 | 12061.7122 | 0.5 |
| 21-10 | 9421.4806 | 1.3 | | | 33-23 | 12812.0516 | 3.6 | | |
| 12-11 | 9421.5852 | -1.9 | | | 34-23 | 12812.0839 | 3.0 | 12061.7729 | 1.7 |
| 11-12 | 9421.5934 | 0.6 | | | 32-21 | 12812.1179 | 2.0 | 12061.8071 | 1.2 |
| 12-12 | 9421.6083 | -0.6 | | | 11-01 | 12812.2942 | 0.6 | 12061.9822 | -0.2 |
| | | | | | 12-01 | 12812.3095 | 0.5 | 12061.9981 | -0.6 |
| 303-202 | | | | | | | | | |
| 23-23 | 12300.9917 | 1.5 | | | 322-212 | | | | |
| 22-22 | 12301.0235 | 1.0 | | | 21-22 | 17851.1641 | -1.5 | 16906.8459 | 0.2 |
| 43-32 | 12301.2856 | 2.0 | 11570.1452 | -0.7 | 33-22 | 17851.1641 | -1.5 | 16906.8459 | 0.2 |
| 45-34 | 12301.2856 | 0.7 | 11570.1452 | -1.4 | 22-22 | 17851.1641 | -1.5 | 16906.8459 | 0.2 |
| 21-10 | 12301.3019 | 2.3 | | | 32-22 | 17851.1641 | -1.5 | 16906.8459 | 0.2 |
| 44-33 | 12301.3156 | 1.5 | 11570.1792 | 3.3 | 43-22 | 17851.1641 | -1.5 | 16906.8459 | 0.2 |
| 22-11 | 12301.3376 | 0.9 | | | 23-23 | 17851.2079 | -1.1 | 16906.8899 | 0.5 |
| 32-21 | | | 11570.2235 | 4.5 | 22-23 | 17851.2079 | -1.1 | 16906.8899 | 0.5 |
| 34-23 | 12301.3657 | 0.7 | | | 34-23 | 17851.2079 | -1.1 | 16906.8899 | 0.5 |
| 33-22 | 12301.4025 | 2.1 | 11570.2648 | 1.8 | 33-23 | 17851.2079 | -1.1 | 16906.8899 | 0.5 |
| 34-34 | 12301.5695 | 1.0 | | | 21-21 | 17851.2243 | -1.3 | 16906.9047 | -1.3 |
| | | | | | 22-21 | 17851.2243 | -1.3 | 16906.9047 | -1.3 |
| 312-211 | | | | | 32-21 | 17851.2243 | -1.3 | 16906.9047 | -1.3 |
| 23-12 | 13924.5981 | 0.1 | 13274.3852 | 0.1 | 43-33 | 17851.3911 | -0.6 | 16907.0708 | -0.5 |
| 22-11 | 13924.5981 | -1.2 | 13274.3852 | -3.5 | 44-33 | 17851.3911 | -0.6 | 16907.0708 | -0.5 |
| 33-33 | 13924.5981 | -2.0 | | | 34-33 | 17851.3911 | -0.6 | 16907.0708 | -0.5 |
| 43-32 | 13924.6301 | -1.8 | 13274.4214 | 1.1 | 33-33 | 17851.3911 | -0.6 | 16907.0708 | -0.5 |
| 45-34 | 13924.6435 | 2.4 | 13274.4300 | 0.2 | 45-34 | 17851.4584 | -0.5 | 16907.1404 | 1.5 |
| 44-33 | 13924.6544 | -2.7 | | | 34-34 | 17851.4584 | -0.5 | 16907.1404 | 1.5 |
| 34-23 | 13924.7070 | -0.1 | 13274.4985 | -2.2 | 44-34 | 17851.4584 | -0.5 | 16907.1404 | 1.5 |
| 33-22 | 13924.7150 | 1.1 | | | 43-32 | 17851.4859 | -1.5 | 16907.1670 | -0.6 |

Table A3.3. (continued)

| $J'K_a'K_c'$-$J''K_a''K_c''$ $F_1'F_2'$-$F_1''F_2''$ | $\nu_{obs}$[a] | $\Delta\nu$[b] | $\nu_{obs}$[a] | $\Delta\nu$[b] | $J'K_a'K_c'$-$J''K_a''K_c''$ $F_1'F_2'$-$F_1''F_2''$ | $\nu_{obs}$[a] | $\Delta\nu$[b] | $\nu_{obs}$[a] | $\Delta\nu$[b] |
|---|---|---|---|---|---|---|---|---|---|
| | $^{20}Ne^{20}Ne$-$^{14}N^{14}NO$ | | $^{22}Ne^{22}Ne$-$^{14}N^{14}NO$ | | | $^{20}Ne^{20}Ne$-$^{14}N^{14}NO$ | | $^{22}Ne^{22}Ne$-$^{14}N^{14}NO$ | |
| | | | | | 32-32 | 17851.4859 | -1.5 | 16907.1670 | -0.6 |
| 313-212 | | | | | 21-11 | 17851.5512 | -0.1 | 16907.2280 | -2.9 |
| 23-23 | 12006.3790 | -0.5 | 11317.8970 | -0.6 | 22-11 | 17851.5512 | -0.1 | 16907.2280 | -2.9 |
| 22-22 | 12006.4090 | -0.1 | 11317.9269 | -1.1 | 23-12 | 17851.5812 | -1.6 | 16907.2629 | 0.4 |
| 45-34 | 12006.7287 | 1.0 | 11318.2451 | -0.7 | 22-12 | 17851.5812 | -1.6 | 16907.2629 | 0.4 |
| 43-32 | 12006.7287 | -1.3 | 11318.2451 | -2.6 | | | | | |
| 44-33 | 12006.7501 | -0.9 | 11318.2700 | -0.0 | 321-211 | | | | |
| 23-12 | 12006.7501 | -3.1 | 11318.2700 | -0.7 | 32-32 | | | 16076.0624 | 1.6 |
| 21-10 | 12006.7644 | -0.6 | | | 34-34 | | | 16076.0624 | 0.1 |
| 32-21 | 12006.7748 | -2.9 | 11318.2949 | -1.9 | 33-23 | | | 16076.1474 | -0.0 |
| 34-23 | 12006.7831 | -1.0 | | | 22-12 | 16950.7241 | 0.1 | | |
| 22-11 | | | 11318.3117 | -1.5 | 33-22 | 16950.7241 | -0.2 | 16076.1690 | 0.7 |
| 44-34 | | | 11318.3380 | 0.4 | 44-34 | 16950.7241 | -2.5 | | |
| 33-22 | 12006.8148 | -2.2 | 11318.3380 | 0.7 | 34-23 | | | 16076.1873 | -0.5 |
| 33-23 | 12006.8601 | -0.3 | | | 32-21 | 16950.7465 | 1.3 | | |
| 34-34 | 12007.0331 | -0.8 | 11318.5521 | -0.9 | 44-33 | 16950.7599 | -1.0 | 16076.2087 | -2.9 |
| | | | | | 23-12 | 16950.7599 | -2.0 | | |
| 312-202 | | | | | 43-32 | 16950.7758 | 3.2 | 16076.2286 | 1.3 |
| 33-22 | 16411.9842 | 1.4 | 15717.4207 | 0.5 | 45-34 | 16950.7758 | 2.2 | 16076.2286 | 1.5 |
| 34-23 | 16412.0367 | 3.3 | 15717.4716 | 1.8 | 32-22 | 16950.7758 | -0.1 | | |
| 32-21 | 16412.0496 | -1.9 | 15717.4880 | 0.4 | | | | | |
| | | | | | | | | | |
| 322-221 | | | | | | | | | |
| 23-12 | 13136.6882 | -0.4 | | | | | | | |
| 22-12 | 13136.6882 | -0.4 | | | | | | | |
| 43-32 | 13136.7378 | 1.5 | | | | | | | |
| 32-32 | 13136.7378 | 1.5 | | | | | | | |
| 45-34 | 13136.7492 | -1.0 | | | | | | | |
| 34-34 | 13136.7492 | -1.0 | | | | | | | |
| 44-34 | 13136.7492 | -1.0 | | | | | | | |
| 33-33 | 13136.7839 | 0.8 | | | | | | | |
| 44-33 | 13136.7839 | 0.8 | | | | | | | |
| 23-33 | 13136.7839 | 0.8 | | | | | | | |
| 23-23 | 13136.8760 | 1.9 | | | | | | | |
| 22-23 | 13136.8760 | 1.9 | | | | | | | |
| 34-23 | 13136.8760 | 1.9 | | | | | | | |
| 33-23 | 13136.8760 | 1.9 | | | | | | | |
| 21-22 | 13136.8952 | -0.2 | | | | | | | |
| 23-22 | 13136.8952 | -0.2 | | | | | | | |
| 22-22 | 13136.8952 | -0.2 | | | | | | | |
| 32-22 | 13136.8952 | -0.2 | | | | | | | |
| 33-22 | 13136.8952 | -0.2 | | | | | | | |

[a] Measured frequencies in MHz, [b] Observed-calculated frequencies in kHz.

Table A3.4. Observed transition frequencies of the $^{14}N$-hyperfine structure of $^{20}Ne^{22}Ne$-$^{14}N_2O$.

| $J'K_a'K_c'$-$J''K_a''K_c''$ $F_1'F_2'$-$F_1''F_2''$ | $\nu_{obs}$[a] | $\Delta\nu$[b] | $J'K_a'K_c'$-$J''K_a''K_c''$ $F_1'F_2'$-$F_1''F_2''$ | $\nu_{obs}$[a] | $\Delta\nu$[b] | $J'K_a'K_c'$-$J''K_a''K_c''$ $F_1'F_2'$-$F_1''F_2''$ | $\nu_{obs}$[a] | $\Delta\nu$[b] |
|---|---|---|---|---|---|---|---|---|
| 101-000 | | | 303-202 | | | 221-111 | | |
| 01-12 | 4264.7913 | 0.6 | 22-22 | 11926.5293 | 0.6 | 32-21 | 12452.0649 | 1.4 |
| 01-11 | 4264.7913 | 0.6 | 43-32 | 11926.7939 | 0.7 | 11-01 | 12452.2403 | 0.7 |
| 01-10 | 4264.7913 | 0.6 | 45-34 | 11926.7939 | 0.2 | 12-01 | 12452.2559 | -0.5 |
| 21-12 | 4264.9295 | -2.0 | 21-10 | 11926.8100 | 0.2 | | | |
| 21-11 | 4264.9295 | -2.0 | 44-33 | 11926.8241 | 1.6 | 322-212 | | |
| 21-10 | 4264.9295 | -2.0 | 22-12 | 11926.8730 | -0.2 | 21-22 | 17380.5691 | -0.0 |
| 23-12 | 4264.9523 | -2.0 | 34-23 | 11926.8730 | -0.7 | 33-22 | 17380.5691 | -0.0 |
| 22-12 | 4264.9800 | -1.4 | 33-22 | 11926.9107 | 1.5 | 22-22 | 17380.5691 | -0.0 |
| 22-11 | 4264.9800 | -1.4 | 34-34 | 11927.0815 | 2.2 | 32-22 | 17380.5691 | -0.0 |
| 11-12 | 4265.0629 | -2.8 | 32-32 | 11927.0815 | -0.6 | 43-22 | 17380.5691 | -0.0 |
| 11-11 | 4265.0629 | -2.8 | | | | 23-23 | 17380.6109 | -1.9 |
| 11-10 | 4265.0629 | -2.8 | 312-211 | | | 22-23 | 17380.6109 | -1.9 |
| 12-12 | 4265.0764 | -0.6 | 23-12 | 13574.1289 | 1.3 | 34-23 | 17380.6109 | -1.9 |
| 12-11 | 4265.0764 | -0.6 | 22-11 | 13574.1289 | -2.4 | 33-23 | 17380.6109 | -1.9 |
| 10-11 | 4265.1031 | -1.0 | 33-33 | 13574.1289 | -4.0 | 21-21 | 17380.6295 | 0.2 |
| | | | 43-32 | 13574.1596 | -2.6 | 22-21 | 17380.6295 | 0.2 |
| 110-000 | | | 45-34 | 13574.1729 | 1.6 | 32-21 | 17380.6295 | 0.2 |
| 10-11 | 5796.0625 | -0.4 | 34-23 | 13574.2383 | -0.2 | 43-33 | 17380.7931 | -1.4 |
| 12-12 | 5796.1140 | 0.7 | | | | 44-33 | 17380.7931 | -1.4 |
| 12-11 | 5796.1140 | 0.7 | 313-212 | | | 34-33 | 17380.7931 | -1.4 |
| 11-12 | 5796.1343 | -0.9 | 23-23 | 11647.6825 | -0.2 | 33-33 | 17380.7931 | -1.4 |
| 11-11 | 5796.1343 | -0.9 | 22-22 | 11647.7140 | 1.1 | 45-34 | 17380.8624 | 0.4 |
| 11-10 | 5796.1343 | -0.9 | 45-34 | 11648.0301 | 0.0 | 34-34 | 17380.8624 | 0.4 |
| 22-12 | 5796.3075 | -0.6 | 43-32 | 11648.0301 | -1.9 | 44-34 | 17380.8624 | 0.4 |
| 22-11 | 5796.3075 | -0.6 | 44-33 | 11648.0525 | -1.8 | 43-32 | 17380.8925 | 1.9 |
| 23-12 | 5796.3584 | -0.1 | 23-12 | 11648.0525 | -2.8 | 32-32 | 17380.8925 | 1.9 |
| 21-12 | 5796.3959 | -3.9 | 32-21 | 11648.0812 | 1.1 | 21-11 | 17380.9528 | -1.1 |
| 21-11 | 5796.3959 | -3.9 | 22-11 | 11648.0979 | 0.2 | 22-11 | 17380.9528 | -1.1 |
| 21-10 | 5796.3959 | -3.9 | 44-34 | 11648.1195 | -2.2 | 23-12 | 17380.9863 | 0.9 |
| 01-12 | 5796.6887 | 0.4 | 33-22 | 11648.1195 | -1.0 | 22-12 | 17380.9863 | 0.9 |
| 01-11 | 5796.6887 | 0.4 | 34-34 | 11648.3354 | -0.6 | 21-10 | 17381.0373 | -0.6 |
| 01-10 | 5796.6887 | 0.4 | | | | | | |
| | | | 312-202 | | | 321-211 | | |
| 111-000 | | | 33-22 | 16036.5002 | -1.2 | 32-32 | 16506.6334 | 1.2 |
| 01-12 | 5128.9505 | 0.0 | 34-23 | 16036.5530 | 3.0 | 34-34 | 16506.6334 | -0.1 |
| 01-11 | 5128.9505 | 0.0 | 44-33 | 16036.7426 | 0.0 | 33-23 | 16506.7206 | 0.2 |
| 01-10 | 5128.9505 | 0.0 | 45-34 | 16036.8164 | 2.7 | 33-22 | 16506.7397 | -0.6 |
| 21-12 | 5129.0979 | -0.3 | 43-32 | 16036.8402 | -1.9 | 34-23 | 16506.7620 | 3.3 |
| 21-11 | 5129.0979 | -0.3 | 23-12 | 16036.9356 | 1.5 | 32-21 | 16506.7620 | -0.5 |
| 21-10 | 5129.0979 | -0.3 | | | | 22-11 | 16506.7620 | 1.7 |
| 23-12 | 5129.1171 | 0.3 | 212-111 | | | 21-10 | 16506.7769 | -1.8 |
| 22-12 | 5129.1407 | 0.7 | 34-23 | 7862.0228 | 3.0 | 44-33 | 16506.7769 | -2.1 |
| 22-11 | 5129.1407 | 0.7 | 33-22 | 7862.0638 | - 0.2 | 23-12 | 16506.7769 | -5.5 |
| 11-12 | 5129.2299 | 1.1 | 12-01 | 7862.0638 | 1.1 | 43-32 | 16506.7949 | 1.2 |

Table A3.4. (continued)

| $J'K_a'K_c'$-$J''K_a''K_c''$ $F_1'F_2'$-$F_1''F_2''$ | $\nu_{obs}$[a] | $\Delta\nu$[b] | $J'K_a'K_c'$-$J''K_a''K_c''$ $F_1'F_2'$-$F_1''F_2''$ | $\nu_{obs}$[a] | $\Delta\nu$[b] | $J'K_a'K_c'$-$J''K_a''K_c''$ $F_1'F_2'$-$F_1''F_2''$ | $\nu_{obs}$[a] | $\Delta\nu$[b] |
|---|---|---|---|---|---|---|---|---|
| 11-11 | 5129.2299 | 1.1 | 21-10 | 7862.1083 | 1.6 | 45-34 | 16506.7949 | 1.4 |
| 11-10 | 5129.2299 | 1.1 | 23-12 | 7862.1486 | 2.1 | 21-11 | 16506.8163 | -1.1 |
| 12-12 | 5129.2402 | 0.9 | 22-11 | 7862.2020 | 1.4 | | | |
| 12-11 | 5129.2402 | 0.9 | 23-23 | 7862.2706 | 1.6 | 322-221 | | |
| 10-11 | 5129.2632 | 0.7 | 21-21 | 7862.2706 | -0.4 | 23-12 | 12790.7914 | -0.3 |
| | | | | | | 22-12 | 12790.7914 | -0.3 |
| 202-101 | | | 211-101 | | | 43-32 | 12790.8373 | 0.5 |
| 12-12 | 8264.0773 | -2.1 | 23-12 | 10726.6974 | -0.6 | 32-32 | 12790.8373 | 0.5 |
| 11-10 | 8264.0773 | -1.7 | 23-23 | 10726.8212 | 0.5 | 45-34 | 12790.8525 | -0.0 |
| 11-12 | 8264.1051 | -1.0 | 33-22 | 10726.8871 | -0.8 | 34-34 | 12790.8525 | -0.0 |
| 32-21 | 8264.3022 | 0.5 | 32-22 | 10726.9292 | -2.6 | 44-34 | 12790.8525 | -0.0 |
| 34-23 | 8264.3022 | -1.3 | 34-23 | 10726.9457 | -0.2 | 33-33 | 12790.8896 | 0.6 |
| 33-22 | 8264.3318 | -2.2 | 32-21 | 10726.9807 | -1.0 | 44-33 | 12790.8896 | 0.6 |
| 21-10 | 8264.3458 | 0.4 | 12-22 | 10726.9807 | -0.8 | 23-33 | 12790.8896 | 0.6 |
| 12-01 | 8264.3653 | -0.4 | 12-01 | 10727.1718 | -0.4 | 23-23 | 12790.9761 | -0.5 |
| 23-12 | 8264.3848 | -1.7 | | | | 22-23 | 12790.9761 | -0.5 |
| 22-11 | 8264.4339 | -1.2 | 220-110 | | | 34-23 | 12790.9761 | -0.5 |
| 23-23 | 8264.5072 | -2.0 | 11-01 | 12048.7588 | -0.5 | 33-23 | 12790.9761 | -0.5 |
| | | | 22-23 | 12048.7735 | 2.1 | 21-22 | 12790.9989 | -1.5 |
| 212-101 | | | 21-21 | 12048.7838 | 2.5 | 23-22 | 12790.9989 | -1.5 |
| 34-23 | 8726.1828 | 0.5 | 12-01 | 12048.7838 | -2.3 | 22-22 | 12790.9989 | -1.5 |
| 33-22 | 8726.2262 | 3.5 | 23-23 | 12048.8090 | 0.3 | 32-22 | 12790.9989 | -1.5 |
| 23-12 | 8726.3073 | -1.5 | 22-11 | 12048.9962 | 1.5 | 33-22 | 12790.9989 | -1.5 |
| | | | 32-21 | 12048.9962 | -1.4 | | | |
| 211-110 | | | 33-22 | 12049.0044 | -2.8 | 330-220 | | |
| 11-01 | 9195.2601 | 0.2 | 34-23 | 12049.0153 | 0.9 | 33-23 | 18710.8259 | 1.1 |
| 12-01 | 9195.2739 | -0.7 | 22-12 | 12049.0153 | -1.2 | 23-12 | 18710.8259 | -1.5 |
| 23-23 | 9195.4178 | 1.3 | 23-12 | 12049.0559 | 2.0 | 45-34 | 18710.8647 | -1.9 |
| 32-21 | 9195.5155 | 2.2 | 12-23 | 12049.1155 | -0.3 | 34-23 | 18710.8791 | 2.0 |
| 34-23 | 9195.5434 | 1.7 | 21-10 | 12049.1155 | -2.8 | 32-21 | 18710.8791 | 0.4 |
| 33-22 | 9195.5618 | 0.6 | 11-12 | 12049.3333 | -0.9 | 21-11 | 18710.8791 | -2.7 |
| 22-11 | 9195.6208 | 0.8 | 12-11 | 12049.3396 | 0.4 | | | |
| 22-12 | 9195.6427 | 0.9 | 12-12 | 12049.3609 | -0.1 | 331-221 | | |
| 23-12 | 9195.6636 | 1.9 | | | | 33-22 | 18903.0207 | 3.4 |
| 21-10 | 9195.7203 | 0.4 | 221-111 | | | 22-12 | 18903.0456 | -0.9 |
| 12-11 | 9195.8270 | -0.7 | 23-12 | 12451.7816 | -1.1 | 32-21 | 18903.0456 | -1.9 |
| 12-12 | 9195.8504 | 0.9 | 23-23 | 12451.9062 | 1.0 | 22-11 | 18903.0609 | -2.4 |
| | | | 12-12 | 12451.9692 | 1.6 | 44-33 | 18903.0756 | 0.0 |
| 303-202 | | | 33-22 | 12451.9692 | -0.3 | 45-34 | 18903.0993 | 3.0 |
| 23-23 | 11926.4957 | -0.8 | 34-23 | 12452.0312 | 1.9 | 43-32 | 18903.0993 | 2.0 |

[a] Measured frequencies in MHz.

[b] Observed-calculated frequencies in kHz.

Table A3.5. The observed frequencies of the $^{14}N$-hyperfine structure of $^{20}Ne_2$-($^{15}N^{14}NO$, $^{14}N^{15}NO$) and $^{22}Ne_2$-($^{15}N^{14}NO$, $^{14}N^{15}NO$).

| $J'K_a'K_c'$-$J''K_a''K_c''$ F'- F'' | $\nu_{obs}$[a] | $\Delta\nu$[b] | $\nu_{obs}$[a] | $\Delta\nu$[b] | $\nu_{obs}$[a] | $\Delta\nu$[b] | $\nu_{obs}$[a] | $\Delta\nu$[b] |
|---|---|---|---|---|---|---|---|---|
| | $^{20}Ne^{20}Ne$-$^{15}N^{14}NO$ | | $^{22}Ne^{22}Ne$-$^{15}N^{14}NO$ | | $^{20}Ne^{20}Ne$-$^{14}N^{15}NO$ | | $^{22}Ne^{22}Ne$-$^{14}N^{15}NO$ | |
| 101-000 | | | | | | | | |
| 0 - 1 | 4330.1723 | 1.8 | 4117.7098 | -0.2 | 4348.0920 | 1.4 | 4134.2703 | 1.3 |
| 2 - 1 | 4330.2266 | 1.9 | 4117.7640 | -0.9 | 4348.2578 | 2.0 | 4134.4368 | 1.7 |
| 1 - 1 | 4330.2640 | 3.2 | 4117.8017 | 0.2 | 4348.3678 | 1.9 | 4134.5471 | 1.3 |
| 110-000 | | | | | | | | |
| 1 - 1 | 5883.0351 | -1.1 | 5572.7234 | 0.2 | 5932.3673 | 0.4 | 5616.8643 | -0.3 |
| 2 - 1 | 5883.1131 | 1.3 | 5572.8002 | 2.1 | 5932.5875 | 0.3 | 5617.0851 | 0.3 |
| 0 - 1 | 5883.2252 | 0.1 | 5572.9114 | 0.9 | 5932.9172 | -0.5 | 5617.4144 | -0.7 |
| 202-101 | | | | | | | | |
| 1 - 1 | 8424.5224 | -3.5 | 7964.1668 | -0.7 | 8452.1118 | -2.6 | 7989.0142 | -2.2 |
| 3 - 2 | 8424.5952 | -2.6 | 7964.2412 | 0.1 | 8452.3290 | -1.9 | 7989.2349 | -2.2 |
| 1 - 0 | 8424.6134 | -2.9 | 7964.2600 | 0.9 | 8452.3871 | -2.6 | 7989.2934 | 0.3 |
| 2 - 1 | 8424.6239 | -2.1 | 7964.2715 | 0.4 | 8452.4097 | -2.5 | 7989.3225 | -2.0 |
| 2 - 2 | 8424.6590 | -3.2 | 7964.3083 | 0.6 | 8452.5199 | -2.4 | 7989.4332 | -2.0 |
| 211-110 | | | | | | | | |
| 1 - 0 | 9294.5191 | -2.8 | 8889.7309 | 1.7 | | | 8938.9255 | 0.6 |
| 2 - 2 | 9294.5686 | -0.9 | 8889.7763 | -1.5 | 9347.8949 | -1.6 | 8939.0716 | -1.1 |
| 3 - 2 | 9294.6119 | 0.1 | 8889.8208 | 2.0 | 9348.0149 | 0.3 | 8939.1903 | 0.3 |
| 2 - 1 | 9294.6471 | 2.0 | 8889.8530 | 0.3 | 9348.1172 | 0.4 | 8939.2918 | -1.1 |
| 1 - 1 | 9294.7130 | 2.2 | 8889.9162 | -0.3 | 9348.3020 | 1.6 | 8939.4760 | 0.7 |
| 212-111 | | | | | | | | |
| 1 - 1 | 8023.9225 | 0.9 | 7579.1108 | 1.1 | 8042.4828 | 2.2 | 7596.2563 | 1.5 |
| 3 - 2 | 8024.0092 | 3.3 | 7579.1927 | 0.2 | 8042.7244 | 2.5 | 7596.4977 | 2.3 |
| 1 - 0 | 8024.0233 | 3.2 | 7579.2061 | 0.7 | 8042.7561 | 0.1 | | |
| 2 - 1 | 8024.0470 | -0.5 | 7579.2331 | -1.4 | 8042.8500 | 2.2 | 7596.6238 | 2.0 |
| 2 - 2 | 8024.0879 | 1.0 | 7579.2708 | -2.0 | 8042.9602 | 2.3 | | |
| 211-101 | | | | | | | | |
| 2 - 1 | 10847.4197 | -0.8 | 10344.7718 | -2.6 | 10932.1165 | -1.4 | 10421.6109 | -0.8 |
| 2 - 2 | 10847.4571 | 0.5 | 10344.8112 | 0.2 | 10932.2261 | -1.9 | 10421.7215 | -0.9 |
| 1 - 1 | 10847.4850 | -1.2 | 10344.8384 | 0.3 | 10932.3016 | 0.1 | 10421.7954 | 1.3 |
| 3 - 2 | 10847.4990 | 0.1 | 10344.8513 | -0.7 | 10932.3456 | -0.4 | 10421.8395 | -0.2 |
| 1 - 0 | 10847.5758 | -0.7 | 10344.9290 | -0.7 | 10932.5757 | -1.1 | 10422.0701 | -0.8 |
| 220-110 | | | | | | | | |
| 1 - 0 | 12276.9370 | 0.9 | 11554.6973 | -1.1 | 12380.5387 | -0.7 | 11646.7644 | -0.7 |
| 2 - 2 | 12276.9502 | 0.8 | 11554.7069 | -0.3 | 12380.5714 | -0.6 | 11646.7874 | 0.1 |
| 3 - 2 | 12277.0134 | -0.3 | 11554.7738 | 0.1 | 12380.7643 | 0.9 | 11646.9863 | 1.0 |
| 2 - 1 | 12277.0258 | 0.9 | 11554.7831 | 1.0 | 12380.7920 | -0.3 | 11647.0066 | -0.9 |

Table A3.5. (continued)

| $J'K_a'K_c'$-$J''K_a''K_c''$ F'- F'' | $\nu_{obs}$[a] | $\Delta\nu$[b] | $\nu_{obs}$[a] | $\Delta\nu$[b] | $\nu_{obs}$[a] | $\Delta\nu$[b] | $\nu_{obs}$[a] | $\Delta\nu$[b] |
|---|---|---|---|---|---|---|---|---|
| | $^{20}Ne^{20}Ne$-$^{15}N^{14}NO$ | | $^{22}Ne^{22}Ne$-$^{15}N^{14}NO$ | | $^{20}Ne^{20}Ne$-$^{14}N^{15}NO$ | | $^{22}Ne^{22}Ne$-$^{14}N^{15}NO$ | |
| 1 - 1 | 12277.1247 | -0.3 | 11554.8860 | 0.4 | 12381.0898 | -0.3 | 11647.3151 | -0.5 |
| 221-111 | | | | | | | | |
| 2 - 1 | 12678.2913 | -0.2 | 11940.4318 | -0.3 | 12790.9688 | 0.6 | 12040.2418 | 0.1 |
| 2 - 2 | 12678.3296 | -1.3 | 11940.4685 | -1.9 | 12791.0771 | -1.3 | 12040.3512 | 0.0 |
| 1 - 1 | 12678.3520 | 0.3 | 11940.4943 | 1.1 | 12791.1540 | 2.2 | 12040.4272 | 1.0 |
| 3 - 2 | 12678.3705 | 0.9 | 11940.5107 | 1.0 | 12791.1981 | 1.7 | 12040.4708 | 1.0 |
| 1 - 0 | 12678.4507 | 0.5 | 11940.5885 | -0.4 | 12791.4272 | 0.0 | 12040.7002 | 0.3 |
| 303-202 | | | | | | | | |
| 2 - 2 | 12202.8216 | 1.9 | 11477.8086 | 0.5 | 12230.8122 | 1.9 | 11502.6015 | 1.2 |
| 4 - 3 | 12202.9186 | 2.1 | 11477.9069 | -0.9 | 12231.0984 | 1.3 | 11502.8968 | 0.7 |
| 3 - 2 | 12202.9456 | 1.1 | 11477.9363 | 0.5 | 12231.1793 | 1.4 | 11502.9781 | 0.5 |
| 3 - 3 | 12203.0101 | 1.1 | 11478.0020 | -0.3 | 12231.3708 | 1.4 | 11503.1774 | 1.8 |
| 312-211 | | | | | | | | |
| 2 - 1 | 13750.9503 | 1.9 | 13108.2815 | 1.0 | 13823.8672 | -2.7 | 13174.8731 | -1.9 |
| 4 - 3 | 13750.9639 | -0.3 | 13108.2965 | -0.1 | 13823.9178 | 2.6 | 13174.9209 | -1.0 |
| 3 - 2 | 13750.9834 | -1.1 | 13108.3172 | -1.3 | 13823.9734 | -2.0 | 13174.9893 | 2.5 |
| 313-212 | | | | | | | | |
| 2 - 2 | 11905.8704 | 0.2 | 11221.2989 | 1.5 | 11929.3072 | -0.9 | | |
| 4 - 3 | 11905.9866 | 0.1 | 11221.4129 | 0.0 | 11929.6460 | -1.4 | 11242.9834 | -0.4 |
| 2 - 1 | 11905.9940 | -2.1 | 11221.4215 | -0.7 | 11929.6765 | 1.3 | 11243.0100 | -1.1 |
| 3 - 2 | 11906.0047 | -1.7 | 11221.4332 | -0.1 | 11929.7053 | -1.3 | 11243.0425 | -2.1 |
| 3 - 3 | 11906.0862 | -1.2 | 11221.5131 | -0.4 | 11929.9401 | -2.5 | | |
| 312-202 | | | | | | | | |
| 3 - 2 | 16173.7813 | 2.3 | 15488.8215 | -0.3 | 16303.6823 | 1.2 | 15607.2750 | 1.0 |
| 2 - 2 | | | | | | | 15607.3429 | -1.8 |
| 3 - 3 | | | | | | | 15607.4720 | -0.1 |
| 4 - 3 | 16173.8657 | 0.4 | 15488.9080 | 0.5 | 16303.9323 | 1.9 | 15607.5266 | 2.2 |
| 2 - 1 | 16173.9079 | -0.8 | 15488.9513 | 0.2 | 16304.0583 | 1.3 | 15607.6535 | 0.7 |
| 321-211 | | | | | | | | |
| 3 - 3 | 16751.0070 | 1.1 | 15884.8120 | -0.5 | 16881.1662 | -0.3 | | |
| 3 - 2 | 16751.0452 | 2.9 | 15884.8516 | -1.9 | 16881.2850 | 0.5 | 16002.6043 | -0.4 |
| 2 - 1 | | | | | 16881.3032 | -0.2 | | |
| 4 - 3 | 16751.0598 | 1.6 | 15884.8680 | 1.7 | 16881.3173 | 0.9 | 16002.6441 | 0.2 |
| 2 - 2 | 16751.1180 | -0.9 | 15884.9270 | 0.8 | 16881.4856 | -1.4 | | |
| 322-212 | | | | | | | | |
| 3 - 2 | 17641.0238 | -0.8 | 16710.9893 | -1.0 | 17789.0902 | -1.2 | 16843.5141 | -0.3 |
| 2 - 2 | 17641.0238 | -0.8 | 16710.9893 | -1.0 | 17789.0902 | -1.2 | 16843.5141 | -0.3 |

Table A3.5. (continued)

| $J'K_a'K_c'$-$J''K_a''K_c''$ F'- F'' | $\nu_{obs}$[a] | $\Delta\nu$[b] | $\nu_{obs}$[a] | $\Delta\nu$[b] | $\nu_{obs}$[a] | $\Delta\nu$[b] | $\nu_{obs}$[a] | $\Delta\nu$[b] |
|---|---|---|---|---|---|---|---|---|
| | $^{20}Ne^{20}Ne$-$^{15}N^{14}NO$ | | $^{22}Ne^{22}Ne$-$^{13}N^{14}NO$ | | $^{20}Ne^{20}Ne$-$^{14}N^{15}NO$ | | $^{22}Ne^{22}Ne$-$^{14}N^{15}NO$ | |
| 3 - 3 | 17641.1056 | 0.0 | 16711.0720 | 1.4 | 17789.3279 | 0.5 | 16843.7507 | 0.4 |
| 4 - 3 | 17641.1056 | 0.0 | 16711.0720 | 1.4 | 17789.3279 | 0.5 | 16843.7507 | 0.4 |
| 2 - 1 | 17641.1502 | -0.4 | 16711.1150 | -0.2 | 17789.4573 | -1.2 | 16843.8800 | -1.4 |

[a] Measured frequencies in MHz.
[b] Observed-calculated frequencies in kHz.

Table A3.6. Observed frequencies of the $^{14}N$-hyperfine structure of $^{20}Ne^{22}Ne$-($^{15}N^{14}NO$, $^{14}N^{15}NO$).

| $J'K_a'K_c'$-$J''K_a''K_c''$ | | | | | $J'K_a'K_c'$-$J''K_a''K_c''$ | | | | | $J'K_a'K_c'$-$J''K_a''K_c''$ | | | | |
|---|---|---|---|---|---|---|---|---|---|---|---|---|---|---|
| F'-F'' | $\nu_{obs}$[a] | $\Delta\nu$[b] | $\nu_{obs}$[a] | $\Delta\nu$[b] | F'-F'' | $\nu_{obs}$[a] | $\Delta\nu$[b] | $\nu_{obs}$[a] | $\Delta\nu$[b] | F'-F'' | $\nu_{obs}$[a] | $\Delta\nu$[b] | $\nu_{obs}$[a] | $\Delta\nu$[b] |
| | $^{20}Ne^{22}Ne$-$^{15}N^{14}NO$ | | $^{20}Ne^{22}Ne$-$^{14}N^{15}NO$ | | | $^{20}Ne^{22}Ne$-$^{15}N^{14}NO$ | | $^{20}Ne^{22}Ne$-$^{14}N^{15}NO$ | | | $^{20}Ne^{22}Ne$-$^{15}N^{14}NO$ | | $^{20}Ne^{22}Ne$-$^{14}N^{15}NO$ | |
| 101-000 | | | | | 212-111 | | | | | 303-202 | | | | |
| 0-1 | 4215.7215 | 1.7 | 4232.8601 | -0.8 | 2-1 | 7789.8763 | 0.2 | 7807.8703 | 2.9 | 3-2 | 11831.2232 | -1.0 | 11857.8829 | 1.3 |
| 2-1 | 4215.7767 | 1.9 | 4233.0269 | 1.2 | 2-2 | 7789.9148 | 0.0 | 7807.9784 | 0.7 | 3-3 | 11831.2898 | 0.3 | 11858.0769 | 1.9 |
| 1-1 | 4215.8133 | 1.8 | 4233.1369 | 1.3 | | | | | | | | | | |
| | | | | | 212-101 | | | | | 312-211 | | | | |
| 111-000 | | | | | 3-2 | 8661.5494 | -1.4 | 8692.4569 | 0.1 | 2-1 | 13404.5131 | -0.2 | 13474.0077 | -1.0 |
| 0-1 | 5087.4326 | -0.9 | 5117.5748 | -0.5 | 2-1 | 8661.5953 | 0.5 | 8692.5825 | -0.3 | 4-3 | 13404.5305 | 1.4 | 13474.0561 | 1.5 |
| 2-1 | 5087.4922 | 0.7 | 5117.7396 | -1.1 | 2-2 | 8661.6322 | 0.7 | 8692.6942 | 1.5 | 3-2 | 13404.5503 | 0.3 | 13474.1152 | -1.2 |
| 1-1 | 5087.5301 | -0.0 | 5117.8496 | -1.4 | | | | | | | | | | |
| | | | | | 211-101 | | | | | 313-212 | | | | |
| 110-000 | | | | | 2-1 | 10583.7165 | -1.0 | 10664.2875 | -0.9 | 2-2 | 11549.1325 | 0.6 | | |
| 1-1 | 5728.4424 | -0.3 | 5775.1817 | 0.3 | 2-2 | 10583.7553 | 1.2 | 10664.3970 | -1.3 | 4-3 | 11549.2484 | 0.5 | 11571.7868 | -2.2 |
| 2-1 | 5728.5199 | 1.9 | 5775.4027 | 1.1 | 1-1 | 10583.7801 | -1.8 | | | 2-1 | 11549.2563 | -1.1 | 11571.8141 | -2.5 |
| 0-1 | 5728.6311 | 0.2 | 5775.7321 | 0.2 | 3-2 | 10583.7952 | -0.3 | 10664.5160 | -0.5 | 3-2 | 11549.2673 | -0.8 | 11571.8475 | -1.1 |
| | | | | | 1-0 | 10583.8747 | 1.2 | 10664.7464 | -0.6 | 3-3 | 11549.3477 | -1.0 | | |
| 202-101 | | | | | | | | | | | | | | |
| 1-1 | 8184.2518 | -0.1 | 8210.4234 | -3.2 | 220-110 | | | | | 312-202 | | | | |
| 3-2 | 8184.3231 | -1.7 | 8210.6425 | -1.5 | 1-0 | 11928.8535 | -0.5 | 12026.8408 | -0.0 | 3-2 | 15803.9117 | -2.2 | 15927.6777 | 0.5 |
| 1-0 | 8184.3410 | -2.5 | 8210.6970 | -4.4 | 2-2 | 11928.8647 | -0.6 | 12026.8694 | -0.8 | 4-3 | 15804.0024 | 2.6 | 15927.9287 | 1.6 |
| 2-1 | 8184.3528 | -0.8 | 8210.7263 | -1.3 | 3-2 | 11928.9304 | -0.3 | 12027.0644 | 0.8 | 2-1 | 15804.0420 | -1.3 | 15928.0554 | 1.1 |
| 2-2 | 8184.3895 | -0.7 | 8210.8346 | -2.9 | 2-1 | 11928.9430 | 2.4 | 12027.0899 | -0.5 | | | | | |
| | | | | | 1-1 | 11929.0414 | -0.9 | 12027.3916 | 0.3 | 321-211 | | | | |
| 211-110 | | | | | | | | | | 3-3 | 16311.9103 | -1.1 | 16435.6596 | -0.2 |
| 1-0 | 9070.9621 | -0.3 | 9121.8758 | -0.1 | 221-111 | | | | | 3-2 | 16311.9513 | -1.5 | 16435.7796 | 1.7 |
| 2-2 | 9071.0121 | 1.1 | 9122.0227 | 0.3 | 2-1 | 12324.0074 | -0.6 | 12430.4590 | 0.7 | 2-1 | | | 16435.7987 | -1.5 |
| 3-2 | 9071.0518 | -0.6 | 9122.1413 | 0.7 | 2-2 | 12324.0467 | 0.1 | 12430.5691 | 0.5 | 4-3 | 16311.9667 | 2.6 | 16435.8131 | 0.7 |
| 2-1 | 9071.0852 | -1.1 | 9122.2430 | 0.4 | 1-1 | 12324.0707 | 1.6 | | | 2-2 | 16312.0239 | -0.0 | 16435.9824 | -1.6 |

Table A3.6. (continued)

| $J'K_a'K_c'$-$J''K_a''K_c''$ F′-F″ | $\nu_{obs}$[a] | $\Delta\nu$[b] | $\nu_{obs}$[a] | $\Delta\nu$[b] | $J'K_a'K_c'$-$J''K_a''K_c''$ F′-F″ | $\nu_{obs}$[a] | $\Delta\nu$[b] | $\nu_{obs}$[a] | $\Delta\nu$[b] | $J'K_a'K_c'$-$J''K_a''K_c''$ F′-F″ | $\nu_{obs}$[a] | $\Delta\nu$[b] | $\nu_{obs}$[a] | $\Delta\nu$[b] |
|---|---|---|---|---|---|---|---|---|---|---|---|---|---|---|
| | $^{20}Ne^{22}Ne$-$^{15}N^{14}NO$ | | $^{20}Ne^{22}Ne$-$^{14}N^{15}NO$ | | $^{20}Ne^{22}Ne$-$^{15}N^{14}NO$ | | | $^{20}Ne^{22}Ne$-$^{14}N^{15}NO$ | | | $^{20}Ne^{22}Ne$-$^{15}N^{14}NO$ | | $^{20}Ne^{22}Ne$-$^{14}N^{15}NO$ | |
| 1-1 | 9071.1511 | 0.4 | 9122.4261 | -0.3 | 3-2 | 12324.0863 | 0.4 | 12430.6880 | 1.7 | | | | | |
| | | | | | 1-0 | 12324.1640 | -1.7 | 12430.9175 | 0.3 | 322-212 | | | | |
| 212-111 | | | | | | | | | | 3-2 | 17177.5634 | -0.9 | 17317.8620 | 0.6 |
| 1-1 | 7789.7513 | 0.7 | 7807.5033 | 2.9 | 303-202 | | | | | 2-2 | 17177.5634 | -0.9 | 17317.8620 | 0.6 |
| 3-2 | 7789.8347 | 0.6 | 7807.7436 | 1.8 | 2-2 | 11831.0991 | 1.0 | 11857.5120 | 1.4 | 3-3 | 17177.6455 | 0.5 | 17317.0995 | 1.0 |
| 3-2 | 7789.8347 | 0.6 | 7807.7436 | 1.8 | 2-2 | 11831.0991 | 1.0 | 11857.5120 | 1.4 | 3-3 | 17177.6455 | 0.5 | 17317.0995 | 1.0 |
| 1-0 | 7789.8473 | 0.0 | 7807.7788 | 2.6 | 4-3 | 11831.1981 | 2.0 | 11857.8019 | 1.6 | 4-3 | 17177.6455 | 0.5 | 17318.0995 | 1.0 |
| | | | | | | | | | | 2-1 | 17177.6901 | 0.3 | 17318.2271 | -2.5 |

[a] Measured frequencies in MHz.
[b] Observed-calculated frequencies in kHz.

# A4

# TABLES OF THE MEASURED TRANSITION FREQUENCIES FOR CHAPTER SIX

Table A4.1. The observed transition frequencies of the $^{14}N$-hyperfine structure of $Ar^{20}Ne$-$N_2O$ and $Ar^{22}Ne$-$N_2O$

| $J'K_a'K_c'$-$J''K_a''K_c''$ $F_1'F_2'$-$F_1''F_2''$ | $\nu_{obs}$[a] | $\Delta\nu$[b] | $\nu_{obs}$[a] | $\Delta\nu$[b] | $J'K_a'K_c'$-$J''K_a''K_c''$ $F_1'F_2'$-$F_1''F_2''$ | $\nu_{obs}$[a] | $\Delta\nu$[b] | $\nu_{obs}$[a] | $\Delta\nu$[b] |
|---|---|---|---|---|---|---|---|---|---|
| | $Ar^{20}Ne$-$N_2O$ | | $Ar^{22}Ne$-$N_2O$ | | | $Ar^{20}Ne$-$N_2O$ | | $Ar^{22}Ne$-$N_2O$ | |
| 110-000 | | | | | 221-111 | | | | |
| 10-11 | 4582.1195 | 3.1 | 4424.2068 | 0.6 | 23-12 | 10295.4877 | -0.7 | 9827.8439 | 0.7 |
| 12-12 | 4582.1672 | 0.4 | 4424.2566 | 0.2 | 22-21 | 10295.6121 | 0.8 | | |
| 12-11 | 4582.1672 | 0.4 | 4424.2566 | 0.2 | 23-23 | 10295.6121 | 0.5 | 9827.9673 | 1.9 |
| 11-12 | 4582.1860 | -2.8 | 4424.2755 | -2.8 | 12-12 | 10295.6782 | 1.9 | 9828.0340 | 1.6 |
| 11-11 | 4582.1860 | -2.7 | 4424.2755 | -2.8 | 33-22 | 10295.6782 | -0.2 | 9828.0340 | 1.0 |
| 11-10 | 4582.1860 | -2.8 | 4424.2755 | -2.8 | 34-23 | 10295.7379 | 0.7 | 9828.0928 | 0.8 |
| 22-12 | 4582.3629 | -0.1 | 4424.4525 | -0.5 | 32-21 | 10295.7763 | 4.0 | 9828.1277 | 1.2 |
| 22-11 | 4582.3629 | -0.1 | 4424.4525 | -0.5 | 12-22 | 10295.7763 | 2.3 | 9828.1277 | -2.5 |
| 23-12 | 4582.4146 | 1.2 | 4424.5048 | 1.6 | 11-01 | 10295.9505 | 0.9 | 9828.3065 | 3.0 |
| 21-12 | 4582.4526 | -2.1 | 4424.5431 | -1.2 | 12-01 | 10295.9633 | -1.9 | 9828.3194 | -0.2 |
| 21-11 | 4582.4526 | -2.1 | 4424.5431 | -1.2 | | | | | |
| 21-10 | 4582.4526 | -2.1 | 4424.5431 | -1.2 | 220-111 | | | | |
| 01-12 | 4582.7446 | -0.8 | 4424.8346 | -1.0 | 22-11 | 10401.3796 | 1.4 | 9961.7659 | 0.3 |
| 01-11 | 4582.7446 | -0.8 | 4424.8346 | -1.0 | 23-12 | 10401.3964 | -1.7 | 9961.7878 | -0.2 |
| 01-10 | 4582.7446 | -0.8 | 4424.8346 | -1.0 | 23-23 | 10401.5222 | 0.8 | 9961.9101 | -0.1 |
| | | | | | 21-21 | 10401.5556 | 1.4 | | |
| 202-101 | | | | | 11-10 | | | 9962.0257 | 3.3 |
| 12-12 | 5910.1456 | -1.2 | 5807.8730 | 1.8 | 33-22 | 10401.6275 | -0.2 | 9962.0257 | 2.0 |
| 11-10 | 5910.1456 | 1.2 | 5807.8730 | 3.8 | 12-12 | | | 9962.0715 | 0.8 |
| 32-21 | 5910.3585 | -0.8 | 5808.0887 | -0.3 | 32-22 | | | 9962.1006 | 4.0 |
| 34-23 | 5910.3585 | -0.9 | 5808.0887 | -0.8 | 34-23 | 10401.7020 | 0.8 | 9962.1006 | 1.3 |
| 33-22 | 5910.3807 | -1.8 | 5808.1162 | 1.4 | 32-21 | 10401.7447 | 2.2 | 9962.1379 | -2.9 |
| 21-11 | 5910.4165 | 1.5 | 5808.1162 | 0.6 | 11-01 | 10401.9344 | 0.8 | 9962.3341 | 0.0 |
| 23-12 | 5910.4165 | 0.6 | 5808.1555 | 2.9 | 12-01 | 10401.9556 | -0.5 | 9962.3589 | 0.9 |
| 22-11 | 5910.4570 | -0.7 | 5808.1555 | 1.5 | | | | | |
| 11-01 | 5910.4570 | -1.9 | 5808.1982 | 0.0 | 221-110 | | | | |
| | | | | | 12-01 | | | 9355.0021 | -0.7 |
| 211-110 | | | | | 23-23 | | | 9355.1466 | 0.5 |
| 12-01 | 6457.1825 | -0.4 | 6414.1233 | -2.4 | 32-21 | 9854.0380 | -2.8 | 9355.2472 | 0.9 |
| 21-21 | 6457.2928 | -2.0 | 6414.2372 | -1.5 | 34-23 | 9854.0713 | 3.2 | 9355.2752 | 2.6 |
| 23-23 | 6457.3272 | -0.5 | 6414.2702 | -1.5 | 33-22 | 9854.0839 | -1.4 | 9355.2878 | -0.5 |
| 32-21 | 6457.4222 | -4.0 | 6414.3672 | -1.7 | 22-11 | 9854.1483 | 2.5 | 9355.3483 | -0.3 |
| 34-23 | 6457.4509 | -2.0 | 6414.3980 | 1.8 | 23-12 | 9854.1877 | -1.4 | 9355.3924 | -0.5 |
| 33-22 | 6457.4648 | -4.3 | 6414.4125 | -1.4 | | | | | |
| 22-11 | 6457.5291 | -1.1 | 6414.4775 | 1.9 | 303-202 | | | | |
| 23-12 | 6457.5722 | -2.1 | 6414.5195 | 1.0 | 43-32 | 8634.8174 | -0.9 | 8434.8136 | -2.3 |
| | | | | | 45-34 | 8634.8174 | -1.9 | 8434.8136 | -3.2 |
| 211-101 | | | | | 44-33 | 8634.8443 | -0.4 | 8434.8447 | 1.0 |
| 22-12 | 8031.3263 | -2.1 | 7867.4752 | -0.9 | 22-12 | 8634.8871 | -0.5 | 8434.8906 | 1.9 |
| 23-12 | 8031.3504 | -0.2 | 7867.4975 | 0.4 | 34-23 | 8634.8871 | -1.7 | 8434.8906 | -0.8 |
| 22-21 | 8031.4759 | 3.9 | 7867.6236 | 1.7 | 33-22 | 8634.9201 | 0.4 | | |
| 23-23 | 8031.4759 | 2.0 | 7867.6236 | 1.9 | | | | | |
| 33-22 | 8031.5401 | 0.1 | 7867.6868 | -1.0 | 312-202 | | | | |

Table A4.1. (continued)

| $J'K_a'K_c'$-$J''K_a''K_c''$ $F_1'F_2'$-$F_1''F_2''$ | $\nu_{obs}$[a] | $\Delta\nu$[b] | $\nu_{obs}$[a] | $\Delta\nu$[b] | $J'K_a'K_c'$-$J''K_a''K_c''$ $F_1'F_2'$-$F_1''F_2''$ | $\nu_{obs}$[a] | $\Delta\nu$[b] | $\nu_{obs}$[a] | $\Delta\nu$[b] |
|---|---|---|---|---|---|---|---|---|---|
| | $Ar^{20}Ne$-$N_2O$ | | $Ar^{22}Ne$-$N_2O$ | | | $Ar^{20}Ne$-$N_2O$ | | $Ar^{22}Ne$-$N_2O$ | |
| 34-23 | 8031.6014 | 2.3 | 7867.7481 | 1.9 | 33-22 | 11730.2071 | 1.4 | 11580.8311 | -1.0 |
| 32-21 | 8031.6333 | -0.7 | 7867.7805 | -0.7 | 34-23 | 11730.2564 | 0.6 | 11580.8821 | 0.8 |
| 12-22 | 8031.6333 | -2.9 | 7867.7805 | -1.8 | 32-21 | 11730.2733 | -0.1 | 11580.9000 | 1.2 |
| 11-01 | 8031.8114 | -0.0 | 7867.9631 | 2.9 | 34-34 | 11730.4396 | 3.9 | 11581.0681 | -2.3 |
| 12-01 | 8031.8282 | 0.8 | 7867.9743 | -1.3 | 44-33 | 11730.4396 | 0.6 | 11581.0681 | -0.7 |
| 10-01 | 8031.8552 | 1.2 | 7868.0000 | -0.9 | 45-34 | 11730.5112 | 1.6 | 11581.1407 | 1.5 |
| | | | | | 43-32 | 11730.5362 | -0.3 | 11581.1672 | 0.8 |
| 212-101 | | | | | 22-11 | 11730.5814 | -0.4 | 11581.2142 | -1.4 |
| 10-01 | 6706.7784 | -0.0 | | | 23-12 | 11730.6222 | -0.3 | 11581.2543 | -0.8 |
| 32-22 | | | 6449.4414 | 1.5 | | | | | |
| 32-21 | 6706.7784 | -2.2 | | | 321-211 | | | | |
| 34-23 | 6706.7902 | 1.3 | 6449.4950 | 0.8 | 44-34 | 12912.9092 | 3.6 | 12462.6801 | 0.2 |
| 33-22 | 6706.8308 | -0.8 | 6449.5358 | 0.2 | 22-11 | 12912.9092 | 3.4 | | |
| 12-01 | 6706.8308 | -0.1 | 6449.5358 | -1.3 | 21-10 | 12912.9092 | 0.5 | 12462.6991 | 6.1 |
| 11-01 | 6706.8604 | -2.1 | | | 33-22 | 12912.9378 | 0.9 | 12462.6991 | 2.7 |
| 23-12 | 6706.9150 | -1.4 | | | 23-12 | | | 12462.6991 | -1.7 |
| 22-11 | 6706.9708 | -0.1 | | | 43-32 | 12912.9378 | -0.2 | 12462.7134 | -3.5 |
| 23-23 | 6707.0393 | -0.4 | | | 44-33 | 12912.9378 | -2.1 | 12462.7134 | 1.0 |
| 21-21 | 6707.0393 | -4.1 | | | 45-34 | 12912.9378 | -4.2 | 12462.7134 | -5.8 |
| | | | | | 34-23 | 12912.9445 | -0.9 | 12462.7134 | 4.9 |
| 212-111 | | | | | 32-21 | 12912.9445 | -1.7 | 12462.7134 | 2.9 |
| 32-22 | 5574.2599 | 2.3 | 5468.9097 | -1.0 | | | | | |
| 34-23 | 5574.3157 | 3.9 | 5468.9637 | 0.1 | 322-212 | | | | |
| 12-01 | 5574.3576 | 4.4 | 5469.0045 | 0.5 | 21-22 | 13742.4421 | -0.4 | 13268.9536 | 0.0 |
| 33-22 | 5574.3576 | 3.8 | 5469.0045 | -1.9 | 23-22 | 13742.4421 | -0.4 | 13268.9536 | 0.0 |
| 33-23 | 5574.3830 | 3.7 | 5469.0342 | 3.5 | 22-22 | 13742.4421 | -0.4 | 13268.9536 | 0.0 |
| 11-01 | 5574.3830 | -1.7 | 5469.0342 | -1.3 | 32-22 | 13742.4421 | -0.4 | 13268.9536 | 0.0 |
| 21-10 | 5574.4011 | 3.9 | 5469.0502 | -1.3 | 33-22 | 13742.4421 | -0.4 | 13268.9536 | 0.0 |
| 23-12 | 5574.4418 | 2.5 | 5469.0926 | 0.2 | 23-23 | 13742.4873 | 1.2 | 13268.9985 | 1.6 |
| 22-11 | 5574.4971 | 3.1 | | | 22-23 | 13742.4873 | 1.2 | 13268.9985 | 1.6 |
| | | | | | 34-23 | 13742.4873 | 1.2 | 13268.9985 | 1.6 |
| 220-110 | | | | | 33-23 | 13742.4873 | 1.2 | 13268.9985 | 1.6 |
| 22-21 | | | 9489.0153 | -1.4 | 21-21 | 13742.5008 | -1.9 | 13269.0122 | -1.3 |
| 11-01 | 9959.7656 | -1.3 | 9489.0153 | -2.0 | 22-21 | 13742.5008 | -1.9 | 13269.0122 | -1.3 |
| 12-01 | 9959.7887 | -0.7 | 9489.0422 | 1.0 | 32-21 | 13742.5008 | -1.9 | 13269.0122 | -1.3 |
| 22-23 | 9959.8199 | -1.4 | 9489.0577 | -0.1 | 33-33 | 13742.6691 | -0.3 | 13269.1808 | -0.0 |
| 21-21 | 9959.8199 | -2.9 | 9489.0577 | -4.7 | 34-33 | 13742.6691 | -0.3 | 13269.1808 | -0.0 |
| 23-23 | 9959.8526 | 0.4 | 9489.0900 | -0.9 | 44-33 | 13742.6691 | -0.3 | 13269.1808 | -0.0 |
| 32-21 | 9960.0097 | -1.4 | 9489.2588 | -1.8 | 43-33 | 13742.6691 | -0.3 | 13269.1808 | -0.0 |
| 34-23 | 9960.0331 | 1.0 | 9489.2791 | -0.9 | 45-34 | 13742.7393 | 2.4 | 13269.2495 | 1.5 |
| 33-22 | 9960.0331 | -1.5 | 9489.2791 | 0.1 | 34-34 | 13742.7393 | 2.4 | 13269.2495 | 1.5 |
| 22-11 | | | 9489.2791 | -3.6 | 44-34 | 13742.7393 | 2.4 | 13269.2495 | 1.5 |
| 23-12 | 9960.0999 | 1.1 | 9489.3366 | -1.1 | 43-32 | 13742.7652 | -0.3 | 13269.2763 | -0.2 |
| 21-10 | | | 9489.3988 | -1.7 | 32-32 | 13742.7652 | -0.3 | 13269.2763 | -0.2 |

Table A4.1. (continued)

| $J'K_aK_c'$-$J''K_aK_c''$ $F_1'F_2'$-$F_1''F_2''$ | $\nu_{obs}$[a] | $\Delta\nu$[b] | $\nu_{obs}$[a] | $\Delta\nu$[b] | $J'K_aK_c'$-$J''K_aK_c''$ $F_1'F_2'$-$F_1''F_2''$ | $\nu_{obs}$[a] | $\Delta\nu$[b] | $\nu_{obs}$[a] | $\Delta\nu$[b] |
|---|---|---|---|---|---|---|---|---|---|
| | $Ar^{20}Ne$-$N_2O$ | | $Ar^{22}Ne$-$N_2O$ | | | $Ar^{20}Ne$-$N_2O$ | | $Ar^{22}Ne$-$N_2O$ | |
| 11-12 | 9960.3438 | -1.6 | 9489.5958 | -0.7 | 21-11 | 13742.8284 | -1.2 | 13269.3400 | -1.1 |
| 12-11 | 9960.3438 | -2.2 | 9489.5958 | -2.8 | 22-11 | 13742.8284 | -1.2 | 13269.3400 | -1.1 |
| 12-12 | 9960.3672 | -0.7 | 9489.6183 | -2.2 | 23-12 | 13742.8601 | -1.1 | 13269.3715 | -1.1 |
| | | | | | 22-12 | 13742.8601 | -1.1 | 13269.3715 | -1.1 |
| 221-111 | | | | | 21-10 | 13742.9130 | -0.7 | 13269.4241 | -0.7 |
| 21-10 | 10295.4713 | 0.3 | 9827.8269 | -0.3 | | | | | |

[a] Observed frequencies (MHz).

[b] Observed-calculated frequencies (kHz).

Table A4.2. The observed frequencies of the $^{14}N$-hyperfine structure of $Ar^{20}Ne$-($^{15}N^{14}NO$, $^{14}N^{15}NO$) and $Ar^{22}Ne$-($^{15}N^{14}NO$, $^{14}N^{15}NO$)

| $J'K_aK_c'J''K_aK_c''$ F' - F'' | $\nu_{obs}$[a] | $\Delta\nu$[b] | $\nu_{obs}$[a] | $\Delta\nu$[b] | $\nu_{obs}$[a] | $\Delta\nu$[b] | $\nu_{obs}$[a] | $\Delta\nu$[b] |
|---|---|---|---|---|---|---|---|---|
| | $Ar^{20}Ne$-$^{15}N^{14}NO$ | | $Ar^{22}Ne$-$^{15}N^{14}NO$ | | $Ar^{20}Ne$-$^{14}N^{15}NO$ | | $Ar^{22}Ne$-$^{14}N^{15}NO$ | |
| 110-000 | | | | | | | | |
| 1 - 1 | 4530.2524 | -1.5 | 4374.4656 | -2.9 | 4560.7245 | -0.3 | 4402.6010 | -1.6 |
| 2 - 1 | 4530.3296 | 0.5 | 4374.5423 | -0.6 | 4560.9466 | -0.1 | 4402.8235 | -0.3 |
| 0 - 1 | 4530.4416 | -0.4 | 4374.6509 | -3.5 | 4561.2770 | -2.6 | 4403.1545 | -1.1 |
| 202-101 | | | | | | | | |
| 1 - 1 | 5853.0347 | -1.4 | 5753.1420 | -3.6 | 5868.2414 | 0.1 | 5767.8495 | -0.6 |
| 3 - 2 | 5853.1029 | 0.3 | 5753.2153 | -0.6 | 5868.4461 | -1.4 | 5768.0592 | -1.2 |
| 1 - 0 | 5853.1193 | -5.6 | 5753.2376 | -0.9 | 5868.5064 | 0.0 | 5768.1270 | 0.0 |
| 2 - 1 | 5853.1193 | -3.5 | 5753.2376 | -0.6 | 5868.5196 | -0.5 | 5768.1270 | -1.8 |
| 2 - 2 | 5853.1558 | -2.5 | 5753.2740 | -1.4 | 5868.6176 | -0.3 | 5768.2367 | -1.8 |
| 211-110 | | | | | | | | |
| 1 - 0 | 6383.2084 | -0.6 | 6342.0480 | 0.5 | 6409.0619 | -0.2 | 6367.7643 | -0.4 |
| 2 - 2 | 6383.2557 | 0.0 | 6342.0981 | 1.1 | 6409.2088 | -2.2 | 6367.9143 | 0.7 |
| 3 - 2 | 6383.2977 | -0.6 | 6342.1374 | 0.5 | 6409.3286 | -0.7 | 6368.0304 | -0.6 |
| 2 - 1 | 6383.3318 | 0.9 | 6342.1716 | 0.2 | 6409.4338 | 0.9 | 6368.1358 | 1.0 |
| 1 - 1 | 6383.4003 | 3.1 | 6342.2317 | -1.7 | 6409.6186 | 1.7 | 6368.3176 | -0.1 |
| 212-111 | | | | | | | | |
| 1 - 1 | 5524.6496 | 0.3 | 5420.9339 | 0.6 | 5534.1489 | -1.0 | 5430.3354 | -1.2 |
| 3 - 2 | 5524.7356 | 1.8 | 5421.0163 | 1.5 | 5534.3919 | -0.4 | 5430.5782 | 0.2 |
| 1 - 0 | 5524.7490 | 0.4 | 5421.0287 | 2.3 | 5534.4262 | 0.5 | 5430.6113 | 0.4 |
| 2 - 1 | 5524.7749 | 0.2 | 5421.0560 | -1.3 | 5534.5210 | 1.3 | 5430.7077 | 2.4 |
| 2 - 2 | 5524.8155 | 1.1 | 5421.0943 | -0.2 | 5534.6310 | 0.9 | 5430.8157 | 0.7 |
| 212-101 | | | | | | | | |
| 1 - 1 | 6648.3177 | 0.4 | 6393.7610 | 1.6 | 6671.2907 | -0.2 | 6414.3830 | 2.0 |
| 3 - 2 | 6648.3989 | 1.2 | 6393.8412 | 0.4 | 6671.5352 | 0.7 | 6414.6263 | 2.1 |
| 1 - 0 | 6648.4070 | 0.8 | 6393.8551 | 2.8 | 6671.5697 | -0.0 | 6414.6597 | -0.0 |
| 2 - 1 | 6648.4427 | -0.1 | 6393.8847 | 1.4 | 6671.6613 | 0.6 | 6414.7485 | -1.2 |
| 2 - 2 | 6648.4763 | -2.0 | 6393.9210 | 0.5 | 6671.7714 | -0.8 | 6414.8612 | 0.1 |
| 221-110 | | | | | | | | |
| 1 - 0 | 9753.4042 | 1.1 | 9259.8249 | -1.2 | 9819.6657 | 0.3 | 9319.1836 | -0.8 |
| 2 - 2 | 9753.4571 | 0.3 | 9259.8759 | 0.2 | 9819.8123 | -0.0 | 9319.3294 | -1.0 |
| 3 - 2 | 9753.4930 | -1.9 | 9259.9158 | 0.3 | 9819.9322 | 0.4 | 9319.4506 | 0.8 |
| 2 - 1 | 9753.5326 | 0.6 | 9259.9489 | -1.2 | 9820.0352 | 1.0 | 9319.5517 | 0.2 |
| 1 - 1 | 9753.5914 | 0.2 | 9260.0110 | -1.0 | 9820.2218 | 1.7 | 9319.7358 | -1.5 |
| 220-111 | | | | | | | | |
| 2 - 1 | 10284.0617 | 0.0 | 9849.1902 | 1.3 | 10361.0477 | -0.5 | 9919.6278 | -0.9 |
| 2 - 2 | 10284.1000 | -1.4 | 9849.2281 | 2.0 | 10361.1581 | -0.4 | 9919.7381 | -0.3 |
| 1 - 1 | 10284.1481 | -0.3 | 9849.2876 | 6.1 | 10361.3137 | 0.4 | 9919.9070 | 1.4 |

Table A4.2. (continued)

| $J'K_aK_c$-$J''K_aK_c''$ F'- F'' | $\nu_{obs}$[a] | $\Delta\nu$[b] | $\nu_{obs}$[a] | $\Delta\nu$[b] | $\nu_{obs}$[a] | $\Delta\nu$[b] | $\nu_{obs}$[a] | $\Delta\nu$[b] |
|---|---|---|---|---|---|---|---|---|
| $Ar^{20}Ne$-$^{15}N^{14}NO$ | | | $Ar^{22}Ne$-$^{15}N^{14}NO$ | | $Ar^{20}Ne$-$^{14}N^{15}NO$ | | $Ar^{22}Ne$-$^{14}N^{15}NO$ | |
| 3 - 2 | 10284.1586 | 1.5 | 9849.2876 | 1.9 | 10361.3298 | 0.9 | 9919.9171 | 0.7 |
| 1 - 0 | 10284.2462 | -1.5 | 9849.3765 | 2.0 | 10361.5902 | 1.1 | 9920.1822 | 2.3 |
| 211-101 | | | | | | | | |
| 2 - 1 | 7936.2181 | -0.5 | 7775.5017 | -1.8 | 7983.7928 | -0.1 | 7820.6617 | -0.5 |
| 2 - 2 | 7936.2552 | 1.0 | 7775.5404 | -0.3 | 7983.9040 | -0.5 | 7820.7747 | 1.1 |
| 1 - 1 | 7936.2852 | 0.3 | 7775.5653 | -0.3 | 7983.9796 | 2.8 | 7820.8459 | 0.9 |
| 3 - 2 | 7936.2968 | 0.1 | 7775.5804 | -0.2 | 7984.0236 | 0.9 | 7820.8911 | -0.1 |
| 1 - 0 | 7936.3731 | -0.6 | 7775.6591 | 0.7 | 7984.2553 | -0.4 | 7821.1212 | -2.5 |
| 220-110 | | | | | | | | |
| 1 - 0 | 9854.7417 | 1.1 | 9388.5902 | 0.7 | 9923.5404 | 0.9 | 9450.8708 | 1.1 |
| 2 - 2 | 9854.7671 | 0.3 | 9388.6089 | 0.5 | 9923.6061 | -1.1 | 9450.9253 | 0.8 |
| 3 - 2 | 9854.8239 | 1.3 | 9388.6689 | 0.9 | 9923.7775 | -0.2 | 9451.1033 | 0.8 |
| 2 - 1 | 9854.8421 | 0.0 | 9388.6829 | 0.1 | 9923.8273 | -1.8 | 9451.1465 | 0.8 |
| 1 - 1 | 9854.9286 | -0.1 | 9388.7750 | -0.4 | 9924.0917 | -2.5 | 9451.4220 | -0.6 |
| 221-111 | | | | | | | | |
| 2 - 1 | 10182.7503 | -1.4 | 9720.4544 | -1.8 | 10257.2537 | 0.5 | 9788.0333 | -1.2 |
| 2 - 2 | 10182.7925 | 1.1 | 9720.4923 | -1.1 | 10257.3649 | 1.3 | 9788.1444 | 0.2 |
| 1 - 1 | 10182.8116 | 0.7 | 9720.5166 | -1.5 | 10257.4395 | 0.3 | 9788.2207 | 0.4 |
| 3 - 2 | 10182.8293 | -0.2 | 9720.5333 | 0.1 | 10257.4829 | -0.2 | 9788.2628 | -0.8 |
| 1 - 0 | 10182.9108 | 0.6 | 9720.6106 | -0.6 | 10257.7138 | -1.2 | 9788.4942 | -0.4 |
| 303-202 | | | | | | | | |
| 2 - 2 | 8557.9761 | -0.2 | 8361.9873 | 0.3 | 8575.6695 | -1.8 | 8378.5055 | -1.5 |
| 4 - 3 | 8558.0606 | 0.6 | 8362.0763 | 0.0 | 8575.9255 | -0.5 | 8378.7732 | -0.5 |
| 2 - 1 | 8558.0606 | -2.4 | 8362.0763 | -3.3 | 8575.9360 | -0.4 | 8378.7844 | 0.5 |
| 3 - 2 | 8558.0857 | 1.4 | 8362.1030 | 1.3 | 8575.9981 | 1.6 | 8378.8493 | 0.2 |
| 3 - 3 | 8558.1407 | 0.6 | 8362.1606 | -0.6 | 8576.1681 | 1.2 | 8379.0281 | 1.0 |
| 312-202 | | | | | | | | |
| 3 - 2 | 11584.6876 | -1.5 | 11439.5533 | -1.4 | 11654.0886 | 0.3 | 11506.4650 | -0.2 |
| 2 - 2 | 11584.7273 | 1.5 | 11439.5862 | 0.7 | 11654.1843 | -0.3 | 11506.5549 | 0.0 |
| 3 - 3 | 11584.7467 | 1.9 | 11439.6142 | 0.0 | 11654.2600 | 1.3 | 11506.6442 | 1.0 |
| 4 - 3 | 11584.7704 | -1.6 | 11439.6376 | 0.6 | 11654.3298 | -0.2 | 11506.7117 | 2.1 |
| 2 - 1 | 11584.8132 | 0.7 | 11439.6805 | 2.5 | 11654.4486 | -1.0 | 11506.8304 | -1.4 |
| 321-211 | | | | | | | | |
| 3 - 3 | 12773.0521 | -0.9 | 12326.7883 | -1.0 | 12851.5591 | 0.7 | 12399.7193 | 0.5 |
| 2 - 1 | 12773.0834 | -0.7 | 12326.8249 | -1.1 | 12851.6532 | 2.7 | 12399.8271 | -1.3 |
| 4 - 3 | 12773.0964 | 2.8 | 12326.8359 | 3.0 | 12851.6738 | -1.5 | 12399.8362 | -0.2 |
| 3 - 2 | 12773.0964 | 0.8 | 12326.8249 | -4.3 | 12851.6738 | -2.8 | 12399.8476 | -0.8 |
| 2 - 2 | 12773.1491 | -1.2 | 12326.8881 | 0.0 | 12851.8335 | -0.9 | 12400.0112 | -0.1 |

Table A4.2. (continued)

| $J'K_a'K_c'$-$J''K_a''K_c''$ F'- F'' | $\nu_{obs}$[a] | $\Delta\nu$[b] | $\nu_{obs}$[a] | $\Delta\nu$[b] | $\nu_{obs}$[a] | $\Delta\nu$[b] | $\nu_{obs}$[a] | $\Delta\nu$[b] |
|---|---|---|---|---|---|---|---|---|
| | $Ar^{20}Ne$-$^{15}N^{14}NO$ | | $Ar^{22}Ne$-$^{15}N^{14}NO$ | | $Ar^{20}Ne$-$^{14}N^{15}NO$ | | $Ar^{22}Ne$-$^{14}N^{15}NO$ | |
| 322-212 | | | | | | | | |
| 2 - 2 | 13586.5985 | 1.1 | 13119.4611 | -0.2 | 13678.1648 | 0.0 | 13204.0309 | 0.1 |
| 3 - 2 | 13586.5985 | 1.1 | 13119.4611 | -0.2 | 13678.1648 | 0.1 | 13204.0309 | 0.1 |
| 4 - 3 | 13586.6754 | -2.6 | 13119.5404 | -0.6 | 13678.4031 | 0.6 | 13204.2690 | 1.2 |
| 3 - 3 | 13586.6754 | -2.6 | 13119.5404 | -0.6 | 13678.4031 | 0.6 | 13204.2690 | 1.2 |
| 2 - 1 | 13586.7233 | 0.5 | 13119.5861 | 0.9 | 13678.5327 | -1.8 | 13204.3982 | -1.3 |

[a] Observed frequencies (MHz).
[b] Observed-calculated frequencies (kHz).

# A5

# TABLES OF THE MEASURED TRANSITION FREQUENCIES FOR CHAPTER SEVEN

Table A5.1. Observed Transition Frequencies (in MHz) for CO-$^{14}N^{14}NO$ Isotopomers.

| $J'K_a'K_c'$ -$J''K_a''K_c''$ | $^{12}C^{16}O$-NNO | | $^{13}C^{16}O$-NNO | | $^{13}C^{18}O$-NNO | | $J'K_a'K_c'$ -$J''K_a''K_c''$ | $^{12}C^{16}O$-NNO | | $^{13}C^{16}O$-NNO | | $^{13}C^{18}O$-NNO | |
|---|---|---|---|---|---|---|---|---|---|---|---|---|---|
| $F_1'$ $F'$- $F_1''$ $F''$ | $\nu_{obs}$ | $\Delta\nu$ | $\nu_{obs}$ | $\Delta\nu$ | $\nu_{obs}$ | $\Delta\nu$ | $F_1'$ $F'$- $F_1''$ $F''$ | $\nu_{obs}$ | $\Delta\nu$ | $\nu_{obs}$ | $\Delta\nu$ | $\nu_{obs}$ | $\Delta\nu$ |
| 111-000 | | | | | | | 211-110 | | | | | | |
| 10-11 | 14516.5094 | -4.5 | 14486.8959 | 2.4 | 14407.9507 | -2.1 | 11-10 | 7396.9353 | 1.3 | 7315.9992 | -0.6 | 6932.1152 | -0.4 |
| 12-12 | 14516.5614 | -1.5 | 14486.9439 | 1.1 | 14408.0009 | -1.0 | 12-12 | 7396.9353 | 1.1 | 7315.9992 | 0.2 | 6932.1152 | -1.3 |
| 12-11 | 14516.5614 | -1.5 | 14486.9439 | 1.1 | 14408.0009 | -1.0 | 32-21 | 7397.1921 | 0.1 | 7316.2561 | 1.2 | 6932.3741 | -1.3 |
| 11-12 | 14516.5831 | -1.3 | 14486.9671 | 2.7 | 14408.0235 | 0.0 | 34-23 | 7397.1921 | -1.2 | 7316.2561 | -1.2 | 6932.3741 | -1.8 |
| 11-11 | 14516.5831 | -1.3 | 14486.9671 | 2.7 | 14408.0235 | 0.0 | 33-22 | 7397.2289 | 1.1 | 7316.2923 | -0.8 | 6932.4095 | -0.4 |
| 11-10 | 14516.5831 | -1.3 | 14486.9671 | 2.7 | 14408.0235 | 0.0 | 12-01 | 7397.2488 | 0.5 | 7316.3123 | -0.4 | 6932.4301 | -1.0 |
| 22-12 | 14516.7587 | -0.1 | 14487.1417 | 3.7 | 14408.1980 | 0.3 | 33-23 | 7397.2618 | 3.1 | 7316.3244 | 1.2 | 6932.4409 | -0.7 |
| 22-11 | 14516.7587 | -0.1 | 14487.1417 | 3.7 | 14408.1980 | 0.3 | 21-10 | 7397.2618 | 1.3 | 7316.3244 | 0.8 | 6932.4409 | -1.1 |
| 23-12 | 14516.8097 | 1.9 | 14487.1925 | 5.1 | 14408.2501 | 3.3 | 11-01 | 7397.2796 | 0.6 | 7316.3452 | 1.5 | 6932.4611 | -0.9 |
| 21-12 | 14516.8452 | -2.4 | 14487.2301 | 2.6 | 14408.2865 | -0.3 | 23-12 | 7397.3080 | 0.3 | 7316.3728 | 1.2 | 6932.4894 | -0.5 |
| 21-11 | 14516.8452 | -2.4 | 14487.2301 | 2.6 | 14408.2865 | -0.3 | 22-12 | 7397.3521 | 2.2 | 7316.4164 | 2.2 | 6932.5314 | -0.8 |
| 21-10 | 14516.8452 | -2.4 | 14487.2301 | 2.6 | 14408.2865 | -0.3 | 22-11 | 7397.3630 | 0.5 | 7316.4268 | 0.2 | 6932.5463 | 1.4 |
| 01-12 | 14517.1359 | -2.5 | 14487.5191 | 2.0 | 14408.5757 | -1.6 | 23-23 | 7397.4407 | -2.0 | 7316.5084 | 2.1 | 6932.6219 | -3.5 |
| 01-11 | 14517.1359 | -2.5 | 14487.5191 | 2.0 | 14408.5757 | -1.6 | 21-21 | 7397.4537 | 0.8 | 7316.5183 | 2.9 | 6932.6352 | -1.1 |
| 01-10 | 14517.1359 | -2.5 | 14487.5191 | 2.0 | 14408.5757 | -1.6 | | | | | | | |
| | | | | | | | 212-101 | | | | | | |
| 110-101 | | | | | | | 22-12 | 17826.1998 | -2.7 | 17764.0933 | -3.3 | 17530.5949 | 2.2 |
| 01-12 | 11205.2008 | -1.7 | 11208.1375 | -0.3 | 11283.8676 | -2.6 | 22-11 | 17826.2132 | 2.1 | 17764.1031 | -2.4 | 17530.6029 | 1.9 |
| 01-11 | 11205.2100 | -1.1 | 11208.1468 | 0.1 | 11283.8787 | 0.2 | 21-10 | 17826.2241 | 2.2 | 17764.1145 | 0.7 | 17530.6151 | 1.4 |
| 21-10 | 11205.3355 | -1.9 | 11208.2736 | 1.2 | 11284.0051 | 0.0 | 23-12 | 17826.2306 | 0.7 | 17764.1212 | -2.0 | 17530.6204 | -0.4 |
| 23-12 | 11205.3825 | 0.9 | 11208.3207 | 3.8 | 11284.0503 | 0.9 | 23-23 | 17826.3401 | 0.0 | 17764.2327 | -0.6 | 17530.7307 | 0.0 |
| 21-22 | 11205.4488 | 1.2 | 11208.3868 | 4.3 | 11284.1144 | -0.6 | 21-21 | 17826.3623 | -1.1 | 17764.2547 | -3.0 | 17530.7533 | -0.2 |
| 21-21 | 11205.4797 | 0.8 | 11208.4191 | 2.9 | 11284.1434 | -1.4 | 33-22 | 17826.4172 | 0.6 | 17764.3078 | -1.8 | 17530.8065 | -0.6 |
| 23-23 | 11205.4930 | 1.2 | 11208.4310 | 4.0 | 11284.1583 | -0.9 | 12-12 | 17826.4323 | 0.1 | 17764.3248 | -0.8 | 17530.8227 | -0.6 |
| 11-12 | 11205.5032 | -0.8 | 11208.4407 | 1.7 | 11284.1740 | 1.9 | 33-23 | 17826.4323 | -2.1 | 17764.3248 | -3.8 | 17530.8227 | -1.4 |
| 22-22 | 11205.5032 | -1.8 | 11208.4407 | 2.6 | 11284.1740 | 0.2 | 10-11 | 17826.4756 | 2.3 | 17764.3655 | -0.6 | 17530.8696 | 4.6 |
| 22-23 | 11205.5209 | -1.8 | 11208.4627 | 5.6 | 11284.1901 | -0.8 | 34-23 | 17826.4756 | -0.6 | 17764.3655 | -3.7 | 17530.8696 | 2.6 |

Table A5.1. (Continued)

| $J'K_a'K_c'$ -$J''K_a''K_c''$ $F_i'$ $F'$- $F_i''$ $F''$ | $^{12}C^{16}O$-NNO $\nu_{obs}$ | $\Delta\nu$ | $^{13}C^{16}O$-NNO $\nu_{obs}$ | $\Delta\nu$ | $^{13}C^{18}O$-NNO $\nu_{obs}$ | $\Delta\nu$ | $J'K_a'K_c'$ -$J''K_a''K_c''$ $F_i'$ $F'$- $F_i''$ $F''$ | $^{12}C^{16}O$-NNO $\nu_{obs}$ | $\Delta\nu$ | $^{13}C^{16}O$-NNO $\nu_{obs}$ | $\Delta\nu$ | $^{13}C^{18}O$-NNO $\nu_{obs}$ | $\Delta\nu$ |
|---|---|---|---|---|---|---|---|---|---|---|---|---|---|
| 12-11 | 11205.5209 | -4.3 | 11208.4627 | 2.3 | 11284.1901 | -3.1 | 32-22 | 17826.4756 | -1.0 | 17764.3655 | -2.2 | 17530.8696 | 1.0 |
| 22-21 | 11205.5347 | -1.5 | 11208.4750 | 3.2 | 11284.2031 | -0.6 | 32-21 | 17826.5078 | 0.0 | 17764.4009 | -0.6 | 17530.8982 | -0.3 |
| 12-23 | 11205.6262 | -0.6 | 11208.5629 | 1.3 | 11284.2951 | 0.4 | 11-01 | 17826.6767 | 1.2 | 17764.5652 | -2.9 | 17531.0658 | 0.0 |
| 11-21 | 11205.6262 | -1.5 | 11208.5629 | -1.0 | 11284.2951 | 0.3 | 12-01 | 17826.6941 | -0.4 | 17764.5856 | -1.1 | 17531.0836 | -1.6 |
| 11-01 | 11205.7669 | 0.6 | 11208.7024 | 2.2 | 11284.4340 | 0.0 | 10-01 | 17826.7250 | -2.1 | 17764.6177 | -0.6 | 17531.1166 | -2.0 |
| 12-01 | 11205.7768 | -2.1 | 11208.7152 | 2.6 | 11284.4478 | 1.0 | | | | | | | |
| | | | | | | | 211-202 | | | | | | |
| 202-101 | | | | | | | 12-23 | 11467.0821 | 0.2 | 11464.5986 | -0.6 | 11514.7095 | -0.3 |
| 12-12 | 7135.2047 | 0.8 | 7059.6904 | 3.0 | 6701.4272 | 1.4 | 11-22 | 11467.0966 | -2.2 | 11464.6128 | -2.2 | 11514.7294 | 2.1 |
| 12-11 | 7135.2159 | 3.4 | 7059.6980 | 1.6 | 6701.4352 | 1.0 | 32-21 | 11467.1870 | 2.8 | 11464.7033 | 2.1 | 11514.8137 | 1.9 |
| 11-12 | 7135.2159 | 1.2 | 7059.6980 | -1.0 | 6701.4352 | -1.1 | 10-11 | 11467.1870 | 1.9 | 11464.7033 | 3.0 | 11514.8137 | -0.3 |
| 32-22 | 7135.3463 | 3.2 | 7059.8262 | 2.4 | 6701.5693 | 3.2 | 34-23 | 11467.2051 | -0.9 | 11464.7248 | 2.0 | 11514.8366 | 2.8 |
| 21-10 | 7135.3463 | 1.1 | 7059.8262 | 0.1 | 6701.5693 | 0.5 | 12-11 | 11467.2354 | -0.6 | 11464.7516 | 0.0 | 11514.8629 | -2.2 |
| 33-22 | 7135.3726 | -1.7 | 7059.8542 | -3.4 | 6701.5902 | -5.9 | 12-12 | 11467.2483 | 1.5 | 11464.7636 | 0.5 | 11514.8750 | -0.5 |
| 34-23 | 7135.3726 | 2.7 | 7059.8542 | 1.6 | 6701.5902 | -1.6 | 34-33 | 11467.2961 | 3.1 | 11464.8103 | 2.6 | 11514.9243 | 2.3 |
| 21-11 | 7135.3726 | 1.1 | 7059.8542 | 0.2 | 6701.5902 | -4.0 | 11-10 | 11467.2961 | 1.2 | 11464.8103 | -2.3 | 11514.9243 | 1.4 |
| 23-12 | 7135.3726 | 3.8 | 7059.8542 | 2.9 | 6701.5902 | -1.3 | 32-32 | 11467.2961 | -0.4 | 11464.8103 | -3.3 | 11514.9243 | 0.0 |
| 32-21 | 7135.3726 | -1.8 | 7059.8542 | -3.4 | 6701.5902 | -5.8 | 34-34 | 11467.3138 | -1.4 | 11464.8319 | 0.3 | 11514.9444 | 1.0 |
| 22-11 | 7135.3942 | 2.9 | 7059.8783 | 2.9 | 6701.6110 | -2.2 | 33-33 | 11467.3600 | 1.5 | 11464.8760 | 2.4 | 11514.9877 | 0.0 |
| 33-23 | 7135.3942 | 2.2 | 7059.8783 | 1.7 | 6701.6110 | -2.1 | 23-22 | 11467.4445 | 3.0 | 11464.9591 | 2.4 | 11515.0697 | -0.2 |
| 12-01 | 7135.4675 | 1.2 | 7059.9526 | 4.0 | 6701.6895 | 1.7 | 21-21 | 11467.4445 | -0.6 | 11464.9591 | -2.6 | 11515.0697 | -3.0 |
| 22-22 | 7135.4803 | 5.1 | 7059.9612 | 3.6 | 6701.6998 | 2.2 | 23-23 | 11467.4556 | 0.1 | 11464.9718 | 0.0 | 11515.0846 | 1.4 |
| 11-01 | 7135.4803 | 3.2 | 7059.9612 | 1.1 | 6701.6998 | 1.6 | 22-22 | 11467.4840 | 0.3 | 11464.9989 | -0.3 | 11515.1107 | -1.5 |
| 23-23 | 7135.4803 | 1.3 | 7059.9612 | -0.2 | 6701.6998 | -1.5 | 22-23 | 11467.4990 | 1.3 | 11465.0139 | -0.4 | 11515.1240 | -1.6 |
| | | | | | | | 23-34 | 11467.5648 | 0.2 | 11465.0803 | -0.3 | 11515.1934 | 0.6 |
| 212-111 | | | | | | | 23-12 | 11467.6211 | 0.8 | 11465.1361 | 0.4 | 11515.2502 | 1.3 |
| 11-01 | 6879.4183 | 0.0 | 6809.0761 | -3.5 | 6474.9557 | -1.7 | 22-11 | 11467.6510 | -0.8 | 11465.1671 | 0.4 | 11515.2811 | 0.3 |
| 12-01 | 6879.4405 | 3.2 | 6809.0984 | 0.2 | 6474.9733 | -3.6 | | | | | | | |

Table A5.1. (continued)

| $J'K_a'K_c'$ -$J''K_a''K_c''$ $F_i'$ $F'$- $F''$ $F_i''$ | $^{12}C^{16}O$-NNO $\nu_{obs}$ | $\Delta\nu$ | $^{13}C^{16}O$-NNO $\nu_{obs}$ | $\Delta\nu$ | $^{13}C^{18}O$-NNO $\nu_{obs}$ | $\Delta\nu$ | $J'K_a'K_c'$ -$J''K_a''K_c''$ $F_i'$ $F'$- $F''$ $F_i''$ | $^{12}C^{16}O$-NNO $\nu_{obs}$ | $\Delta\nu$ | $^{13}C^{16}O$-NNO $\nu_{obs}$ | $\Delta\nu$ | $^{13}C^{18}O$-NNO $\nu_{obs}$ | $\Delta\nu$ |
|---|---|---|---|---|---|---|---|---|---|---|---|---|---|
| 21-21 | 6879.5380 | 2.4 | 6809.1963 | 1.2 | 6475.0721 | -2.8 | 303-202 | | | | | | |
| 22-23 | 6879.5380 | -0.2 | 6809.1963 | -2.8 | 6475.0721 | -4.6 | 32-21 | 10691.2402 | -0.9 | 10578.4384 | -0.6 | 10043.1886 | 0.6 |
| 23-23 | 6879.5650 | -0.6 | 6809.2222 | -3.4 | 6475.1016 | -3.3 | 34-23 | 10691.2402 | -1.0 | 10578.4384 | -0.7 | 10043.1886 | 0.5 |
| 32-21 | 6879.6788 | -1.2 | 6809.3365 | -2.4 | 6475.2202 | 0.3 | 45-34 | 10691.2473 | 1.7 | 10578.4467 | 3.1 | 10043.1942 | 2.6 |
| 34-23 | 6879.7023 | 0.7 | 6809.3602 | -1.3 | 6475.2397 | -1.5 | 21-11 | 10691.2473 | 1.3 | 10578.4467 | 4.6 | 10043.1942 | 1.7 |
| 33-22 | 6879.7100 | 1.1 | 6809.3699 | -0.3 | 6475.2462 | -1.2 | 44-33 | 10691.2473 | 1.4 | 10578.4467 | 2.5 | 10043.1942 | 2.2 |
| 22-11 | 6879.7614 | -0.2 | 6809.4196 | -2.4 | 6475.3002 | 0.1 | 33-22 | 10691.2473 | 1.4 | 10578.4467 | 2.2 | 10043.1942 | 1.4 |
| 12-23 | 6879.7675 | -0.4 | 6809.4287 | 0.7 | 6475.3091 | 1.8 | 43-32 | 10691.2473 | -1.0 | 10578.4467 | 0.3 | 10043.1942 | 0.1 |
| 32-22 | 6879.7675 | -1.3 | 6809.4287 | 0.3 | 6475.3091 | 0.1 | 23-12 | 10691.2663 | -0.6 | 10578.4675 | 2.9 | 10043.2142 | 1.5 |
| 22-12 | 6879.7816 | -1.5 | 6809.4417 | -1.9 | 6475.3221 | 0.4 | 44-34 | 10691.2663 | -1.8 | 10578.4675 | -0.6 | 10043.2142 | 0.9 |
| 23-12 | 6879.8117 | 1.2 | 6809.4678 | -2.4 | 6475.3499 | 0.1 | 21-10 | 10691.2749 | 0.9 | 10578.4733 | 1.1 | 10043.2222 | 2.7 |
| 21-10 | 6879.8704 | 1.1 | 6809.5288 | -0.3 | 6475.4094 | 0.5 | 22-11 | 10691.2749 | 0.5 | 10578.4733 | 0.3 | 10043.2222 | 2.2 |
| 12-11 | 6879.9920 | 0.7 | 6809.6502 | -0.8 | 6475.5322 | 1.5 | | | | | | | |
| 11-12 | 6879.9920 | -1.8 | 6809.6502 | -3.7 | 6475.5322 | -0.6 | | | | | | | |
| 12-12 | 6880.0151 | 2.3 | 6809.6694 | -3.2 | 6475.5529 | 0.6 | | | | | | | |
| 313-212 | | | | | | | 322-221 | | | | | | |
| 32-32 | 10316.2216 | -1.5 | 10210.8369 | 0.4 | 9710.2062 | 1.6 | 22-21 | 10700.8803 | -3.4 | 10587.7566 | 1.2 | | |
| 34-34 | 10316.2335 | 2.1 | 10210.8441 | -0.4 | 9710.2151 | 2.0 | 21-21 | 10700.8803 | -3.4 | 10587.7566 | 1.2 | | |
| 22-12 | 10316.2792 | 2.0 | 10210.8912 | -0.7 | 9710.2606 | 2.7 | 23-23 | 10700.8889 | -1.0 | 10587.7636 | 1.7 | | |
| 21-10 | 10316.2979 | 2.6 | 10210.9083 | -0.4 | 9710.2780 | 1.1 | 34-23 | 10700.8889 | -1.0 | 10587.7636 | 1.7 | | |
| 22-11 | 10316.2979 | 1.6 | 10210.9083 | -2.2 | 9710.2780 | 0.7 | 44-23 | 10700.8889 | -1.0 | 10587.7636 | 1.7 | | |
| 23-12 | 10316.3129 | 3.2 | 10210.9209 | -2.0 | 9710.2915 | 0.1 | 22-23 | 10700.8889 | -1.0 | 10587.7636 | 1.7 | | |
| 33-23 | 10316.3346 | 1.9 | 10210.9490 | 1.6 | 9710.3155 | 2.0 | 33-23 | 10700.8889 | -1.0 | 10587.7636 | 1.7 | | |
| 43-32 | 10316.3346 | -0.8 | 10210.9490 | 0.4 | 9710.3155 | -1.6 | 43-23 | 10700.8889 | -1.0 | 10587.7636 | 1.7 | | |
| 45-34 | 10316.3440 | 2.6 | 10210.9566 | 2.0 | 9710.3231 | -0.0 | 33-22 | 10700.9017 | -2.9 | 10587.7796 | 1.8 | | |
| 44-33 | 10316.3440 | 1.5 | 10210.9566 | 0.2 | 9710.3231 | -0.8 | 22-22 | 10700.9017 | -2.9 | 10587.7796 | 1.8 | | |
| 21-11 | 10316.3440 | -2.9 | 10210.9566 | -2.3 | 9710.3301 | 0.5 | 23-22 | 10700.9017 | -2.9 | 10587.7796 | 1.8 | | |

Table A5.1. (continued)

| $J'K_a'K_c'$ -$J''K_a''K_c''$ F' F'- F'' F'' | $^{12}C^{16}O$-NNO $\nu_{obs}$ | $\Delta\nu$ | $^{13}C^{16}O$-NNO $\nu_{obs}$ | $\Delta\nu$ | $^{13}C^{18}O$-NNO $\nu_{obs}$ | $\Delta\nu$ | $J'K_a'K_c'$ -$J''K_a''K_c''$ F' F'- F'' F'' | $^{12}C^{16}O$-NNO $\nu_{obs}$ | $\Delta\nu$ | $^{13}C^{16}O$-NNO $\nu_{obs}$ | $\Delta\nu$ | $^{13}C^{18}O$-NNO $\nu_{obs}$ | $\Delta\nu$ |
|---|---|---|---|---|---|---|---|---|---|---|---|---|---|
| 34-23 | 10316.3692 | 1.8 | 10210.9789 | -1.5 | 9710.3484 | -1.0 | 21-22 | 10700.9017 | -2.9 | 10587.7796 | 1.8 | | |
| 32-21 | 10316.3692 | 1.7 | 10210.9789 | -1.5 | 9710.3484 | -1.2 | | | | | | | |
| 43-33 | 10316.3966 | 1.3 | 10211.0050 | -1.8 | 9710.3782 | -0.4 | 321-220 | | | | | | |
| 22-22 | 10316.5083 | 1.3 | 10211.1186 | -2.2 | 9710.4904 | 1.9 | 23-12 | 10718.7103 | -3.5 | 10604.7939 | 3.0 | | |
| 23-23 | 10316.5143 | 2.3 | 10211.1235 | -1.8 | 9710.4904 | -3.4 | 22-12 | 10718.7103 | -6.3 | 10604.7939 | 0.2 | | |
| | | | | | | | 22-11 | 10718.7235 | -3.9 | 10604.8059 | 0.7 | | |
| 312-211 | | | | | | | 43-32 | 10718.7598 | -3.3 | 10604.8409 | 2.1 | | |
| 23-23 | 11092.0638 | 0.7 | 10970.7874 | -0.6 | 10395.5513 | -0.6 | 45-34 | 10718.7715 | -1.7 | 10604.8509 | 1.3 | | |
| 22-22 | 11092.0850 | 0.1 | 10970.8095 | -0.7 | 10395.5743 | 0.8 | 32-32 | 10718.7715 | -3.2 | 10604.8509 | 0.7 | | |
| 21-11 | 11092.3709 | 0.4 | 10971.0935 | -0.3 | 10395.8602 | 1.1 | 44-34 | 10718.7715 | -5.2 | 10604.8509 | -2.2 | | |
| 32-22 | 11092.3709 | -1.6 | 10971.0935 | -2.3 | 10395.8602 | -1.1 | 44-33 | 10718.7961 | -2.8 | 10604.8803 | 3.3 | | |
| 45-34 | 11092.4032 | -0.1 | 10971.1268 | -0.5 | 10395.8945 | 2.5 | 32-21 | 10718.8865 | -0.6 | 10604.9633 | 0.7 | | |
| 43-32 | 11092.4032 | -4.8 | 10971.1342 | 2.2 | 10395.8945 | -2.4 | 21-22 | 10718.8951 | 4.1 | 10604.9735 | 5.0 | | |
| 44-33 | 11092.4174 | 0.4 | 10971.1410 | -0.5 | 10395.9080 | 2.5 | 23-22 | 10718.8951 | 2.5 | 10604.9735 | 3.5 | | |
| 32-21 | 11092.4287 | -2.2 | 10971.1555 | 0.9 | 10395.9250 | 5.1 | 34-23 | 10718.8951 | 1.3 | 10604.9735 | 3.9 | | |
| 34-23 | 11092.4357 | 0.8 | 10971.1600 | 1.3 | 10395.9250 | 1.2 | 22-22 | 10718.8951 | -0.3 | 10604.9735 | 0.8 | | |
| 23-12 | 11092.4357 | -0.9 | 10971.1600 | -0.6 | 10395.9250 | -0.3 | 33-23 | 10718.8951 | -1.7 | 10604.9735 | 1.0 | | |
| 21-10 | 11092.4512 | -1.0 | 10971.1750 | -1.0 | 10395.9407 | -0.3 | 33-22 | 10718.9102 | -0.5 | 10604.9889 | 1.2 | | |
| 33-22 | 11092.4612 | 1.8 | 10971.1847 | 1.0 | 10395.9489 | 0.8 | | | | | | | |
| 22-11 | 11092.4721 | 2.3 | 10971.1955 | 1.1 | 10395.9590 | 0.6 | 322-413 | | | | | | |
| 22-12 | 11092.4986 | -2.0 | 10971.2225 | -2.8 | 10395.9894 | 0.2 | 43-44 | 17657.1421 | 0.0 | | | | |
| 33-23 | 11092.4986 | -3.0 | 10971.2225 | -3.7 | 10395.9894 | -1.0 | 34-44 | 17657.1421 | 0.0 | | | | |
| 34-34 | 11092.6836 | -0.8 | 10971.4068 | -0.9 | 10396.1725 | -0.7 | 33-44 | 17657.1421 | 0.0 | | | | |
| 33-33 | 11092.6836 | -1.9 | 10971.4068 | -2.5 | 10396.1725 | -1.7 | 34-45 | 17657.2200 | -0.1 | | | | |
| 32-32 | 11092.6930 | 1.2 | 10971.4118 | -3.4 | 10396.1806 | -0.2 | 44-45 | 17657.2200 | -0.1 | | | | |
| | | | | | | | 45-45 | 17657.2200 | -0.1 | | | | |
| 312-303 | | | | | | | 23-43 | 17657.2388 | 0.1 | | | | |
| 23-34 | 11868.2776 | 0.2 | 11857.3209 | 0.2 | 11867.4482 | 1.2 | 32-43 | 17657.2388 | 0.1 | | | | |

Table A5.1. (continued)

| $J'K_a'K_c'$ -$J''K_a''K_c''$ $F_i'$ $F'$- $F_i''$ $F''$ | $^{12}C^{16}O$-NNO $\nu_{obs}$ | $\Delta\nu$ | $^{13}C^{16}O$-NNO $\nu_{obs}$ | $\Delta\nu$ | $^{13}C^{18}O$-NNO $\nu_{obs}$ | $\Delta\nu$ | $J'K_a'K_c'$ -$J''K_a''K_c''$ $F_i'$ $F'$- $F_i''$ $F''$ | $^{12}C^{16}O$-NNO $\nu_{obs}$ | $\Delta\nu$ | $^{13}C^{16}O$-NNO $\nu_{obs}$ | $\Delta\nu$ | $^{13}C^{18}O$-NNO $\nu_{obs}$ | $\Delta\nu$ |
|---|---|---|---|---|---|---|---|---|---|---|---|---|---|
| 22-33 | 11868.3210 | -1.6 | 11857.3658 | 0.9 | 11867.4931 | 0.2 | 22-43 | 17657.2388 | 0.1 | | | | |
| 21-21 | 11868.3916 | 0.3 | 11857.4319 | -2.3 | 11867.5628 | 0.4 | 43-43 | 17657.2388 | 0.1 | | | | |
| 23-23 | 11868.4165 | -0.1 | 11857.4569 | -2.2 | 11867.5888 | 0.7 | 33-43 | 17657.2388 | 0.1 | | | | |
| 43-43 | 11868.4562 | -0.1 | 11857.4969 | -2.2 | 11867.6288 | 1.7 | 34-55 | 17657.4322 | 3.5 | | | | |
| 22-22 | 11868.4631 | 0.8 | 11857.5029 | -1.0 | 11867.6355 | 1.2 | 44-55 | 17657.4322 | 3.5 | | | | |
| 45-45 | 11868.4717 | -1.2 | 11857.5119 | -3.4 | 11867.6441 | 0.3 | 45-55 | 17657.4322 | 3.5 | | | | |
| 44-44 | 11868.5299 | 0.4 | 11857.5689 | -2.1 | 11867.7016 | 0.4 | 23-33 | 17657.5085 | 0.6 | | | | |
| 32-32 | 11868.6348 | -0.1 | 11857.6753 | -2.1 | 11867.8034 | -1.1 | 22-33 | 17657.5085 | 0.6 | | | | |
| 34-34 | 11868.6484 | -0.8 | 11857.6877 | -3.7 | 11867.8198 | 0.8 | 32-33 | 17657.5085 | 0.6 | | | | |
| 33-33 | 11868.6957 | -1.4 | 11857.7379 | -0.5 | 11867.8677 | 0.2 | 33-33 | 17657.5085 | 0.6 | | | | |
| 34-45 | 11868.7551 | 1.1 | 11857.7952 | -0.5 | 11867.9258 | 0.8 | 43-33 | 17657.5085 | 0.6 | | | | |
| 34-23 | 11868.7868 | -1.6 | 11857.8294 | -0.4 | 11867.9606 | 0.6 | 45-56 | 17657.5143 | -0.1 | | | | |
| 33-22 | 11868.8360 | -0.8 | 11857.8765 | -0.9 | 11868.0091 | 0.2 | 33-54 | 17657.5322 | -1.2 | | | | |
| | | | | | | | 44-54 | 17657.5322 | -1.2 | | | | |
| 322-221 | | | | | | | 34-54 | 17657.5322 | -1.2 | | | | |
| 21-10 | 10700.7000 | 0.0 | 10587.5733 | 1.5 | | | 43-54 | 17657.5322 | -1.2 | | | | |
| 22-12 | 10700.7183 | 0.1 | 10587.5932 | 1.8 | | | 23-54 | 17657.5322 | -1.2 | | | | |
| 32-12 | 10700.7183 | 0.1 | 10587.5932 | 1.8 | | | 34-34 | 17657.5845 | -1.0 | | | | |
| 23-12 | 10700.7183 | 0.1 | 10587.5932 | 1.8 | | | 44-34 | 17657.5845 | -1.0 | | | | |
| 33-12 | 10700.7183 | 0.1 | 10587.5932 | 1.8 | | | 33-34 | 17657.5845 | -1.0 | | | | |
| 22-11 | 10700.7293 | -0.3 | 10587.6055 | 2.0 | | | 23-34 | 17657.5845 | -1.0 | | | | |
| 32-11 | 10700.7293 | -0.3 | 10587.6055 | 2.0 | | | 22-32 | 17657.6104 | -1.8 | | | | |
| 21-11 | 10700.7293 | -0.3 | 10587.6055 | 2.0 | | | 21-32 | 17657.6104 | -1.8 | | | | |
| 33-32 | 10700.7635 | -3.1 | 10587.6387 | 0.4 | | | | | | | | | |
| 32-32 | 10700.7635 | -3.1 | 10587.6387 | 0.4 | | | 404-303 | | | | | | |
| 22-32 | 10700.7635 | -3.1 | 10587.6387 | 0.4 | | | 45-34 | 14232.9846 | -1.9 | 14083.4622 | -2.3 | 13373.7697 | -1.8 |
| 43-32 | 10700.7635 | -3.1 | 10587.6387 | 0.4 | | | 44-33 | 14232.9846 | -1.9 | 14083.4622 | -2.6 | 13373.7697 | -2.1 |
| 23-32 | 10700.7635 | -3.1 | 10587.6387 | 0.4 | | | 43-32 | 14232.9846 | -3.3 | 14083.4622 | -3.6 | 13373.7697 | -3.1 |

Table A5.1. (continued)

| $J'K_a'K_c'$ - $J''K_a''K_c''$ | $^{12}C^{16}O$-NNO | | $^{13}C^{16}O$-NNO | | $^{13}C^{18}O$-NNO | | $J'K_a'K_c'$ - $J''K_a''K_c''$ | $^{12}C^{16}O$-NNO | | $^{13}C^{16}O$-NNO | | $^{13}C^{18}O$-NNO | |
|---|---|---|---|---|---|---|---|---|---|---|---|---|---|
| $F_1'$ $F'$ - $F_1''$ $F''$ | $\nu_{obs}$ | $\Delta\nu$ | $\nu_{obs}$ | $\Delta\nu$ | $\nu_{obs}$ | $\Delta\nu$ | $F_1'$ $F'$ - $F_1''$ $F''$ | $\nu_{obs}$ | $\Delta\nu$ | $\nu_{obs}$ | $\Delta\nu$ | $\nu_{obs}$ | $\Delta\nu$ |
| 34-34 | 10700.7742 | -2.0 | 10587.6492 | 0.5 | | | 55-44 | 14232.9923 | 0.0 | 14083.4711 | 0.7 | 13373.7779 | 1.5 |
| 45-34 | 10700.7742 | -2.0 | 10587.6492 | 0.5 | | | 56-45 | 14232.9923 | -1.8 | 14083.4711 | -0.8 | 13373.7779 | 0.0 |
| 33-33 | 10700.7973 | -2.3 | 10587.6750 | 1.2 | | | 54-43 | 14232.9923 | -3.6 | 14083.4711 | -2.8 | 13373.7779 | -1.7 |
| 44-33 | 10700.7973 | -2.3 | 10587.6750 | 1.2 | | | 34-23 | 14233.0028 | -1.9 | 14083.4826 | 0.2 | 13373.7899 | 1.6 |
| 34-33 | 10700.7973 | -2.3 | 10587.6750 | 1.2 | | | 33-22 | 14233.0028 | -2.4 | 14083.4826 | -0.7 | 13373.7899 | 0.9 |
| 43-33 | 10700.7973 | -2.3 | 10587.6750 | 1.2 | | | 44-34 | 14233.0028 | -2.5 | 14083.4826 | -2.7 | 13373.7899 | 0.0 |
| 23-33 | 10700.7973 | -2.3 | 10587.6750 | 1.2 | | | 32-21 | 14233.0028 | -5.5 | 14083.4826 | -3.6 | 13373.7899 | -1.9 |
| 32-21 | 10700.8803 | -3.4 | 10587.7566 | 1.2 | | | | | | | | | |
| 414-313 | | | | | | | 413-404 | | | | | | |
| 32-21 | 13749.1603 | 1.0 | 13608.8672 | -1.8 | 12942.3666 | -1.7 | 32-32 | 12418.8284 | 0.3 | 12395.9350 | -0.5 | 12349.8916 | 0.5 |
| 33-22 | 13749.1603 | 0.1 | 13608.8672 | -3.0 | 12942.3666 | -2.4 | 34-33 | 12418.8284 | -1.0 | 12395.9350 | 0.5 | 12349.8916 | -1.3 |
| 34-23 | 13749.1660 | 1.2 | 13608.8717 | -2.5 | 12942.3731 | -0.8 | 34-34 | 12418.8475 | -0.8 | 12395.9541 | -1.3 | 12349.9116 | 0.2 |
| 54-43 | 13749.1762 | 3.5 | 13608.8829 | 0.6 | 12942.3832 | 1.4 | 54-54 | 12418.8812 | 0.2 | 12395.9877 | -0.6 | 12349.9412 | -2.2 |
| 55-44 | 13749.1762 | 1.2 | 13608.8829 | -2.0 | 12942.3832 | -0.8 | 56-56 | 12418.8956 | 0.1 | 12395.9999 | -2.6 | 12349.9561 | -1.9 |
| 56-45 | 13749.1762 | 0.7 | 13608.8829 | -2.1 | 12942.3832 | -1.4 | 33-33 | 12418.9069 | -0.2 | 12396.0109 | -2.4 | 12349.9688 | -1.7 |
| 44-33 | 13749.1865 | 5.4 | 13608.8915 | 0.6 | 12942.3942 | 3.8 | 55-55 | 12418.9608 | 0.3 | 12396.0653 | -1.3 | 12350.0217 | -1.7 |
| 43-32 | 13749.1865 | 3.6 | 13608.8915 | -0.7 | 12942.3942 | 1.9 | 43-43 | 12419.0786 | 0.0 | 12396.1851 | -0.3 | 12350.1387 | -0.2 |
| 45-34 | 13749.1865 | 2.3 | 13608.8915 | -2.1 | 12942.3942 | 0.5 | 45-45 | 12419.0925 | -0.1 | 12396.1976 | -1.6 | 12350.1528 | -0.2 |
| | | | | | | | 44-44 | 12419.1527 | 0.8 | 12396.2562 | -1.4 | 12350.2127 | 0.1 |
| 413-312 | | | | | | | | | | | | | |
| 56-45 | 14783.4173 | 0.6 | 14621.9621 | 3.0 | 13856.0944 | 2.4 | 505-404 | | | | | | |
| 54-43 | 14783.4246 | 4.0 | 14621.9675 | 4.4 | 13856.1000 | 4.0 | 55-44 | 17756.0780 | 4.2 | 17570.5741 | 2.5 | 16689.7756 | -2.8 |
| 55-44 | 14783.4246 | 1.3 | 14621.9675 | 1.5 | 13856.1000 | 1.4 | 56-45 | 17756.0780 | 1.9 | 17570.5741 | 0.5 | 16689.7756 | -4.6 |
| 45-34 | 14783.4301 | 0.2 | 14621.9769 | 4.7 | 13856.1060 | 0.5 | 54-43 | 17756.0780 | 0.6 | 17570.5741 | -0.8 | 16689.7756 | -5.9 |
| 43-32 | 14783.4301 | -1.4 | 14621.9769 | 3.0 | 13856.1060 | -1.2 | 66-55 | 17756.0895 | 6.2 | 17570.5808 | 0.0 | 16689.7875 | 1.1 |
| 34-23 | 14783.4383 | 2.0 | 14621.9834 | 4.7 | 13856.1126 | 1.0 | 67-56 | 17756.0895 | 3.0 | 17570.5808 | -3.0 | 16689.7875 | -1.7 |
| 44-33 | 14783.4383 | -3.0 | 14621.9834 | -0.6 | 13856.1200 | 3.1 | 65-54 | 17756.0895 | 1.6 | 17570.5808 | -4.5 | 16689.7875 | -3.0 |

Table A5.1. (continued)

| $J'K_a'K_c'$ -$J''K_a''K_c''$ $F_1'$ $F'$- $F_1''$ $F''$ | $^{12}C^{16}O$-NNO $\nu_{obs}$ | $\Delta\nu$ | $^{13}C^{16}O$-NNO $\nu_{obs}$ | $\Delta\nu$ | $^{13}C^{18}O$-NNO $\nu_{obs}$ | $\Delta\nu$ | $J'K_a'K_c'$ -$J''K_a''K_c''$ $F_1'$ $F'$- $F_1''$ $F''$ | $^{12}C^{16}O$-NNO $\nu_{obs}$ | $\Delta\nu$ | $^{13}C^{16}O$-NNO $\nu_{obs}$ | $\Delta\nu$ | $^{13}C^{18}O$-NNO $\nu_{obs}$ | $\Delta\nu$ |
|---|---|---|---|---|---|---|---|---|---|---|---|---|---|
| 32-21 | 14783.4464 | 1.3 | 14621.9922 | 4.7 | 13856.1200 | -0.4 | 44-33 | 17756.0961 | 5.0 | 17570.5912 | 2.6 | 16689.7955 | 1.5 |
| 33-22 | 14783.4464 | -3.6 | 14621.9922 | -0.5 | | | 55-45 | 17756.0961 | 3.6 | 17570.5912 | -1.2 | 16689.7955 | -1.2 |
| | | | | | | | 45-34 | 17756.0961 | 2.8 | 17570.5912 | 0.7 | 16689.7955 | -0.3 |
| 423-322 | | | | | | | 43-32 | 17756.0961 | 0.6 | 17570.5912 | -1.7 | 16689.7955 | -2.5 |
| 32-21 | 14263.3424 | 0.9 | | | | | | | | | | | |
| 32-22 | 14263.3424 | 0.9 | | | | | 515-414 | | | | | | |
| 34-23 | 14263.3424 | -2.4 | | | | | 43-32 | 17177.0482 | 2.5 | | | 16170.4930 | 0.8 |
| 34-33 | 14263.3424 | -2.4 | | | | | 44-33 | 17177.0482 | 2.4 | | | 16170.4930 | 0.7 |
| 34-34 | 14263.3424 | -2.4 | | | | | 45-34 | 17177.0482 | -0.3 | | | 16170.4930 | -2.1 |
| 34-44 | 14263.3424 | -2.4 | | | | | 65-54 | 17177.0582 | 6.2 | | | 16170.5025 | 3.9 |
| 54-43 | 14263.3565 | 2.7 | | | | | 66-55 | 17177.0582 | 5.6 | | | 16170.5025 | 3.2 |
| 54-33 | 14263.3565 | 2.7 | | | | | 67-56 | 17177.0582 | 4.6 | | | 16170.5025 | 2.2 |
| 54-44 | 14263.3565 | 2.7 | | | | | 55-44 | 17177.0582 | 4.2 | | | 16170.5025 | 1.5 |
| 54-34 | 14263.3565 | 2.7 | | | | | 54-43 | 17177.0582 | 3.1 | | | 16170.5025 | 0.4 |
| 54-23 | 14263.3565 | 2.7 | | | | | 56-45 | 17177.0582 | 2.0 | | | 16170.5025 | -0.7 |
| 33-23 | 14263.3565 | 2.0 | | | | | | | | | | | |
| 33-33 | 14263.3565 | 2.0 | | | | | 514-413 | | | | | | |
| 33-32 | 14263.3565 | 2.0 | | | | | 67-56 | 18468.7364 | 0.8 | | | 17311.8103 | 1.0 |
| 33-22 | 14263.3565 | 2.0 | | | | | 65-54 | 18468.7364 | -2.1 | | | 17311.8103 | -1.9 |
| 33-43 | 14263.3565 | 2.0 | | | | | 66-55 | 18468.7364 | -2.5 | | | 17311.8103 | -2.3 |
| 56-45 | 14263.3565 | 0.4 | | | | | 56-45 | 18468.7364 | -5.1 | | | 17311.8103 | -5.3 |
| 55-4 5 | 14263.3671 | 0.4 | | | | | 54-43 | 18468.7415 | -2.3 | | | 17311.8210 | 3.2 |
| 55-44 | 14263.3671 | 0.4 | | | | | 55-44 | 18468.7415 | -5.8 | | | 17311.8210 | -0.5 |
| 55-34 | 14263.3671 | 0.4 | | | | | 45-34 | 18468.7415 | -7.0 | | | 17311.8210 | -1.1 |
| 43-23 | 14263.4021 | 2.2 | | | | | 43-32 | 18468.7536 | -0.4 | | | 17311.8306 | 3.0 |
| 43-33 | 14263.4021 | 2.2 | | | | | 44-33 | 18468.7536 | -1.4 | | | 17311.8306 | 2.0 |
| 43-22 | 14263.4021 | 2.2 | | | | | | | | | | | |
| 43-32 | 14263.4021 | 2.2 | | | | | 505-414 | | | | | | |

Table A5.1. (continued)

| $J'K_a'K_c'$ -$J''K_a''K_c''$ $F_1'$ $F'$- $F_1''$ $F''$ | $^{12}C^{16}O$-NNO $\nu_{obs}$ | $\Delta\nu$ | $^{13}C^{16}O$-NNO $\nu_{obs}$ | $\Delta\nu$ | $^{13}C^{18}O$-NNO $\nu_{obs}$ | $\Delta\nu$ | $J'K_a'K_c'$ -$J''K_a''K_c''$ $F_1'$ $F'$- $F_1''$ $F''$ | $^{12}C^{16}O$-NNO $\nu_{obs}$ | $\Delta\nu$ | $^{13}C^{16}O$-NNO $\nu_{obs}$ | $\Delta\nu$ | $^{13}C^{18}O$-NNO $\nu_{obs}$ | $\Delta\nu$ |
|---|---|---|---|---|---|---|---|---|---|---|---|---|---|
| 43-43 | 14263.4021 | 2.2 | | | | | 43-32 | 7923.6438 | -1.3 | | | | |
| 45-45 | 14263.4021 | -0.1 | | | | | 45-34 | 7923.6605 | -1.6 | | | | |
| 45-44 | 14263.4021 | -0.1 | | | | | 65-54 | 7923.6919 | 1.4 | | | | |
| 45-34 | 14263.4021 | -0.1 | | | | | 67-56 | 7923.7005 | -2.5 | | | | |
| 44-43 | 14263.4111 | -0.8 | | | | | 44-33 | 7923.7141 | -1.5 | | | | |
| 44-34 | 14263.4111 | -0.8 | | | | | 66-55 | 7923.7626 | 0.9 | | | | |
| 44-33 | 14263.4111 | -0.8 | | | | | 54-43 | 7923.8794 | 0.2 | | | | |
| | | | | | | | 56-45 | 7923.8889 | -2.2 | | | | |
| 422-321 | | | | | | | 55-44 | 7923.9452 | -0.1 | | | | |
| 32-21 | 14308.2728 | 2.8 | | | | | | | | | | | |
| 33-33 | 14308.2728 | 1.4 | | | | | 514-505 | | | | | | |
| 34-23 | 14308.2728 | -1.0 | | | | | 43-43 | 13131.4881 | 1.6 | | | | |
| 33-32 | 14308.2728 | -2.5 | | | | | 45-45 | 13131.5045 | 1.0 | | | | |
| 54-23 | 14308.2879 | 1.6 | | | | | 66-55 | 13131.5333 | 2.9 | | | | |
| 56-45 | 14308.2879 | 1.5 | | | | | 65-65 | 13131.5333 | 1.6 | | | | |
| 33-22 | 14308.2879 | 1.2 | | | | | 67-67 | 13131.5446 | 0.0 | | | | |
| 33-23 | 14308.2879 | -1.6 | | | | | 44-44 | 13131.5729 | 1.9 | | | | |
| 55-44 | 14308.3010 | 0.8 | | | | | 66-66 | 13131.6186 | 2.5 | | | | |
| 55-45 | 14308.3010 | -2.8 | | | | | 54-54 | 13131.7463 | 1.3 | | | | |
| 43-32 | 14308.3420 | 3.0 | | | | | 56-56 | 13131.7590 | 1.0 | | | | |
| 45-34 | 14308.3420 | 0.1 | | | | | 55-55 | 13131.8274 | 2.0 | | | | |
| 45-44 | 14308.3552 | 5.3 | | | | | | | | | | | |
| 43-43 | 14308.3552 | 4.6 | | | | | | | | | | | |
| 45-45 | 14308.3552 | 1.8 | | | | | | | | | | | |
| 44-33 | 14308.3552 | 0.5 | | | | | | | | | | | |
| 44-34 | 14308.3552 | -2.4 | | | | | | | | | | | |

$\nu_{obs}$=measured frequencies, $\Delta\nu$=observed-calculated frequencies.

Table A5.2. Observed Transition Frequencies (in MHz) for $^{13}C^{16}O$-$^{15}N^{14}NO$ and $^{13}C^{16}O$-$^{14}N^{15}NO$

| $J'K_a'K_c'$ -$J''K_a''K_c''$ | | | | | $J'K_a'K_c'$ -$J''K_a''K_c''$ | | | | |
|---|---|---|---|---|---|---|---|---|---|
| F'- F'' | $\nu_{obs}$ | $\Delta\nu^a$ | $\nu_{obs}$ | $\Delta\nu$ | F'- F'' | $\nu_{obs}$ | $\Delta\nu$ | $\nu_{obs}$ | $\Delta\nu$ |
| | $^{13}C^{16}O$-$^{15}N^{14}NO$ | | $^{13}C^{16}O$-$^{14}N^{15}NO$ | | | $^{13}C^{16}O$-$^{15}N^{14}NO$ | | $^{13}C^{16}O$-$^{14}N^{15}NO$ | |
| 111-000 | | | | | 303-202 | | | | |
| 1 - 0 | 14067.2319 | -2.6 | 14474.6867 | -0.8 | 2 - 2 | 10453.9215 | 2.3 | 10494.1089 | -0.2 |
| 2 - 0 | 14067.3100 | 2.5 | 14474.9089 | 0.6 | 3 - 2 | 10453.9547 | 2.2 | 10494.2509 | 2.8 |
| 0 - 0 | 14067.4171 | 0.1 | 14475.2379 | -1.6 | 4 - 3 | 10453.9547 | 0.8 | 10494.2509 | 0.3 |
| | | | | | 2 - 1 | 10453.9628 | 3.0 | 10494.2733 | 0.2 |
| 110-101 | | | | | 3 - 3 | 10453.9777 | -0.9 | 10494.3573 | 3.7 |
| 0 - 1 | 10831.5147 | -3.0 | 11220.1180 | -2.1 | | | | | |
| 2 - 1 | 10831.5892 | 0.7 | 11220.2995 | 1.6 | 313-212 | | | | |
| 2 - 2 | 10831.6153 | 1.0 | 11220.4008 | 0.7 | 3 - 3 | 10084.4823 | -0.9 | 10132.2299 | -1.2 |
| 1 - 1 | 10831.6329 | -2.8 | 11220.4179 | 1.5 | 2 - 1 | 10084.5153 | -1.6 | 10132.3012 | -0.5 |
| 1 - 2 | 10831.6601 | -1.4 | 11220.5183 | -0.3 | 4 - 3 | 10084.5273 | -1.7 | 10132.3354 | -0.2 |
| 1 - 0 | 10831.7012 | 1.0 | 11220.6712 | -0.8 | 3 - 2 | 10084.5358 | 2.0 | 10132.3573 | -0.7 |
| | | | | | 2 - 2 | 10084.5964 | 0.8 | 10132.4997 | 0.5 |
| 202-101 | | | | | | | | | |
| 1 - 1 | 6977.1679 | -1.5 | 7003.3249 | 1.5 | 312-211 | | | | |
| 3 - 2 | 6977.2107 | 1.0 | 7003.4861 | 1.9 | 2 - 2 | 10850.0355 | 0.8 | 10880.1329 | -0.1 |
| 2 - 1 | 6977.2107 | 0.7 | 7003.4861 | -1.4 | 4 - 3 | 10850.1439 | 0.3 | 10880.4649 | 0.1 |
| 1 - 0 | 6977.2348 | 0.8 | 7003.5809 | 1.9 | 3 - 2 | 10850.1529 | -0.3 | 10880.5013 | 0.6 |
| 2 - 2 | 6977.2348 | -1.1 | 7003.5910 | 1.3 | 2 - 1 | 10850.1529 | -3.5 | 10880.5013 | 0.4 |
| | | | | | 3 - 3 | 10850.2301 | -1.3 | 10880.7367 | -0.5 |
| 212-101 | | | | | | | | | |
| 2 - 1 | 17301.4143 | -0.6 | 17727.6424 | 0.8 | 312-303 | | | | |
| 2 - 2 | 17301.4408 | 0.1 | 17727.7439 | 0.0 | 2 - 3 | 11486.2368 | 1.3 | 11858.6872 | 0.0 |
| 1 - 1 | 17301.4929 | 1.6 | 17727.8382 | -0.9 | 4 - 3 | 11486.2671 | 0.9 | 11858.7822 | -0.3 |
| 3 - 2 | 17301.4929 | -0.6 | 17727.8713 | 0.5 | 2 - 2 | 11486.2671 | -1.7 | 11858.8259 | -0.3 |
| 1 - 0 | 17301.5584 | 0.3 | 17728.0944 | -0.3 | 4 - 4 | 11486.2892 | -1.7 | 11858.8857 | 0.2 |
| | | | | | 3 - 3 | 11486.3537 | -0.3 | 11859.0552 | 0.4 |
| 211-110 | | | | | 3 - 4 | 11486.3799 | 1.2 | 11859.1570 | -0.8 |
| 1 - 1 | 7235.6052 | -0.8 | 7255.5052 | -0.3 | 3 - 2 | 11486.3880 | 0.6 | 11859.1943 | 0.5 |
| 3 - 2 | 7235.6970 | 0.3 | 7255.7549 | -0.5 | | | | | |
| 1 - 0 | 7235.7223 | -1.8 | 7255.7974 | -4.3 | 404-303 | | | | |
| 2 - 1 | 7235.7291 | 1.4 | 7255.8740 | 0.6 | 3 - 3 | 13916.4917 | 0.0 | 13971.7554 | -2.0 |
| 2 - 2 | 7235.7736 | -1.4 | 7255.9908 | -1.1 | 4 - 3 | 13916.5216 | 2.2 | 13971.8773 | -1.5 |
| | | | | | 5 - 4 | 13916.5216 | -0.5 | 13971.8863 | 1.1 |
| 212-111 | | | | | 3 - 2 | 13916.5216 | -3.5 | 13971.8940 | -2.4 |
| 1 - 0 | 6725.0784 | 0.1 | 6756.6296 | 0.9 | 4 - 4 | 13916.5432 | -0.9 | 13971.9808 | -1.0 |
| 2 - 2 | 6725.1080 | -1.2 | 6756.7604 | -1.9 | | | | | |
| 3 - 2 | 6725.1597 | 0.0 | 6756.8891 | -0.2 | 414-313 | | | | |
| 2 - 1 | 6725.1826 | 0.4 | 6756.9829 | -0.2 | 4 - 4 | 13440.0670 | 0.4 | 13504.1296 | 0.0 |
| 1 - 1 | 6725.2621 | 1.2 | 6757.1810 | 0.4 | 3 - 2 | 13440.1061 | -0.6 | 13504.2155 | 0.1 |
| | | | | | 5 - 4 | 13440.1129 | 1.7 | 13504.2265 | -0.5 |
| 211-202 | | | | | 4 - 3 | 13440.1129 | 0.5 | 13504.2362 | 2.0 |
| 1 - 2 | 11090.0336 | 1.9 | 11472.4347 | 0.3 | 3 - 3 | 13440.1680 | -0.5 | 13504.3579 | 1.3 |
| 3 - 2 | 11090.0745 | 2.2 | 11472.5670 | 1.2 | | | | | |

Table A5.2. (continued)

| $J'K_a'K_c'$ -$J''K_a''K_c''$ F'- F'' | $\nu_{obs}$ | $\Delta\nu^a$ | $\nu_{obs}$ | $\Delta\nu$ | $J'K_a'K_c'$ -$J''K_a''K_c''$ F'- F'' | $\nu_{obs}$ | $\Delta\nu$ | $\nu_{obs}$ | $\Delta\nu$ |
|---|---|---|---|---|---|---|---|---|---|
| | $^{13}C^{16}O$-$^{15}N^{14}NO$ | | $^{13}C^{16}O$-$^{14}N^{15}NO$ | | | $^{13}C^{16}O$-$^{15}N^{14}NO$ | | $^{13}C^{16}O$-$^{14}N^{15}NO$ | |
| 1 - 1 | 11090.0745 | -0.6 | 11472.5987 | 0.3 | 413-312 | | | | |
| 3 - 3 | 11090.1011 | -0.1 | 11472.6713 | 0.1 | 3 - 3 | 14460.3164 | 1.5 | 14500.9159 | 0.2 |
| 2 - 2 | 11090.1526 | -0.8 | 11472.8027 | 0.4 | 5 - 4 | 14460.4267 | 0.3 | 14501.2630 | 0.9 |
| 2 - 3 | 11090.1801 | 0.6 | 11472.9076 | -0.2 | 4 - 3 | 14460.4321 | 1.6 | 14501.2772 | -0.6 |
| 2 - 1 | 11090.1949 | 0.9 | 11472.9657 | -0.6 | 3 - 2 | 14460.4321 | 1.6 | 14501.2851 | 1.8 |
| | | | | | 4 - 4 | 14460.5152 | -3.1 | 14501.5498 | -0.3 |

[a] $\nu_{obs}$-$\nu_{calc}$ in kHz.